

**Biological insights into the
mechanisms underpinning
the pathogenic success of
*Acinetobacter baumannii***

by

Felise Grace Adams

*Thesis
Submitted to Flinders University
for the degree of*

Doctor of Philosophy
College of Science and Engineering
July 2020

TABLE OF CONTENTS

TABLE OF CONTENTS	II
LIST OF TABLES.....	VI
TABLE OF FIGURES	VII
THESIS SUMMARY.....	IX
DECLARATION	XI
ACKNOWLEDGEMENTS	XII
ABSTRACTS	XIII
CONTRIBUTIONS	XIV
PUBLICATIONS.....	XV
CHAPTER 1: General introduction.....	1
1.1 <i>Acinetobacter baumannii</i> ; a global threat to human health	2
1.2 The <i>Acinetobacter</i> genus.....	3
1.3 Disease and impact of <i>A. baumannii</i> infections.....	4
1.3.1 Nosocomial infections	4
1.3.2 Community-acquired infections	6
1.4 Characteristics of <i>A. baumannii</i> that contribute to pathogenicity and virulence.....	6
1.4.1 Formation of biofilms and pellicles	7
1.4.2 Outer membrane protein A	9
1.4.3 Chaperone-usher pili.....	9
1.4.4 Motility	11
1.4.5 Desiccation tolerance.....	13
1.4.6 Capsular polysaccharide	14
1.4.7 Type VI secretion system	15
1.4.8 Micronutrient acquisition systems	17
1.4.9 Antimicrobial resistance mechanisms employed by <i>A. baumannii</i>	18
1.5 Evolution of <i>A. baumannii</i> virulence by mobile genetic elements	23
1.5.1 Insertion sequence elements	24
1.5.2 Miniature inverted-repeat transposable elements	28
1.5.3 Transposons	30
1.5.4 Integrons	30
1.5.5 Plasmids	31
1.5.6 Genomic islands.....	32
1.6 Regulatory mechanisms employed by <i>A. baumannii</i>	32
1.6.1 Two component signal transduction systems	33
1.7 Scope of thesis	56

CHAPTER 2: Resistance to pentamidine is mediated by AdeAB, regulated by AdeRS, and influenced by growth conditions in <i>Acinetobacter baumannii</i> ATCC 17978.....	59
2.1 Preface.....	61
2.2 Abstract.....	61
2.3 Introduction.....	61
2.4 Materials and methods	63
2.4.1 Bacterial strains, plasmids and growth conditions.....	63
2.4.2 Antimicrobial susceptibility testing.....	69
2.4.3 Construction of <i>A. baumannii</i> ATCC 17978 deletion strains and genetic complementation	70
2.4.4 Cell treatments and RNA isolation	70
2.4.5 Bioinformatic analysis	71
2.4.6 Quantitative Real-Time PCR.....	71
2.4.7 Phenotypic microarray analysis	72
2.5 Results.....	72
2.5.1 Generation of $\Delta adeRS$ and complemented strains	72
2.5.2 Transcriptomic profiling of $\Delta adeRS$	72
2.5.3 Deletion of <i>adeRS</i> in ATCC 17978 reduced susceptibility to a limited number of antimicrobial agents	75
2.5.4 Both AdeA and AdeB are required for intrinsic antimicrobial resistance in ATCC 17978.....	77
2.5.5 AdeRS is critical for increased expression of <i>adeAB</i> following pentamidine exposure	77
2.5.6 Carbon source utilisation alters resistance to pentamidine.....	80
2.5.7 Bioavailability of iron correlates with pentamidine resistance.....	84
2.6 Discussion.....	84
2.7 Conclusions.....	90
CHAPTER 3: Deletion of a two component signal transduction system in <i>Acinetobacter baumannii</i> ATCC 17978 promotes secondary loss-of-function mutations in the AdeN global regulator	92
3.1 Preface.....	94
3.2 Abstract.....	94
3.3 Introduction.....	94
3.4 Methods.....	96
3.4.1 Strains and growth conditions.....	96
3.4.2 Construction of <i>A. baumannii</i> deletion strains.....	96
3.4.3 Transcriptome profiling and qRT-PCR validation	100
3.4.4 Bioinformatics	100
3.5 Results.....	100

3.5.1	The ACX60_11155/60 genes encode a LuxR-type response regulator and a solute symporter family fused hybrid histidine kinase	100
3.5.2	11155 and 11160 are co-transcribed in ATCC 17978	102
3.5.3	Architecture of 11160 differs to characterised bacterial SLC fused histidine kinases	104
3.5.4	Absence of distinct Hpt proteins in <i>A. baumannii</i> genomes infers utilisation of multi-TCS signalling pathways for signal transfer.....	104
3.5.5	Deletion of <i>11155</i> from ATCC 17978 promoted selection for secondary loss-of-function mutations in the AdeN regulator.	106
3.5.6	11160 orthologues are present across different classes of the Proteobacteria phyla, frequently co-clustering with ABC transporter genes.	110
3.6	Discussion	111

CHAPTER 4:	MITE_{Aba12}, a novel mobile miniature inverted-repeat transposable element identified in <i>Acinetobacter baumannii</i> ATCC 17978 and its prevalence across the <i>Moraxellaceae</i> family	116
4.1	Preface.....	118
4.2	Abstract.....	118
4.2.1	Importance	118
4.3	Introduction.....	119
4.4	Materials and methods	121
4.4.1	Bacterial strains, plasmids, media and growth conditions.....	121
4.4.2	Construction of deletion and complementation derivatives	121
4.4.3	Desiccation survival assay	121
4.4.4	Gene cloning and DNA sequencing.....	126
4.4.5	Stability of MITE _{Aba12} in <i>hns</i>	126
4.4.6	Motility assays	126
4.4.7	Comparative genomics, alignments and clustering	126
4.4.8	Characterisation of MITE _{Aba12} target site duplications	128
4.5	Results.....	128
4.5.1	Construction of <i>qseBC</i> and <i>ygiW</i> deletion derivatives in <i>A. baumannii</i> ATCC 17978	128
4.5.2	Disruption of the <i>hns</i> gene after desiccation stress.....	128
4.5.3	Identification and characterisation of a novel active MITE in <i>A. baumannii</i> ATCC 17978	130
4.5.4	IS _{Aba12} is the proposed autonomous parent of the novel MITE in <i>A. baumannii</i> ATCC 17978	135
4.5.5	MITE _{Aba12} is present in a diverse range of species from the <i>Moraxellaceae</i> family	135

4.5.6	MITE _{Aba12} is a highly conserved mobile element with potential to affect expression of neighbouring host genes.....	136
4.5.7	MITE _{Aba12} in <i>M. osloensis</i> CCUG 350 is located within a novel composite transposon.....	148
4.6	Discussion.....	148
CHAPTER 5: Final discussion.....		155
5.1	<i>A. baumannii</i> ATCC 17978, a good model organism?.....	156
5.1.1	Strain to strain variation, a cause for concern?.....	157
5.2	New genetic tools to analyse <i>A. baumannii</i> pathogenesis	157
5.3	MGEs play a role in the genetic plasticity of <i>A. baumannii</i> ATCC 17978	159
5.3.1	Does disruption of H-NS enhance survival under desiccation stress in ATCC 17978?	159
5.3.2	Insights and implications of MITE _{Aba12} elements in host genome evolution	160
5.4	The contribution of the AdeRS/AdeAB(C) cluster in the pathogenic success of <i>A. baumannii</i>	162
5.4.1	Does BaeSR communicate with AdeRS?	164
5.4.2	AdeA and AdeB function together to confer intrinsic resistance in <i>A. baumannii</i> ATCC 17978	165
5.4.3	Does strain specific phenotypes affect pentamidine efficacy against <i>A. baumannii</i> ?.....	167
5.5	The role of the 11155/60 TCS in <i>A. baumannii</i> ATCC 17978	167
5.6	How to define the regulatory role of the QseBC TCS in <i>A. baumannii</i>	169
5.7	Challenges associated with defining phenotypes for bacterial TCSs	170
5.8	Deciphering interactions between TCS in <i>A. baumannii</i>	171
5.9	Conclusions.....	172
CHAPTER 6: Appendices		173
	Appendix A - Genes significantly down- and up-regulated (≥ 2 -fold) in $\Delta adeRS$ compared against ATCC 17978 (CP012004) by RNA-seq	174
	Appendix B - Comparative analysis of kinetic response curves obtained from Biolog PM plates for $\Delta adeRS$ cells untreated and subjected to increasing concentrations of pentamidine.....	183
	Appendix C - Genes significantly down- and up-regulated (≥ 2 -fold) in $\Delta 11155 \Delta adeN::ISAbal2$ compared against WT ATCC 17978 (CP012004) by RNA-seq.....	184
	Appendix D - Adams <i>et al.</i> , 2018; <i>PLoS ONE</i>	191
	Appendix E - Adams and Brown, 2019; <i>mSphere</i>	211
	Appendix F – Adams, 2017; <i>Microbiology Australia</i>	228
	Appendix G – List of Abbreviations.....	233
CHAPTER 7: References		237

LIST OF TABLES

Table 2.1: Strains and plasmids used in the study	64
Table 2.2: Primers used in this study	66
Table 2.3: Antibiotic susceptibility of <i>A. baumannii</i> ATCC 17978, deletion mutants and complemented strains.....	76
Table 2.4: Zones of clearing obtained from growth on M9 minimal medium with the addition of different carbon sources after exposure to pentamidine.....	81
Table 2.5: Zones of clearing for <i>A. baumannii</i> ATCC 17978 and deletion mutants grown on Mueller-Hinton agar with the addition or chelation of iron after pentamidine exposure.....	86
Table 3.1: Strains and plasmids used in the study	97
Table 3.2: Primers used in the study	98
Table 3.3: Bacterial strains harbouring orthologues of <i>11160</i> used in gene alignments	101
Table 4.1: Strains and plasmids used in this study.....	122
Table 4.2: Primers used in the study	124
Table 4.3: Bacterial strains that harbour full length MITE _{Aba12} elements.....	137
Table 4.4: IS with TIR closely related to those of IS _{Aba12} and MITE _{Aba12}	140
Table 4.5: List of MITE _{Aba12} elements and their corresponding strain names that formulate MITE _{Aba12} Sub-groups 1-10.....	144

TABLE OF FIGURES

Figure 1.1: The six families of drug transporters with characterised systems from <i>A. baumannii</i> used as representatives	20
Figure 1.2: Mobile genetic elements found in bacteria.....	25
Figure 1.3: The signalling cascade and conserved domain architecture of prototypical two component signal transduction systems	36
Figure 1.4: Diagrammatic representation of the three different mechanisms of stimulus perception adopted by bacterial HKs	38
Figure 1.5: Domain organisation and phosphorelay events of prototypical, hybrid and unorthodox two component signal transduction systems	41
Figure 1.6: Domain architecture of TCS proteins encoded in <i>A. baumannii</i> ATCC 17978, AYE and SDF genomes.....	50
Figure 2.1: Global transcriptomic response differences of <i>A. baumannii</i> ATCC 17978 after deletion of <i>adeRS</i>	73
Figure 2.2: Validation of RNA-sequencing results.....	74
Figure 2.3: Structures of dicationic antimicrobial compounds to which $\Delta adeRS$, $\Delta adeA$, $\Delta adeB$ and $\Delta adeAB$ deletion mutant derivatives showed a decrease in resistance when compared to WT ATCC 17978.....	78
Figure 2.4: Increased expression of <i>adeA</i> following pentamidine stress is dependent on the presence of AdeRS in ATCC 17978	79
Figure 2.5: Resistance to pentamidine is modulated by carbon sources available in the growth medium	83
Figure 2.6: Kinetic response curves paralleling bacterial growth from Biolog PM01 and PM2A plates identify ten carbon sources that increase pentamidine resistance in $\Delta adeRS$	85
Figure 2.7: Pentamidine resistance is affected by the concentration of iron within the growth medium.....	87
Figure 3.1: Overview of structural and genetic organisation of 11155 and 11160 present in <i>A. baumannii</i> ATCC 17978	103
Figure 3.2: Comparison of structural domains of 11160 to CbrA and CrbS from <i>P. fluorescens</i> SBW25.....	105
Figure 3.3: Growth kinetics of ATCC 17978, $\Delta 11155 \Delta adeN::ISAbal2$ and $\Delta 11155 adeN_{Gly54Asp}$	107
Figure 3.4: Identification of loss-of-function mutations in the global regulator AdeN from an 11155 deletion background.....	109
Figure 3.5: Alignment of the genetic region from different proteobacterial species carrying orthologues of the 11155/11160 TCS	112
Figure 4.1: Identification of hyper-motile variants from <i>A. baumannii</i> ATCC 17978 wildtype, $\Delta qseBC$, and $\Delta ygiW$ strains after desiccation stress	129
Figure 4.2: Insertions in the <i>hns</i> locus from hyper-motile variants and relationship between <i>ISAbal2</i> and <i>MITE_{Aba12}</i>	132

Figure 4.3: Motility of <i>A. baumannii</i> ATCC 17978 variants and complemented derivatives	134
Figure 4.4: Nucleotide alignment of all MITE _{Aba12} elements identified in this study .	143
Figure 4.5: Characterisation of target site duplications flanking MITE _{Aba12}	145
Figure 4.6: Putative σ 70 promoter sequences identified in MITE _{Aba12} (c)	147
Figure 4.7: MITE _{Aba12} is located within Tn6645 in <i>Moraexella osloensis</i> CCUG 350.....	150

THESIS SUMMARY

Acinetobacter baumannii is a Gram-negative human pathogen that is the causative agent of several life-threatening disease states in susceptible individuals. A range of persistence and resistance mechanisms contribute to the success of this bacterium, including an ability to sense and respond to rapidly changing environments mediated by the concerted action of regulatory proteins. One key regulatory strategy *A. baumannii* employ is through two component signal transduction systems (TCSs). TCSs consist of two modular multi-domain proteins; a membrane-bound histidine kinase (HK) and cytosolic response regulator (RR). The HK senses alterations in the extracellular milieu, relays the signal to the RR, triggering appropriate cellular modifications. Despite regulating a plethora of virulent phenotypes in other bacterial pathogens, the role of TCSs encoded by *A. baumannii* remains largely ill defined. The broad aim of this study was to examine the relative role of three distinct TCS in regulating virulence-associated strategies employed by *A. baumannii*.

The AdeRS TCS is known to regulate the AdeABC tripartite efflux pump in a number of clinical *A. baumannii* isolates. Deletion derivatives targeting *adeRS*, *adeAB*, *adeA* and *adeB* genes were generated in the well-characterised *A. baumannii* ATCC 17978 strain. Antibioassay analyses revealed that the genetically modified strains displayed decreased resistance to a subset of dicationic compounds compared to wildtype (WT). *Trans*-complementation of these mutants partially or fully restored resistance back to WT levels. The global transcriptional landscape of the Δ *adeRS* derivative was determined using RNA-sequencing, and revealed significant variation in expression levels of over 290 genes compared to WT. Transcriptional analyses after shock experiments with pentamidine, a newly identified intrinsic substrate, confirmed AdeRS was directly responsible for activating expression of *adeAB* genes. Alternate resistance mechanisms against pentamidine were further explored, revealing that resistance levels were influenced by the presence of cations and different carbon sources in the growth media.

The second TCS analysed was the putative TCS encoded at the ACX60_11155/60 loci (*11155/60*). This system was chosen for further investigation due to its absence in the avirulent *A. baumannii* SDF strain, and thus was hypothesised to regulate virulence-associated genes. *In silico* analyses revealed a unique architecture for the 11160 hybrid HK, categorising the protein into an uncommon family. Construction and analysis of the Δ *11155* derivative in ATCC 17978 identified an autonomous insertion sequence that

disrupted the function of a distal transcriptional regulator. Regeneration of $\Delta 11155$ utilising a different gene deletion method also harboured a loss-of-function mutation in the same transcriptional regulator, revealing a novel regulatory network. Broader level investigations identified that the TCS was conserved across various bacterial species from the Proteobacteria phyla, co-localising with a transport gene cluster.

In other Gram-negative pathogens, the QseBC TCS is involved in modulating an array of different virulence-associated mechanisms. A homologue of this system and its proposed target, a putative signal peptide (*ygiW*), are present in *A. baumannii*; this system was chosen for further analysis. Independent deletion derivatives targeting *qseBC* and *ygiW* genes were generated in ATCC 17978 and phenotypically analysed. Fortuitously, desiccation stress analyses of $\Delta qseBC$ and $\Delta ygiW$ derivatives compared to WT led to the identification of a novel *trans*-activated miniature inverted-repeat transposable element (MITE), disrupting function of a known global regulator of *A. baumannii*. Further characterisation of the element identified its presence amongst numerous strains across the *Moraxellaceae* family. The unique element showed potential to influence host gene expression, identifying a unique mechanism of ‘mobile’ regulation.

Overall, studies performed on multiple TCS have identified how some pathogenic traits are regulated in *A. baumannii*. The work also highlights how stressors can lead to unexpected changes in the genome, as represented by movement of known and novel mobile genetic elements. As we enter the post-antibiotic era, knowledge of the regulatory mechanisms responsible for virulence factor expression could prove to be invaluable, as proteins such as TCS offer an alternative target for the treatment of infections caused by this formidable pathogen.

DECLARATION

I certify that this thesis does not incorporate without acknowledgment any material previously submitted for a degree or diploma in any university; and that to the best of my knowledge and belief it does not contain any material previously published or written by another person except where due reference is made in the text.

Felise G. Adams

ACKNOWLEDGEMENTS

Firstly, I would like to thank Professor Melissa Brown for giving me the opportunity to undertake my Ph.D. in her laboratory. Your guidance and ongoing support throughout my journey has been instrumental in the completion of this thesis. I would also like to thank Dr Uwe Stroehler for his mentorship throughout the early stages of my Ph.D. The continual encouragement from you both has helped me to see my full potential as a research scientist.

This work was made possible by the financial support offered by AJ and IM Naylor (Flinders University) and Playford Trust Ph.D. scholarships and thus I would like to extend my gratitude to the aforementioned funding bodies.

I would also like to extend my gratitude to many Brown lab members. Sylvia, Jenny, Sarah, Betty, Abol, and Mohsen, thank you for helping me along the way and making my time here such a memorable experience. Sylvia, I am so grateful that pursuing a career in microbiology brought me to you! Your encouragement to travel and see the world, our lengthy phone calls and our shared passion for learning new things and of course, our love of animals will be fondly remembered. Jenny, my love poodle, I don't think we could have done this without each other. From the ups and downs of lab life, thesis writing and supervision of various students over the years, I am so glad we were able to share these experiences together. I will be forever grateful for your ongoing positivity, tenacity and kindness, but mostly your ability to help me realise what is important in life. I have made lifelong friends with you both.

To my family, thank you for continual support and helping me through all those tough times. To my loving partner Ben, thank you for your endless encouragement and taking such a great interest in my work. It was a roller coaster of a ride, but we made it! I love you more than words can ever express, and I am looking forward to starting the next chapter of our lives together.

Overall, I would like to dedicate my Ph.D. to my dad, even though you didn't get to see me complete this stage of my life, I know you were there, encouraging me every step of the way. You gave me the strength to never give up, I love you dad, this one's for you ♥

ABSTRACTS

Presenting author is underlined

Adams, F.G., Stroehler, U.H., and Brown, M.H. Stress induces translocation of insertion sequence element in the human pathogen *Acinetobacter baumannii*, Oral presentation, Adelaide, Flinders University Post Graduate Conference, 2017.

Adams, F.G., Stroehler, U.H., Hassan, K.A., Marri, S., and Brown, M.H. Cellular and regulatory mechanisms involved in pentamidine resistance in *Acinetobacter baumannii*, Poster presentation, *Molecular Analysis of Bacterial Pathogens (BacPath)*, Hahndorf, Australia, 2017.

Adams, F.G., Stroehler, U.H., Hassan, K.A., Marri, S., and Brown, M.H. Cellular and regulatory mechanisms involved in pentamidine resistance in *Acinetobacter baumannii*, Poster presentation, *Bacterial Networks*, Sant Feliu de Guixols, Spain, 2017.

Adams, F.G., Stroehler, U.H., Hassan, K.A., Marri, S., and Brown, M.H. Is pentamidine resistance in *Acinetobacter baumannii* ATCC 17978 regulated by *adeRS*?, Oral presentation, *ASM Annual Scientific Meeting*, Perth, Australia, 2016.

Adams, F.G., Stroehler, U.H. and Brown M.H. The two component signal transduction system *adeRS* and its role in regulating pentamidine resistance in *Acinetobacter baumannii* ATCC 17978, Poster presentation, *Gordon Research Conference on Sensory Transduction in Microorganisms*, Ventura, USA, 2016.

Adams, F.G., Stroehler, U.H., Hassan, K.A., Marri, S., and Brown, M.H. The role *adeR* plays in regulation of genes critical for virulence and cell survival in *Acinetobacter baumannii* ATCC 17978, Poster presentation, *Molecular Analysis of Bacterial Pathogens (BacPath)*, Phillip Island, Australia, 2015.

Adams, F.G., Stroehler, U.H., Hassan, K.A., Marri, S., and Brown, M.H. A transcriptomic approach to elucidate the role *adeR* plays in regulation genes critical for virulence and cell survival in *Acinetobacter baumannii* ATCC 17978, Poster presentation, *10th International Symposium on the Biology of Acinetobacter*, Athens, Greece, 2015.

Adams, F.G., Stroehler, U.H. and Brown M.H. How is virulence regulated in the human pathogen *Acinetobacter baumannii*? Oral presentation, *Flinders University Post Graduate Conference*, Adelaide, 2014. .

CONTRIBUTIONS

Dr. Karl Hassan undertook carbon source utilisation experiments on *A. baumannii* ATCC 17978 and $\Delta adeRS$ strains.

RNA-sequencing was performed by the Australian genome research facility (AGRF) with Dr Shashikanth Marri (Flinders University, Australia) assisting with processing the obtained transcriptomic data.

Mr Jason Young (Flinders University) conducted ICP-MS analysis on *A. baumannii* ATCC 17978 and $\Delta adeRS$ strains.

PUBLICATIONS

Published work arising from data compiled in this thesis

Adams, F.G. and Brown M.H. (2019) MITE_{Aba12}, a novel mobile miniature inverted-repeat transposable element identified in *Acinetobacter baumannii* ATCC 17978 and its prevalence across the *Moraxellaceae* family. *mSphere* **4**, e00028-19. DOI: 10.1128/mSphereDirect.00028-19.

Adams, F.G., Stroehler, U.H., Hassan, K.A., Marri, S. and Brown, M.H. (2018) Resistance to pentamidine is mediated by AdeAB, regulated by AdeRS, and influenced by growth conditions in *Acinetobacter baumannii* ATCC 17978. *PLoS ONE* **13**, e197412. DOI: 10.1371/journal.pone.0197412

Adams, F.G. (2017) A key regulatory mechanism of antimicrobial resistance in pathogenic *Acinetobacter baumannii*. *Microbiology Australia* **38**, 122-26

Additional published work

Singh, J., **Adams, F.G.** and Brown, M.H. (2019) Diversity and function of capsular polysaccharide in *Acinetobacter baumannii*. *Frontiers in Microbiology* **9**:3301. DOI: 10.3389/fmicb.2018.03301.

Manuscript prepared for submission

Adams, F.G., Stroehler, U.H., Marri, S. and Brown M.H. Deletion of a two component signal transduction system in *Acinetobacter baumannii* ATCC 17978 promotes secondary loss-of-function mutations in the AdeN global regulator. Submitted to *Frontiers in Cellular and Infection Microbiology* as a Brief Research Report.

CHAPTER 1: General introduction

1.1 *Acinetobacter baumannii*; a global threat to human health

The human bacterial pathogen *Acinetobacter baumannii* is an ubiquitous aerobic, Gram-negative bacterium that belongs to the group of γ -proteobacteria and the *Acinetobacter* genus. *A. baumannii* grows under strictly aerobic conditions and their shape can change from rod to coccoidal depending on the growth conditions. *A. baumannii* is a versatile organism, assimilating a variety of carbon and nitrogen sources and can grow in a vast range of temperatures and pH conditions (Bouvet and Grimont, 1987; Bergogne-Bérézin and Towner, 1996; Peleg *et al.*, 2008a). These properties help to explain the ability of *A. baumannii* to persist in a wide variety of ecological niches, with an alarming potential to flourish within clinical settings. This has transformed this bacterium from being originally perceived as a general contaminant in diagnostic samples, to a serious opportunistic nosocomial and an occasional community-acquired pathogen.

The designation of *A. baumannii* as a troublesome pathogen is due to a combination of acquired and intrinsic mechanisms. Examples of the latter include an ability to form robust biofilms on various inanimate surfaces and survive desiccating conditions (Harding *et al.*, 2018). This increased persistence can provide a reservoir for infection and facilitate transmission throughout clinical settings, contributing to hospital outbreaks and clonal spread of isolates. Furthermore, the ability of the organism to rapidly acquire and effectively regulate expression of a diverse suite of virulence-associated and antimicrobial resistance determinants has led to the rapid emergence of multi- (resistant to three or more classes of effective antimicrobial compounds), extensively- (resistant to all but one or two) and even pan-drug (resistant to all classes) resistant isolates (Durante-Mangoni and Zarrilli, 2011; Rolain *et al.*, 2013; Rivera *et al.*, 2016; Giammanco *et al.*, 2017; Nowak *et al.*, 2017). These attributes have propelled *A. baumannii* to be one of the leading bacterial species (sp.) threatening the current antibiotic era. As such, the World Health Organisation (WHO) listed carbapenem-resistant *A. baumannii* isolates as one of the top three critical priorities for research and development towards new therapeutic treatments for antibiotic-resistant bacterial sp. (World Health Organisation, 2017).

With a lack of effective treatment options and a dwindling antibiotic pipeline, understanding the molecular mechanisms underpinning the pathogenic success of *A. baumannii* is imperative for the generation of novel treatment strategies to combat infections caused by this formidable pathogen.

1.2 The *Acinetobacter* genus

The genus *Acinetobacter* has had an interesting taxonomical history. The first to report an *Acinetobacter* strain (originally named *Micrococcus calco-aceticus*) was in 1911 by Bijernick (Baumann, 1968). However, in 1968 over 60 years later, the originally identified strain along with various other bacteria were clustered together to formulate the *Acinetobacter* genus (Baumann, 1968). This genus was formally acknowledged in 1971 (Lessel, 1971) but it wasn't until 1986 through the use of DNA-DNA hybridisation technologies that sp. level discrimination was determined (Bouvet and Grimont, 1986).

Acinetobacter sp. are ubiquitous in nature and have been isolated from both environmental and clinical samples, as well as in human and animal specimens (Adegoke *et al.*, 2012). To date, the *Acinetobacter* genus is comprised of over 50 distinct genomic sp., of which the majority are classed as non-pathogenic (Al Atrouni *et al.*, 2016). It is often difficult to discriminate between different *Acinetobacter* sp. using current taxonomic methods or commercial identification systems due to their close genetic relatedness and similar phenotypic properties. A clear example can be demonstrated by *A. baumannii*, *A. nosocomialis* (previously genomospecies 13TU), *A. calcoaceticus*, *A. seifertii*, *A. dijkschoorniae* and *A. pittii* (previously genomospecies 3) strains which are often classified under the “*A. calcoaceticus*-*A. baumannii* complex” (Acb) (Nemec *et al.*, 2015; Cosgaya *et al.*, 2016). However, antibiotic susceptibility profiles and thus, the clinical significance of these six sp., can differ greatly from each other and therefore this classification is considered to be largely inadequate (Lee *et al.*, 2007). Through the use of molecular technologies such as amplified 16S ribosomal DNA (rDNA) restriction analysis, amplified fragment length polymorphism and matrix-associated laser desorption ionisation-time of flight mass spectrometry (Marí-Almirall *et al.*, 2017), sp. identification has been greatly improved. However, as these methods are not routinely used across pathology labs, misidentification is still an ongoing problem.

From the Acb complex, *A. baumannii*, *A. nosocomialis* and *A. pittii* have the greatest clinical significance and are most commonly isolated from human specimens (Nemec *et al.*, 2011; Chusri *et al.*, 2014). Infections caused by *A. baumannii*, however, are by far the most frequent and often associated with increased antimicrobial resistance and higher rates of morbidity and mortality compared to that of sp. from a non-*baumannii* origin (Roca *et al.*, 2012). It is uncommon for *A. baumannii* to be isolated outside of clinical settings, although the bacterium has been found to be a part of the normal flora of the skin and the gastrointestinal and upper respiratory tracts (Seifert *et al.*, 1997; Berlau *et al.*,

1999). Despite these findings, the natural reservoir for *A. baumannii* still remains uncertain.

1.3 Disease and impact of *A. baumannii* infections

1.3.1 Nosocomial infections

A. baumannii has a predilection to infect the severely injured, immune compromised and the elderly, with the highest density of infections occurring amongst patients whom are admitted to intensive care units (ICUs) (Ansaldi *et al.*, 2011; Lee *et al.*, 2012b). *A. baumannii* can cause a wide variety of infections across several anatomical sites. Most commonly these infections are localised to the respiratory tract and bloodstream but are also present across skin and soft tissues, urinary tract and the nervous system (Peleg *et al.*, 2008a). A general commonality identified across these manifestations is the disruption to an anatomical barrier promoting direct entry of the bacterium to the site of infection.

Nosocomial infections caused by multidrug resistant (MDR) *A. baumannii* isolates, particularly those resistant to carbapenem antibiotics, a first line treatment, have been linked to increased morbidity and mortality (Lemos *et al.*, 2014). A number of risk factors are associated with the acquisition of carbapenem-resistant or MDR isolates; socioeconomic status, recent surgery or treatment with antimicrobial agents, presence of catheters or respiratory intubation, location in an ICU, and length of hospital stay (Zheng *et al.*, 2013; Chopra *et al.*, 2014; Henig *et al.*, 2015).

It has been estimated in the U.S. that *A. baumannii* was responsible for 45,900 (range of 41,400 to 83,000) cases with 1 million (range of 600,000 to 1,400,000) cases reported globally per year (Spellberg and Rex, 2013). Furthermore, the use of surveillance data during 2009-10 by the U.S. National Healthcare Safety Network identified that *Acinetobacter* sp. were accountable for 1.8% of all healthcare-associated infections with similar rates being identified in Europe (Lob *et al.*, 2016). Worryingly, surveillance studies revealed that *A. baumannii* nosocomial infections are approximately double that across Asian, Middle Eastern and South American countries, where in some of these areas. *Acinetobacter* is one of the three most common causative agents responsible for bacteraemia and nosocomial pneumonia (Kuo *et al.*, 2012; Luna *et al.*, 2014; Levy-Blitchtein *et al.*, 2018).

1.3.1.1 Global spread of successful *A. baumannii* lineages

The clinical relevance of *A. baumannii* has substantially increased since the 1980s, with the emergence and dissemination of three distinct clonal groups (Dijkshoorn *et al.*, 1996; Nemec *et al.*, 2004; van Dessel *et al.*, 2004). These major *A. baumannii* clones were initially named European clones, but were renamed to international clonal lineages (IC) 1, 2 and 3 due to their presence in clinical institutions worldwide (van Dessel *et al.*, 2004; Whitman *et al.*, 2008; Post and Hall, 2009). To date, a total of eight ICs (IC1-IC8) have been identified, where the additional five epidemic lineages were identified from a large survey of imipenem-resistant isolates (Higgins *et al.*, 2010). However, the majority of outbreak isolates are generally restricted to isolates from IC1 and IC2, as they commonly display MDR phenotypes (Diancourt *et al.*, 2010). The dissemination of clonal lineages can be caused by the movement of infected patients between different wards or hospitals whilst intercontinental spread is mainly thought to occur via air travel (Dijkshoorn *et al.*, 2007).

Global epidemiological characterisation of MDR *A. baumannii* is required to help provide insight into the prevalence of epidemic lineages and resistance phenotypes as well as assist in predicting future treatment options. Various typing methods have been utilised to investigate *A. baumannii* outbreaks, offering varying levels of discrimination (Zarrilli *et al.*, 2013). Generally, typing methods are chosen based on the nature of the investigation, for example, pulsed-field gel electrophoresis (PFGE) is currently the favoured method for the assessment of outbreaks (Adams-Haduch *et al.*, 2011), whilst repetitive element palindromic PCR (Rep-PCR, Diversilab) is suited for analysis of a large number of isolates (Higgins *et al.*, 2010). However, issues in result reproducibility and dissemination of data to other hospitals/laboratories are common limitations (Higgins *et al.*, 2012). Multi-locus sequence typing (MLST) is considered the best option for population structure investigations (Maiden *et al.*, 1998; Urwin and Maiden, 2003), however this method offers poor resolution when assessing outbreaks as it cannot discern person-to-person spread (Pérez-Losada *et al.*, 2013).

Decreasing costs associated with whole genome sequencing (WGS) have enabled clonal typing of hospital-acquired bacterial pathogens utilising this technique more popular (Eyre *et al.*, 2012; Turabelidze *et al.*, 2013; Ruppitsch *et al.*, 2015). Despite generating more robust data to that of MLST and PFGE typing schemes, which generally only assess a small number of housekeeping genes, limitations in the ability to analyse the large data set is a common drawback (Fricke and Rasko, 2014; Schurch *et al.*, 2018).

Recently, a core genome MLST scheme using WGS was generated for *A. baumannii* (Higgins *et al.*, 2017). By defining the core genome using well-characterised reference strains, the scheme could discriminate between IC types and identify separate outbreaks with good precision. Furthermore, the authors adopted a standardised nomenclature which will support inter-laboratory exchange and comparison of generated data.

1.3.2 Community-acquired infections

Although rare, community-acquired *A. baumannii* infections have also been reported, where typing analyses have identified these isolates represent a distinct lineage to *Acinetobacter* infections acquired from health care-associated environments (Eveillard *et al.*, 2013). Cases predominantly occur in sub-tropical and tropical environments, including Northern Australia and South East Asia (Dexter *et al.*, 2015). Thus far, community-acquired infections are often highly susceptible to antibiotic treatment and tend to be associated with individuals whom have underlying co-morbidities, including alcoholism, chronic lung disease, diabetes mellitus and cancer (Dexter *et al.*, 2015). *A. baumannii* has been also isolated from infected wounds of military personnel and civilians in war zones (Davis *et al.*, 2005; Scott *et al.*, 2007) and from survivors of natural disasters (Oncul *et al.*, 2002; Uckay *et al.*, 2008; Wang *et al.*, 2010). A study from the National Naval Medical Centre (U.S.) on post war wounds in American troops from Iraq and Afghanistan elucidated that *A. baumannii* was the most prevalent bacterial organism, accounting for 63% of all isolates identified (Eveillard *et al.*, 2013). Similarly, *A. baumannii* was also the leading cause of bacterial infection from victims of the Bali bombing (~65%) that were admitted to Perth Royal hospital in Australia (Heath *et al.*, 2003). Although these types of *A. baumannii* infections are largely seen as sporadic and oftendeemed as individual events, high mortality rates of 40-60% have been correlated with community-acquired pneumonia, underscoring its clinical impact (Leung *et al.*, 2006).

1.4 Characteristics of *A. baumannii* that contribute to pathogenicity and virulence

A. baumannii strains have a number of characteristics that contribute to their pathogenicity. These factors include: its ability to adhere to abiotic and biotic surfaces (Eijkelkamp *et al.*, 2011b); production of capsular polysaccharide (Russo *et al.*, 2010); the ability to scavenge iron from iron-restricted environments (Eijkelkamp *et al.*, 2011a); and the ability to rapidly acquire resistance to antimicrobials, via horizontal gene

transfer (HGT), homologous recombination (Snitkin *et al.*, 2011) or DNA damage-inducible responses (Norton *et al.*, 2013).

As mentioned earlier, *A. baumannii* causes a broad range of disease states, however, unlike for other bacterial pathogens, the disease progression cycle is not well defined. Through advancements in WGS and the application of mutagenesis, crucial factors contributing to *A. baumannii* pathogenicity have been identified revealing its ability to persist in the environment, evade antibiotic treatments and interact with host cells, as reviewed in (Weber *et al.*, 2015a; Lee *et al.*, 2017; Harding *et al.*, 2018). Some of the best-studied examples will be discussed in greater detail below.

1.4.1 Formation of biofilms and pellicles

Biofilms are defined as a structured community of microorganisms encased in an extracellular polymeric matrix, comprised of exopolysaccharides, proteins and/ or extracellular DNA (López *et al.*, 2010). The matrix is imperative for adhesion to biotic and abiotic surfaces and maintenance of a cohesive structure and has been found to enhance motility, promote cell-to-cell signalling and HGT between bacteria (Dragoš and Kovács, 2017). Switching to this sessile lifestyle occurs in response to different environmental cues, with cells displaying distinct physiological and behavioural differences compared to their planktonic counterparts (Moreno-Paz *et al.*, 2010).

The vast majority of *A. baumannii* isolates can form biofilms on inanimate surfaces including medical-associated devices, such as endotracheal tubing and intravascular catheters (Greene *et al.*, 2016). Similar to other bacteria, *A. baumannii* cells encased within a biofilm display increased tolerance to various stressors, promoting persistence within host niches and clinical environments, thus providing sources for recurrent infections and reservoirs of transmission, respectively (Eze *et al.*, 2018). Within the *A. baumannii* genome, genes coding for cell surface structures that contribute to biofilm production and maintenance include the outer membrane porin OmpA (Section 1.4.2), the CsuA/BABCDE pilus chaperone-usher assembly system (Tomaras *et al.*, 2003; Gaddy *et al.*, 2009) (Section 1.4.3), and other putative chaperone-usher pili systems (Martí *et al.*, 2011a; Eijkelkamp *et al.*, 2014; Álvarez-Fraga *et al.*, 2016). Similar to the biofilm-associated protein (Bap) originally identified in the Gram-positive pathogen, *Staphylococcus aureus* (Cucarella *et al.*, 2001), the *A. baumannii* homologue (Bap_{Ab}) is also important in biofilm formation (Loehfelm *et al.*, 2008). Bap_{Ab} is a large surface-exposed protein that is exported via a type I secretion system (Harding *et al.*, 2017) and

is implicated in biovolume and intercellular adhesion of mature biofilms across *A. baumannii* isolates (Goh *et al.*, 2013). Additional Bap-like proteins have been identified with their deletion resulting in similar biofilm defects as described for Bap_{Ab} deletion derivatives (De Gregorio *et al.*, 2015). Protein *O*-glycosylation mediated via a bifurcated pathway involving capsular polysaccharide synthesis (Section 1.4.6) was also found to be critical for biofilm formation (Iwashkiw *et al.*, 2012). Inactivation of the *O*-oligosaccharyltransferase, *pglL*, affected initial attachment as well as biofilm density and maturation, in both static and flow cell models. Deletion of the initiating transferase, *pglC*, involved in both protein *O*-glycosylation and capsule production led to an irregular biofilm structure but did not affect biofilm biomass (Lees-Miller *et al.*, 2013). Like other bacterial sp., such as *Escherichia coli* (Wang *et al.*, 2004), production of the polysaccharide poly- β -(1-6)-*N*-acetylglucosamine (PNAG), was shown to be critical for *A. baumannii* biofilm formation, as deletion of the *pgaABCD* gene cluster abolished biofilm mass (Choi *et al.*, 2009). Antibodies raised against PNAG eliminated *A. baumannii* cells in opsonophagocytic assays and led to reduced bacterial loads in murine models, signifying the potential of PNAG as a possible vaccine target (Bentancor *et al.*, 2012).

A specific type of biofilm occurring at the air-liquid interface is defined as a pellicle. Due to the absence of solid substrata, pellicles require a higher level of organisation, generating more complex structures than biofilms formed at the solid-liquid interface (Branda *et al.*, 2005). A select number of *Acinetobacter* sp. can produce pellicles, with a greater frequency identified across pathogenic sp. including *A. baumannii* and *A. nosocomialis* (Martí *et al.*, 2011b). Pellicles are more prominent from cells incubated at room temperature compared to cells incubated at 37°C, supporting a defined role as an abiotic persistence strategy (Martí *et al.*, 2011b). To identify proteins involved in pellicle biogenesis, a proteomic analysis on 1- and 4-day pellicles were compared to that of their planktonic counterparts, revealing 620 differentially expressed proteins (Kentache *et al.*, 2017). This supported findings described by Marti *et al.*, (2011) who showed this sessile mode of growth increased expression of virulence factors, including iron uptake systems, outer membrane porins and adhesion factors, widening their involvement in not only abiotic persistence but also as a potential virulence associated strategy. Another factor involved in pellicle formation, the histone-like nucleoid-structuring protein (H-NS), was identified through insertional inactivation of the *hns* gene in *A. baumannii* ATCC 17978 (Eijkelkamp *et al.*, 2013). A further study using random transposon (Tn) mutagenesis on

the same *hns* mutant derivative identified that disruptions located within genes directly involved in secondary metabolite homeostasis abolished pellicle formation (Giles *et al.*, 2015). Examination of pellicle matrices from three representative *A. baumannii* strains harbouring different morphological pellicles were found to be comprised of a diverse set of extracellular polymeric substances (Nait Chabane *et al.*, 2014). Collectively, these findings show that biofilm and pellicle formation by *A. baumannii* is a multistep process involving several cellular structures and functions and is an important persistence determinant of this organism.

1.4.2 Outer membrane protein A

The most abundant protein of the *A. baumannii* outer membrane is OmpA (termed OmpA_{Ab}) a 38 kDa β -barrel trimeric porin belonging to the OmpA-like family of proteins (Sugawara and Nikaido, 2012). OmpA_{Ab} is involved in biofilm formation (Gaddy *et al.*, 2009; Cabral *et al.*, 2011) and adherence to and subsequent invasion of host epithelia (Choi *et al.*, 2008b; Gaddy *et al.*, 2009). Upon entry into epithelial cells, OmpA_{Ab} was found to localise in the mitochondria and nucleus, leading to the induction of host inflammatory responses and apoptosis (Choi *et al.*, 2005; Choi *et al.*, 2008a; Lee *et al.*, 2010b). OmpA_{Ab}-dependent disruption of cells forming the mucosal lining allows penetration and invasion into deeper tissues and thus is considered important during the early stages of infection. Using a murine pneumonia infection model, an *A. baumannii* *ompA_{Ab}* deletion derivative displayed significantly reduced bacterial loads and failed to efficiently disseminate from the lungs to the bloodstream (Choi *et al.*, 2008b). Results from transposon (Tn) insertion site sequencing experiments further underscored the importance of OmpA_{Ab}, where derivatives harbouring insertional disruptions in this gene led to an approximate 6-fold reduction in persistence within murine lungs (Wang *et al.*, 2014). The porin also plays an important role in host immune evasion, as OmpA_{Ab} was found to directly bind to the complement regulator, factor H, masking cells from complement attack (Kim *et al.*, 2009).

1.4.3 Chaperone-usher pili

Pili are filamentous surface appendages composed of protein subunits called pilins or fimbrins and range between 1-2 micrometres in length. They have a ubiquitous presence on the outer surface of Gram-negative bacteria and are known to act as tethers mediating bacterial adhesion to biotic and abiotic surfaces (Pratt and Kolter, 1998; Spaulding *et al.*, 2018). Four types of assembly pathways for bacterial pili are currently known; extracellular nucleation-precipitation pathway (curli pili), alternate chaperone pathway

(CS1 pili), general secretion pathway (type IV pili) and the chaperone-usher pathway (including P and type I pili) (Gohl *et al.*, 2006). Of these classes, the chaperone-usher pili are the best characterised. Comparative analyses of eight *A. baumannii* genomes from various clonal groups identified four gene clusters encoding various chaperone-usher type pili systems, namely, A1S_1507-1510 (fimbriae cluster), A1S_2088-2091 and A1S_2213-2218 (Csu-cluster) in ATCC 17978, and the AB57_2003-2007 (P pili cluster) in *A. baumannii* AB0057 (Eijkelkamp *et al.*, 2014).

The Csu cluster encodes the CsuA/ABCDE proteins and belongs to the archaic family of chaperone-usher systems (Pakharukova *et al.*, 2015). The CsuA/B, CsuA and CsuB proteins are pilin subunits that are translocated to the outer membrane by the CsuC chaperone. The CsuA/B, CsuA and CsuB monomers are polymerised by the CsuD usher protein, generating the pilin fibre. The CsuE tip adhesion and the minor pilins CsuA and CsuB are involved in pilin polymerisation. This cluster is well conserved and found in the majority of sequenced *A. baumannii* clinical isolates (Moriel *et al.*, 2013). Using an X-ray structure of the *A. baumannii* CsuC-CsuE chaperone–adhesin preassembly complex, the mechanism for cell attachment to inanimate surfaces was recently defined (Pakharukova *et al.*, 2018). This revealed that CsuE exposes three highly hydrophobic flexible finger-like loops at the tip of the pilus, mutation of which drastically reduced attachment and biofilm formation on plastic surfaces. This study also strengthens previous work implicating the limited involvement of Csu pili in attachment to biotic surfaces such as host cells (de Breij *et al.*, 2009).

Several regulatory proteins and environmental conditions can influence expression of chaperone-usher pili systems in *A. baumannii*. For instance, inactivation of the response regulator (RR) component (*bfmR*) of the two component signal transduction system (TCS) BfmRS, abolished *csu* expression, resulting in loss of Csu pili production, adhesive properties, and biofilm formation on plastic (Tomaras *et al.*, 2008) (Section 1.6.1.7.4). Furthermore, sub-inhibitory concentrations of two anti-folate antibiotics used for maintenance of the pAB3 plasmid in ATCC 17978 cells repressed *csuA/B* expression, defining a link between pilus expression and folate metabolism (Moon *et al.*, 2017). The same study also identified putative riboswitches in the *csu* promoter region and upstream from the *bfmRS* operon, postulating that these genes may be altered by mRNA secondary structures and are co-ordinately regulated. However, further experimental evidence is required to delineate if any such links exist.

An investigation into genes prone to genetic variation during host infection and treatment revealed the *csu* region as a significant mutational hotspot (Wright *et al.*, 2017a). Differential effects were observed, where expression of *csu* was both increased and decreased compared to the isogenic isolates from various patients (Wright *et al.*, 2017a). Furthermore, previous work examining the location of insertion sequences (IS) within over 1,000 *A. baumannii* genomes found that the genetic region harbouring the *csu* gene cluster (~5 kilobase [kb]) had over 90 independent insertion events, which was estimated to be three times greater than any other 5 kb genomic region (Wright *et al.*, 2016). Taken together, these studies suggest that the Csu cluster is under significant selection and despite a key role in *A. baumannii* virulence, expression of these proteins under certain conditions may be unfavourable.

Recently, a putative type I chaperone/usher pilus assembly system in *A. baumannii* was functionally characterised (Wood *et al.*, 2018). Expression of the gene cluster was upregulated in cells cultured in darkness at 24°C through a mechanism dependent on the photoreceptor, BlsA (Mussi *et al.*, 2010). Disruption of the pilin A subunit, significantly reduced surface-associated motility and pellicle formation whilst biofilm formation on plastic was increased when cultured under dark conditions. Given these findings, this gene cluster was named the *photo-regulated pilus ABCD (prpABCD)* operon. Furthermore, inactivation of *prpA* significantly reduced virulence *in vivo*, highlighting its importance in the pathogenic potential of *A. baumannii*.

1.4.4 Motility

Bacteria belonging to the *Acinetobacter* sp. were traditionally known as non-motile. This is illustrated by the word ‘*Acinetobacter*’ which is derived from the Greek language, translating to ‘non-motile rod’. The non-motile phenotype was categorised by the inability of the bacterium to actively migrate through liquid medium, predominately due to the absence of flagella (Baumann, 1968). However, since this initial observation, two forms of *A. baumannii* locomotion have been described, namely, twitching and surface-associated motility.

Twitching motility is a well-characterised type of bacterial motility, and according to Semmler *et al.*, (1999) is defined as migration of bacteria within the surface/plastic interface of solid agar (Semmler *et al.*, 1999). This form of movement works through a ‘pulling’ mechanism, using extension and retraction for forward orientated migration. In *Acinetobacter* several studies have confirmed links between twitching and a functional

type IV pili system (Clemmer *et al.*, 2011; Harding *et al.*, 2013; Wilharm *et al.*, 2013; Leong *et al.*, 2017). Twitching motility has been shown to be the most prevalent form of motility found in IC 1 isolates (Eijkelkamp *et al.*, 2011b).

Surface-associated motility occurs at the interface of growth medium and air. The earliest description of surface-associated motility was published in the mid 1980's, where the phenomenon was thought to be intimately linked to twitching motility (Henrichsen, 1984). A number of factors are critical in *A. baumannii* surface-associated motility, including quorum sensing (Clemmer *et al.*, 2011), production of lipooligosaccharide (LOS) (McQueary *et al.*, 2012), the compound 1,3-diaminopropane (Skiebe *et al.*, 2012), iron availability in the growth medium (Eijkelkamp *et al.*, 2011a) and a functioning type II N6-adenine DNA methyltransferase (Blaschke *et al.*, 2018). Interestingly, the presence of blue light at 24°C inhibited motility in ATCC 17978 cells through the action of the BlsA protein (Mussi *et al.*, 2010). This protein contains blue-light-sensing domains found to be responsible for the observed phenotype, as when cultured under blue light, motility was restored in a $\Delta blsA$ derivative to levels similar to those obtained under dark conditions (Mussi *et al.*, 2010). Interestingly, this phenomenon was not paralleled at 37°C, inferring *blsA* expression is temperature responsive. Impaired surface-associated motility phenotypes have been identified across spontaneous rifampicin mutants derived from amino acid (aa) substitutions in the β subunit of the bacterial RpoB RNA polymerase (Pérez-Varela *et al.*, 2017). Using RNA transcriptomics six genes were found to be down-regulated across two $\Delta rpoB$ derivatives, including transporters and metabolic enzymes. Deletion of four of the six genes led to defective surface associated motility phenotypes and reduced virulence in an *in vivo* nematode model in both poor- and hyper-biofilm producing *A. baumannii* backgrounds. This is thought to be the first example linking virulence and surface-associated motility in *A. baumannii*.

Several studies have demonstrated conflicting results/conclusions in terms of motility phenotypes. For example, *A. nosocomialis* M2 (formally known as *A. baumannii* M2) mutants defective in type IV pili production could not display twitching motility and showed no impairment towards surface-associated motility (Harding *et al.*, 2013). These findings contrasted previous work by Wilharm *et al.*, (2013) who showed that in the same strain type IV pili retraction mutants did in fact impair surface-associated motility (Wilharm *et al.*, 2013). Furthermore, in *A. baumannii* isolates, surface-associated motility was reported to only occur in non-clonal lineages (Eijkelkamp *et al.*, 2011b), however, this has not been supported across other studies (Skiebe *et al.*, 2012). It has been

postulated that recently identified phase-variant phenotypes or conditions used to test for motility (nutrient content and type of solidifying matrix, respectively) could contribute to the reported inconsistencies (Tipton *et al.*, 2015).

1.4.5 Desiccation tolerance

Desiccation tolerance is defined as the ability to maintain viability under dry conditions. In *A. baumannii*, resistance to desiccating conditions greatly varies across strains with viability of some strains exceeding 100 days (Jawad *et al.*, 1998; Catalano *et al.*, 1999; Antunes *et al.*, 2011a; Farrow *et al.*, 2018). Desiccation reduces the free water content in cells, leading to drastic changes at molecular, structural and physiological levels.

Structural configurations of the outer membrane (Boll *et al.*, 2015), presence of capsular polysaccharide (Ophir and Gutnick, 1994), and production of a biofilm (Espinal *et al.*, 2012), are contributing factors that affect the level of desiccation tolerance afforded by *Acinetobacter* sp.. Deletion of a lipid A acyltransferase involved in production of underacylated LOS significantly reduced desiccation survival in human serum and rich growth media (Boll *et al.*, 2015). It was hypothesised that variations in outer membrane fluidity resulting from perturbations in the lipid composition of this deletion derivative facilitated lethal leakage of water and vital nutrients out of the cell. Exopolysaccharides such as capsule (Section 1.4.6) are proposed to protect against desiccation by holding a reservoir of water in the immediate microenvironment which can be readily lost with negligible effects on the internal water potential (Roberson and Firestone, 1992). Clinical *A. baumannii* isolates forming robust biofilms displayed increased survival under desiccating conditions compared to non-biofilm forming strains (Espinal *et al.*, 2012). As biofilms are encased in a polymeric matrix, this observation further supports the hypothesis that extracellular polysaccharides can act as a buffer, increasing protection from desiccative conditions.

Desiccation tolerance in bacteria is also linked to the ability to limit protein oxidation and DNA damage. Proteomic analysis of desiccation-stressed *A. baumannii* AbH12O-A2 cells revealed increased expression of proteins involved in DNA repair and detoxification of reactive oxygen species (ROS) (Gayoso *et al.*, 2014). The presence of RecA, a protein involved in homologous recombination/repair and activation of the ‘SOS response’ upon DNA damage, was critical in *A. baumannii* desiccation survival (Aranda *et al.*, 2011). Furthermore, *recA* expression was required for the generation of rifampicin resistant

isolates via *rpoB* mutations after desiccation stress, concluding that this unfavourable condition can induce mutations that fortuitously lead to a MDR phenotype (Norton *et al.*, 2013). Proteins, phospholipids and nucleic acids are more prone to oxidation during desiccation because of increased solute concentrations and ROS within cells (Potts, 1994). Similar to other bacterial sp., a number of proteins involved in neutralising ROS were upregulated during desiccation stress, including superoxide dismutase, glutathione peroxidase and catalase enzymes (Gayoso *et al.*, 2014). Given the highly plastic nature of *A. baumannii*, whether any of the differentially expressed proteins identified within the study were altered by means of mobile genetic elements (MGEs) such as ISs was not analysed. Recently, the KatE catalase enzyme known to detoxify hydrogen peroxide was found to be essential in desiccation resistance of *A. baumannii* ATCC 17961, with its expression controlled by the BfmRS TCS (Farrow *et al.*, 2018) (Section 1.6.1.7.4).

1.4.6 Capsular polysaccharide

Like other human pathogens, *A. baumannii* possess a capsule that surrounds the bacterial cell surface. This capsule is composed of polysaccharide repeat units and is defined as a key virulence determinant (Russo *et al.*, 2010). Currently, over 100 distinct capsule types have been identified across *A. baumannii* isolates, which are all generated via the Wzx/Wzy-dependent pathway (Shashkov *et al.*, 2017). Capsule types vary extensively in their chemical structure due to differences in genetic content at the chromosomal capsular biosynthesis locus (KL), a syntenic block harbouring genes required for capsule biosynthesis, assembly and export (Hu *et al.*, 2013). The chromosomal location of the KL is conserved across the majority of *A. baumannii* strains (between the *fkpA* and *lldP* genes) and generally ranges between ~20-35 kb, where the length of this region is reflective on the capsule type produced (Kenyon and Hall, 2013). However, production of some capsules require additional genes that are distal from the KL region (Kenyon and Hall, 2013; Kenyon *et al.*, 2016).

Due to the utilisation of a shared pathway, *Acinetobacter* sp. generate capsular polysaccharide repeating units that are identical to carbohydrate structures attached to glycoproteins (Lees-Miller *et al.*, 2013). The first step in this bifurcated pathway involves the initiating glycosyltransferase, ItrA, that transfers the first sugar of the repeating carbohydrate to a lipid carrier, followed by addition of subsequent sugars by glycosyltransferase enzymes to the growing unit (Hug and Feldman, 2011). The integral membrane protein Wzx flips the sugar repeat unit into the periplasm and is the last step before the divergence of capsule and protein glycosylation pathways. Capsule production

involves polymerisation of individual sugar repeat units before being exported to the outer membrane whereas for protein glycosylation, this single repeat unit is attached to selected outer membrane proteins via the PglL *O*-oligosaccharyltransferase (Iwashiki *et al.*, 2012).

A number of studies have identified that capsule is a significant contributor in *A. baumannii* virulence. For example, a number of acapsular derivatives from multiple *A. baumannii* strains display alterations in antimicrobial resistance profiles as well as decreased survival in human serum, ascites fluid and infection models (Russo *et al.*, 2010; Umland *et al.*, 2012; Lees-Miller *et al.*, 2013; Geisinger and Isberg, 2015; Sanchez-Larrayoz *et al.*, 2017). Furthermore, up-regulation of capsule production increased serum resistance *in vitro* and virulence *in vivo* (Geisinger and Isberg, 2015). Capsule has also been linked with other virulence-associated attributes such as motility (McQueary *et al.*, 2012) and biofilm formation (Umland *et al.*, 2012; Lees-Miller *et al.*, 2013). Recently, a novel link between the phase-variable phenotype of *A. baumannii* strain AB5075 and capsule production was revealed, with the more virulent opaque variant producing a 50% thicker capsule layer than their translucent counterparts (Chin *et al.*, 2018). Further assessment utilising a mutant derivative from an opaque background that could no longer export capsule to the outer membrane revealed impaired survival when subjected to lysozyme, disinfectants and desiccating conditions compared to the WT parent (Tipton *et al.*, 2018). Additionally, the presence of capsule was required for full virulence, as the capsule deficient mutant derivative displayed an eight log-fold reduction in survival compared to WT cells.

1.4.7 Type VI secretion system

To assist in inter- and intra-bacterial competition or to elicit responses in eukaryotic cells, some Gram-negative bacterial sp., including *A. baumannii*, excrete protein toxins through specialised molecular machinery via type VI secretion system (T6SS) (Bingle *et al.*, 2008). T6SS consist of three distinct substructures; the baseplate, the membrane complex and the sheath-tube complex, which once assembled is anchored to the cell envelope where contraction of the sheath ejects effector molecules across the membrane (Zoued *et al.*, 2014; Chang *et al.*, 2017). Proteins excreted by T6SS, known as effector molecules, are sp. or strain specific and are delivered into the extracellular space or prey cells as cargo of T6SS needle proteins (VgrG/Hcp/PAAR) or as translation fusions with these proteins (Durand *et al.*, 2014). The vast majority of effector proteins display anti-bacterial properties, whilst some also possess anti-host properties (Jamet and Nassif,

2015; Cianfanelli *et al.*, 2016). Known T6SS effector proteins include; phospholipases, lipases, DNases, RNases and peptidoglycan hydrolases, all of which display differing effectiveness of cell lysis (Durand *et al.*, 2014). To prevent self- or sibling-intoxication, T6SS effectors are co-expressed with an immunity protein, which neutralises their cognate antibacterial effectors (Jamet and Nassif, 2015).

Various research groups have described the genetic organisation and activity of T6SS in *Acinetobacter* sp. including *A. baumannii* (Weber *et al.*, 2013; Repizo *et al.*, 2015; Weber *et al.*, 2015b; Weber *et al.*, 2016; Fitzsimons *et al.*, 2018; Wang *et al.*, 2018), *A. nosocomialis* (Carruthers *et al.*, 2013) and *A. baylyi* (Ringel *et al.*, 2017). Functional analyses of *A. baumannii* isolates harbouring an active T6SS have been found to ‘out-compete’ laboratory *E. coli* strains as well as other *Acinetobacter* strains (Repizo *et al.*, 2015; Weber *et al.*, 2015b; Weber *et al.*, 2016; Fitzsimons *et al.*, 2018). Furthermore, the active T6SS from *A. baumannii* DSM30011 and Ab04 outcompeted *Pseudomonas aeruginosa* and *Klebsiella pneumoniae* strains, respectively, common competitors of clinical and host niches (Repizo *et al.*, 2015). The T6SS present in the naturally competent *A. baylyi* ADP1 strain produces five different effectors with varying lytic abilities (Ringel *et al.*, 2017). Interestingly, the level of DNA transfer from prey to predator correlated with the degree of prey cell lysis, inferring that lytic effectors play an integral role in T6SS-dependent HGT in naturally competent bacteria. These findings reveal a unique mechanism that may assist in the spread of resistance determinants across different bacterial sp. (Ringel *et al.*, 2017).

The regulatory mechanisms influencing T6SS expression and assembly vary across *A. baumannii* isolates. Some T6SS are constitutively expressed whilst others are repressed due to the action of regulatory proteins. For example, the presence of two TetR-type transcriptional regulators carried on a large conjugative plasmid repressed T6SS gene expression (Weber *et al.*, 2015b). Loss of this plasmid relieved T6SS repression and enabled effective killing of *E. coli* prey cells. Complementation of either regulator *in trans* decreased T6SS gene expression back to WT levels (Weber *et al.*, 2015b). The T6SS gene cluster in *A. baumannii* is rich in adenosine (A) and thiamine (T) nucleotides, and is thus thought to be acquired via HGT events. Given its AT-rich nature, the system has been found to also be under the regulatory control of H-NS, a transcriptional repressor that preferentially binds AT-rich DNA including genetic material acquired by HGT (Ali *et al.*, 2012). Transcriptome analyses of *hns*-inactivated variants from two distinct *A. baumannii* isolates identified a significant increase in T6SS gene expression compared

to their respective WT counterparts (Eijkelkamp *et al.*, 2013; Deveson Lucas *et al.*, 2018). However, differences in the inter- and intra-bacterial killing capabilities of these mutants were not investigated.

1.4.8 Micronutrient acquisition systems

A key requirement for survival, successful colonisation, and invasion of bacterial pathogens, is the ability to scavenge transition metals from their surrounding environment. Trace elements such as iron, zinc, and manganese play crucial roles in many processes involved in metabolism as well as virulence-associated traits such as motility and biofilm formation (Palmer and Skaar, 2016). As a result, competition to obtain micronutrients is continual, across both human host niches and inanimate surfaces. However, vertebrate hosts have developed a number of innate defence strategies to limit the availability of these metals to bacteria, a process now known as ‘nutritional immunity’ (Hood and Skaar, 2012).

1.4.8.1 *A. baumannii* iron scavenging mechanisms

Iron is required for many essential processes in bacteria and plays a relevant role in pathogenesis (Cassat and Skaar, 2013). *A. baumannii* is known to survive under iron-limiting conditions and combats iron deprivation by exploiting multiple acquisition strategies (Zimblér *et al.*, 2009; Antunes *et al.*, 2011b; Eijkelkamp *et al.*, 2011a). These include the FeoABC system, proteins embedded on the cell surface that directly bind and translocate Fe²⁺ iron or heme from the extracellular environment into cells (Cartron *et al.*, 2006). Deletion of either *feoA* or *feoB* significantly reduced survival of *A. baumannii* *in vivo* (Subashchandrabose *et al.*, 2016; Álvarez-Fraga *et al.*, 2018). However, the most effective iron scavenging mechanism is production of high-affinity iron chelating molecules termed siderophores. These molecules are secreted into the extracellular environment and are capable of capturing and solubilising free Fe³⁺. In some cases siderophores can even ‘steal’ from host proteins due to their higher affinity to the metal ion (Carrano and Raymond, 1979). Uptake of iron-loaded siderophores into the cell involves cell surface receptors and TonB-dependent transport systems (Miethke and Marahiel, 2007).

Multiple siderophore systems have been identified in the *A. baumannii* genome (Yamamoto *et al.*, 1994; Eijkelkamp *et al.*, 2011a; Proschak *et al.*, 2013; Penwell *et al.*, 2015), with acinetobactin being the most conserved across *A. baumannii* isolates. Genes encoding proteins involved in acinetobactin production are generally localised in a single

cluster (Antunes *et al.*, 2011b), however, some strains require production of additional proteins outside of this genetic region (Penwell *et al.*, 2012). Depending on extracellular pH levels, acinetobactin can isomerise into one of two forms, promoting iron sequestration capabilities across most of the pH spectra, conditions likely to be encountered throughout the infection process (Shapiro and Wencewicz, 2016). Acinetobactin is also required for full virulence in various infection models across a number of different strains, clearly underscoring its importance in *A. baumannii* pathogenesis (Gaddy *et al.*, 2012; Penwell *et al.*, 2012; Wang *et al.*, 2014).

1.4.8.2 *A. baumannii* zinc scavenging mechanisms

Zinc, the second most abundant transition metal cofactor, is essential for *A. baumannii* survival. Similar to iron, human and other mammalian hosts have developed sequestration mechanisms to reduce zinc accessibility to invading bacterial pathogens. One well studied example is calprotectin, a protein complex released from host neutrophils that is capable of chelating Zn^{2+} and Mn^{2+} ions (Damo *et al.*, 2013; Zackular *et al.*, 2015). During an *A. baumannii* infection, calprotectin is produced over the full infection period (Moore *et al.*, 2014). To circumvent host defences including calprotectin-mediated nutritional immunity, *A. baumannii* employs a high-affinity zinc-binding uptake system, named ZnuABC, to obtain zinc from the environment (Hood *et al.*, 2012) and is mandatory for full virulence in *A. baumannii*.

Recently, a putative cell wall-modifying enzyme, termed ZrlA, was found to play a key role in *A. baumannii* zinc sequestration from extracellular environments (Lonergan *et al.*, 2019). Expression of *zrlA* was previously found to be regulated by the zinc-uptake regulator and its expression significantly upregulated following exposure to calprotectin (Mortensen *et al.*, 2014). Deletion of *zrlA* led to impaired growth during zinc starvation and cells displayed an altered membrane composition including increased cell envelope permeability and aberrant peptidoglycan muropeptide levels. Furthermore, the absence of *zrlA* increased antibiotic efficacy compared to WT in *in vitro* and *in vivo* studies, highlighting its appeal as a novel therapeutic target.

1.4.9 Antimicrobial resistance mechanisms employed by *A. baumannii*

A key feature attributed to the pathogenic success of *A. baumannii* is its ability to rapidly acquire antimicrobial resistance. Epidemiological studies assessing the incidence of MDR isolates have revealed it is an increasing problem worldwide, with some now displaying pan-resistance (Nowak *et al.*, 2017). Multiple mechanisms combat the

presence and influx of foreign toxic compounds, including antibiotics, disinfectants and antiseptics, as well as host-derived defence molecules. Examples include; the production of antibiotic inactivating enzymes (Corvec *et al.*, 2003; Lin and Lan, 2014), target binding site modifications (Lopes and Amyes, 2013), permeability defects, and overproduction of multidrug efflux pumps (Vila *et al.*, 2007). The latter characteristic is one of the most widespread mechanisms facilitating multidrug resistance across nosocomial pathogens and is discussed in more detail.

1.4.9.1 Efflux mediated resistance

Drug efflux as a means of antibiotic resistance is achieved by membrane-localised proteins that can actively extrude antimicrobial compounds into the periplasm or to the extracellular environment thus preventing accumulation to toxic levels within the cell. Aside from expulsion of antibiotics (Kumar and Schweizer, 2005), membrane transport proteins are involved in other vital physiological roles including essential nutrient uptake, trafficking of quorum sensing molecules and extrusion of metabolic waste products and host-defence molecules (Kohler *et al.*, 2001; Piddock, 2006). Genes that encode efflux proteins can either be located on the chromosome or on MGEs such as plasmids.

Efflux proteins vary greatly in their substrate profile, with some specific for only one substrate or alternatively, have the capacity to expel an array of chemically and structurally diverse compounds. When a pump can provide resistance towards three or more different classes of antibiotics they are classified as multidrug efflux pumps. Based on their energy source, structural arrangement, and protein sequence homology, bacterial efflux proteins have been categorised into seven distinct families/superfamilies (Chitsaz and Brown, 2017), of these, six are present in the *A. baumannii* genome. These include the ATP-binding cassette (ABC) superfamily, the major facilitator superfamily (MFS), the multidrug and toxic compound extrusion family, the small multidrug resistance family, the resistance-nodulation-division (RND) family and the most recently identified proteobacterial antimicrobial compound efflux (PACE) protein superfamily (Hassan *et al.*, 2013) (Figure 1.1). As illustrated in Figure 1.1, these proteins are located within the cell membrane either as single component transporters, catalysing transport of substrates across the cytoplasmic membrane, or as a ternary complex, containing a membrane transporter, periplasmic fusion protein (MFP) and an outer membrane porin (OMP), capable of translocating substrates across both inner and outer membranes (Li and Nikaido, 2004).

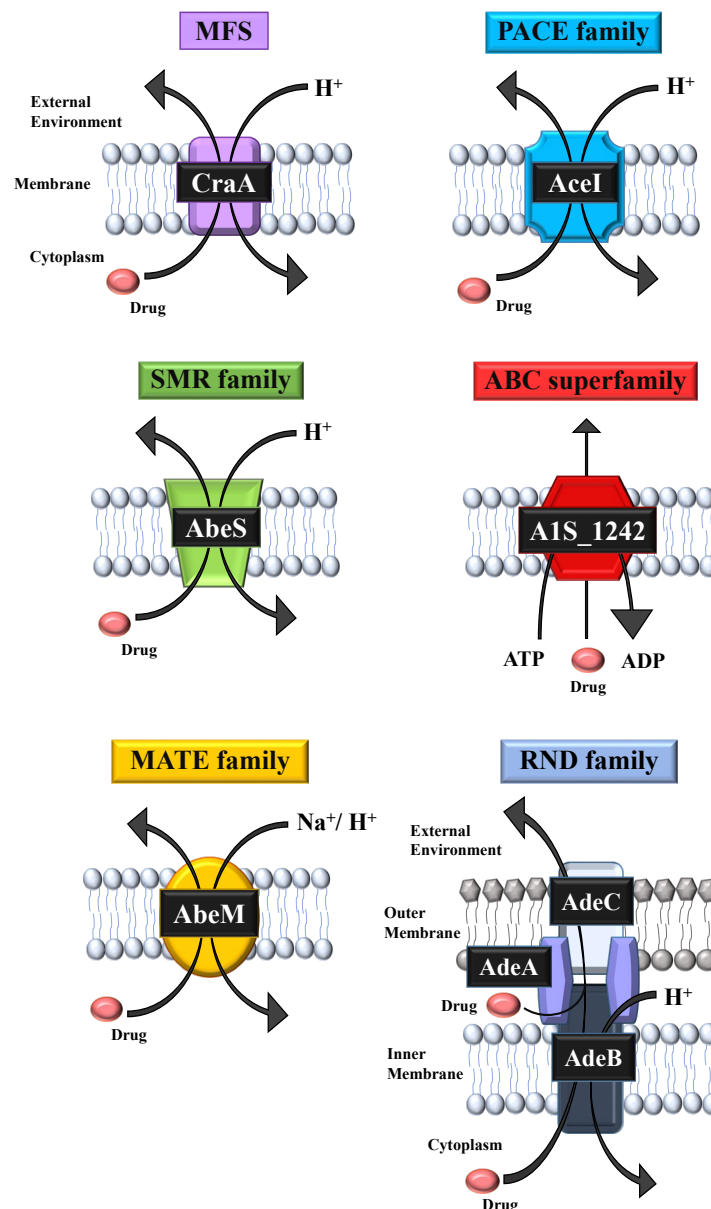


Figure 1.1: The six families of drug transporters with characterised systems from *A. baumannii* used as representatives

Transporter proteins are divided into six different families based on sequence identity and secondary structure prediction; major facilitator superfamily (MFS), small multidrug resistance (SMR), multidrug and toxic compound extrusion (MATE), proteobacterial antimicrobial compound efflux (PACE), ATP binding cassette (ABC), and resistance-nodulation-cell division (RND). These export system family members typically transport their substrates (red oval) across the inner membrane using either an ion gradient (H⁺ or Na⁺) or use ATP hydrolysis energy coupling mechanism. The RND protein complex is comprised of an inner membrane protein (AdeB), an outer membrane protein (AdeC) and a membrane fusion protein (AdeA), facilitating direct expulsion of substrates into the external environment. Figure modified from Sapula and Brown (2016).

The large majority of tripartite efflux systems are categorised into the RND superfamily and are predominately identified across Gram-negative bacteria (Nikaido, 2011). Efflux systems have been identified across a number of strains from *A. baumannii*, *A. baylyi*, *A. nosocomialis*, *A. pittii*, *A. radioresistens* and *A. oleivorans* sp., however, their overexpression in *A. baumannii* is most frequently associated with MDR phenotypes. Analysis of fully sequenced MDR *A. baumannii* isolates have identified a high number of putative drug efflux pumps (www.membranetransport.org). A large portion of these putative *A. baumannii* transporter proteins have been functionally assessed. These include: from the ABC family, an unnamed system at the A1S_1535 gene locus from ATCC 17978 (Li *et al.*, 2016a); the MFS family, AbaF (Sharma *et al.*, 2016), AedC (Hassan *et al.*, 2011), AedF (Hassan *et al.*, 2011), AmvA (Rajamohan *et al.*, 2010a), CraA (Roca *et al.*, 2009), Tet(A) (Ribera *et al.*, 2003), Tet(B) (Coyne *et al.*, 2011) and two unnamed MFS systems positioned at the A1S_2795 and ABAYE_0913 loci from ATCC 17978 and AYE isolates, respectively (Li *et al.*, 2016a); from the SMR family, AbeS (Srinivasan *et al.*, 2009); from the MATE family, AbeM (Su *et al.*, 2005), from the PACE family, AceI (Hassan *et al.*, 2013; Hassan *et al.*, 2015) and from the RND superfamily, AdeABC (Magnet *et al.*, 2001), AdeDE (Chau *et al.*, 2004) and AdeFGH (Coyne *et al.*, 2010) and AdeIJK (Damier-Piolle *et al.*, 2008), CAP01997, an EmrA homologue (Nowak-Zaleska *et al.*, 2016) and ArpAB (Tipton *et al.*, 2017). The two efflux systems most frequently linked to multidrug resistance in *A. baumannii* and directly associated with results presented in this thesis are described in further detail below.

1.4.9.1.1 *adeABC*

The AdeABC system abbreviated after *Acinetobacter* drug efflux belongs to the RND superfamily and was the first efflux pump to be characterised in *A. baumannii* (Magnet *et al.*, 2001). The *adeABC* operon encodes: a MFP, AdeA; the transporter, AdeB; and the OMP, AdeC. The *adeABC* genes are located directly downstream from the divergently transcribed *adeRS* TCS genes which exert tight regulatory control of the operon (Marchand *et al.*, 2004) (Section 1.6.1.7.1). AdeABC is suggested to play a minimal role in intrinsic resistance as an *adeB* mutant produced indistinguishable resistance patterns to an array of antimicrobial compounds to that of the parental strain (Yoon *et al.*, 2015). However, when AdeABC is overexpressed, the pump confers resistance to a wide range of compounds from multiple antibiotic classes, including the majority of β -lactams and aminoglycosides, fluoroquinolones, tetracyclines and tigecycline, the macrolides including lincosamides, and chloramphenicol.

Different variations of the *adeRS* and *adeABC* operons have been identified in clinical *A. baumannii* isolates. For example, in a set of 116 genotypically and geographically distinct clinical isolates, 80% harboured the *adeABC* genes whilst *adeC* was only detected in approximately 41% of isolates that had both *adeAB* and *adeRS* genes present (Nemec *et al.*, 2007). The latter finding infers that AdeC is dispensable for efflux and AdeAB may recruit another OMP to assist in formation of a functional tripartite complex. This proposition was confirmed experimentally by two independent studies demonstrating that the AdeK OMP from the AdeIJK pump complex could function with AdeAB leading to decreased susceptibility to various compounds (Sugawara and Nikaido, 2014; Leus *et al.*, 2018). Despite dissimilar substrate specificities, inactivation of AdeFGH, an additional RND pump present in *A. baumannii* (Coyne *et al.*, 2010) triggered overproduction of AdeAB in ATCC 17978 cells (Leus *et al.*, 2018). This finding indicates that activity of at least one of the two pumps is required for survival with authors postulating cross-regulation of the two operons, however, a clear mechanism is yet to be defined.

Phenotypic examination of a laboratory-induced isolate that overexpressed AdeABC found that this derivative had reduced biofilm formation and DNA uptake compared to WT cells (Yoon *et al.*, 2015). A further study using the same set of derivatives found overproduction of AdeABC significantly decreased fitness after intraperitoneal inoculation whilst minimal changes were observed after intranasal inoculation (Yoon *et al.*, 2016). Transmission of cells overproducing AdeABC via the latter route led to increased virulence and stimulated an enhanced neutrophil activation response in the lungs. These findings provide a plausible rationale for the frequent association of AdeABC overexpressed isolates as the causative agent of respiratory tract infections.

1.4.9.1.2 *adeIJK*

The *adeIJK* operon encodes AdeIJK, the second RND-type efflux pump discovered in *A. baumannii* (Damier-Piolle *et al.*, 2008). Unlike AdeABC, AdeIJK is present in all *A. baumannii* strains and is constitutively expressed, displaying a broad substrate profile (Damier-Piolle *et al.*, 2008; Rajamohan *et al.*, 2010b; Sugawara and Nikaido, 2014; Hassan *et al.*, 2016). The genes are co-transcribed in an operon and encode the AdeI membrane fusion protein, the AdeJ transporter, and the AdeK OMP, respectively. In *A. baumannii*, AdeIJK not only plays a role in antibiotic resistance but has been recently shown to be involved membrane maintenance and lipid homeostasis (Leus *et al.*, 2018; Jiang *et al.*, 2019), defining novel roles for this efflux system.

Expression of AdeIJK is negatively regulated by the AdeN TetR-type transcriptional repressor. The *adeN* locus is distally located to *adeIJK* and was found to be constitutively expressed but not self-regulated in *A. baumannii* BM4587 (Rosenfeld *et al.*, 2012). In addition to *A. baumannii*, AdeN homologues are present across various *Acinetobacter* sp. genomes including *A. calcoaceticus*, *A. nosocomialis* and *A. pittii* (Rosenfeld *et al.*, 2012). A number of studies have shown AdeN as a mutational hotspot in clinical *A. baumannii* isolates (Fernando *et al.*, 2014; Saranathan *et al.*, 2017; Gerson *et al.*, 2018). Inactivation of *adeN* results in over-expression of *adeIJK*, providing increased resistance to AdeIJK substrates (Rosenfeld *et al.*, 2012; Fernando *et al.*, 2014; Saranathan *et al.*, 2017) and reduced biofilm formation and DNA uptake, similar to an AdeABC overexpressed derivative (Yoon *et al.*, 2015; Saranathan *et al.*, 2017). Furthermore, an *adeN* deletion derivative was more virulent in a *Galleria mellonella* infection model compared to WT cells (Yoon *et al.*, 2015; Saranathan *et al.*, 2017), underscoring its role as an important regulator involved in *A. baumannii* pathogenesis.

1.5 Evolution of *A. baumannii* virulence by mobile genetic elements

The transfer of genetic information is a widespread phenomenon and a key facilitator in bacterial genome evolution. These processes are often driven by environmental selection pressures, where the scale of such changes can vary greatly. Small alterations can occur by errors during DNA replication or DNA damage repair, often leading to single nucleotide polymorphisms (SNPs) or insertion/deletion events. Larger changes can be generated by genetic recombination, where homologous DNA segments are exchanged, or acquisition of foreign DNA via HGT. Several different MGEs exist in bacteria, including; ISs, Tns, integrons, phage, genomic islands (GEIs), and plasmids, all of which can be acquired via HGT (Patel, 2016).

Since sequencing of the first *A. baumannii* genome in 2007 (Smith *et al.*, 2007), the number of *Acinetobacter* sequences and annotated genomes has increased at an exponential rate. As of August 2019, 3868 *A. baumannii* genome sequences and 374 plasmid sequences are accessible on the NCBI database (<http://www.ncbi.nlm.nih.gov>). The extensive repertoire of available sequences have facilitated robust comparative genomic analyses, identifying phylogenetic relationships and population structures of *Acinetobacter* sp. as well as tracking the origins and dissemination of numerous antimicrobial resistance and virulence determinants (Diancourt *et al.*, 2010; Eijkelkamp *et al.*, 2014; Adams *et al.*, 2016; Royer *et al.*, 2018).

Adding to the already formidable list of virulence determinants, many *Acinetobacter* sp. are well adapted for genetic exchange, and can be categorised into the unique collection of Gram-negative bacteria labelled “naturally transformable” (Barbe *et al.*, 2004; Vaneechoutte *et al.*, 2006; Ramirez *et al.*, 2010; Wilharm *et al.*, 2013). Clinical *A. baumannii* isolates are known to share a relatively small core genome with a diverse accessory genome (Imperi *et al.*, 2011; Farrugia *et al.*, 2013; Liu *et al.*, 2014). Aside from natural competence mechanisms (Wilharm *et al.*, 2013), accessory genes can be acquired by HGT, with an estimated 25-46% of genes (predominately encoding hypothetical proteins, Tns and ISs) being classified as unique to each *A. baumannii* strain (Adams *et al.*, 2008; Imperi *et al.*, 2011). The highly plastic nature of *A. baumannii* genomes has played a key role in their adaptation to strong selection pressures found within nosocomial and host environments, thus promoting their evolution toward multidrug-, extensively-drug and pan-resistant phenotypes (Wright *et al.*, 2017a).

1.5.1 Insertion sequence elements

ISs are defined as genetic entities capable of independent transposition facilitating movement to non-homologous loci within a genome (Vandecraen *et al.*, 2017). These ubiquitous sequences are small and compact, ranging between 700-2,500 base pairs (bp) in length. Generally, these elements contain one or two open reading frames (ORFs) which span the entire length of the IS and are most often flanked by short terminal inverted repeat sequences (TIRs) (Figure 1.2 A). The ORFs within ISs encode transposases which are imperative for their movement, and in some instances, also carry regulatory genes (Siguier *et al.*, 2014). The TIR sequences usually found at the ends of an element are used as recognition sites by the coding transposases, assisting in cleavage and excision of the genetic sequence, allowing the IS to translocate to a new location within a given genome. IS insertion in the host DNA often generates a staggered cut, and is repaired by host DNA polymerases and ligases, and thus the integration sequence becomes duplicated (Mahillon and Chandler, 1998). The length of these target site duplications (TSDs) are short (2-14 bp), specific for a given IS and act as useful markers for identification of recent transposition events.

ISs are prevalent in all domains of life, where in prokaryotes, it has been estimated that more than 4000 different ISs from 29 families currently exist (Siguier *et al.*, 2015). These elements are found in both chromosomes and plasmids, and are often associated with the mobilisation of genes, either by the formation of composite Tns or by carrying genes as passenger genes, known as ‘transporter ISs’ (Siguier *et al.*, 2015). Additionally, ISs can

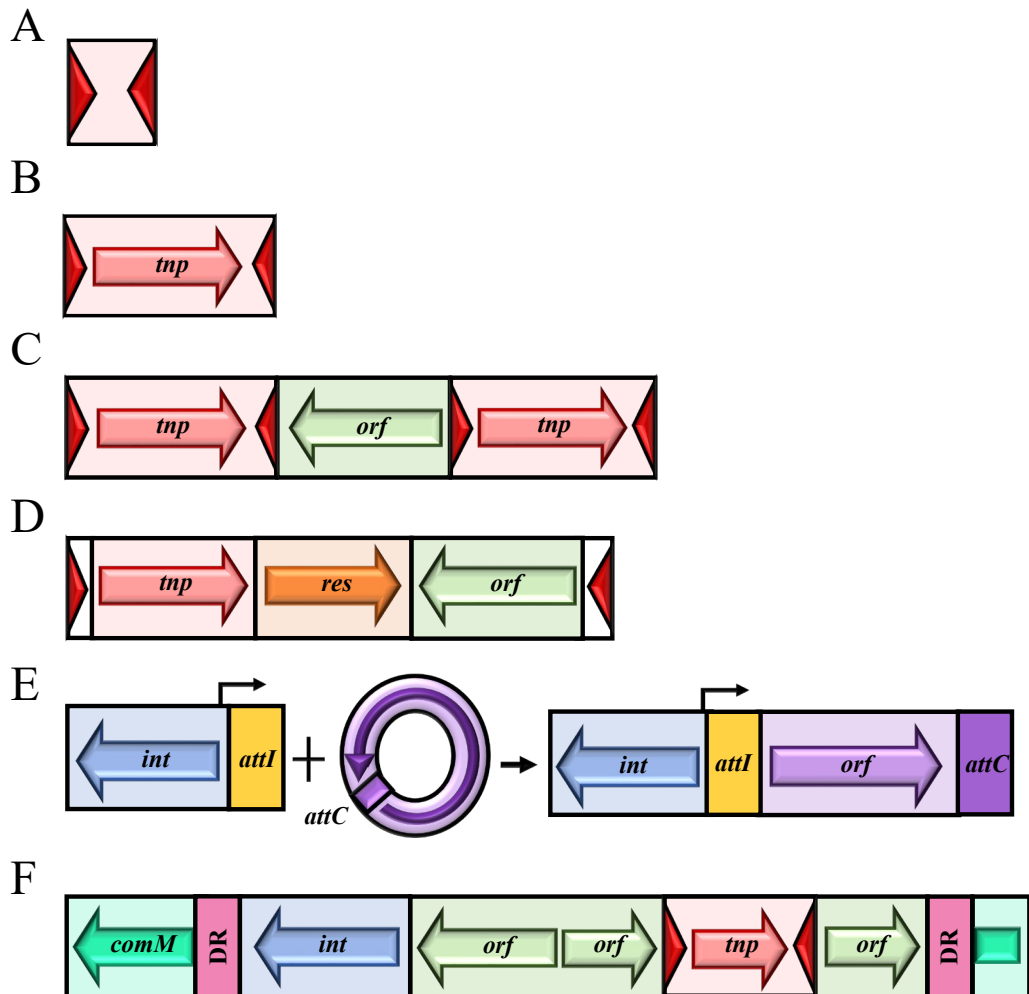


Figure 1.2: Mobile genetic elements found in bacteria

(A) A miniature inverted-repeat transposable element (MITE), comprised of two similar terminal inverted repeat (TIR; dark red triangles) sequences; these structures are AT-rich and generally do not contain coding sequences. **(B)** An insertion sequence (IS), generally containing a transposase gene (*tnp*; red arrow) flanked by TIR sequences. **(C and D)** The two different types of transposons (Tn) found in bacteria, composite and non-composite, respectively. Composite transposons contain genes/open reading frames (ORF; green arrow) that are flanked by ISs. Non-composite transposons are deemed more complex, requiring production of a transposase and resolvase (orange arrow) for transposition. ORFs can also be contained within these structures. **(E)** Integrons comprised of an integrase gene (*int*; blue arrow) and *attI* site (yellow box), capable of capturing gene cassettes (purple circle), which insert alongside the *attI* sequence. Gene cassettes contain a single promoter-less gene and a recombination site (generally *attC*) and in their free form, are circular and linearise upon integration (Collis and Hall, 1992). Expression of captured genes is facilitated by the promoter sequence located on the integron (black arrow), between *int* and *attI*. **(F)** An example of a genomic island. Genomic islands identified in *A. baumannii* are commonly located within the *comM* gene and generate direct repeat (DR) sequences upon insertion. Genomic islands usually carry integrase genes, as well as multiple ISs. Figure adapted from Hawkey (2017).

influence host gene expression as insertion into intragenic regions can often lead to gene inactivation or if integrated directly upstream of a gene can result in overexpression through the addition of outward-facing promoter sequences (Vandecraen *et al.*, 2017).

IS movement is generally seen when bacteria are placed under stressful conditions, with integration into new locations offering genomic variation, helping sp. like *A. baumannii* evolve new traits within relatively short timeframes (Wen *et al.*, 2014; Wright *et al.*, 2017b). The distribution of IS in *A. baumannii* genomes has been investigated, and over 5,000 different insertion sites for 29 IS were found across 976 *A. baumannii* genomes (Adams *et al.*, 2016). *A. baumannii* is one of the few bacterial sp. currently undergoing transient expansion of some IS families, with predictions estimating that up to ~3% of its genome is generated from IS, representing more than 100 IS copies per genome (Wright *et al.*, 2017b). The acquisition and movement of numerous IS is often associated with resistance and persistence mechanisms within *A. baumannii*.

1.5.1.1 IS mediated host adaptation

As previously mentioned, some ISs carry strong outward-facing promoter sequences or may also generate hybrid promoters upon insertion. Once integrated into a proximal area upstream of a gene, the element can facilitate over-expression of the downstream host gene or operon. This has been demonstrated for different ISs present in *A. baumannii*, namely IS*Aba1* and to a lesser extent, IS*Aba125* and IS*Aba825*, all of which have been associated with conferring clinically relevant levels of resistance towards routinely used as well as last line antimicrobial treatments (Lopes and Amyes, 2012). Due to the selective advantages they can provide to hospital-borne bacteria, a number of IS-activated antimicrobial resistance genes are frequently mobilised within different genetic contexts and disseminate across *Acinetobacter* sp. and other genera including to sp. from the *Enterobacteriaceae* family (Potron *et al.*, 2011; Hamidian and Hall, 2014; La *et al.*, 2014; Wright *et al.*, 2014; Zhang *et al.*, 2014; Krahn *et al.*, 2016; Nigro and Hall, 2016b). Gene inactivation by IS transposition has also had a significant influence shaping *A. baumannii* genomes. A number of studies have investigated how *A. baumannii* copes under various selective pressures, namely antimicrobial treatment, where pseudogene formation from IS integration has promoted increased survival, giving valuable insights into the mechanistic nature to how some resistance phenotypes can arise (Mussi *et al.*, 2005; Lee *et al.*, 2011; Moffatt *et al.*, 2011; Lopes *et al.*, 2012; Eijkelkamp *et al.*, 2013; Kim and Ko, 2015; Trebosc *et al.*, 2016; Saranathan *et al.*, 2017; Deveson Lucas *et al.*, 2018; Mirshekar *et al.*, 2018; Singkham-In and Chatsuwana, 2018).

ISs are also known to facilitate extensive DNA rearrangements and large scale gene loss (Siguier *et al.*, 2014). For example, when numerous copies of the same IS are present within a genome, they offer sites of homology, and recombination events can lead to deletion of the genetic material between two identical elements. An interesting trend in areas commonly subjected to deletion within *A. baumannii* have shown to favour regions carrying genetic loci that code for proteins that are exposed on the cell surface, and thus their deletion is suggested to provide a selective advantage by limiting detection by host defence molecules (Snitkin *et al.*, 2011; Wright *et al.*, 2014).

1.5.1.2 Regulation of IS transposition

A number of regulatory mechanisms facilitating bacterial IS transposition have been identified, where many are IS specific (Nagy and Chandler, 2004). For example, the frameshifting rate of some ISs can determine the transposition frequency of an element (Chandler and Fayet, 1993). IS*AbaI* harbours two genes between its TIR sequences and is present at a high frequency in a large number of *A. baumannii* genomes (Héritier *et al.*, 2006; Lopes and Amyes, 2012; Adams *et al.*, 2016). The element differs to the closely related IS1133-like elements by one nucleotide resulting in a frameshift, that leads to a truncated yet functional transposase and fusion of the two encoded ORFs (Héritier *et al.*, 2006). It has been speculated that this frameshift might contribute to the high abundance of this element across *A. baumannii* genomes, however, it was demonstrated that it was instead a mechanism that reduced transposition, as reversal of the frameshift increased transposition frequency by 1000-fold (Mugnier *et al.*, 2009).

Aside from element-specific regulatory mechanisms, several host factors have been shown to alter transposition of MGEs in bacteria, obstructing transposition at varying stages (Nagy and Chandler, 2004). Prokaryotic DNA chaperones have been associated with regulating IS transposition (Shiga *et al.*, 2001; Wardle *et al.*, 2005). Of these chaperones, the integration host factor (IHF) protein was required for transposition of some ISs present in enteric bacterial sp. (Sewitz *et al.*, 2003). A homologue of the *E. coli* IHF has been identified in *Acinetobacter* and is known to influence gene transcription in *Acinetobacter junii* (Krawczyk and Kur, 1998). It was also found to be essential for *A. baumannii* persistence within the lung (Wang *et al.*, 2014). Whether global regulators like IHF affect IS translocation in *A. baumannii* is yet to be examined.

Transposition frequency of ISs are also modulated by environmental pressures such as temperature (Ohtsubo *et al.*, 2005; Takahashi *et al.*, 2007). However, very little is known

about how transposition rates vary across different bacterial sp., the type of IS, or how different selective pressures may influence this process. To give more insight into these unknowns, an adapted method termed “IS-seq” was developed to track IS movement (Wright *et al.*, 2017b). Through exposure of *A. baumannii* cells to a selective condition (e.g., sub-minimum inhibitory concentration [MIC] levels of hydrogen peroxide), new IS insertions within a mixed cellular population were identified, classifying the type of IS and transposition frequency within the host genome. Furthermore, IS-seq could identify integration hotspots that may provide a selective advantage under the condition tested. This effective and economic approach to characterise the transposition potential of different IS is not restricted to *A. baumannii* but can be adopted for any bacterial sp..

1.5.2 Miniature inverted-repeat transposable elements

Miniature inverted-repeat transposable elements (MITEs) are defined as short, non-autonomous elements that contain truncated stretches of non-coding DNA (Delihias, 2011). These AT-rich elements are present in both prokaryotic and eukaryotic genomes and generally range between 50–400 bp in length. Similar to ISs, most MITEs also harbour TIR sequences at their terminal ends and generate TSDs upon insertion. As they do not code for a functional transposase, MITEs are proposed to be transposed *in trans* by co-resident ISs that can recognise their TIR sequences. This has been confirmed experimentally, where MITEs have been translocated by transposases *in vivo* in both prokaryote and eukaryote sp. (Poirel *et al.*, 2009; Yang *et al.*, 2009; Hancock *et al.*, 2010). MITEs can be categorised into two types (Type I or Type II); generated either by internal deletion of an IS/Tn or through convergence of two similar TIR sequences by random events, respectively (Brügger *et al.*, 2002).

Bacterial MITEs are predominantly located intergenically, but can also be found in intragenic regions of host chromosomes and plasmids (Ogata *et al.*, 2000; Delihias, 2007). A number of bacterial MITEs carry ORFs that fuse with host ORFs, which can alter their expression and/ or function. As mentioned, MITEs do not encode genes, making identification and tracking their evolution difficult. In order to overcome this drawback, many computational programs have been dedicated to aid in identification within prokaryotic and eukaryotic genomes such as ‘detectMITE’ (Ye *et al.*, 2016), MITE Uncovering sysTem (Chen *et al.*, 2009) and MITE Digger (Yang, 2013).

MITEs are multifaceted and can play diverse roles within their host genomes, mainly via influencing host gene expression. Their movement can result in disruption of genes,

where in some cases they can affect the virulence potential of the organism (Robertson *et al.*, 2004). Some MITEs have shown to harbour outward facing promoter sequences and thus also have the potential to alter gene expression levels (Siddique *et al.*, 2011). These elements can also alter messenger RNA (mRNA) stability, e.g. by providing cleavage sites for RNase proteins or affect post-translational processing of neighbouring genes, as seen in Correia elements of *Neisseria* (De Gregorio *et al.*, 2002; 2003; Enríquez *et al.*, 2010). Furthermore, they can promote large-scale genomic rearrangements (Brügger *et al.*, 2004) or offer hotspots for DNA recombination (Buisine *et al.*, 2002). Like ISs and Tns, MITEs can also formulate composite Tns, and thus have the potential to provide a selective advantage to their hosts. This has been demonstrated across *Pseudomonas putida* isolates, where two copies of the MITE, ARMphe, flank an operon that encode genes involved in phenol degradation (Peters *et al.*, 2004).

To date, two different MITEs have been identified in *Acinetobacter* sp. The first MITE was characterised in the prawn associated *Acinetobacter johnsonii* isolate, NFM2, where two identical copies of the 439 bp element flanked a Tn402-like class 1 integron (Gillings *et al.*, 2009). This arrangement formulated a composite Tn and was shown to be active due to the presence of five bp flanking TSDs. Since this initial identification by Gilling *et al.*, (2009), the same element has been found to flank similar Tn402-like class 1 integrons harbouring different gene cassette arrays in *Acinetobacter* sp., including within nosocomial *A. baumannii* isolates (Zong, 2014; Wibberg *et al.*, 2018). In addition to one other documented example (Poirel *et al.*, 2009), *Acinetobacter* is the only bacterial sp. where MITEs are known to flank and mobilise integrons.

The second MITE, MITE-297, was identified within conjugative plasmids from *A. baumannii* GC1 isolates (Hamidian *et al.*, 2016a). MITE-297 is 502 bp, which is typically larger than most prokaryotic MITEs. Its longer length was accounted for by the presence of an 102 aa protein of unknown function straddled between 26 bp TIRs. The element was proposed to have been generated from internal deletion of a Tn from the Tn6019/Tn6022 family (Hamidian and Hall, 2011). Two identical copies of MITE-297 flanked a 77.5 kb fragment within the large conjugative plasmid pA297-3, with 5 bp TSDs identified either side of the MITE-297 elements. The genetic material between the two MITE-297 copies harboured numerous IS and a *mer* module, capable of conferring mercury resistance. Several plasmids closely related to pA297-3 were also found to carry copies of MITE-297, differing by the genetic material located between the MITEs,

potentially resulting from deletions adjacent to identical ISs present in the sequence or by homologous recombination occurring at MITE-297 element (Hamidian and Hall, 2011).

1.5.3 Transposons

Tns are defined as linear segments of DNA (3-40 kb) which contain a transposase and TIR at each end and have the capacity to carry multiple genes. In bacteria, three different groups of Tns have been identified; composite, non-composite and Mu-type (Lupski, 1987; Kleckner, 1990). In *Acinetobacter*, composite Tns are the most frequently identified. Composite Tns are generally comprised of two ISs that express transposases at each end of the Tn that may or may not be identical (Figure 1.2 C). Instead of each MGE moving independently, the full length of DNA situated between one end of the element to the other is transposed as a entire unit. Composite Tns found in *A. baumannii* carry many genes, usually related to antibiotic resistance such as *bla*-*OXA23* providing resistance to carbapenems in Tn2006, Tn2007, Tn2008 and Tn2009, or *aphA6* in the context of Tn*aphA6*, conferring aminoglycoside resistance with IS*Aba1* and IS*Aba125* elements driving their over-expression, respectively (Corvec *et al.*, 2007; Wang *et al.*, 2011b; Zhou *et al.*, 2011; Nigro and Hall, 2016b). To date, Tn2006 is the most widespread MGE facilitating carbapenem resistance, with a great propensity to disseminate amongst *A. baumannii* isolates (Lee *et al.*, 2012a; Nigro and Hall, 2016b).

1.5.4 Integrons

Integrons are genetic elements carrying a site-specific recombination system essential for the capture/integration, expression and exchange of DNA elements, termed gene cassettes (Cambray *et al.*, 2010). Integrons are not deemed self-mobile, but are often transferred through MGEs (Domingues *et al.*, 2012). Site-specific recombination events are required for integron insertion, with the *attC* sequence on the gene cassette recognising the corresponding *attI* site on the target integron and inserting next to it (Figure 1.2 E). This gene capturing system facilitates accumulation of multiple similarly orientated cassettes (in some instances over 100) in a tandem array extending from the *attI* site, providing large scale genomic diversity and can facilitate acquisition of adaptive phenotypes (Partridge *et al.*, 2009). Integron classes are based on the type of integrases they encode (Boucher *et al.*, 2007). In *A. baumannii*, Class 1 integrons are the most commonly identified integron, and are a key facilitator in the rapid spread of resistance genes, mainly due to their residence within MGEs (Lin *et al.*, 2013; Zhu *et al.*, 2014; Hamidian *et al.*, 2015; Martins *et al.*, 2015; Lean and Yeo, 2017; Mirshekar *et al.*, 2018).

1.5.5 Plasmids

Plasmids are usually circular genetic elements that are present in prokaryotic cells and undergo self-controlled replication. The plasmids characterised in *A. baumannii* range from two to 100 kb and vary significantly in genetic content (Gallagher *et al.*, 2015; Hamidian *et al.*, 2016a; Wibberg *et al.*, 2018). These ‘selfish’ genetic entities are considered one of the primary vehicles driving bacterial evolution, as they typically encode numerous accessory genes, many that can increase fitness and thus promote bacterial survival (Barlow, 2009; Weingarten *et al.*, 2018). Furthermore, these elements are capable of intra- and inter-sp. transfer by passive or active mechanisms (Smillie *et al.*, 2010; Hülter *et al.*, 2017). As previously stated in Section 1.5, *A. baylyi* and some *A. baumannii* isolates are naturally transformable, with this passive form of genetic transfer accounting for the high abundance of non-conjugative plasmids identified within these sp..

Differences in the number and type of plasmids in *A. baumannii* clinical isolates have been determined using a novel typing method involving variation in plasmid replication genes, leading to the designation of 19 different replication groups (Bertini *et al.*, 2010). Using this identification method, a recent assessment into a subset of nosocomial and environmentally acquired *A. baumannii* plasmids highlighted a predominance of plasmids from the Rep-3 superfamily across both groups, with many sharing conserved backbones (Salto *et al.*, 2018). Plasmids greater than 10 kb are of greater interest compared to their smaller counterparts due to their ability to rapidly disseminate MDR phenotypes (Nigro *et al.*, 2015; Hamidian *et al.*, 2016a; Nigro and Hall, 2017; Wibberg *et al.*, 2018). However, small plasmids (~2-10 kb) present across sequenced *A. baumannii* isolates have been recently reviewed, shedding light on their functions and overall significance (Lean and Yeo, 2017).

Aside from carrying resistance determinants, virulence associated genes have also been found on *A. baumannii* plasmids (Lean *et al.*, 2015; Weber *et al.*, 2015b; Hamidian *et al.*, 2016b; Lucidi *et al.*, 2018). As previously mentioned in Section 1.4.7, pAB04-1 and its related variants hold the regulatory switch controlling expression of a chromosomally encoded type VI secretion system (Weber *et al.*, 2015b). The study also demonstrated that without antibiotic selection, the ~170 kb plasmid was readily lost in a subset of the population, resulting in a loss of multidrug resistance and instead gaining an ability to kill co-resident bacteria in a T6SS dependent manner. It has been suggested that *A. baumannii* has partitioned two phenotypes depending on its surrounding environment,

evolving a clever plasmid-based strategy to balance two distinct, yet fitness-costly mechanisms (Weber *et al.*, 2015b).

1.5.6 Genomic islands

A number of accessory genes acquired by HGT accumulate as syntenic blocks termed GEIs. GEIs are large segments of DNA (10-200 kb) (Juhás *et al.*, 2009) that can harbour a variety of genes, including resistance genes and MGEs such as ISs, Tns and integrons which are required for mobilisation of genetic material in and out of the island (Figure 1.2 F). GEIs commonly insert at the terminal end of tRNA genes and differ in their GC content compared to the corresponding host genome, assisting in their identification (Schmidt and Hensel, 2004). Site-specific recombinases are responsible for GEI integration into the genome and as a result of insertion are usually flanked by DR, which can be subsequently utilised as recognition sequences for future excision events (Dobrindt *et al.*, 2004).

Similar to other pathogens, the presence of GEIs in *A. baumannii* genomes have had a significant impact on antimicrobial resistance and to some extent metabolic versatility, facilitating more virulent phenotypes (Schmidt and Hensel, 2004). For example, the AbaR1 GEI which inserted into the *comM* gene within the AYE *A. baumannii* isolate spanned 86 kb and harboured 45 resistance genes, conferring resistance to numerous antibiotics from multiple classes (Fournier *et al.*, 2006; Adams *et al.*, 2008). This GEI was intimately linked to the isolates MDR phenotype, a contributing factor for epidemic outbreaks across 54 healthcare facilities in France, which led to 26% mortality in infected patients (Poirel *et al.*, 2003). Since the characterisation of AbaR1 back in 2006, various AbaR1-associated and distinct GEIs have been identified in *A. baumannii* isolates (Iacono *et al.*, 2008; Post *et al.*, 2010; Krizova *et al.*, 2011; Bonnin *et al.*, 2012; Nigro and Hall, 2012; Nigro *et al.*, 2013; Wright *et al.*, 2014; Kenyon *et al.*, 2016). Collectively, these studies demonstrate not only the diversity but the similarities of GEI integration sites, as well as their overall architecture and genetic content.

1.6 Regulatory mechanisms employed by *A. baumannii*

The survival and pathogenic success of bacteria requires an ability to rapidly sense and respond to changing microenvironments. Bacteria have therefore evolved a repertoire of regulatory mechanisms that can independently respond to a myriad of environmental cues providing coordinate expression of their genes. The regulation and timing of virulence factor expression is imperative for successful colonisation, growth and survival within

the host and transmission. Hence, identifying the proteins responsible as well as unravelling the intricate mechanisms that facilitate these changes is imperative for understanding the pathobiology of *A. baumannii*.

To date, protein-based regulation systems are the most predominate control mechanism characterised in *A. baumannii* (Casella *et al.*, 2017). Only one RNA-based mechanism has been functionally characterised, with this work undertaken in *A. baylyi* (Withers *et al.*, 2014). Genomic comparisons of *A. baumannii* and *A. baylyi* ADP1 have revealed that *A. baumannii* contains approximately double the amount of transcriptional regulators, correlating with the ability of the organism to survive within a greater range of environments compared to that of *A. baylyi* (Adams *et al.*, 2008).

Most regulatory systems characterised in *A. baumannii* control genes associated with antimicrobial resistance and/ or virulent phenotypes. Key examples amongst others include: the transcription factor (also referred to as one component systems) H-NS, a global regulator involved in regulation of AT-rich genetic material (Eijkelkamp *et al.*, 2013; Deveson Lucas *et al.*, 2018); ferric and zinc uptake regulators responsible for iron and zinc uptake and homeostasis, respectively (Daniel *et al.*, 1999; Mortensen *et al.*, 2014); AbaR, a quorum-sensing responsive regulator (Niu *et al.*, 2008); SoxR, a MerR-like regulator known to regulate expression of AbuO, a protein involved in oxidative and osmotic stress resistance phenotypes (Srinivasan *et al.*, 2015); AdeN, the regulator of the AdeIJK MDR efflux pump (Rosenfeld *et al.*, 2012) (Section 1.4.9.1.2); 1645, the master regulator of the phase-variable phenotype (Chin *et al.*, 2018); TetR1 and TetR2, two TetR-like regulatory proteins controlling T6SS expression (Weber *et al.*, 2015b) (Section 1.4.7); ArpR, regulator of the ArpAB efflux pump (Tipton *et al.*, 2017); and AdeL and AceR, LysR-type regulators known to control expression of AdeFGH and AceI efflux pumps, respectively (Coyne *et al.*, 2010; Liu *et al.*, 2018). Similar to transcription factors, TCS proteins can reprogram diverse aspects of microbial physiology in response to environmental cues. These systems are a key signalling strategy afforded by *A. baumannii* and insights into their structure and function in addition to characterised systems present in *A. baumannii* will be discussed in further detail.

1.6.1 Two component signal transduction systems

Protein phosphorylation via TCS is a fundamental strategy allowing organisms to elicit appropriate cellular responses upon sensing their external environment (Hoch, 2000). Canonical TCSs consist of two modular proteins, a histidine kinase (HK) and a cognate

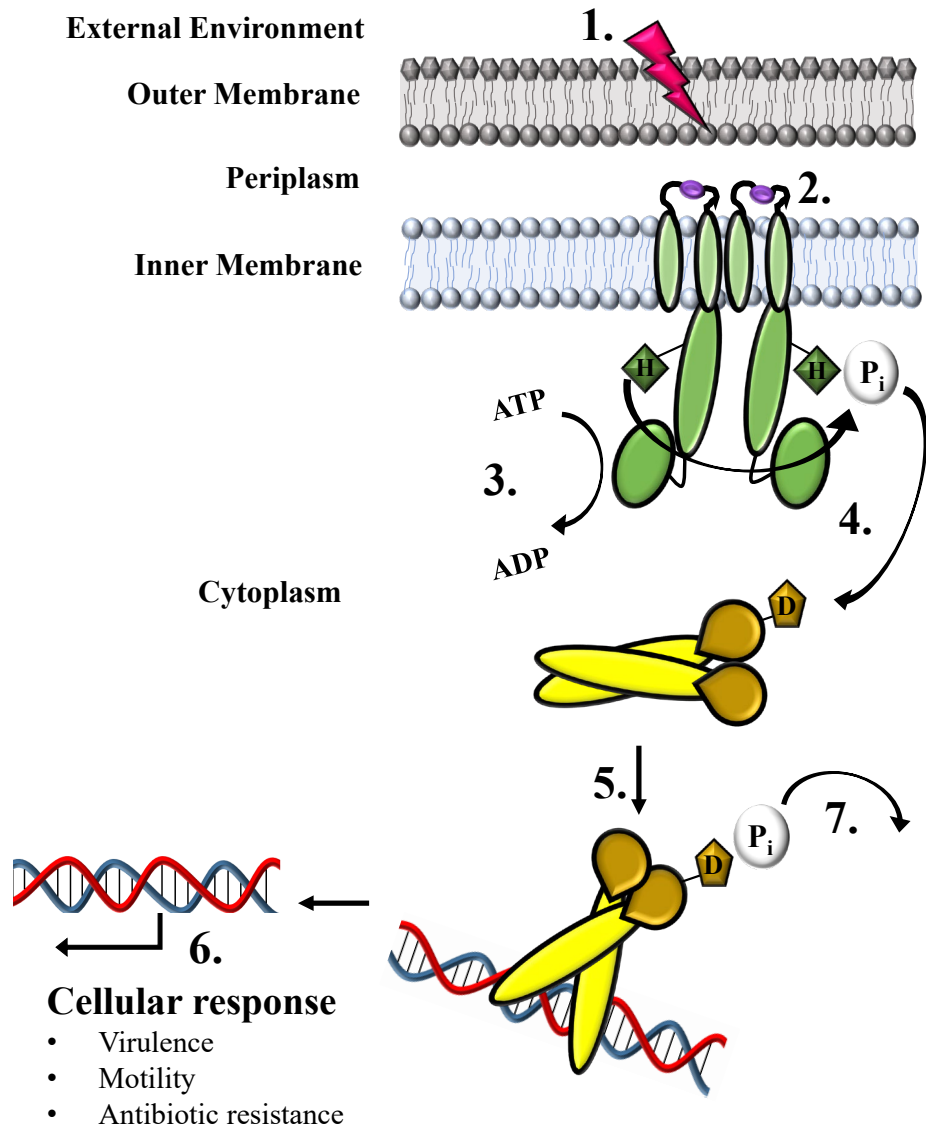
RR that contain heterologous and homologous domains linked via a phosphorelay system (West and Stock, 2001; Williams and Whitworth, 2010). TCSs are widespread in bacteria and are present in more than 95% of sequenced bacterial genomes, with their absence only seen in a small number of endosymbionts and obligate pathogens with significantly reduced genomes (Wuichet *et al.*, 2010). Generally, HK and RR genes are co-transcribed in an operon, however, there are many examples where these genes exist in the genome distal located from their cognate partner, and are defined as orphans (Williams and Whitworth, 2010) (Section 1.6.1.3). In 2015, a total of 164 651 TCS proteins from 2758 sequenced prokaryotic genomes were uploaded into P2CS, a specialised database dedicated to prokaryotic TCS (Ortet *et al.*, 2015). A number of factors influence the quantity of genes encoding TCS within a bacterial genome, e.g. the size of the genome and the diversity of environments the bacterium may encounter (Galperin, 2005; 2006).

1.6.1.1 *Histidine kinases*

Prototypical HKs are located in the cell membrane and contain two transmembrane (TM) helices that are linked by a variable periplasmic sensor domain that can sense particular stimuli within the extracellular milieu (Pirrung, 1999; Sevvana *et al.*, 2008) (Figure 1.3 A). Very little sequence homology is shared between sensing domains of HKs, supporting the notion they have evolved for highly specific ligand/stimulus interactions. Located at the C-terminal end of the protein is a highly conserved cytoplasmic kinase core consisting of the histidine kinase phosphoacceptor (HisKA) and catalytic ATP (CA) domains, and are defined as the unifying structures of HKs (Gao and Stock, 2009) (Figure 1.3 B). The HisKA domain contains the H-box harbouring the conserved histidine residue required for autophosphorylation whilst the CA domain is composed of four aa motifs/boxes (N, G1, F and G2) which are known to be responsible for ATP binding (Stock *et al.*, 1989) (Figure 1.3 B).

When a stimulus is detected from the external environment, the conformational change from the TM helices present in the HK lead to autophosphorylation between homodimers where the CA region catalyses phosphorylation of the histidine residue energised by ATP (Figure 1.3 A). This phosphate is subsequently transferred by direct binding of the cognate RR to the HK (Podgornaia and Laub, 2013). In most cases, HKs have bi-functional activity meaning when they are not stimulated to autophosphorylate, they can act as phosphatases for their cognate RR (Khorchid and Ikura, 2006). This function has been shown to eliminate crosstalk and unwanted phosphorylation of the cognate RR by other HKs or small molecule donors (Siryaporn and Goulian, 2008).

A



B

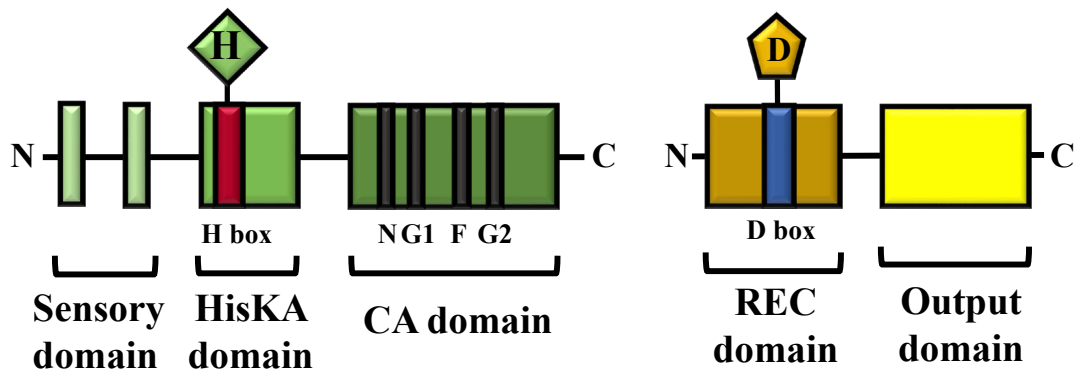


Figure 1.3: The signalling cascade and conserved domain architecture of prototypical two component signal transduction systems

(A) TCS are comprised of a HK (green) and RR (gold) protein. HK proteins are generally embedded within the inner membrane whilst RR proteins reside in the cytoplasm. The HK detects an external stimuli (1) and interactions of the stimulating agent (purple circles) with the periplasmic sensing domain induce conformational changes in the HK (2) promoting ATP-dependent *trans*-autophosphorylation of the conserved histidine (H) residue of its homodimeric partner (3). This phosphate (P_i) is then transferred to the conserved aspartate (D) residue on the RR protein (4). Phosphorylation of the RR promotes conformational changes that modulate its interaction with DNA (5) leading to alterations in target gene expression (6). These systems can regulate a plethora of different phenotypes such as virulence, motility and antibiotic resistance. The circuit can be reset to a pre-stimulus state by dephosphorylation of the RR (7) by: auto-dephosphorylation, HK phosphatase or alternate phosphatase activities. **(B)** HKs contain a variable N terminal extracellular sensing domain required for stimulus perception. Two transmembrane (TM) segments (green vertical bars) are usually identified within the N terminus, functioning to anchor the HK to the membrane and link the sensing domain to the His kinase A (HisKA) domain. This HisKA domain is required for phosphate transfer reactions, containing the H box (red) which harbours the highly conserved phospho-accepting H residue. The catalytic and ATP binding (CA) domain contains the conserved N, G1, F and G2 boxes (dark green) and is required for energising the autophosphorylation reaction between two HK homodimers. The RR harbours a C-terminal receiver (REC) domain which contains the highly conserved phosphoaccepting D residue. Phosphorylation of the D residue activates the C-terminal output domain, most often leading to DNA binding.

The HKs are a member of the protein kinase family which are classified by their mode of autophosphorylation (Mascher *et al.*, 2006) and delineates the HK family from the larger Ser/Thr/Tyr kinase family, proteins which function by transferring a phosphate from ATP to a given protein substrate (Deutscher and Saier, 2005). Additionally, unlike classic protein kinase amplification cascades, HKs do not phosphorylate multiple targets but generally act only upon their cognate RR (Robinson *et al.*, 2000; Casino *et al.*, 2009).

Despite their dissimilarity at the protein level, work has proceeded to classify HKs based on their membrane topology. Mascher *et al.*, (2006) categorised HKs into three principal groups, the first and largest group is represented by prototypical HKs, defined by a periplasmic sensory domain flanked by two TM helices (Figure 1.4 A). This periplasmic sensor domain is generally where stimuli interact with the HK, activating a signal to modulate kinase/phosphatase activities. This group of proteins are typical for sensing solutes, nutrients and ions. The second group of HKs have multiple TM helices, ranging from 2- to 20 (Figure 1.4 B). However, unlike group one, these HKs do not have a periplasmic sensing domain and the stimuli for these HKs are thought to be membrane associated changes such as ionic strength, osmolarity or turgor (Mascher *et al.*, 2006). The third group of HKs, denoted as the cytoplasmic-sensing HKs, contain membrane bound or soluble proteins with their sensing domains located within the cell cytosol and are known to sense intracellular signals (Figure 1.4 C).

Aside from the principal features of HKs, combinations of additional sensory and linker domains have been identified. A number of these domains serve to transmit the signal from the N-terminus to the catalytic core domains or alternatively function as an additional signal sensing domain. The best studied of these is the HAMP domain, named after their presence in mediating signalling in HKs, adenylyl cyclases, methyl-accepting chemotaxis proteins, and some phosphatases. HAMP domains are found in approximately 30% of all HKs and are generally located as immediate extensions of the C-terminal TM helix, connecting this region to the cytoplasmic kinase core (Aravind and Ponting, 1999). Although the mechanism of signal transduction through HAMP domains is not clearly defined, it is believed that HAMP domains exist in two states and switching between these conformations is required for kinase activation (Zschiedrich *et al.*, 2016). Many HKs also harbour domains that can sense additional cytoplasmic signals. The most common are the PAS (Per-Arnt-Sim) and GAF (c-GMP-specific and c-GMP-stimulated phosphodiesterases, *Anabaena* adenylyl cyclases and *E. coli* FhlA) domains. Approximately 40% of all HKs carry at least one of these cytoplasmic domains and in

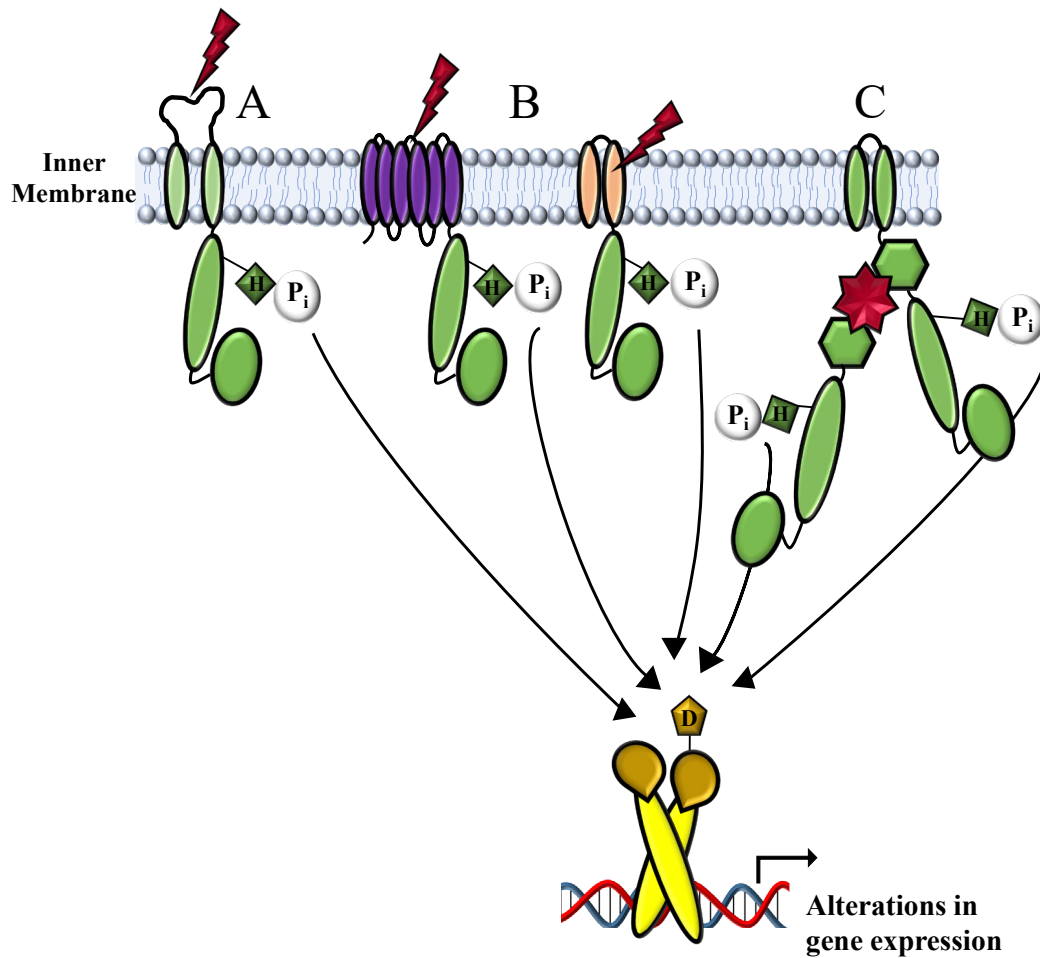


Figure 1.4: Diagrammatic representation of the three different mechanisms of stimulus perception adopted by bacterial HKs

(A) Periplasmic sensing HKs. (B) HKs with sensing mechanisms linked to TM regions. (C) Cytoplasmic sensing HKs. The areas of the HK proteins that are involved in stimulus perception are highlighted in colour and the stimuli which activate the HK are represented by a red thunderbolt or star. See text for details. Figure adapted from Mascher *et al.*, (2006).

some experimentally examined examples these domains can detect intracellular stimuli such as secondary messenger molecules, redox potential, gases and even photons (Henry and Crosson, 2011; Mann *et al.*, 2016).

1.6.1.2 Response regulators

RRs are typically found in the cytosol of a cell and function as phosphorylation-activated switches that regulate output responses (Jenal and Galperin, 2009). These proteins generally consist of two domains; a conserved N-terminal receiver (REC) domain (termed Response_reg in the pfam database) and a variable C-terminal effector domain (Bourret, 2010) (Figure 1.3 B). The RR REC domain directly interacts with its phosphorylated cognate HK and catalyses transfer of the phosphoryl group from the phospho-histidine residue to their own phospho-acceptor site, a conserved aspartate residue located within the D box (Figure 1.3 B). Whilst the effector domain regulates output responses RRs are present in two different conformations dependent on whether they are in their active or inactive state. The inactive conformation of a RR is favoured in the unphosphorylated protein, whereas phosphorylation shifts the conformation toward the active state. When the REC domain becomes phosphorylated, the conformational changes that occur from phosphate binding affect the properties of the effector domain (Williams and Whitworth, 2010) (Figure 1.3 A). Effector domains are diverse in structure and regulate a variety of output mechanisms (Robinson *et al.*, 2000). Most effector domains facilitate DNA binding and operate as transcriptional regulators (Erickson *et al.*, 2005; de Been *et al.*, 2008; Gao and Stock, 2009), whilst others are known to be involved in protein-, RNA- or ligand-binding (Galperin, 2006). In addition to these core domains, the flexible interdomain linker of some RR have been found to be important in increasing the affinity of the RR to bind to its target DNA (Walthers *et al.*, 2003).

The heterogeneity observed across C-terminal effector domains has been used to classify RR proteins into subfamilies (Stock *et al.*, 1989). These groupings are named after representative and/ or best-studied members (Galperin, 2006; 2010). The two most abundant subfamilies found across bacterial genomes are the OmpR/PhoB (Mizuno and Tanaka, 1997; Itou and Tanaka, 2001) and NarL/FixJ families (Baikalov *et al.*, 1996), both utilising variations of the helix-turn-helix (HTH) DNA-binding structural motif. Although rare, the REC domain can function as a stand-alone module, promoting protein-protein interactions, controlling such functions as bacterial motility and participating in signalling phosphorelays, such as CheY and Spo0F, respectively (Jenal and Galperin, 2009).

1.6.1.3 Orphan RRs/HKs

Through the investigation of co-evolutionary relationships between cognate HK-RR pairs, orphan HKs/RRs were discovered (Koretke *et al.*, 2000). Computational analysis of bacterial genomic data has assisted in the rapid identification and abundance of orphan TCSs within different bacterial sp. (Ulrich and Zhulin, 2007; Procaccini *et al.*, 2011). Unlike classical TCS, where the HK and its cognate RR gene lie adjacently in the bacterial chromosome, orphans exist without their cognate RR/HK counterparts encoded within the same operon. Orphan HKs and RRs vary greatly amongst bacterial sp.; in *E. coli* only 6.4% of TCSs are encoded as orphans compared to 57% in *Caulobacter crescentus* (Skerker *et al.*, 2005). Orphan HK/RRs function in the same manner as cognate systems (Muller *et al.*, 2007), however, a modified communication process of ‘one to many’ or ‘many to one’ HK:RR ratio has been observed (Laub *et al.*, 2007). This observation highlighted questions regarding the identity of the partners for orphan HKs and RRs, and if they have true cognate partners at all. To help elucidate this gap in the knowledge, an *in vitro* system level approach denoted ‘phosphotransfer profiling’ was created that adopts a methodical examination of the ability of a HK to transfer a phosphoryl group to the collection of RRs in a genome of interest (Laub *et al.*, 2007). This approach has been a monumental step forward in identifying cognate partners for orphan HKs/RRs in many bacterial sp. (Biondi *et al.*, 2006; Ryan, 2006; Lassak *et al.*, 2010).

1.6.1.4 Hybrid and unorthodox histidine kinases

In bacteria, prototypical HKs represent the primary form of sensory input for signal transduction, however, unorthodox and hybrid histidine kinases (HHK) also play a role in this process (West and Stock, 2001). These unorthodox HK and HHK proteins are more complex than classical HKs as they also possess a REC domain at their C terminus (Figure 1.5 B and C). Instead of the single histidine-aspartate transfer, a histidine-aspartate-histidine-aspartate relay is adopted. To achieve this, unorthodox and HHKs require an intermediate histidine phosphotransfer (Hpt) domain. In HHKs, the Hpt protein is encoded as a separate protein (Figure 1.5 C), whereas in unorthodox HKs this Hpt domain is fused (Figure 1.5 B). Although the receiver domains of atypical HKs are analogous to RR receiver domains, to illicit a response in the cell, RR proteins are still necessary as they contain the effector domain (Gao *et al.*, 2007).

It is not entirely clear how these HHKs evolved, as phylogenetic analyses can not identify a common ancestor (Zhang and Shi, 2005). It is believed that their origin and expansion was most likely achieved by lateral recruitment of a receiver domain into an

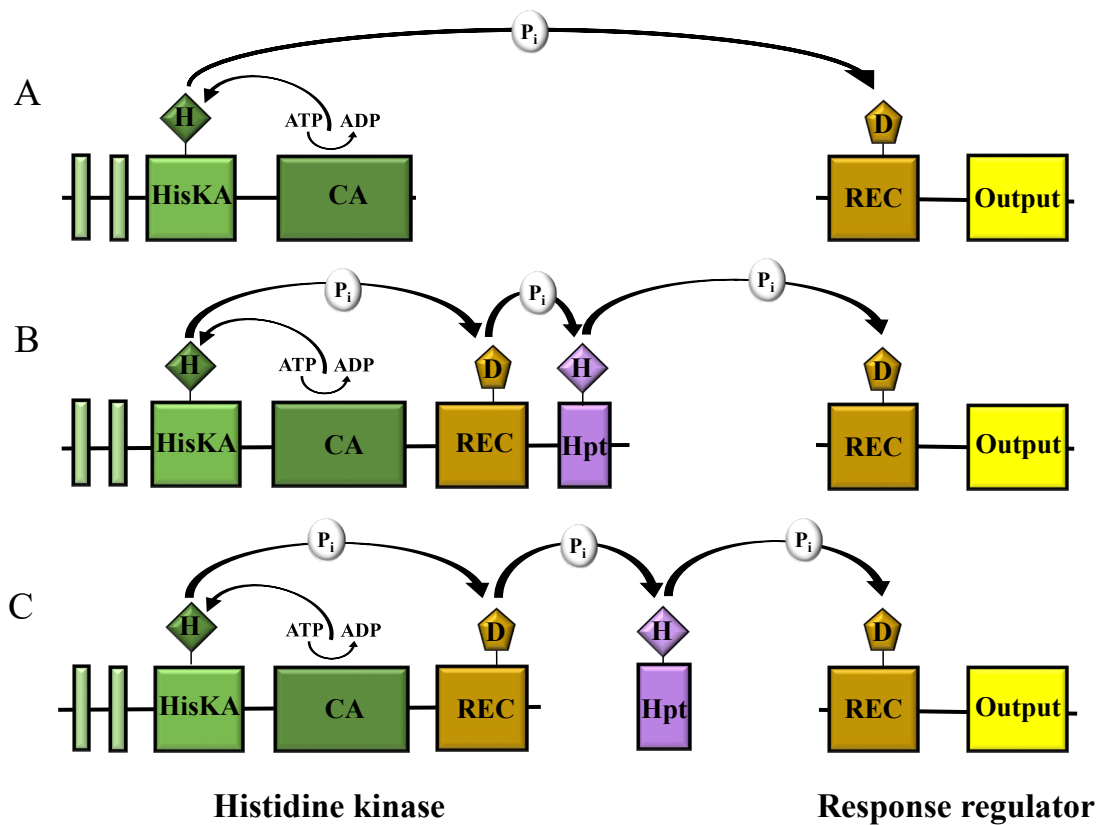


Figure 1.5: Domain organisation and phosphorelay events of prototypical, hybrid and unorthodox two component signal transduction systems

(A) Prototypical HKs transfer the phosphate (P_i) from the conserved H residue within the HisKA domain directly to the D residue within the REC domain of the cognate RR. **(B)** Unorthodox HKs transfer the phosphate to an additional REC (gold) and Hpt (purple) domain within the HK protein before phosphoryl transfer to the REC domain of the cognate RR. **(C)** Hybrid HKs similarly transfer the phosphate to a REC domain located within the HK protein, but subsequently transfer the phosphoryl group to an Hpt domain located on another protein (purple) before transfer of the phosphoryl group to the REC domain of the cognate RR.

adjoining HK gene and then duplication as one unit (Zhang and Shi, 2005). Despite being less common in bacteria, some advantages of unorthodox and HHKs over their classical counterparts have been identified, including minimisation of crosstalk between non-cognate RRs through the packaging of REC and kinase domains into a single protein (Zhang and Shi, 2005; Capra *et al.*, 2012).

1.6.1.5 Specificity mechanisms employed by TCS

To date, there are three main mechanisms bacteria have evolved at the phosphotransfer level to ensure specificity of two-component pathways; molecular recognition, substrate competition and phosphatase activity (Podgornaia and Laub, 2013). Molecular recognition is the most prominent, where an auto-phosphorylated HK can identify its cognate RR and avoid phosphorylating other non-cognate RR partners. Kinetic studies into the VanS HK of *Enterococcus* found phosphorylation of its cognate RR, VanR, was 10^4 -fold greater than that of the non-cognate RR, PhoB (Fisher *et al.*, 1996). These findings were also supported *in vitro* by phosphotransfer profiling experiments which demonstrated that HKs have a strong kinetic preference for their cognate RR compared to all possible regulators in a given genome (Skerker *et al.*, 2005). Relative cellular concentrations of HKs and their cognate RRs can also increase specificity (Li *et al.*, 2014a). For example, the EnvZ HK and its RR partner OmpR of *E. coli* are found at an approximate 1:35 ratio in the cell (Cai and Inouye, 2002). The higher abundance of the cognate RR ensures that it can outcompete other non-cognate RR for binding to the HK, preventing unwanted phosphotransfer events. Further research has elucidated that only a small set of amino acid residues located primarily in one α -helix within the HK dimerisation domain are required for cognate RR recognition (Casino *et al.*, 2009; Willett and Kirby, 2012). As previously stated, many HKs have bi-functional activity that promote either forward phosphoryl transfer or dephosphorylation of its cognate phosphorylated RR partner (Dutta and Inouye, 1996; Porter *et al.*, 2008). Phosphatases control the timing and rate of information being passed through each signalling pathway (McCleary *et al.*, 1993) and can dephosphorylate the cognate RR preventing unwanted phosphorylation by non-cognate HKs or small molecule phosphodonors (Willett *et al.*, 2013).

1.6.1.6 Targeting TCS for development of novel antimicrobial therapies

With a lack of currently effective antimicrobial treatments and a less than promising pipeline for the generation of new antibiotics, research into the production of alternate antimicrobial therapies is of significant interest. Whilst TCS genes are also present in the

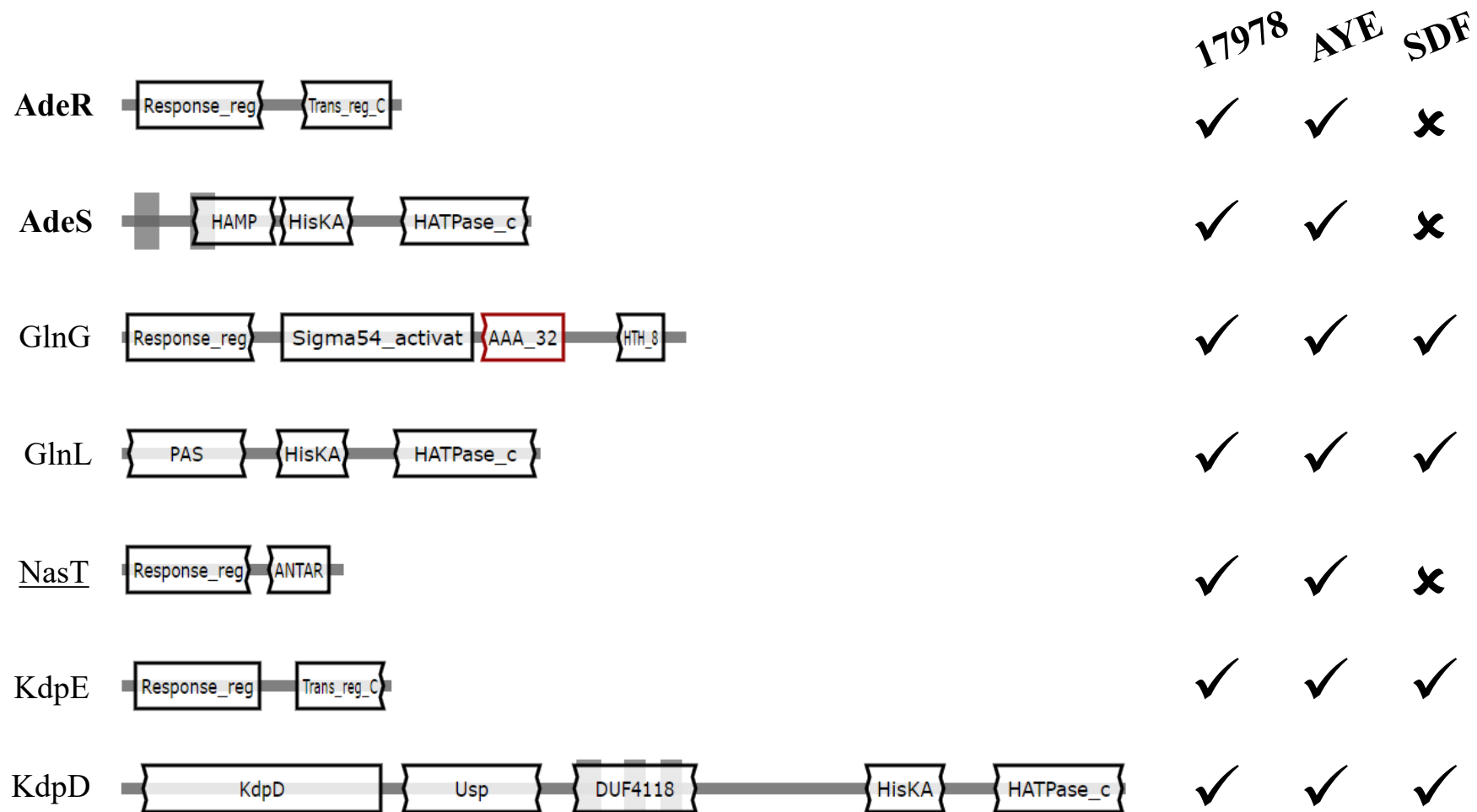
genomes of yeasts, fungi, moulds, and plants, their absence from higher eukaryotes and metazoans combined with their association in regulating virulence in clinically important pathogens, have made these proteins attractive targets as an alternative strategy for the development of novel therapeutics (Worthington *et al.*, 2013; Tiwari *et al.*, 2017).

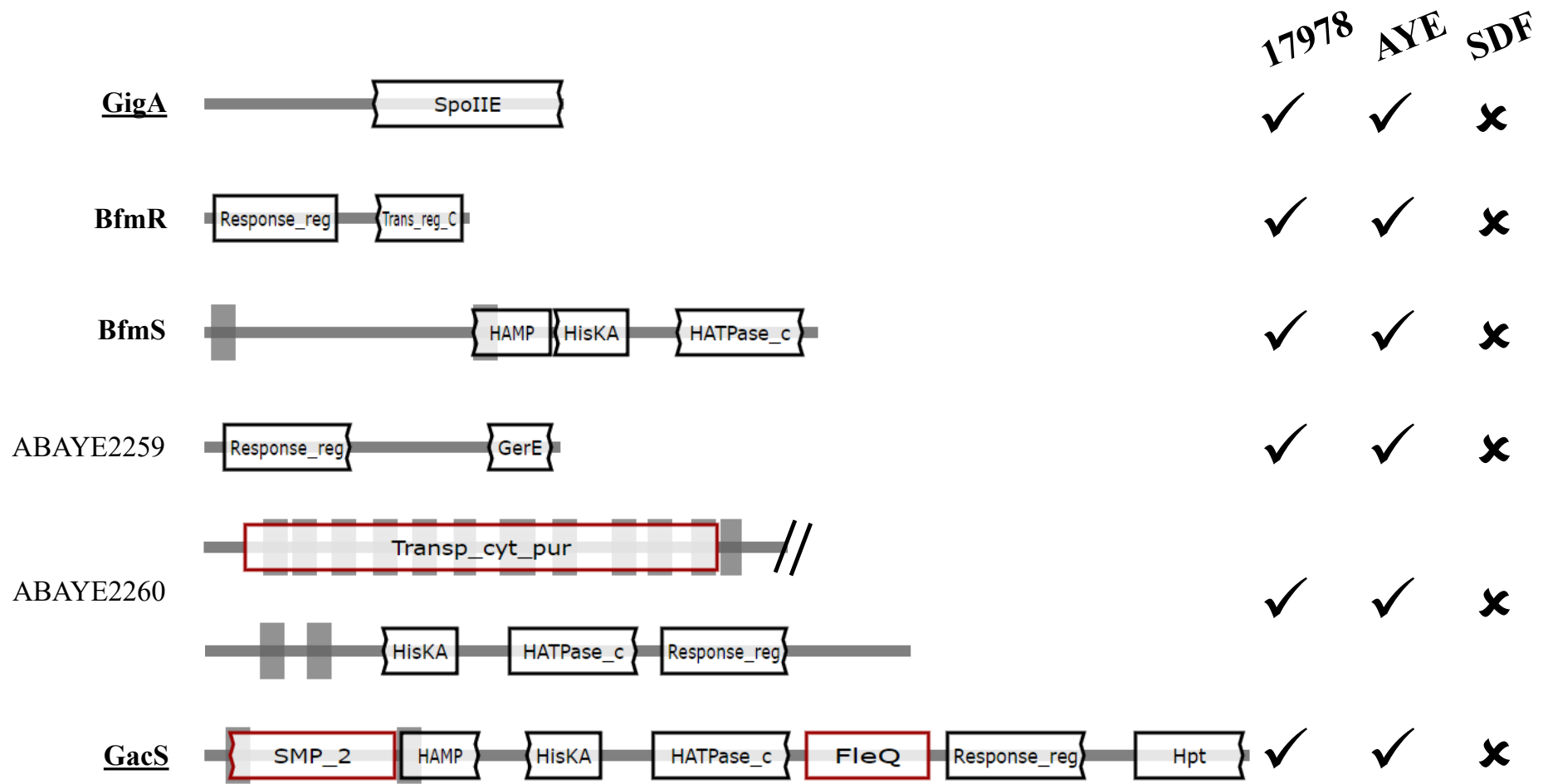
To date, a number of TCSs have been defined as ideal candidates, including the *A. baumannii* BfmRS system (Milton *et al.*, 2018) (Section 1.6.1.7.4). Thus far, studies have focused on targeting conserved TCS reactions, including autophosphorylation of HKs or the phosphotransfer from HKs to their cognate RRs, in the hope of generating a single compound that can simultaneously inhibit activity of multiple TCSs. Research groups have focused on identifying inhibitors using a number of different technologies, most commonly through high throughput and structure-based virtual screening methods (Rasko *et al.*, 2008; Gotoh *et al.*, 2010; Tang *et al.*, 2012). A handful of compounds have demonstrated inhibition against TCS systems (Bem *et al.*, 2015), however, no compounds have progressed to clinical trials.

1.6.1.7 TCS present in the *A. baumannii* genome

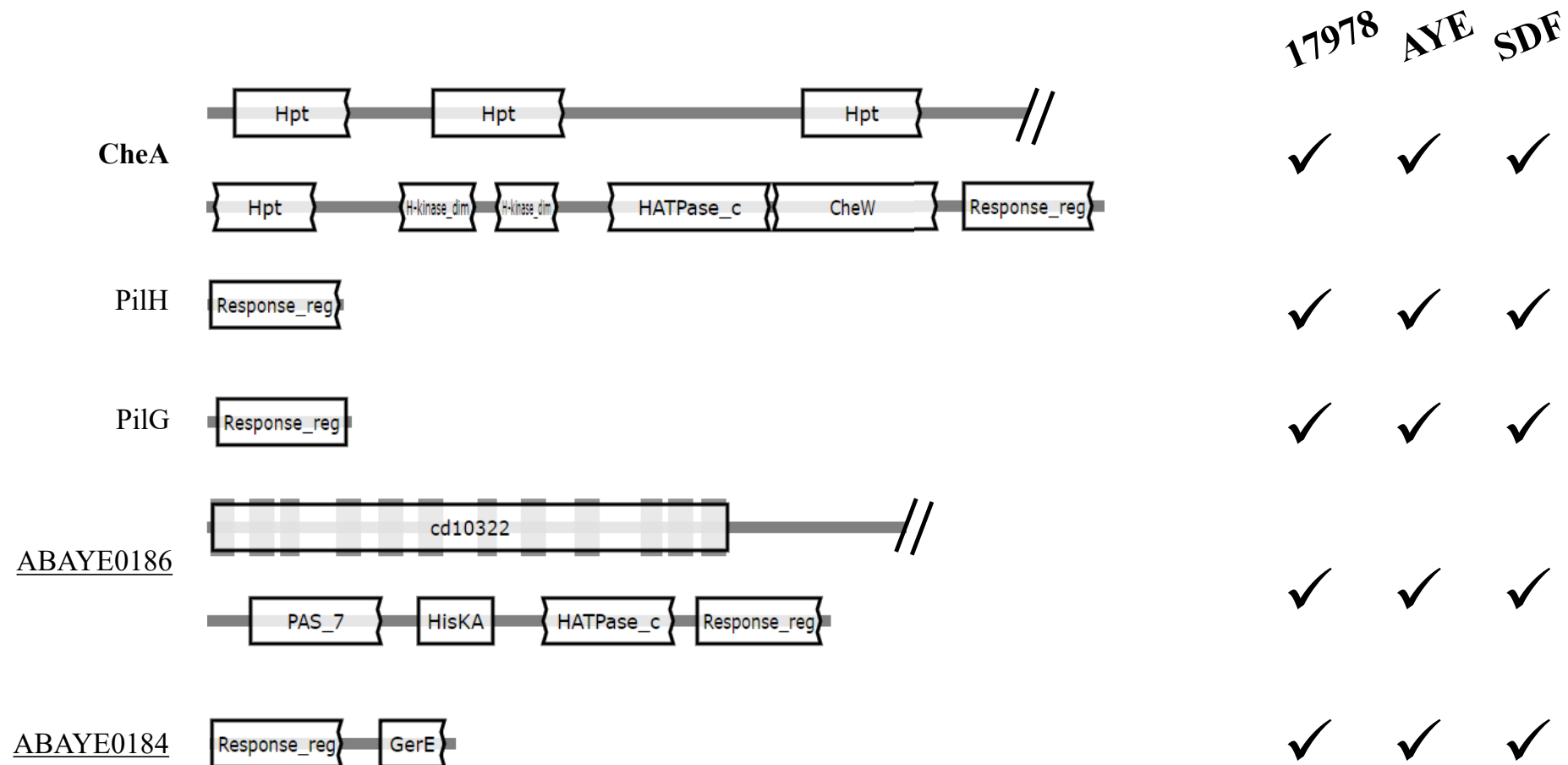
The number of TCS present in *A. baumannii* can be seen as largely isolate specific (Adams *et al.*, 2008). This is demonstrated in Figure 1.6, where the domain architecture of TCS proteins from three *A. baumannii* isolates that differ in their pathogenic potential were analysed. The avirulent *A. baumannii* SDF strain, isolated from a human louse (Fournier *et al.*, 2006), has the least number of TCS proteins (10 RRs and 6 HKs), the drug-susceptible ATCC 17978 strain, isolated from a fatal case of meningitis in 1956 (Smith *et al.*, 2007) has a total of 34 TCS proteins (18 RRs and 16 HKs) whilst the MDR AYE strain, (Fournier *et al.*, 2006) isolated from the urinary tract of a patient in 2001 during an epidemic outbreak, has the greatest number of TCS proteins (20 RRs and 18 HKs). These numbers were derived from the identification of TCS proteins that carry at least both of the HK essential domains, HisKA, HATPase or the essential REC domain of RRs. When comparing TCS from ATCC 17978 to that of the more recently isolated AYE strain, only two new systems were acquired over the 45 years between their isolation, inferring minimal TCS expansion over this period. Collectively, a slight overrepresentation of RR proteins could be identified across each of the strains examined, and is likely to indicate a level of cross-talk amongst these systems. In addition to the essential domains present in TCS proteins, a wide variety of additional domains were

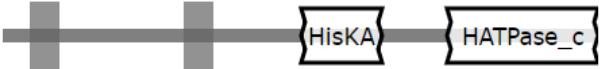

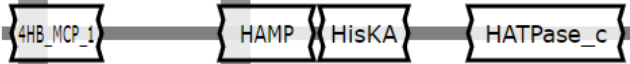
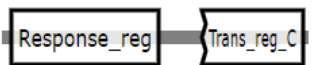
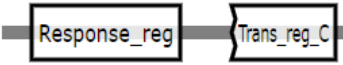

		17978	AYE	SDF
PilR		✓	✓	✗
PilS		✓	✓	✗
<u>GacA</u>		✓	✓	✓
AlgS		✓	✓	✗
AlgR		✓	✓	✓
CusR		✓	✓	✗
CusS		✓	✓	✗





		17978	AYE	SDF
ABAYE0600		✓	✓	✓
ABAYE0599		✓	✓	✓
QseB		✓	✓	✓
QseC		✓	✓	✗
PmrA		✓	✓	✗
PmrB		✓	✓	✗
ABAYE0575		✓	✓	✗



		17978	AYE	SDF
ABAYE1349		x	✓	x
ABAYE1350		x	✓	x
ABAYE1341		x	✓	x
ABAYE1340		x	✓	x
OmpR		✓	✓	✓
EnvZ		✓	✓	✓

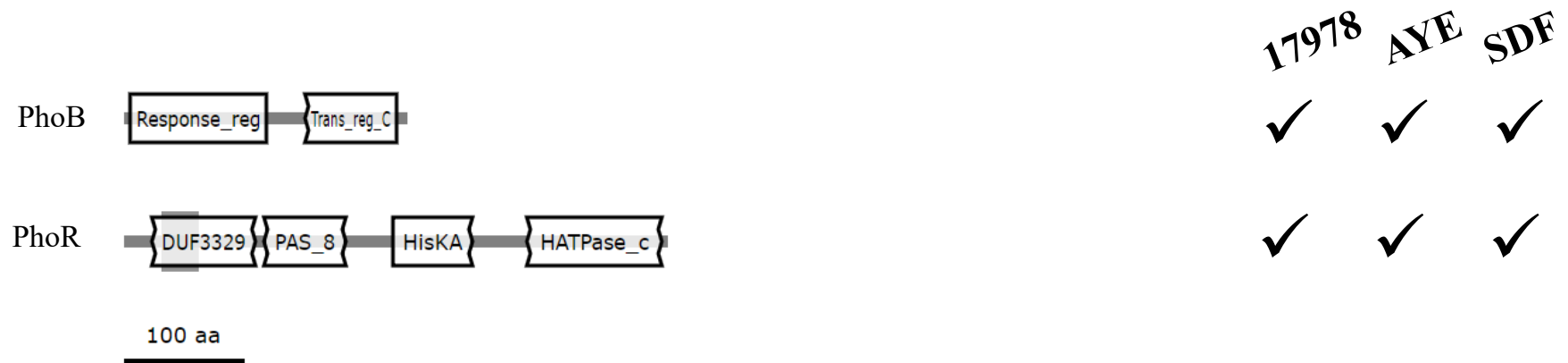


Figure 1.6: Domain architecture of TCS proteins encoded in *A. baumannii* ATCC 17978, AYE and SDF genomes

The figure is based on the output of TCS protein sequences obtained from *A. baumannii* AYE using the CDvist program (Adebali *et al.*, 2015). The relative position and size of the identified conserved domains are indicated by the labelled symbols. Dark grey boxes represent putative transmembrane (TM) helices and black angled bars a break in the sequence. Protein names/locus tags were assigned using *A. baumannii* AYE protein annotation. Underlined and bolded TCS names/locus tags represent orphan TCS proteins and experimentally characterised systems, respectively. Presence or absence of HK/RR proteins in ATCC 17978 (GenBank accession: CP000521), AYE (GenBank accession: CU459141) and SDF (GenBank accession: CU468230) are represented by black ticks or crosses, respectively.

identified, some more common (e.g. HAMP and PAS domains, Section 1.6.1.1) than others (e.g. the RNA binding domain AN TAR named after AmiR and NasR transcription antitermination regulators) (Galperin, 2006). Overall, prototypical TCS were found to dominate, with only two hybrid and two unorthodox HKs identified. Interestingly, the HKs, GlnL and ABAYE5075 lacked putative TM helices, and like other bacteria adopting HKs with similar structures (Mascher *et al.*, 2006), it would suggest that these are also soluble proteins residing in the *A. baumannii* cytosol.

Although *A. baumannii* encodes a relatively low number of TCS compared to some other human pathogens, such as *E. coli* and *P. aeruginosa* (approximately 40 and 90 TCS, respectively), during host infection different TCSs present in the *A. baumannii* genome have been enriched with mutations (Wright *et al.*, 2017a). These findings illustrate the importance of these systems in regulating genes that enhance the overall fitness and virulence potential of *A. baumannii*. The TCS that have been experimentally examined in *A. baumannii* will each be discussed in further detail.

1.6.1.7.1 *adeR/S*

As described in Section 1.4.9.1, AdeRS regulates expression of the tripartite multidrug efflux pump, AdeABC. AdeS and AdeR encode HK and RR proteins, respectively and are located directly upstream of the divergently transcribed *adeAB(C)* operon. AdeRS is defined as a transcriptional activator of *adeABC* expression, with recent studies demonstrating that AdeR binds to a perfect 10-bp direct repeat located within the intercistronic region between these two operons (Chang *et al.*, 2016; Wen *et al.*, 2017). Only one direct repeat was found in the *A. baumannii* genome, inferring *adeABC* is the sole target within the AdeRS regulon. Given the importance of this regulatory system in conferring clinically relevant levels of resistance to a range of antimicrobials, AdeRS holds great potential as a target for novel inhibitor development. The binding domain of AdeR has now been solved, detailing the interactions between AdeR to the direct repeat sequence (Wen *et al.*, 2017). Unphosphorylated AdeR demonstrated high affinity binding to its target sequence, even exceeding levels of other similar RRs in their active state (Li *et al.*, 2014b). It was suggested that this interaction may maintain basal levels of transcription for *adeAB(C)* and facilitate almost instantaneous upregulation of gene expression upon activation.

The overproduction of AdeABC seen across multiple *A. baumannii* clinical isolates was frequently linked to mutations or insertions in *adeRS* genes, resulting in constitutive

expression of *adeABC* and subsequent increased resistance levels (Sun *et al.*, 2012; Nowak *et al.*, 2016; Wright *et al.*, 2017a; Gerson *et al.*, 2018). Aside from modulation in resistance, targeted deletion of *adeRS* genes has been shown to affect motility, biofilm formation and virulence, albeit strain specific phenotypic changes (Richmond *et al.*, 2016; De Silva and Kumar, 2017).

1.6.1.7.2 *pmrA/B*

Polymyxin B and polymyxin E (colistin) are cyclic cationic peptides, with the latter being one of the last-line therapeutic options to treat MDR *A. baumannii* infections (Karaikos *et al.*, 2013; Viehman *et al.*, 2014). However, resistance towards these antibiotics has increased in recent years (Valencia *et al.*, 2009; Cai *et al.*, 2012). One such molecular mechanism involved in this resistance is via the PmrAB TCS. The *pmrAB* genes encode RR and HK proteins, respectively, and are co-transcribed with *pmrC*, a gene encoding the lipid A modification enzyme, phosphoethanolamine transferase. In *A. baumannii*, mutations in *pmrA* or *pmrB* that result in constitutive activation of PmrA lead to overexpression of *pmrC* which is correlated with increased polymyxin resistance (Adams *et al.*, 2009; Arroyo *et al.*, 2011; Beceiro *et al.*, 2011). The PmrC-mediated addition of a phosphoethanolamine group to lipid A by PmrC reduces the affinity of the cationic peptide to its lipid A target, decreasing uptake across the outer membrane and resulting in increased resistance (Adams *et al.*, 2009). However, acquisition of resistance by this mechanism can be seen as a trade-off, as bacterial fitness of these isolates is significantly impaired (López-Rojas *et al.*, 2011; Beceiro *et al.*, 2014; Mu *et al.*, 2016). Given this associated fitness cost, resistant isolates have been found to revert mutated aa back to WT or generate compensatory mutations in the *pmr* locus, both reducing expression of *pmrC* (Adams *et al.*, 2009; Snitkin *et al.*, 2013).

1.6.1.7.3 *gacS/A*

The GacSA TCS is an important TCS responsible for regulating many virulence factors across a range of Gram-negative bacteria (Parkins *et al.*, 2001; Gauthier *et al.*, 2010; Zha *et al.*, 2014). GacS in *A. baumannii* shares 43% amino acid identity to GacS of *P. aeruginosa* and is defined as an orphan unorthodox HK (Cerqueira *et al.*, 2014). Peleg and colleagues were the first to confirm a role for GacS in *A. baumannii* virulence, reporting a Tn insertion in *gacS* that significantly reduced killing of the human fungal pathogen *Candida albicans* (Peleg *et al.*, 2008b). RNA-sequencing (RNA-seq) analyses showed the transcription levels of 674 genes were significantly altered in Δ *gacS* derivative compared to WT, with expression changes identified in genes critical for

biofilm formation, motility and pili synthesis (Cerqueira *et al.*, 2014). Growth in human serum demonstrated that $\Delta gacS$ was more susceptible to the killing effects of serum, consistent with results from a septicemia murine model of infection (Cerqueira *et al.*, 2014). Interestingly, *gacS* was found to regulate an aromatic compound degradation pathway known as the phenyl acetic acid catabolic pathway. Further studies using real-time fluorescent microscopy and cell tracking within a zebrafish model revealed that infection with $\Delta gacS$ altered neutrophil behaviour compared to WT cells, causing a rapid influx and prolonged dwelling of neutrophils at the infection site (Bhuiyan *et al.*, 2016). The study defined phenylacetate to be a bacterial chemoattractant and the inability of $\Delta gacS$ to degrade the compound enhanced the neutrophilic response, resulting in reduced bacterial burden and attenuated disease (Bhuiyan *et al.*, 2016). Targeting a metabolic pathway that has capabilities to augment the host innate immune response offers a novel mode of treatment for *A. baumannii* and other MDR pathogens.

1.6.1.7.4 *bfmR/S*

The first phenotypes attributed to the BfmRS TCS of *A. baumannii* were described in 2008, with inactivation of *bfmR* by Tn insertion abolishing biofilm formation on plastic surfaces in a *csu*-dependent manner (Tomaras *et al.*, 2008). However, inactivation of the *bfmS* HK resulted in only a partial reduction of biofilm formation, demonstrating the possibility of cross-talk between other HKs and BfmR. Recent studies have also defined direct links between the BfmRS TCS in maintenance of normal cellular physiology and survival under a diverse set of stress conditions, including desiccation (Farrow *et al.*, 2018; Geisinger *et al.*, 2018). Furthermore, BfmR is essential during *in vivo* growth in human ascites fluid (Umland *et al.*, 2012) and in a murine pneumonia infection model (Wang *et al.*, 2014).

Given its importance in *A. baumannii* survival and virulence, this system was deemed suitable as a potential target for novel inhibitor development. Analysis of the structure of the BfmR REC domain has allowed prediction of a number of small-molecule binding hotspots suitable for inhibiting BfmR binding to its target sequence(s) (Russo *et al.*, 2016). Additionally, a full length structural model of BfmR was recently solved (Logan Draughn *et al.*, 2018), elucidating the binding of BfmR to a seven bp perfect inverted-repeat sequence located near the originally predicted *bfmRS* promoter region (Tomaras *et al.*, 2008). Interestingly, BfmR demonstrated an opposite behaviour to that of RRs from the OmpR/PhoP family, as the binding affinity of BfmR to the target sequence was significantly reduced in its active-state form (Logan Draughn *et al.*, 2018). It was

speculated that this mechanism may act as a novel self-regulatory strategy, preventing unnecessary expression of *bfmRS* genes and other genes within its regulon. However, investigations into binding sites upstream of additional target genes are required to confirm this hypothesis.

1.6.1.7.5 The unorthodox HK *cheA*

In *A. baumannii*, CheA codes for an orphan unorthodox HK that contains a CheW domain (Chen *et al.*, 2017) (Figure 1.6). The protein shares significant identity to CheA and ChpA present in *E. coli* and *P. aeruginosa*, respectively (Chen *et al.*, 2017). In these aforementioned sp., the proteins are known to be involved in chemotactic responses and in controlling motility via flagella and type IV pili (Whitchurch *et al.*, 2004; Baker *et al.*, 2006). Deletion of CheA in *A. baumannii* ATCC 17978 abolished surface-associated motility, pellicle and biofilm formation (Chen *et al.*, 2017). Global transcriptomic analyses confirmed the downregulation of 117 genes in a $\Delta cheA$ derivative, including genes involved in lipopeptide assembly (A1S_0112-0119), Csu pili production, and quorum sensing (Chen *et al.*, 2017). Interestingly, no significant alterations in *pil* gene expression including those co-transcribed with *cheA* were identified. Although not mentioned in the study, two of the genes co-transcribed with *cheA* encode single REC domain proteins (Figure 1.6). These uncommon proteins (termed CheY) are known to function through protein-protein interactions and have been found to be important in CheA-dependent motility phenotypes in other bacteria (Jenal and Galperin, 2009). Supplementation with synthetic quorum sensing molecules restored biofilm and motility phenotypes in $\Delta cheA$ similar to WT levels (Chen *et al.*, 2017). These findings correlate with a previous study which identified the A1S_0112-0119 operon to be regulated by quorum-sensing signals produced by AbaI (Clemmer *et al.*, 2011). Collectively, these results confirm that CheA is a part of the regulatory circuitry that controls expression of the AbaI-dependent quorum-sensing pathway, Csu pili and the lipopeptide produced by A1S_0112-0119 genes.

1.6.1.7.6 *ompR/envZ*

Recently, a phase-variable phenotype was identified in *A. baumannii* AB5075 with colonies interconverting between translucent and opaque variants; the opaque variant is more virulent than its translucent counterpart (Tipton *et al.*, 2015). The rate of this interconversion increased at high densities, signifying an epigenetic mechanism is likely to be involved in controlling phase-variability (Tipton *et al.*, 2015). Using random Tn mutagenesis a colony with a defective cell morphology demonstrated by irregular edging,

interspersed with papillae indicative of translucent variants was isolated (Tipton and Rather, 2017). The Tn insertion mapped within the coding region for a RR, whose protein product shared 70% amino acid identity to *E. coli* OmpR. In *A. baumannii* AB5075, *ompR* is co-transcribed with its cognate HK *envZ*. Inactivation of either *ompR* or *envZ* increased opaque to translucent switching by 401- and 281-fold compared to WT, respectively, indicating that the TCS is responsible for repressing phase-variation switching. In the opaque background, single and double *ompR/envZ* deletion strains were attenuated in a *G. mellonella* infection model, whilst survival of the translucent $\Delta ompR$ variant was the same as WT. The OmpR/EnvZ system is not auto-regulatory and maybe regulated by other molecules and/ or proteins. Despite the clear regulatory influence of this system on phase-variation, a TetR-type transcriptional repressor (defined as 1645) was recently described as the master regulator of this phenotype in AB5075 (Chin *et al.*, 2018). Since overexpression of 1645 did not alter *ompR* expression nor were notable changes in 1645 expression levels seen within $\Delta ompR$ derivative from the opaque background, two independent networks may be responsible for the regulation of phenotypic switching within this isolate.

1.6.1.7.7 *baeS/R*

The BaeSR TCS of *A. baumannii* is a homologue of the *E. coli* BaeRS system sharing 48.1 and 64.6% amino acid identity, respectively (Lin *et al.*, 2014). In ATCC 17978, deletion of the BaeR RR altered growth under osmotic stress conditions and decreased tigecycline resistance 2-fold (Lin *et al.*, 2014). Expression levels of *adeA* and *adeB* were both reduced by over 60% in this $\Delta baeR$ derivative and overexpression of *baeR* increased *adeAB* expression and tigecycline resistance by 2-fold. The authors speculated that BaeSR is a positive regulator of *adeAB*, subsequently leading to changes in tigecycline resistance. However, the correlations from *adeAB* expression alterations and resistance levels was not further explored. An additional study by the same research group identified $\Delta baeR$ was susceptible to the potential antibiotic adjuvant, tannic acid (Lin *et al.*, 2015). It was suggested that BaeSR may also positively regulate AdeIJK, and MacAB-ToIC efflux pumps due to their increased transcription upon exposure to tannic acid in WT cells, whilst minimal expression differences were seen in $\Delta baeR$. Electrophoretic mobility shift assays using BaeR could not bind to *adeA*, *adeI* or *macA* promoter regions suggesting that BaeSR indirectly influences expression of these efflux pumps and thus, may be a member of a larger undefined regulatory network (Lin *et al.*, 2015).

1.6.1.7.8 *gigA/gigB*

The *gigA* and *gigB* genes of *A. baumannii* encode a non-canonical RR and an anti-sigma factor antagonist protein, respectively. Both genes were found to be essential for survival within a *G. mellonella* larvae infection model, indicating they play a direct role in virulence (Gebhardt *et al.*, 2015). In most other bacteria, homologues of these proteins are activated under stress conditions, functioning together to regulate anti-sigma factor activity and assist in alternative sigma factor activation to control expression of genes involved in stress response pathways (Morris and Visick, 2013; Bouillet *et al.*, 2017). In *A. baumannii* 5075, deletion of either *gigA* or *gigB* led to increased sensitivity towards acid pH, zinc ions, temperature stress and aminoglycoside antibiotics (Gebhardt *et al.*, 2015; Gallagher *et al.*, 2017). Mutant derivatives capable of restoring kanamycin resistance back to WT levels in the Δ *gigB* background were enriched in *ptsP*, a gene predicted to encode the Enzyme I component of the nitrogen phosphotransferase system. Independent deletion of two genes from the nitrogen phosphotransferase system suppressed many of the phenotypes observed in Δ *gigA* and Δ *gigB*, inferring a link between these two pathways (Gebhardt *et al.*, 2015). When three of the five sigma factors in *A. baumannii* 5075 were independently deleted, inactivation of the *rpoE* sigma factor produced similar phenotypic responses to Δ *gigA*/ Δ *gigB* derivatives. However, due to limitations in mutant construction and overall experimental design, the authors acknowledged that more definitive studies are required to confirm a direct association (Gebhardt *et al.*, 2015). Collectively, the findings have identified a unique form of regulation imposed by *A. baumannii*, converging a global stress response mechanism with a central metabolic sensing pathway to maintain cellular homeostasis under multiple stress conditions.

1.7 Scope of thesis

In recent decades, *A. baumannii* has propelled itself to be an extremely troublesome hospital-acquired pathogen, aided by an ability to persist within clinically associated environments for extended periods and rapidly acquire resistance to the current armamentarium of therapeutic treatments. Despite the increasing threat this pathogen poses to susceptible individuals and healthcare institutions worldwide, virulence traits including various aspects of antimicrobial resistance, are not completely understood. Furthermore, the regulatory circuitry governing the expression of known and unknown virulence determinants still remains ill defined.

In order to rapidly adapt to changing environmental conditions, *A. baumannii* encodes a variety of different regulatory systems. One such system is TCSs, which function by combining extracellular signals with cellular responses that in turn promote survival under changing environmental conditions. Despite regulating a plethora of virulent phenotypes in other bacterial pathogens, less than half of the TCS encoded by *A. baumannii* have been experimentally investigated. The aim of this study was to further examine the role of TCS in regulating resistance and/ or persistence traits employed by *A. baumannii*. Using the genetically defined isolate, ATCC 17978 as the background strain for all studies presented in this thesis, three TCS were targeted by gene deletion and analysed using a combination of phenotypic and transcriptomic assays. Each research chapter examines a particular TCS, detailing new knowledge about each system as well as fortuitous findings independent of the original research aims.

Chapter 2 investigates the regulatory role of the AdeRS TCS. Although this system has been previously found to regulate expression of the AdeABC tripartite multidrug efflux system, a number of questions still remain to be determined. Work presented in this chapter examined whether the previously observed regulatory properties of AdeRS and efflux capabilities of AdeAB were also maintained in ATCC 17978, a “drug susceptible” clinical isolate which naturally lacks *adeC*. Through the generation of gene deletion derivatives and subsequent antibiogram analyses, it was revealed that AdeAB conferred intrinsic resistance to a limited range of compounds and confirmed that AdeB can function with AdeA alone to confer resistance. Further examination into one of the new substrates identified within this study revealed insights into its mode of action against *A. baumannii*, revealing how the presence of different energy sources and cations in the growth media can modulate the antimicrobial properties of this compound.

Chapter 3 explores the function of the putative TCS named 11155/11160. Basic insights into the topological structure of the proteins were determined, assisting in the identification of a novel domain architecture for the HHK, 11160. Orthologues of the TCS were enriched within species from the Proteobacteria phyla, with genetic alignments revealing a co-localisation with a transport gene cluster. A deletion derivative targeting the 11155 RR was constructed in ATCC 17978 and transcriptome profiling and subsequent analyses revealed translocation of a mobile genetic element into a distal transcriptional regulator, resulting in its inactivation. Regeneration of $\Delta 11155$ utilising an alternative gene mutagenesis protocol also led to a loss-of-function mutation in the same transcriptional regulator. Taken together, these results reveal a novel regulatory circuitry

and suggest that the 11155/11160 TCS is involved in regulating genes that are essential for survival in ATCC 17978.

Chapter 4 sought to examine the regulatory role of the TCS termed QseBC. Homologues of the system have been found to regulate virulence-associated phenotypes in a number of Gram-negative pathogens. Deletion derivatives of *qseBC* and its putative gene target *ygiW* were constructed and phenotypically analysed. During desiccation stress experiments, a number of motile variants were isolated, further examination of which discovered insertional disruption of a known global regulator by MGEs, leading to the identification of a novel MITE. The non-autonomous element was further characterised, providing insights into its overall function and putative roles in adaptive evolution.

The diverse range of experimental approaches and analyses presented in this thesis have unveiled new knowledge on the contribution of TCS in regulating persistence and resistance phenotypes available to *A. baumannii*. The work also underscores the genetic amenability of this pathogen, reporting upon how different stressors can rapidly promote movement of MGEs, leading to alterations in host gene expression levels. Collectively, the results presented here have advanced our understanding into the complex regulatory networks and genetic plasticity that promotes the pathogenic success of *A. baumannii*.

CHAPTER 2: Resistance to pentamidine is mediated by AdeAB, regulated by AdeRS, and influenced by growth conditions in *Acinetobacter baumannii* ATCC 17978

Declaration by candidate

In Chapter 2 the nature and extent of my contribution to the work was as follows:

Nature of contribution	Contribution extent (%)
Conceptualisation, data curation, methodology, performance of experiments, writing, editing and revision of the manuscript	80

The following co-authors contributed to the work

Name	Nature of contribution	Contribution extent (%)
Uwe Stroehler	Conceptualisation, data curation, editing and revision of draft manuscript	5
Karl Hassan	Data curation, methodology, editing and revision of final manuscript	5
Shashikanth Marri	Data curation, formal analysis	5
Melissa Brown	Conceptualisation, data curation, editing and revision of draft and final manuscript	5

The undersigned hereby certify the above declaration correctly reflects the nature and extent of the candidate and co-author contribution to this work.

Candidate signature		17.8.19
---------------------	--	---------

Supervisor signature		17.8.19
----------------------	--	---------

2.1 Preface

This chapter is closely based on the publication by Adams F.G., Stroecher U.H., Hassan K.A. and Brown M.H. (2018) Resistance to pentamidine is mediated by AdeAB, regulated by AdeRS, and influenced by growth conditions in *Acinetobacter baumannii* ATCC 17978. *PLoS ONE* **13**: e0197412 licensed under [Creative Commons Attribution 4.0](#). The printed version of this article can be found in Appendix D.

2.2 Abstract

In recent years, effective treatment of infections caused by *Acinetobacter baumannii* has become challenging due to the ability of the bacterium to acquire or up-regulate antimicrobial resistance determinants. Two component signal transduction systems are known to regulate expression of virulence factors including multidrug efflux pumps. Here, we investigated the role of the AdeRS two component signal transduction system in regulating the AdeAB efflux system, determined whether AdeA and/ or AdeB can individually confer antimicrobial resistance, and explored the interplay between pentamidine resistance and growth conditions in *A. baumannii* ATCC 17978. Results identified that deletion of *adeRS* affected resistance towards chlorhexidine and 4',6-diamidino-2-phenylindole dihydrochloride, two previously defined AdeABC substrates, and also identified an 8-fold decrease in resistance to pentamidine. Examination of $\Delta adeA$, $\Delta adeB$ and $\Delta adeAB$ cells augmented results seen for $\Delta adeRS$ and identified a set of dicationic AdeAB substrates. RNA-sequencing of $\Delta adeRS$ revealed transcription of 290 genes were ≥ 2 -fold altered compared to the wildtype. Pentamidine shock significantly increased *adeA* expression in the wildtype, but decreased it in $\Delta adeRS$, implying that AdeRS activates *adeAB* transcription in ATCC 17978. Investigation under multiple growth conditions, including the use of Biolog phenotypic microarrays, revealed resistance to pentamidine in ATCC 17978 and mutants could be altered by bioavailability of iron or utilisation of different carbon sources. In conclusion, the results of this study provide evidence that AdeAB in ATCC 17978 can confer intrinsic resistance to a subset of dicationic compounds and in particular, resistance to pentamidine can be significantly altered depending on the growth conditions.

2.3 Introduction

Acinetobacter baumannii causes a range of disease states including hospital-acquired pneumonia, blood stream, urinary, wound and bone infections, and is responsible for

epidemic outbreaks of infection worldwide (Peleg *et al.*, 2008a). Such infections are often very difficult to treat due to the MDR character of isolates displayed by this organism (Fournier *et al.*, 2006; Adams *et al.*, 2010). In addition to the impressive propensity of the organism to acquire genetic elements carrying resistance determinants (Fournier *et al.*, 2006; Hamidian *et al.*, 2014; Blackwell *et al.*, 2016a), up-regulation resulting in overproduction of resistance nodulation cell-division (RND) drug efflux systems through integration of insertion sequence elements or mutations in regulatory genes, has also been deemed a major contributor to the MDR phenotype (Coyne *et al.*, 2011; Yoon *et al.*, 2013; Saranathan *et al.*, 2017; Wright *et al.*, 2017a). The best studied RND efflux systems in *A. baumannii* include AdeABC (Magnet *et al.*, 2001), AdeFGH (Coyne *et al.*, 2010) and AdeIJK (Damier-Piolle *et al.*, 2008). Of particular interest is the AdeABC system which affords resistance to diverse antibiotics, biocides and dyes (Magnet *et al.*, 2001; Marchand *et al.*, 2004; Peleg *et al.*, 2007; Rajamohan *et al.*, 2010b), and has gained attention due to its high incidence of over-expression across many MDR *A. baumannii* clinical isolates, primarily from incorporation of point mutations in the genes encoding its positive regulator, AdeRS (Marchand *et al.*, 2004; Yoon *et al.*, 2013; Richmond *et al.*, 2016; Wright *et al.*, 2017a). Typically RND pumps consist of three proteins that form a complex; the absence of any of these components renders the entire complex non-functional (Nikaido and Takatsuka, 2009). Interestingly, deletion of *adeC* in the *A. baumannii* strain BM4454 did not affect resistance towards two substrates of the pump suggesting that AdeAB can utilise an alternative outer membrane protein (OMP) to efflux antimicrobial compounds (Marchand *et al.*, 2004).

The genetic arrangement of the AdeABC system places *adeABC* in an operon that is divergently transcribed to the regulatory *adeRS* two component signal transduction system (TCSTS). Expression of *adeABC* occurs by binding of AdeR to a ten base-pair direct repeat motif found within the intercistronic region separating these operons (Chang *et al.*, 2016; Wen *et al.*, 2017). Many clinical *A. baumannii* isolates harbour different genetic arrangements of the *adeRS* and *adeABC* operons (Nemec *et al.*, 2007), and whether regulation via AdeRS is conserved in these strains is not completely understood.

With an increase in infections caused by MDR isolates across many bacterial sp., including *A. baumannii*, understanding mechanisms of resistance and how resistance to and evasion of treatments has evolved over time has become a key research topic. Furthermore, determining the impact of expression of resistance determinants within the host environment and its effect on the efficacy of therapeutic treatments has gained

attention. For example, when *Pseudomonas aeruginosa* is grown using L-glutamate as the sole carbon source, resistance to the related compounds polymyxin B and colistin increased ≥ 25 - and 9-fold, respectively (Conrad *et al.*, 1979). Other studies have shown that the bioavailability of cations such as iron can have a drastic effect towards the resistance of a number of antimicrobials across a range of pathogenic bacterial sp. (Ezraty and Barras, 2016). Despite *A. baumannii* being recognised as a major human pathogen, these types of studies are limited for this organism.

This study aimed to determine the regulatory role of the AdeRS TCSTS in *A. baumannii* ATCC 17978, a clinical isolate which only encodes the *adeAB* subunits and identify whether AdeA and or AdeB alone can confer antimicrobial resistance in the ATCC 17978 background. Phenotypic characterisation of a constructed panel of deletion strains identified that alterations to the *adeRS* and *adeAB* operons of ATCC 17978 reduced resistance to a subset of dicationic compounds, including pentamidine. As a recent study highlighted the effectiveness of pentamidine in combination therapy to treat infections caused by Gram-negative pathogens (Stokes *et al.*, 2017), we sought to further examine alternative mechanisms of pentamidine resistance in *A. baumannii*. The type of carbon source and availability of iron were identified as affecting pentamidine resistance, thereby revealing interconnectedness between metabolic and resistance strategies within this formidable pathogen.

2.4 Materials and methods

2.4.1 Bacterial strains, plasmids and growth conditions

A. baumannii ATCC 17978 (Smith *et al.*, 2007) was obtained from the ATCC and is designated as wildtype (WT). Bacterial strains, plasmids and primers used in this study are summarised in Table 2.1 and 2.2, respectively. Bacterial strains were cultured using Lysogeny broth (LB) or LB agar plates, under aerobic conditions at 37°C, unless otherwise stated. Antibiotic concentrations used for selection were; ampicillin 100 mg/L, erythromycin (ERY) 25 mg/L, tetracycline (TET) 12 mg/L and gentamicin (GEN) 12.5 mg/L. All antimicrobial agents were purchased from Sigma with the exception of ampicillin which was purchased from AMRESCO. M9 minimal medium agar plates were generated using a stock solution of $5 \times$ M9 salts (200 mM Na₂HPO₄·7H₂O, 110 mM KH₂PO₄, 43 mM NaCl and 93 mM NH₄Cl) and subsequently diluted 1:5 and supplemented with 2 mM MgSO₄, 0.1 mM CaCl₂ and 0.4% (w/v) of various carbon sources on the day of use. M9 minimal medium was supplemented with 0.4% (w/v) of

Table 2.1: Strains and plasmids used in the study

Strain or plasmid	Genotype or description ^a	Reference/ source
<u><i>A. baumannii</i> strains</u>		
ATCC 17978	Non-international type clone; Meninges isolate	ATCC (Smith <i>et al.</i> , 2007)
$\Delta adeRS$	ATCC 17978 with insertion disruption in <i>adeRS</i>	This study
$\Delta adeAB$	ATCC 17978 with insertion disruption in <i>adeAB</i>	This study
$\Delta adeA$	ATCC 17978 with insertion disruption in <i>adeA</i>	This study
$\Delta adeB$	ATCC 17978 with insertion disruption in <i>adeB</i>	This study
$\Delta adeRS$ pWH:: <i>adeRS</i>	$\Delta adeRS$ harbouring pWH:: <i>adeRS</i>	This study
$\Delta adeRS$ pWH1266	$\Delta adeRS$ harbouring pWH1266	This study
$\Delta adeRS$ pWH:: <i>adeAB</i>	$\Delta adeRS$ harbouring pWH:: <i>adeAB</i>	This study
$\Delta adeRS$ pWHgent:: <i>adeAB</i>	$\Delta adeRS$ harbouring pWHgent:: <i>adeAB</i>	This study
$\Delta adeRS$ pWHgent	$\Delta adeRS$ harbouring pWHgent	This study
$\Delta adeA$ pWHgent:: <i>adeAB</i>	$\Delta adeA$ harbouring pWHgent:: <i>adeAB</i>	This study
$\Delta adeA$ pWHgent	$\Delta adeA$ harbouring pWHgent	This study
$\Delta adeB$ pWHgent:: <i>adeAB</i>	$\Delta adeB$ harbouring pWHgent:: <i>adeAB</i>	This study
$\Delta adeB$ pWHgent	$\Delta adeB$ harbouring pWHgent	This study
$\Delta adeAB$ pWHgent:: <i>adeAB</i>	$\Delta adeAB$ harbouring pWHgent:: <i>adeAB</i>	This study
$\Delta adeAB$ pWHgent	$\Delta adeAB$ harbouring pWHgent	This study
<u><i>E. coli</i> strains</u>		
DH5 α	F ⁻ Φ 80 <i>lacZ</i> Δ M15 Δ (<i>lacZYA-argF</i>) U169 <i>recA1 endA1 hsdR17</i> (rK ⁻ , mK ⁺) <i>phoA supE44 λ^- thi-1 gyrA96</i> <i>relA1</i>	(Hanahan, 1983)
<u>Plasmids</u>		
pAT04	TET ^R ; pMMB67EH with Rec _{AB} system	(Tucker <i>et al.</i> , 2014)
pBluescript SK ⁺ II	AMP ^R ; Cloning vector	(Alting-Mees and Short, 1989)

Strain or plasmid	Genotype or description ^a	Reference/ source
pBl ₋ BamHI	AMP ^R ; pBluescript SK ⁺ II with <i>Bam</i> HI restriction site removed via end-filling	This study
pBl _{-adeRS}	AMP ^R ; pBl _{-Bam} HI with <i>adeRS</i> flanking regions and ERY resistance cassette cloned via <i>Xba</i> I	This study
pEX18Tc	TET ^R ; <i>sacB</i> -based suicide vector	(Hoang <i>et al.</i> , 1998)
pEX _{-adeRS}	TET ^R , ERY ^R ; pEX18Tc with <i>adeRS</i> flanking regions and ERY resistance cassette cloned via <i>Xba</i> I	This study
pUCGM	GEN ^R ; Source of GEN resistance cassette	(Schweizer, 1993)
pVA891	CHL ^R , ERY ^R ; Source of ERY resistance cassette	(Macrina <i>et al.</i> , 1983)
pWH1266	AMP ^R , TET ^R ; <i>Acinetobacter/ E. coli</i> shuttle vector	(Hunger <i>et al.</i> , 1990)
pWHgent	AMP ^R , GEN ^R ; pWH1266 with GEN resistance cassette cloned via <i>Bam</i> HI	This study
pWH:: <i>adeRS</i>	AMP ^R ; pWH1266 with <i>adeRS</i> cloned via <i>Bam</i> HI and <i>Sal</i> I	This study
pWH:: <i>adeAB</i>	AMP ^R ; pWH1266 with <i>adeAB</i> cloned via <i>Bam</i> HI and <i>Sph</i> I	This study
pWHgent:: <i>adeAB</i>	AMP ^R , GEN ^R ; pWHgent with <i>adeAB</i> cloned via <i>Bam</i> HI and <i>Sph</i> I	This study

^aAMP, ampicillin; CHL, chloramphenicol; ERY, erythromycin; GEN, gentamicin; ^R, resistant; TET, tetracycline

Table 2.2: Primers used in this study

Primer name/ purpose	Sequence (5' - 3') ^a	Reference/ source
<u>Primers used for construction of $\Delta adeA$, $\Delta adeB$, $\Delta adeAB$ and $\Delta adeRS$</u>		
<u>$\Delta adeRS$</u>		
<i>adeRS_UFR_F</i> ^b	GAGATCTAGATACGCATAGCTTTCTCG GCACC	This study
<i>adeRS_UFR_R</i>	GAGAGGATCCATCGTAGTCATCTTCTA CCAC	This study
<i>adeRS_DFR_F</i>	GAGAGGATCCCGCTATTTTCTGTTAGTA GTGGG	This study
<i>adeRS_DFR_R</i>	GAGATCTAGAGCTCTTAAAAACAGTTA CTC	This study
<i>Ery_BamHI_F</i>	GAGAGGATCCCTTAAGAGTGTGTTGAT AGTGC	This study
<i>Ery_BamHI_R</i>	GAGAGGATCCCTCATAGAATTATTTCCCT CCG	This study
<i>adeRS_check_F</i>	GCAGCCGCGGTAGCAGGC	This study
<i>adeRS_check_R</i>	GGGGTCAAACACAGACGAC	This study
<u>$\Delta adeB$</u>		
<i>adeB_UFR_F</i>	TTACCAATAGCCACGGGC	This study
<i>adeB_UFR_R</i>	CTATCAACACACTCTTAAGGGCAGTTTA GGAATAC	This study
<i>adeB_DFR_F</i> ^b	CGGGAGGAAATAATTCTATGTCAGCCAT TTATAGTC	This study
<i>adeB_DFR_R</i> ^b	GGCCAACGCTTAAATACAT	This study
<i>Ery_F</i>	CTTAAGAGTGTGTTGATAGTGC	This study
<i>Ery_R</i>	CTCATAGAATTATTTCCCTCCG	This study
<i>adeB_NOL_F</i>	CCTTATAACGTCACAGCA	This study
<i>adeB_NOL_R</i> ^b	CGGGTGGTGAGCGTC	This study
<u>$\Delta adeAB$</u>		
<i>adeAB_UFR_F</i>	GAGAGTCTGACTGAGCTTAAACTAATCC AGCC	This study
<i>adeA_UFR_R</i> ^b	CTATCAACACACTCTTAAGGTCCAAACC TAGTGAGTTTTTG	This study
<i>adeB_DFR_F</i> ^b	CGGGAGGAAATAATTCTATGTCAGCCAT TTATAGTC	This study

Primer name/ purpose	Sequence (5' - 3')^a	Reference/ source
<i>adeB</i> _DFR_R ^b	GGCCAACGCTTAAATACAT	This study
Ery_F	CTTAAGAGTGTGTTGATAGTGC	This study
Ery_R	CTCATAGAATTATTTCCCTCCG	This study
<i>adeAB</i> _NOL_F ^b	GCTATGAGTGTTCGGTATCAATTT	This study
<i>adeB</i> _NOL_R ^b	CGGGTGGTGAGCGTC	This study
<u><i>ΔadeA</i></u>		
<i>adeAB</i> _UFR_F	GAGAGT CGACT GAGCTTAAACTAATCC AGCC	This study
<i>adeA</i> _UFR_R ^b	CTATCAACACACTCTTAAGGTCCAAACC TAGTGAGTTTTTG	This study
Ery_F	CTTAAGAGTGTGTTGATAGTGC	This study
Ery_rev_adeA	TCATTTCCTCCCGTTAAATAATAG	This study
<i>adeA</i> _DFR_F	CTATTATTTAACGGGAGGAAATGATGTC ACAATTTTTTATTTCG	This study
<i>adeA</i> _DFR_R	CTTTCAATTGCATACGTG	This study
<i>adeA</i> _NOL_F ^b	GCTATGAGTGTTCGGTATCAATTT	This study
<i>adeA</i> _NOL_R ^b	GAGAT CTAGATA CGCATAGCTTTCTCG GCACC	This study
<u>Primers used for complementation of <i>ΔadeA</i>, <i>ΔadeB</i>, <i>ΔadeAB</i> and <i>ΔadeRS</i></u>		
<i>adeAB</i> _comp_F	GAGAG GATCC ATCGTAGTCATCTTCTA CCAC	This study
<i>adeAB</i> _comp_R	GAGAG CATGCG ACTATAAATGGCTGAC	This study
Gent_comp_F	GAGAG GATCCC GAATTGACATAAGCC	This study
Gent_comp_R	GAGAG GATCCG CTTGAACGAATTGTT	This study
<i>adeRS</i> _comp_F	GAGAG GATCCG TGTGGAGTAAGTGTGG AGA	This study
<i>adeRS</i> _comp_R	GAGAG TCGACG CGAGAAGAGATTCGTA GAAG	This study
<u>Primers used for qRT-PCR</u>		
16S_RT_F ^c	CAGCTCGTGTCTCGTGAGATGT	(Eijkelkamp <i>et al.</i> , 2011a)
16S_RT_R ^c	CGTAAGGGCCATGATGACTT	(Eijkelkamp <i>et al.</i> , 2011a)
<i>GAPDH</i> _RT_F ^c	CAACACTGGTAAATGGCGTG	(Eijkelkamp <i>et al.</i> , 2011a)

Primer name/ purpose	Sequence (5' - 3') ^a	Reference/ source
<i>GAPDH</i> _RT_R ^c	ACAACGTTTTTCATTTTCGCC	(Eijkelkamp <i>et al.</i> , 2011a)
ACX60_17010_F	CAAAAGCAAAGCACCACAA	This study
ACX60_17010_R	GAAGAAGAATCTGGCCATGC	This study
ACX60_15380_F	CCGTGAATGGATTTACAGTTTAGT	This study
ACX60_15380_R	GGTTTGTTAATTGTCCCGTCA	This study
ACX60_14705_F	TTGCCAAAATCTTGAACCAA	This study
ACX60_14705_R	AGTCGCAATACCCAGTCAT	This study
ACX60_11550_F	CGTGATAATCAGGCGAACTG	This study
ACX60_11550_R	GGTTGACCTGGAGCAACTTT	This study
ACX60_07895_F	CATGCTGGTGGTTCAAAAAC	This study
ACX60_07895_R	GCTCTGGTTGAAATGCAATG	This study
<i>csuC</i> _F	GTGGATTAACCGAAGAAAGTCA	This study
<i>csuC</i> _R	GGCTGGCCTTGTTGATTG	This study
<i>csuAB</i> _F	GGTGAACGTACAGACCGCA	This study
<i>csuAB</i> _R	AGTAGCTTGGCCACTTACTGTAGT	This study
<i>adeI</i> _F	AATTGTTCAAGGGCGTTGTTC	This study
<i>adeI</i> _R	GTTTCAACAGGACGGCTCTC	This study
<i>craA</i> _F	CGGCAGTTCCTTGGGTTA	This study
<i>craA</i> _R	AACCATATTGCACGCTCGT	This study
<i>adeA</i> _F	AAGCTGAGGTGGCAAGACTC	This study
<i>adeA</i> _R	TGCTTTCATTTGAGCGACAT	This study
<i>adeS</i> _F	CGGCGACCTCTCTGCTAG	This study
<i>adeS</i> _R	ATGGCTGCATTCCAAACC	This study

^aNucleotides in bold-face type represent incorporated restriction sites, TCTAGA, *Xba*I; GGATTC, *Bam*HI; GTCGAC, *Sal*I; GCATGC, *Sph*I

^bPrimers used for multiple functions

^cPrimers used to amplify genes used as controls/references for qRT-PCR experiments

glucose, or succinic, fumaric, citric, α -ketoglutaric, pyruvic, glutamic or oxaloacetic acids. All carbon compounds were purchased from Sigma with the exception of citric and pyruvic acids which were purchased from Chem-Supply (Gillman, Australia). For solid media, J3 grade agar (Gelita, Australia) was used at a final concentration of 1%.

Iron-chelated and iron-rich conditions were achieved by the addition of dipyriddy (DIP) or $\text{FeSO}_4 \cdot 7\text{H}_2\text{O}$ (Scharlau) at final concentrations of 100 and 200 μM or 2.5 and 5 mM in Mueller-Hinton (MH) agar, respectively.

2.4.2 Antimicrobial susceptibility testing

The resistance profiles of WT and derivative strains were determined via broth microdilution methods (Wiegand *et al.*, 2008) which were performed in duplicate with a minimum of three biological replicates using bacteria cultured in MH broth. Growth was monitored at 600 nm (OD_{600}) using a FLUOstar Omega spectrometer (BMG Labtech, Germany) after overnight incubation at 37°C.

For disk diffusion assays, strains were grown to mid-log phase in MH broth, diluted to $\text{OD}_{600} = 0.1$ in fresh MH broth and 100 μL plated onto MH agar plates on which antimicrobial loaded filter disks were overlaid. Alternatively, when assessing zones of clearing using M9 minimal medium agar, strains were washed three times in phosphate buffered saline (PBS) and diluted to $\text{OD}_{600} = 0.1$ in fresh PBS. Tested antimicrobials were pentamidine isethionate, chlorhexidine dihydrochloride and 4',6-diamidino-2-phenylindole dihydrochloride (DAPI) at the final concentrations of 125, 2.5 and 1.6 μg , respectively. After overnight incubation, callipers were used to measure the diffusion distances which were determined as half of the inhibition zone diameter, less the length of the disk. At least three independent experiments in duplicate were undertaken. Statistical significance was determined using the Student's *t*-test (two-tailed, unpaired) and *P* values <0.0005 were considered significant.

For plate dilution assays, strains were grown to mid-log phase in MH broth, washed three times in PBS and diluted to $\text{OD}_{600} = 0.1$ in fresh PBS. Serial dilutions (10-fold) were prepared of which 5 μl was spotted onto M9 minimal or MH agar containing various concentrations of pentamidine (32, 64, 128, 256 and 512 mg/L) and growth assessed after overnight incubation at 37°C. To test the effect of growth of different carbon sources, M9 minimal media was supplemented with 0.4% (w/v) of succinic, fumaric, citric, α -ketoglutaric or oxaloacetic acids.

2.4.3 Construction of *A. baumannii* ATCC 17978 deletion strains and genetic complementation

Two methods were adopted to generate specific gene deletions in *A. baumannii* ATCC 17978. The first method used to generate $\Delta adeRS$ utilised a *sacB*-based strategy (Kaniga *et al.*, 1991), where genetic sequence flanking the region of interest and the ERY resistance cassette from pVA891 (Macrina *et al.*, 1983) were PCR amplified, purified and subsequently cloned into a modified pBluescript SK⁺ II vector that had the *Bam*HI site removed by end-filling, generating pBl_adeRS. Confirmed clones were re-cloned into *Xba*I-digested pEX18Tc (Hoang *et al.*, 1998). The resulting pEX18Tc_adeRS vector was introduced into ATCC 17978 cells via electroporation, as previously described (Dorsey *et al.*, 2002). Transformants were selected on LB agar supplemented with ERY. Counter-selection was undertaken on M9 minimal agar containing ERY and 5% sucrose. The second method used to generate $\Delta adeA$, $\Delta adeB$ and $\Delta adeAB$ strains utilised the RecET recombinase system with modifications (Tucker *et al.*, 2014). Briefly, 400-600 bp of sequence flanking the gene(s) were used as templates in a nested overlap extension PCR with the ERY resistance cassette from pVA891 (Macrina *et al.*, 1983). Approximately, 3.5-5 μ g of the purified linear PCR product was electroporated into ATCC 17978 cells harbouring the vector pAT04 and recovered as previously described (Tucker *et al.*, 2014). Recombinants were selected on LB agar supplemented with ERY. All mutants generated in this study were confirmed by PCR amplification and Sanger sequencing. Primers utilised to generate mutant strains are listed in Table 2.2.

For genetic complementation of mutant strains, WT copies of *adeRS* and *adeAB* were cloned into pWH1266 (Hunger *et al.*, 1990) where transcription was driven by the TET promoter. Resulting plasmids denoted pWH::*adeRS* and pWH::*adeAB*, respectively were confirmed by Sanger sequencing. The GEN resistance cassette from pUCGM (Schweizer, 1993) was PCR amplified and cloned into *Bam*HI digested pWH::*adeAB* generating pWHgent::*adeAB* thus abrogating transcription from the pWH1266 TET promoter. Plasmids were introduced into appropriate *A. baumannii* cells as previously described (Eijkelkamp *et al.*, 2013). Primers used to generate complementation vectors are listed in Table 2.2.

2.4.4 Cell treatments and RNA isolation

RNA was isolated from WT and $\Delta adeRS$ cells and Hi-seq RNA transcriptome analysis performed following methodologies as outlined previously (Giles *et al.*, 2015). For pentamidine stress assays, WT and $\Delta adeRS$ strains were grown overnight in MH broth,

sub-cultured 1:100 in fresh medium and grown to $OD_{600} = 0.6$; they were subsequently split into two 10 mL cultures. One 10 mL sample was treated with 7.8 mg/L of pentamidine ($0.5 \times \text{MIC}$ for $\Delta adeRS$), whilst the other remained untreated. Cultures were grown for an additional 30 min before total RNA was extracted as outlined previously (Giles *et al.*, 2015).

2.4.5 Bioinformatic analysis

Bioinformatic analysis of RNA-seq data was undertaken as described previously (Giles *et al.*, 2015), with the modification that obtained reads were mapped to the recently re-sequenced *A. baumannii* ATCC 17978 genome (GenBank: CP012004). RNA-seq data have been deposited in the gene expression omnibus database, accession number GSE102711 (<https://www.ncbi.nlm.nih.gov/geo/query/acc.cgi?acc=GSE102711>).

2.4.6 Quantitative Real-Time PCR

Pentamidine stress and RNA-seq validation experiments were achieved using a two-step qRT-PCR method. RNA samples were first purified as previously described (Giles *et al.*, 2015), subsequently DNaseI treated (Promega) and then converted to cDNA using an iScript™ cDNA synthesis kit (Biorad), following the manufacturer's instructions. The cDNA generated was used as a template for qRT-PCR using the SYBR® Green JumpStart™ Taq readymix™ (Sigma) in a 20 µl final volume. Either a Rotor-Gene Q (Qiagen, Australia) or RG-3000 (Corbett Life Science, Australia) instrument was used for quantification of cDNA using the following protocol; 1 min at 95°C, followed by 40 cycles of 10 sec at 95°C, 15 sec at 57°C and 20 sec at 72°C. Melt curve analyses were undertaken to ensure only the desired amplicon was generated. Primers used (Table 2.2) for amplification of cDNA transcripts were designed using NetPrimer (www.premiersoft.com). Transcriptional levels for RNA-seq validation experiments were corrected to *GAPDH* levels prior to normalisation to the ATCC 17978 WT. For pentamidine stress experiments, transcriptional levels of *adeA* were corrected to 16S rDNA levels prior to being normalised to their respective untreated *A. baumannii* cultures. Transcriptional variations were calculated using the $2^{-\Delta\Delta CT}$ method (Livak and Schmittgen, 2001). Results for pentamidine stress experiments display the mean Log_2 fold change (\pm SEM) of three biological replicates each undertaken in triplicate. Statistical analyses were performed by Student's *t*-test, two-tailed, unpaired; ** = $P < 0.01$ and *** = $P < 0.001$.

2.4.7 Phenotypic microarray analysis

A. baumannii $\Delta adeRS$ cells were cultured on LB agar overnight at 37°C. A suspension of cells was made from a single colony in Biolog IF-0 inoculation fluid (Biolog, Inc.) to 85% transmittance and was subsequently diluted 1:200 in Biolog IF-0 containing dye A (Biolog, Inc.) and 0, 8, 16, 32 or 64 mg/L pentamidine. One hundred μ L of each dilution was added to each well of the Biolog PM01 and PM02A MicroPlates and placed in an Omnilog automatic plate reader (Biolog, Inc.) for 72 h at 37°C. Colour formation from the redox active dye (Biolog dye A) was monitored every 15 min. Data obtained from respiration of $\Delta adeRS$ under different pentamidine conditions were individually overlaid against the untreated control using the OmniLog File Management/Kinetic Analysis software v1.20.02, and analysed using OmniLog Parametric Analysis software v1.20.02 (Biolog, Inc.).

2.5 Results

2.5.1 Generation of $\Delta adeRS$ and complemented strains

The *adeRS* operon of *A. baumannii* ATCC 17978 was disrupted through the introduction of an ERY resistance cassette to produce a $\Delta adeRS$ strain. Complementation of $\Delta adeRS$ was achieved via reintroduction of a WT copy of *adeRS* *in trans* on the pWH1266 shuttle vector, generating $\Delta adeRS$ pWH::*adeRS* and comparisons were made to cells carrying the empty vector control ($\Delta adeRS$ pWH1266). To ensure deletion of *adeRS* did not affect viability, growth was monitored by OD₆₀₀ readings in MH broth over an 8 h period; results identified no significant perturbations in the growth rate in laboratory media compared to WT cells (data not shown).

2.5.2 Transcriptomic profiling of $\Delta adeRS$

Transcriptome profiling by RNA-seq of RNA isolated from $\Delta adeRS$ compared to that from WT ATCC 17978 identified 290 differentially expressed (≥ 2 -fold) genes; 210 up-regulated and 80 down-regulated (Figure 2.1 and Appendix A). RNA-seq results were confirmed by quantitative Real-Time PCR (qRT-PCR) for nine genes that displayed different levels of expression in $\Delta adeRS$ compared to WT; a good correlation between methods was observed (Figure 2.2). Expression of a number of efflux proteins was affected by inactivation of *adeRS*. For example, the *craA* major facilitator superfamily transporter (ACX60_01760) shown to confer resistance to chloramphenicol and recently chlorhexidine efflux (Li *et al.*, 2016a) was the highest up-regulated gene (7.1-fold; Figure 2.1) and *adeA* (ACX60_09125), *adeB* (ACX60_09130) and *aceI* (ACX60_07275) which

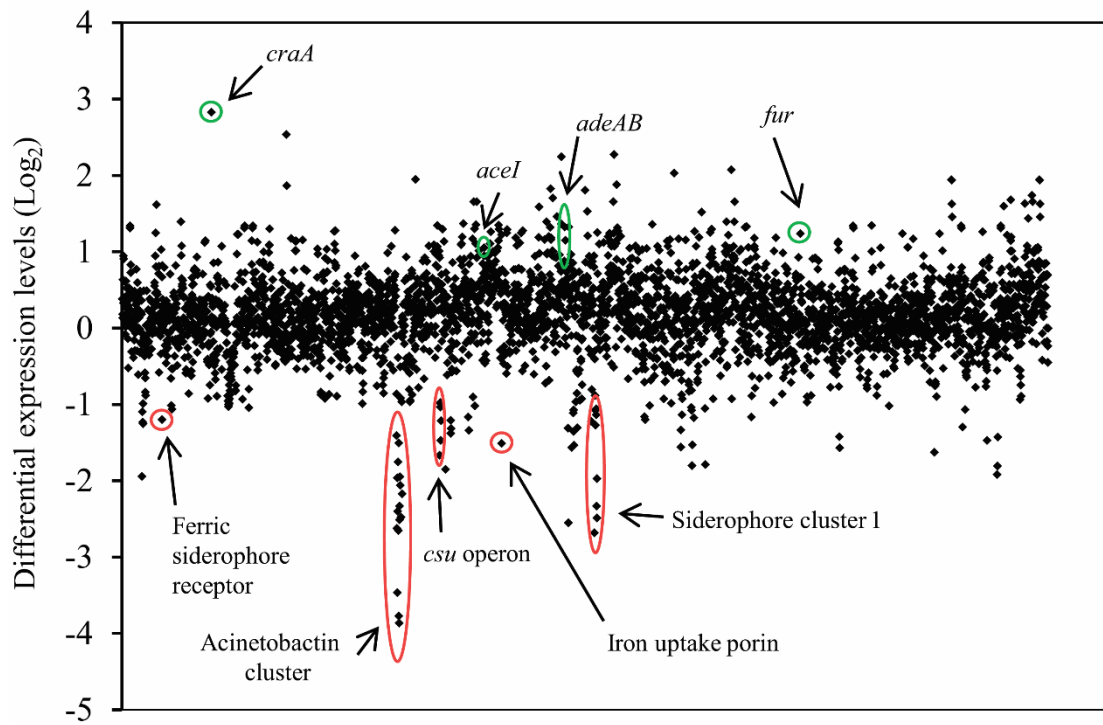


Figure 2.1: Global transcriptomic response differences of *A. baumannii* ATCC 17978 after deletion of *adeRS*

Each diamond marker represents a predicted gene within the genome ordered according to locus tag along the X-axis and differential expression generated from normalised reads per kilobase mapped of WT against $\Delta adeRS$ are displayed on the Y-axis (Log_2). Positive and negative Log_2 -values correlate to up- and down-regulated genes, respectively. Green and red circles highlight genes/gene clusters of interest that have been up- and down-regulated, respectively. See Appendix A for the full list of genes that were differentially expressed ≥ 1 Log_2 fold.

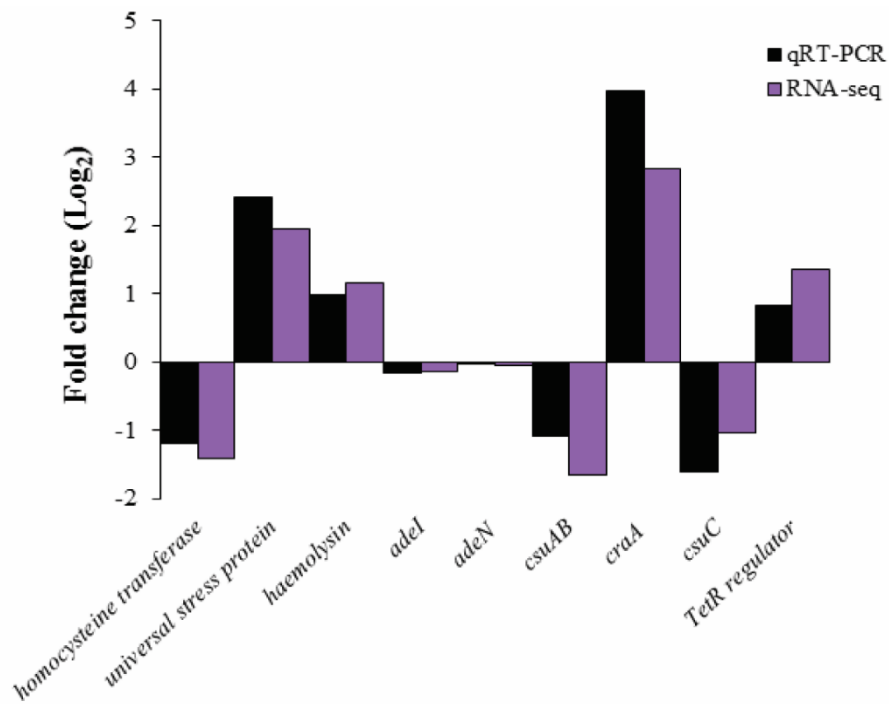


Figure 2.2: Validation of RNA-sequencing results

The transcriptomic results obtained by RNA-seq were validated by qRT-PCR analysis. The level of nine genes that displayed differential expression or remained essentially unchanged between $\Delta adeRS$ and WT ATCC 17978 were chosen for comparison. Expression levels for qRT-PCR experiments were corrected to those obtained for *GAPDH* (ACX60_05065) prior to normalisation against WT ATCC 17978 transcriptional levels. Grey and black bars represent values obtained from RNA-seq and qRT-PCR results, respectively. Differential expression between $\Delta adeRS$ and WT ATCC 17978 are given in Log₂-values.

encode the AdeAB and the AceI efflux pumps, were up-regulated by 2.5-, 1.43-, and 2-fold, respectively, following deletion of *adeRS*.

Expression of multiple genes involved in virulence were down-regulated in the Δ *adeRS* strain, including the type 1 pilus operon *csuA/BABCDE* (ACX60_06480-06505) (3.2- to 2-fold) and the siderophore-mediated iron-acquisition systems acinetobactin (ACX60_05590-05680) and siderophore 1 (ACX60_09665-09720) clusters (7.7- to 1.1-fold and 5.4- to 0.3-fold, respectively). In contrast, the ferric uptake regulator gene (*fur*) (ACX60_13910) was up-regulated 2.4-fold. Despite these alterations in expression levels of iron siderophore clusters and their regulator, no significant growth defects were identified when Δ *adeRS* was grown in the presence of 200 μ M of DIP (data not shown).

2.5.3 Deletion of *adeRS* in ATCC 17978 reduced susceptibility to a limited number of antimicrobial agents

To assess if changes in expression of the *adeAB* and *craA* drug efflux genes identified in the transcriptome of the Δ *adeRS* derivative translated to an alteration in resistance profile, antibiogram analyses were undertaken. Resistance to a number of antibiotics including those that are known substrates of the CraA and AdeABC pumps were assessed. Surprisingly, despite *craA* being the highest up-regulated gene, no change in resistance to the primary substrate of CraA, chloramphenicol (Li *et al.*, 2016a), was seen (data not shown). Previous studies examining the level of antimicrobial resistance conferred by AdeABC indicate that only when deletions are generated in strains which overexpress AdeABC is there a significant impact on the antibiogram (Magnet *et al.*, 2001; Marchand *et al.*, 2004; Rajamohan *et al.*, 2010b; Yoon *et al.*, 2015; Richmond *et al.*, 2016), implying that AdeABC confers only minimal to no intrinsic resistance. This was supported in our analysis as the MIC for TET, tigecycline, GEN, kanamycin, nalidixic acid, ampicillin, streptomycin and amikacin, all previously identified AdeABC substrates, remained unchanged, whilst resistance to norfloxacin and ciprofloxacin increased 2-fold (data not shown) and chlorhexidine decreased 2-fold for the Δ *adeRS* mutant compared to WT (Table 2.3).

A variety of additional compounds were tested, primarily focusing on substrates of other multidrug efflux pumps and/ or clinically relevant compounds, these included; colistin, polymyxin B, rifampicin, triclosan, novobiocin, benzalkonium, methyl viologen, pentamidine, DAPI and dequalinium. Of these, significant differences in the MICs of Δ *adeRS* versus WT were observed only for the diamidine compounds, pentamidine and DAPI, where an 8- and 4-fold reduction in resistance was identified, respectively

Table 2.3: Antibiotic susceptibility of *A. baumannii* ATCC 17978, deletion mutants and complemented strains

Strain	MIC (mg/L) ^{ab}		
	PENT	DAPI	CHX
WT	125	4	8
<i>ΔadeA</i>	15.6	1	4
<i>ΔadeB</i>	15.6	1	4
<i>ΔadeAB</i> ^c	15.6	1	4
<i>ΔadeRS</i> ^d	15.6	1	4
<i>ΔadeRS</i> pWH:: <i>adeRS</i>	125	1	8
<i>ΔadeRS</i> pWH1266	15.6	0.5	4/2
<i>ΔadeRS</i> pWH:: <i>adeAB</i>	31.3	4	4
<i>ΔadeRS</i> pWHgent:: <i>adeAB</i>	15.6	1	4
<i>ΔadeRS</i> pWHgent	7.8	0.5	4
<i>ΔadeA</i> pWHgent:: <i>adeAB</i>	62.5	2	8/4
<i>ΔadeA</i> pWHgent	7.8	0.5	4
<i>ΔadeB</i> pWHgent:: <i>adeAB</i>	62.5	4	4
<i>ΔadeB</i> pWHgent	7.8	1	2
<i>ΔadeAB</i> pWHgent:: <i>adeAB</i>	62.5	4	4
<i>ΔadeAB</i> pWHgent	7.8	1	2

^aPENT, pentamidine; DAPI, 4',6-diamidino-2-phenylindole; CHX, chlorhexidine.

^bValues highlighted in bold-face type indicate MIC values altered two-fold or greater compared to WT.

^cAntimicrobials that did not significantly differ from WT susceptibility levels included gentamicin, kanamycin, norfloxacin, ciprofloxacin, ampicillin, colistin, polymyxin B, dequalinium, tigecycline, triclosan and methyl viologen.

^dAntimicrobials tested that did not significantly differ from WT susceptibility levels included rifampicin, benzylnonium, streptomycin, amikacin and novobiocin as well as antimicrobials listed above in 'c' with the exception of ciprofloxacin and norfloxacin.

(Table 2.3). Thus, taken together the $\Delta adeRS$ strain showed reduced resistance to the bisbiguanide chlorhexidine, and the diamidines pentamidine and DAPI which display structural similarities (Brown and Skurray, 2001) (Figure 2.3). Resistance to these substrates was partially or fully restored by complementation using $\Delta adeRS$ pWH::*adeRS* (Table 2.3).

2.5.4 Both AdeA and AdeB are required for intrinsic antimicrobial resistance in ATCC 17978

Since the 10-bp direct repeat where AdeR has been demonstrated to bind in other *A. baumannii* strains (Chang *et al.*, 2016; Wen *et al.*, 2017) is also present in the ATCC 17978 *adeA-adeR* intercistronic region (data not shown), we hypothesised that the decreased resistance towards the subgroup of dicationic compounds seen in $\Delta adeRS$ resulted from changes in *adeAB* expression. To test this, deletion strains targeting *adeAB*, as well as individual *adeA* and *adeB* mutations were generated in ATCC 17978.

Using $\Delta adeAB$, MIC analyses verified that deletion of the pump resulted in negligible changes in resistance to a subset of the antimicrobials tested for $\Delta adeRS$ (data not shown). However, an identical resistance pattern for the dicationic compounds as that afforded by $\Delta adeRS$ was observed (Table 2.3). Complementation of the inactivated genes partially restored resistance to all compounds, validating that AdeAB plays a direct role in resistance to these dicationic compounds (Table 2.3).

2.5.5 AdeRS is critical for increased expression of *adeAB* following pentamidine exposure

From MIC analysis of the ATCC 17978 derivatives, it was proposed that the presence of the AdeRS TCSTS increased *adeAB* expression consequently providing resistance to pentamidine, chlorhexidine and DAPI (Table 2.3). To confirm this, the level of *adeA* transcription was assessed by qRT-PCR of RNA isolated from WT and $\Delta adeRS$ strains after addition of a sub-inhibitory concentration of pentamidine. Transcription of the *adeAB* operon was significantly up-regulated in WT and down-regulated in $\Delta adeRS$ following pentamidine stress (Figure 2.4). Additionally, qRT-PCR was used to determine if *adeS* expression levels altered after pentamidine stress in WT cells. It was found that *adeS* expression increased less than <2-fold compared to untreated WT cells (data not shown). To phenotypically support the transcriptional evidence that *adeRS* initiates transcription of the ATCC 17978 *adeAB* operon, additional antibiograms were assessed.

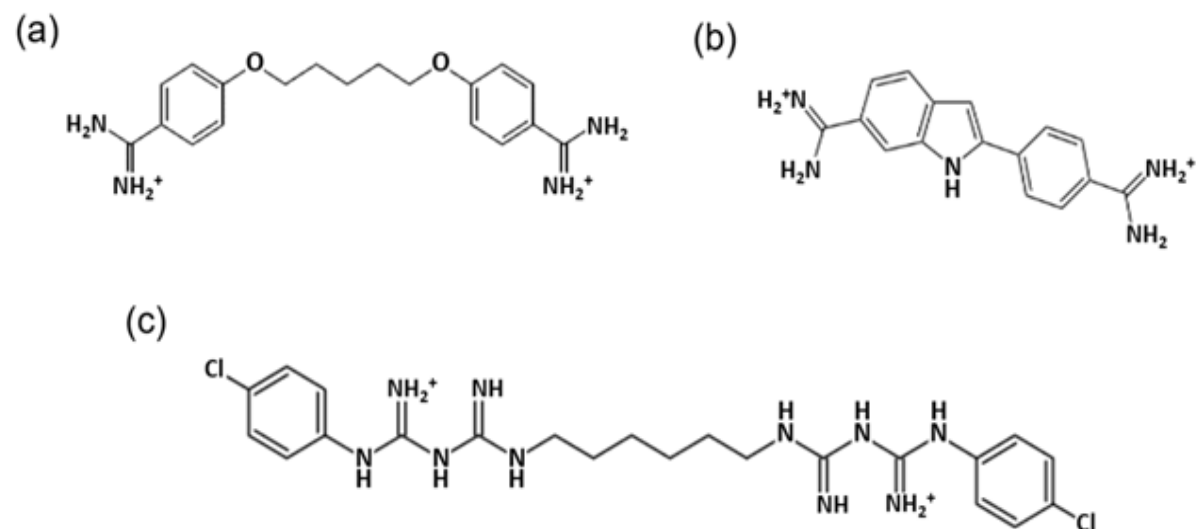


Figure 2.3: Structures of dicationic antimicrobial compounds to which $\Delta adeRS$, $\Delta adeA$, $\Delta adeB$ and $\Delta adeAB$ deletion mutant derivatives showed a decrease in resistance when compared to WT ATCC 17978

Compounds include (a) pentamidine, (b) DAPI and (c) chlorhexidine. For pentamidine and chlorhexidine, the cationic nitrogenous groups are separated by a long carbon chain, forming symmetrical compounds, whereas, DAPI lacks this long linker and is asymmetric.

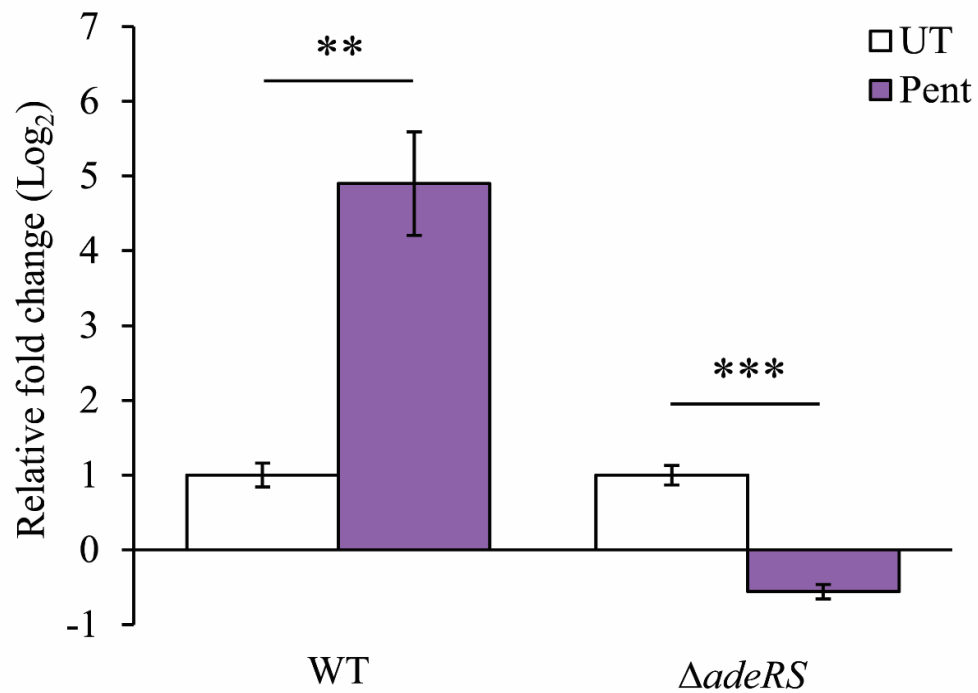


Figure 2.4: Increased expression of *adeA* following pentamidine stress is dependent on the presence of AdeRS in ATCC 17978

Transcriptional levels of *adeA* (ACX60_09125) from WT and $\Delta adeRS$ were determined by qRT-PCR after 30 min shock with 7.8 mg/L of pentamidine (Pent) ($0.5 \times$ MIC of $\Delta adeRS$) and corrected to untreated cells (UT) after normalisation to 16S. Bars represent the mean fold change (Log₂) of three biological replicates undertaken in triplicate, and error bars represent \pm SEM. Statistical analyses were performed by Student's *t*-test, two-tailed, unpaired; ** = $P < 0.01$ and *** = $P < 0.001$.

Using the shuttle vector pWH1266, two clones were constructed; pWH::*adeAB* and pWHgent::*adeAB*, where the GEN resistance cartridge cloned in the latter vector inhibited transcription of *adeAB* from the TET promoter naturally present in pWH1266. MIC analyses determined that the carriage of pWHgent::*adeAB* in Δ *adeRS* did not differ from results obtained for Δ *adeRS*. Conversely, Δ *adeRS* cells with pWH::*adeAB* displayed a 4- and 8-fold increase in pentamidine and DAPI resistance, respectively (Table 2.3). Collectively, these results suggest that expression of *adeAB* and subsequent resistance to the dicationic compounds in ATCC 17978 can only occur when AdeRS is present.

2.5.6 Carbon source utilisation alters resistance to pentamidine

Pentamidine, a drug known to be effective in the treatment of fungal and protozoan infections has gained recent attention in a bacterial context. Pentamidine has shown synergy with Gram-positive antibiotics, potentiating their activity towards Gram-negative bacteria (Stokes *et al.*, 2017). As such, pentamidine has been proposed to be utilised as an adjunct therapy for MDR bacteria, including *A. baumannii* (Stokes *et al.*, 2017). To identify additional pentamidine resistance mechanisms employed by *A. baumannii*, growth in different media was assessed. Disk diffusion assays identified that in *A. baumannii*, resistance to pentamidine was affected by the carbon source provided in M9 minimal medium (Table 2.4), whilst for chlorhexidine and DAPI this pattern was not conserved indicating a pentamidine-specific response (data not shown). To determine the MIC levels for pentamidine, plate dilution experiments were undertaken for WT, Δ *adeRS* and Δ *adeAB* strains provided with varied carbon sources (Figure 2.5). Growth of Δ *adeRS* and Δ *adeAB* cells on MH agar were significantly perturbed at 32 mg/L of pentamidine. This MIC drastically differs when succinic acid was utilised as the sole carbon source, as growth was maintained up to 512 mg/L of pentamidine for all strains tested (Figure 2.5). Fumaric, α -ketoglutaric and oxaloacetic acids also increased pentamidine resistance by 8-fold for Δ *adeRS* and Δ *adeAB* strains when compared to the MIC obtained for MH agar. Growth of Δ *adeRS* and Δ *adeAB* mutants was inhibited at a higher dilution factor in the presence of oxaloacetic acid compared to fumaric and α -ketoglutaric acids whilst growth using citrate as the sole carbon source negatively affected resistance to WT cells, decreasing resistance 2-fold.

Biolog phenotypic arrays were undertaken to identify additional synergistic or antagonistic relationships between carbon sources and pentamidine resistance. Respiration of Δ *adeRS* cells for a total of 190 carbon compounds was assessed at various pentamidine concentrations (Appendix B). From this, an additional ten compounds were

Table 2.4: Zones of clearing obtained from growth on M9 minimal medium with the addition of different carbon sources after exposure to pentamidine

Strain	Zone of clearing (mm) ^{ab}				
	WT	$\Delta adeRS$	$\Delta adeAB$	$\Delta adeA$	$\Delta adeB$
M9 Minimal Medium					
+ glucose	1.8 ± 0.2	5.2 ± 0.1	5.8 ± 0.4	6.2 ± 0.6	6.9 ± 0.3
+ citric acid	2.7 ± 0.8	5.4 ± 0.8	5.1 ± 0.4	5.1 ± 0.5	6.0 ± 0.2
+ isocitric acid	1.2 ± 0.3	5.7 ± 0.1	ND ^c	ND	ND
+ α -ketoglutaric acid	0 ± 0	0 ± 0	0 ± 0	0 ± 0	0 ± 0
+ succinic acid	0 ± 0	0 ± 0	0 ± 0	0 ± 0	0 ± 0
+ fumaric acid	0 ± 0	0 ± 0	0 ± 0	0 ± 0	0 ± 0
+ malic acid	0.9 ± 0.4	5.4 ± 0.5	ND	ND	ND
+ oxaloacetic acid	1.2 ± 0.3	1.6 ± 0.5	1.7 ± 0.5	1.6 ± 0.6	1.7 ± 0.5
+ pyruvic acid	1.3 ± 0.1	4.4 ± 1.3	ND	ND	ND
+ glutamic acid	1.1 ± 0.2	5.4 ± 0.2	ND	ND	ND

^aZones of clearing determined on M9 minimal medium with each carbon source used at a final concentration of 0.4 %. Pentamidine (125 μ g) was deposited onto a paper disc (5 mm diameter) and zones of growth inhibition determined after overnight incubation at 37 °C

^bAverage dimension of inhibition zones was determined by obtaining the diameter from the edge of bacterial growth to the disc (mm), \pm represents standard deviation values determined from averages obtained from at least three independent experiments undertaken in duplicate

^cND, not done

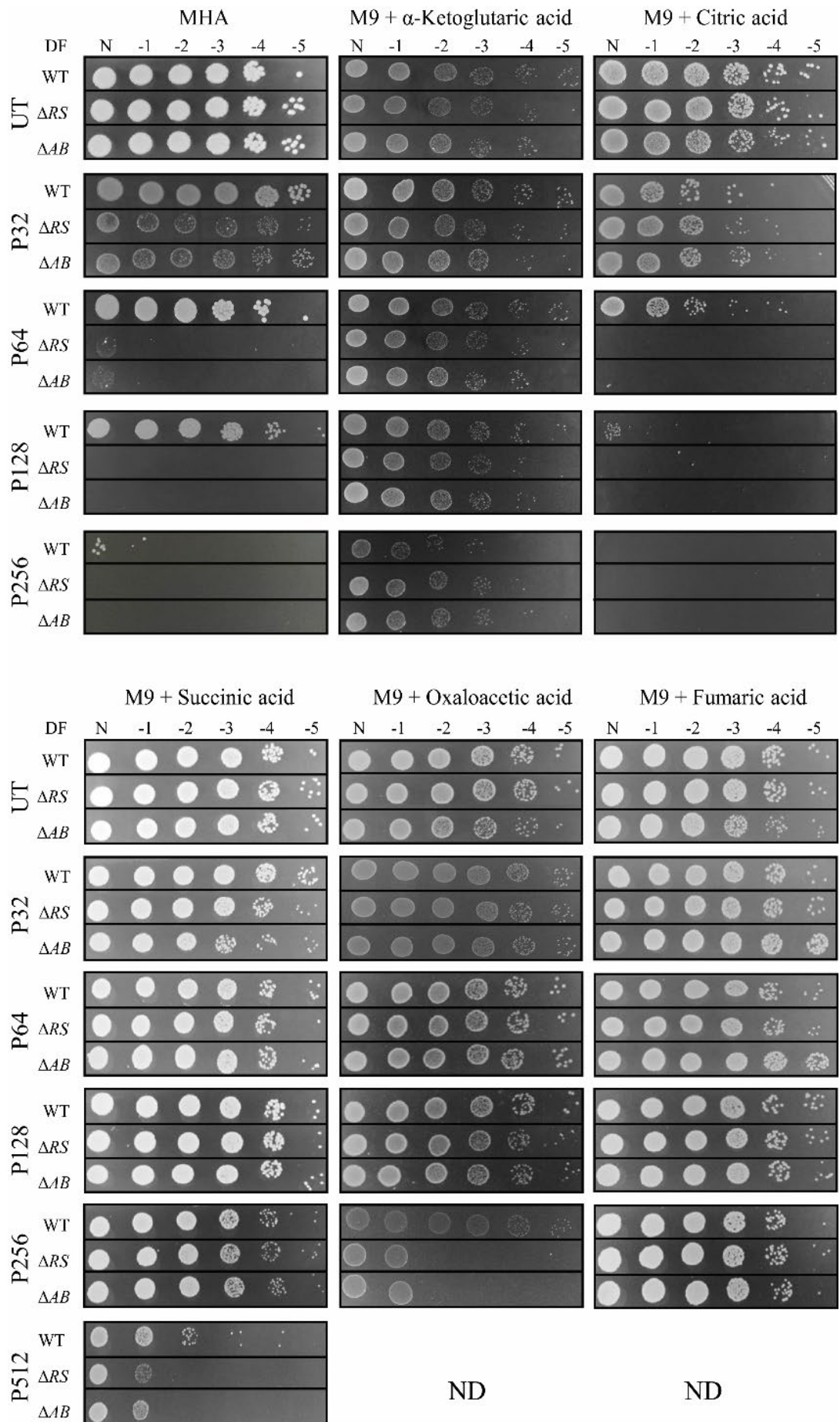


Figure 2.5: Resistance to pentamidine is modulated by carbon sources available in the growth medium

Ten-fold serial dilutions of *A. baumannii* ATCC 17978 (WT), $\Delta adeRS$ (ΔRS) and $\Delta adeAB$ (ΔAB) cells were used to compare the concentration of pentamidine that inhibits growth in different media, Mueller-Hinton agar (MHA) was used as a comparative control. Images display serial 1:10 dilutions after overnight incubation at 37°C, where DF is abbreviated for dilution factor and N represents undiluted cells. Strains were grown in the absence of pentamidine (UT) or presence of 32, 64, 128, 256 and 512 mg/L of pentamidine (P32, P64, P128, P256, and P512, respectively). Carbon sources tested in M9 minimal medium were used at a final concentration of 0.4% (w/v). ND, not done due to precipitation of pentamidine once added into the molten medium. Figures are representative examples of results obtained.

identified that increased resistance to pentamidine in $\Delta adeRS$ at 64 mg/L (Figure 2.6). Despite minimal changes in pentamidine resistance in the presence of citric acid for $\Delta adeRS$ (Figure 2.6), this compound negatively affected respiration at lower pentamidine concentrations (Appendix B). Surprisingly, succinic, α -ketoglutaric and fumaric acids failed to restore respiration at 64 mg/L of pentamidine for $\Delta adeRS$ (Appendix B). By extending the incubation period for another 72 h, respiration in the presence of succinic or fumaric acids was restored to levels similar to the untreated control (data not shown). This may indicate that succinic and fumaric acids significantly lag in their ability to recover the cells from pentamidine in the IF-0 medium (Biolog Inc.) whilst α -ketoglutaric acid recovery is dependent on growth medium.

2.5.7 Bioavailability of iron correlates with pentamidine resistance

Iron has been shown to influence pentamidine resistance in protozoan sp. (Wong and Chow, 2006), thus we assessed if it plays a similar role in *A. baumannii*. The addition of ferrous sulphate to the growth medium significantly reduced the zone of clearing from pentamidine in a dose-dependent manner up to a final concentration of 5 mM for WT and mutant strains (Table 2.5 and Figure 2.7). Furthermore, chelation of iron using DIP resulted in WT cells becoming more susceptible to pentamidine compared to the untreated control (Table 2.5). This modified pentamidine susceptibility is iron specific as inclusion of other cations in the growth medium (zinc, copper, manganese, cobalt, nickel) did not significantly affect the zones of clearing (data not shown). Using inductively-coupled plasma mass spectrometry the internal iron concentration in WT and $\Delta adeRS$ cells was determined in the absence/presence of a sub-inhibitory concentration of pentamidine. Internal iron concentrations remained essentially unchanged in both strains under the different conditions tested (data not shown), indicating that iron/pentamidine interactions may occur outside of the cell and the observed response was not due to a reduced capacity to store iron.

2.6 Discussion

The *adeRS* and *adeABC* operons of *A. baumannii* have gained considerable attention due to their role in regulating and conferring multidrug resistance, respectively (Marchand *et al.*, 2004; Yoon *et al.*, 2013; Nowak *et al.*, 2016; Richmond *et al.*, 2016). Multiple genetic arrangements of the *adeABC* operon in *A. baumannii* clinical isolates exist, where 35% of 116 diverse isolates lack the *adeC* OMP component (Nemec *et al.*, 2007). This is also the case for the clinical isolate *A. baumannii* ATCC 17978, which was

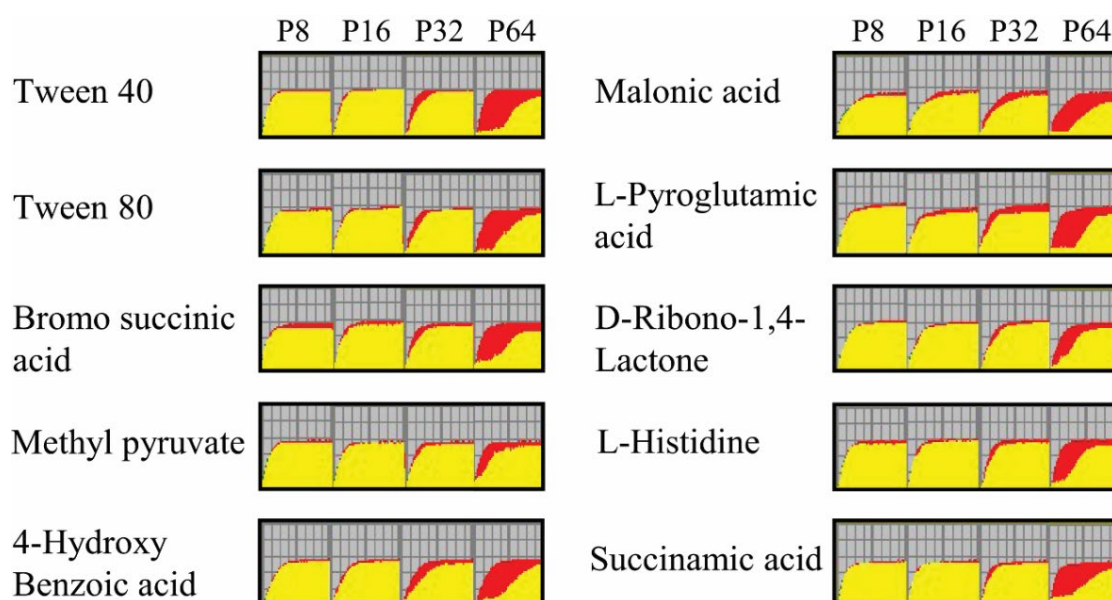


Figure 2.6: Kinetic response curves paralleling bacterial growth from Biolog PM01 and PM2A plates identify ten carbon sources that increase pentamidine resistance in $\Delta adeRS$

P8, P16, P32 and P64 represent kinetic response curves at 8, 16, 32, or 64 mg/L of pentamidine compared to the untreated control, respectively. Red curves represent respiration of untreated $\Delta adeRS$, whilst respiratory activity which overlaps between the control and the sample in the different experimental conditions is represented in yellow. Only carbon compounds that promote at least 50% maximal respiration and induce a recovery response by 36 h are shown. See Appendix B for respiration curves for all tested treatments.

Table 2.5: Zones of clearing for *A. baumannii* ATCC 17978 and deletion mutants grown on Mueller-Hinton agar with the addition or chelation of iron after pentamidine exposure

Strain	Zone of clearing (mm) ^{ab}				
	WT	$\Delta adeRS$	$\Delta adeAB$	$\Delta adeA$	$\Delta adeB$
Medium^c					
MHA control	1.4 ± 0.3	6.9 ± 0.5	6.9 ± 0.3	6.9 ± 0.4	7.2 ± 0.4
+ 2.5 mM FeSO ₄	0.8 ± 0.1*	5.4 ± 0.2*	5.6 ± 0.3*	5.4 ± 0.1***	5.6 ± 0.1***
+ 5 mM FeSO ₄	0.7 ± 0.2*	2.5 ± 0.8***	2.8 ± 0.3***	3.2 ± 0.3***	2.9 ± 0.6***
+ 7.5 mM FeSO ₄	NG	NG	NG	NG	NG
+ 100 μM DIP	1.7 ± 0.1	6.7 ± 0.2	6.9 ± 0.1	6.2 ± 0.2	6.6 ± 0.2
+ 200 μM DIP	5 ± 0.3***	6.7 ± 0.4	6.6 ± 0.4	6.1 ± 0.1	6.4 ± 0.1

^aAveraged values are displayed ± SD. Statistical analyses were performed by Student's *t*-test, two-tailed, unpaired; * = $P < 0.0005$ and *** = $P < 0.000001$.

^bValues given in bold-face type indicate a significant difference between a strain grown under iron-rich or iron-limited conditions versus its respective MHA control.

^cMHA, Mueller-Hinton agar; FeSO₄, ferrous sulphate; DIP, 2',2' dipyridyl; NG, no growth due to iron toxicity

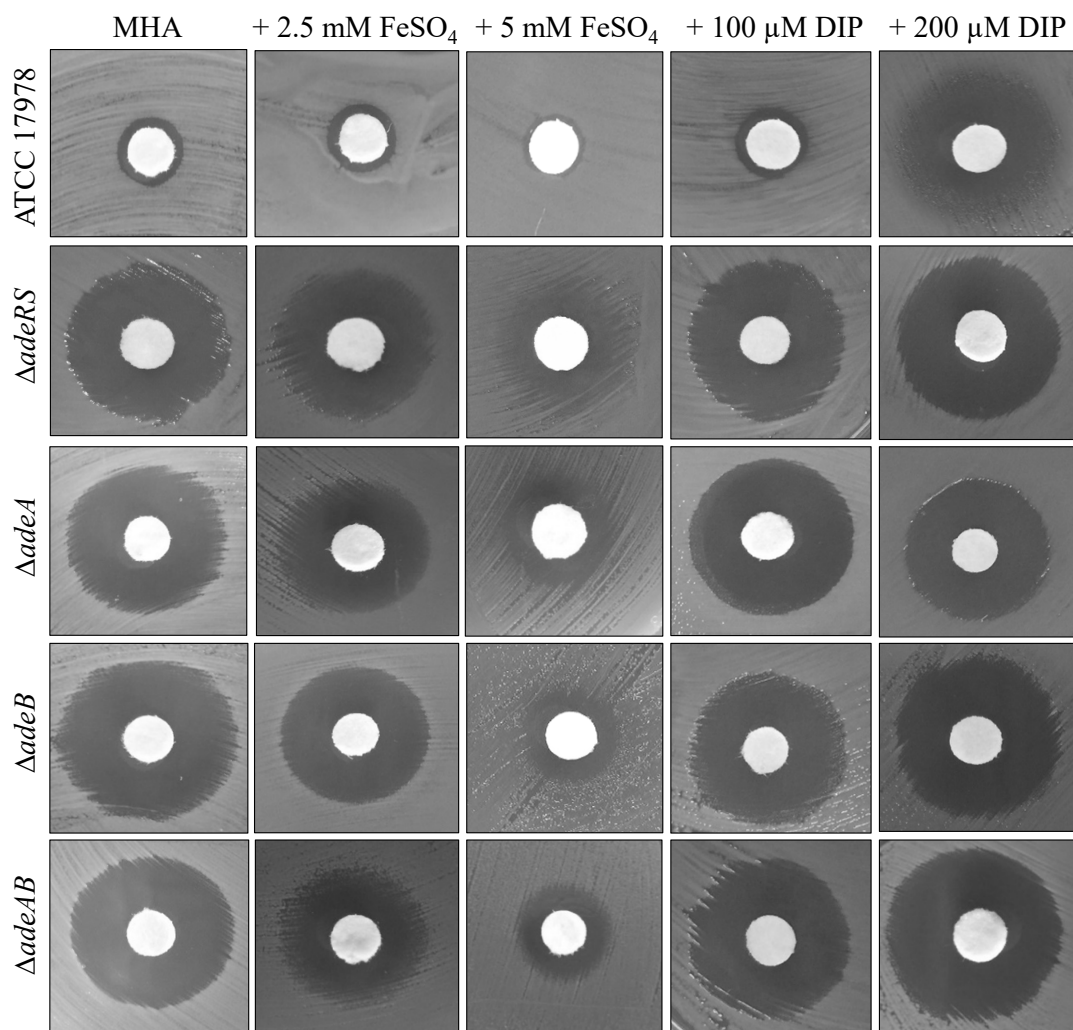


Figure 2.7: Pentamidine resistance is affected by the concentration of iron within the growth medium

Resistance to pentamidine was assessed by disc diffusion assays in Mueller-Hinton agar (MHA) for *A. baumannii* ATCC 17978 and $\Delta adeRS$, $\Delta adeA$, $\Delta adeB$ and $\Delta adeAB$ deletion derivatives. Zones of clearing were compared to iron rich conditions from the addition of ferrous sulphate (FeSO₄) at the final concentrations of 2.5 and 5 mM and iron-chelated conditions obtained by the addition of 2',2' dipyridyl (DIP) at the final concentrations of 100 and 200 μM in MHA. Images displayed are a representative of the typical results obtained.

chosen for further analysis in this study. It is not uncommon for RND pumps to recruit an alternative OMP to form a functional complex (Fralick, 1996; Mine *et al.*, 1999; Chuanchuen *et al.*, 2002). This may also be the situation for AdeAB in *A. baumannii* ATCC 17978, since in an *Escherichia coli* background, *adeAB* can be co-expressed with *adeK*, an OMP belonging to the *A. baumannii* AdeIJK RND complex to confer resistance (Sugawara and Nikaido, 2014). However, whether AdeB can work alone or function with alternative membrane fusion proteins such as *adeI* or *adeF* is not known. As the resistance profile of $\Delta adeA$ was indistinguishable from the $\Delta adeAB$ and $\Delta adeB$ strains, it provides confirmatory evidence that both *adeA* and *adeB* are required for efficient efflux to only a subset of dicationic compounds in ATCC 17978. Further assessments will be required to verify if this phenotype is maintained across other *A. baumannii* isolates and extends to other structurally-similar compounds.

It has been found previously, that the introduction of shuttle vectors expressing WT copies of genes *in trans* do not restore resistance profiles back to WT levels as also seen in this study (Saroj *et al.*, 2012; Liou *et al.*, 2014; Li *et al.*, 2016c; Wang *et al.*, 2018). Using qRT-PCR, *adeS* was expressed at low levels in WT cells even after pentamidine shock (data not shown). Complementation studies with *adeRS* thus could be influenced by copy number effects, which may perturb the native expression levels of these proteins within the cell. Additionally, the differing modes of action of the dicationic compounds may have influenced the MIC results, as fold-shifts in resistance were observed even when the empty pWH1266 vector was being expressed (Table 2.3).

The transcriptomic analysis of ATCC 17978 $\Delta adeRS$ revealed changes in gene expression were not limited to *adeAB* but included many genes, some of which have been shown to be important in *A. baumannii* pathogenesis (Tomaras *et al.*, 2003; Gaddy *et al.*, 2012) and virulence *in vivo* (Murray *et al.*, 2017). Although this had been seen before in an *adeRS* mutant generated in the MDR *A. baumannii* isolate AYE (Richmond *et al.*, 2016), here the transcriptional changes were to a largely different subset of genes. Previously, deletion of *adeRS* in AYE resulted in decreased expression of *adeABC* by 128-, 91-, and 28-fold, respectively (Richmond *et al.*, 2016). This decreased gene expression was expected as AYE naturally contains a point mutation in AdeS (producing an Ala 94 to Val substitution in AdeS) resulting in constitutive expression of *adeABC* and contributing to its MDR phenotype (Fournier *et al.*, 2006; Richmond *et al.*, 2016). Richmond *et al.*, (2016) proposed that the high similarities in phenotypic changes between their *adeRS* and *adeB* AYE deletion derivatives were largely due to downstream

effects caused by reduced expression of *adeABC* (Richmond *et al.*, 2016). We cannot rule out the possibility that some of the changes in gene expression in our study have resulted from the slight increase seen in expression of *adeAB*, most likely caused by polar effects exerted by the ERY resistance cassette. However, our transcriptome data indicated *adeAB* were expressed at low levels and thus represent basal levels of expression; results consistent with ATCC 17978 being labelled as a ‘drug susceptible’ isolate (Smith *et al.*, 2007).

Currently, the environmental signal(s) that interact with the periplasmic sensing domain of AdeS are not known. Antimicrobial compounds can directly stimulate autophosphorylation of specific TCSTS which in turn directly regulate the expression of genes providing resistance to that compound (Koteva *et al.*, 2010; Li *et al.*, 2016b). It is unlikely that pentamidine is the environmental stimulus that is sensed by AdeS, as a number of conditions, including chlorhexidine shock, can also up-regulate *adeAB* expression in ATCC 17978 (Camarena *et al.*, 2010; Eijkelkamp *et al.*, 2011a; Hassan *et al.*, 2013; Lin *et al.*, 2015). Instead, AdeS may respond to stimuli such as solutes that are excreted and accumulate in the periplasm when cells are subjected to various stressors including AdeAB substrates.

This study revealed unique interactions between pentamidine and a number of carbon sources which significantly alter the resistance profile to pentamidine for *A. baumannii* ATCC 17978 and derivatives. Biolog phenotypic arrays identified a number of succinic acid derivatives that also allowed respiration in the presence of a lethal concentration of pentamidine (Figure 2.6). Interestingly, when $\Delta adeRS$ utilised malonic acid as the sole carbon source, a potent inhibitor of the succinate dehydrogenase complex, cells were also able to respire at increased pentamidine concentrations (Figure 2.6). In Gram-negative bacteria, the mechanism of action for pentamidine is thought to primarily occur via binding to the lipid-A component of the outer membrane and not through inhibition of an intracellular target (David *et al.*, 1994; Stokes *et al.*, 2017). Therefore, it seems unlikely that pentamidine interferes with enzymatic functions like that of succinate dehydrogenase, and instead the compounds which showed an increase in pentamidine resistance may contribute to either chelation of the compound or provide protective mechanisms that reduce binding to the lipid-A target. Interestingly, a 1956 study (Amos and Vollmayer, 1957) identified that in the presence of α -ketoglutaric or glutamic acid, resistance to a lethal concentration of pentamidine could be achieved in *E. coli*, leading to the proposition that pentamidine interferes with the transaminase reaction in glutamic

acid production. However, our study shows that glutamic acid does not affect pentamidine resistance (Table 2.4), inferring that a different mechanism might be responsible for the increase in pentamidine resistance in *A. baumannii*.

Iron is an essential metal serving as a co-factor in numerous proteins involved in redox chemistry and electron transport. It is generally a limited resource for pathogenic bacteria such as *A. baumannii* where it is important for virulence and disease progression (Gaddy *et al.*, 2012; Wright *et al.*, 2017a). Our studies showed that altering iron levels also had a marked effect on resistance to pentamidine. This is in agreement with the observation that citric and gluconic acids can act as iron-chelating agents (Hamm *et al.*, 1953; Pecsok and Sandera, 1955) and respiration activity in the presence of these compounds at the pentamidine concentrations tested were significantly altered (Appendix B). Many clinically relevant antimicrobials have shown to be affected by the presence of iron, including compounds belonging to TET, aminoglycoside and quinolone classes (Ezraty and Barras, 2016). Activity of these compounds can be altered by numerous factors, including the formation of stable complexes which can affect drug efficacy or have unfavourable effects on patient health. Understanding the metabolic flux in *A. baumannii* and other MDR bacteria has the potential to lead to more effective therapeutic interventions thus reducing infection rates, knowledge critical to slow the progress towards our re-entry into a pre-antibiotic era.

2.7 Conclusions

Overall, this is the first study which has demonstrated that the AdeAB system in *A. baumannii* ATCC 17978 provides intrinsic resistance to a subset of dicationic compounds, and efflux of these compounds via AdeAB is directly regulated by the AdeRS TCSTS. RNA-seq identified that deletion of *adeRS* produced significant changes in the transcriptome where our results support the notion that strain specific variations are apparent (Richmond *et al.*, 2016). We have provided evidence that in ATCC 17978, AdeRS is directly responsible for the activation of *adeAB* gene expression, as Δ *adeRS* failed to increase expression upon subjection to one of the pumps newly identified intrinsic substrates, pentamidine. It will be of interest to assess whether these dicationic compounds also extend as substrates towards AdeAB(C) pumps present in other *A. baumannii* isolates and if expression levels of *adeAB(C)* upon exposure to these substrates and other potential stressors also occur. This information may help to identify the stimulus that activates the AdeRS TCSTS. We have also demonstrated for the first

time that for pentamidine to exert its antibacterial effect in *A. baumannii*, a dependence on the availability of iron is required, and that growth in the presence of selected carbon sources has a profound effect on its resistance.

**CHAPTER 3: Deletion of a two component
signal transduction system in
Acinetobacter baumannii ATCC 17978
promotes secondary loss-of-function
mutations in the AdeN global regulator**

Declaration by candidate

In Chapter 3 the nature and extent of my contribution to the work was as follows:

Nature of contribution	Contribution extent (%)
Conceptualisation, data curation, methodology performance of experiments, writing, editing and revision of the manuscript	85

The following co-authors contributed to the work

Name	Nature of contribution	Contribution extent (%)
Uwe Stroehler	Initial conceptualisation, data curation	5
Shashikanth Marri	Data curation, formal analysis	5
Melissa Brown	Conceptualisation, editing and revision of draft and final manuscript	5

The undersigned hereby certify the above declaration correctly reflects the nature and extent of the candidate and co-author contribution to this work.

Candidate signature		17.8.19
---------------------	--	---------

Supervisor signature		17.8.19
----------------------	--	---------

3.1 Preface

This chapter formulates a manuscript by **Adams, F.G.**, Stroehrer, U.H., Marri S. and Brown M.H. ‘Deletion of a two component signal transduction system in *Acinetobacter baumannii* ATCC 17978 promotes secondary loss-of-function mutations in the AdeN global regulator’ prepared for submission to *Frontiers in Cellular and Infection Microbiology* as a Brief Research Report.

3.2 Abstract

Two component signal transduction systems are complex regulatory mechanisms that bacteria employ to enable rapid adaptation to a vast array of environmental conditions. Despite their fundamental roles in gene regulation, the signalling networks afforded by these systems in the human pathogen, *A. baumannii*, remain largely unknown. Thus, this study aimed to characterise the putative two component signal transduction system comprised of the response regulator (11155) and hybrid histidine kinase (11160) encoded at the ACX60_11155/60 loci in the strain ATCC 17978. *In silico* analyses revealed 11155 to be a LuxR-type response regulator and 11160 a solute symporter fused hybrid histidine kinase that adopts a novel architecture to previously characterised bacterial histidine kinases. Deletion of the *11155* determinant promoted novel loss-of-function mutations in *adeN*, a TetR-type global transcriptional repressor that controls expression of genes involved in antimicrobial resistance and virulence. Orthologues of 11155/11160 were identified on both chromosomes and plasmids within sp. belonging to the Proteobacteria family and comparative gene alignments of a diverse set of strains from gamma-, beta- and alpha-proteobacteria revealed co-localisation of these with an ABC transporter cluster, inferring a possible co-evolutionary relationship. Overall, this study has identified an essential two component signal transduction system within *A. baumannii* ATCC 17978, demonstrating the first example of adaptive mutagenesis to cope with the deletion of a response regulator in *A. baumannii* and characterised a unique subtype of bacterial regulation, highlighting the complexity of signalling networks adopted by this formidable pathogen.

3.3 Introduction

Acinetobacter baumannii is an opportunistic nosocomial human pathogen responsible for numerous epidemic outbreaks worldwide (Wong *et al.*, 2017). A large portion of its pathogenic success is attributed to its remarkable genetic plasticity, enabling rapid accumulation of numerous resistance and persistence phenotypes (Wright *et al.*, 2017a).

Although some virulence factors have been identified for *A. baumannii* (Harding *et al.*, 2018), information pertaining to the regulatory circuitry responsible for coordination of these known and unknown virulence-associated determinants remains limited.

Two component signal transduction systems (TCSs) are the paradigm for bacterial stimulus-responsive adaptation, playing significant roles in regulating virulence determinants and metabolic processes (Stock *et al.*, 2000; Zschiedrich *et al.*, 2016). In the most basic scheme, a stimulus is detected by the extracytoplasmic sensory domain of a membrane-bound histidine kinase (HK), eliciting conformational changes across the lipid membrane to the cytoplasmic kinase domains, catalysing autophosphorylation of a conserved histidine residue located in the His kinase A domain (HisKA) by the ATPase domain. The phosphoryl group is subsequently transferred to a conserved aspartate residue within the receiver (REC) domain of the cognate response regulator (RR), triggering a cellular response. More complex versions of TCSs exist, requiring additional phosphotransfer reactions, including those involving hybrid histidine kinases (HHKs), which contain kinase domains in addition to a C-terminal REC domain (Appleby *et al.*, 1996). A histidine-containing phosphotransfer domain (Hpt) intermediate is required for transferring a phosphoryl group to its cognate RR, located either on a separate protein or fused to the HHK, the latter termed unorthodox HKs (Appleby *et al.*, 1996). The additional phosphotransfer reactions required by these systems may have evolved to prevent unwanted crosstalk (Capra *et al.*, 2012).

Whilst the principal features facilitating signal flow are highly conserved, the sensory component of HKs are significantly diverse (Mascher *et al.*, 2006). One unique example is proteins that combine solute carrier (SLC) domains with cytosolic TCS domains and are believed to function by coupling solute uptake across the lipid membrane to illicit signals that modulate activity of adjoining HK domains. To date, only three systems adopting this structure have been characterised; the ammonium transporter fused HK *Ks-Amt5* from *Kuenenia stuttgartiensis* (Pflüger *et al.*, 2018) and the CbrSR and CbrAB TCSs, both present within sp. from Gammaproteobacteria (Zhang *et al.*, 2015; Sepulveda and Lupas, 2017; Monteagudo-Cascales *et al.*, 2019). A new structural domain linking N-terminal transporter domains to the C-terminal HK domains termed STAC, due to its presence in SLC and TCS-Associated Component proteins, are present across the majority of symporter fused HKs (Korycinski *et al.*, 2015), however their biological significance remains unclear.

A number of TCS containing hybrid or classical HKs have been characterised in *A. baumannii*, revealing diverse regulons with many directly influencing resistance and overall virulence potential (De Silva and Kumar, 2019). Despite playing key roles in regulating virulence determinants, less than half of the TCS encoded by *A. baumannii* have been experimentally investigated, highlighting a largely unexplored area of research. In this work, the putative TCS encoded at the gene loci ACX60_11155/60 of *A. baumannii* ATCC 17978 was investigated. The *11155* and *11160* genes are co-transcribed in the same polypeptide. Deletion of *11155* promoted secondary loss-of-function mutations in the TetR-type regulator, AdeN. Investigations into the conserved domains and topology of *11160* unveiled a unique architecture, adding to the small list of bacterial solute symporter fused HHKs. Broader level examination revealed that this TCS is enriched across Proteobacterial sp. with a tendency to co-localise with ABC transporter genes, suggestive of a co-evolutionary relationship.

3.4 Methods

3.4.1 Strains and growth conditions

A. baumannii ATCC 17978 (wildtype; WT) and *Escherichia coli* strains were cultured under aerobic conditions using lysogeny broth (LB) or LB agar at 37°C, unless otherwise stated. When required, antibiotics were added at the following concentrations: ampicillin, 100 mg/L; erythromycin (ERY), 25 mg/L; and tetracycline (TET), 12 mg/L. Bacterial strains, plasmids and oligonucleotides used in this study are listed in Table 3.1 and Table 3.2, respectively. Growth kinetics of strains of interest were assessed as outlined previously (Hassan *et al.*, 2017). Briefly, overnight cultures were diluted to an optical density at 600 nm (OD₆₀₀) of 0.01 and growth determined by OD₆₀₀ measurements taken every 15 min on a FLUOstar Omega (BMG Labtech).

3.4.2 Construction of *A. baumannii* deletion strains

Generation of deletion derivatives was achieved using *sacB*- or Rec_{Ab}-based strategies as previously described in Section 2.4.3 with minor modifications. In brief, *sacB*-based gene deletion was achieved by introduction of pEX_11155RR into *E. coli* SM10 cells and mobilised into *A. baumannii* ATCC 17978 by conjugal transfer. *Trans*-conjugates were re-streaked and checked by PCR before counter-selection on M9 minimal agar containing sucrose (5%) and Ery. For mutants constructed by the Rec_{Ab}-deletion method, PCR used pEX_11155RR as template; 30 µg of purified PCR product was introduced into ATCC 17978 harbouring pAT04 and cells recovered as previously described

Table 3.1: Strains and plasmids used in the study

Strain or plasmid	Genotype or description ^a	Reference/ source
<u><i>A. baumannii</i> strains</u>		
ATCC 17978	Non international type clone; meninges isolate (designated as WT)	ATCC (Smith <i>et al.</i> , 2007)
$\Delta 11155$ $\Delta adeN::ISAba12$	ATCC 17978 with ERY ^R insertion disruption in <i>11155</i> and <i>ISAba12</i> in <i>adeN</i>	This study
$\Delta 11155 adeN_{Gly54Asp}$	ATCC 17978 with ERY ^R insertion disruption in <i>11155</i> and <i>adeN_{Gly54Asp}</i>	This study
ATCC 17978 + pAT04	ATCC 17978 with pAT04	This study
<u><i>E. coli</i> strains</u>		
DH5 α	F ⁻ $\Phi 80lacZ\Delta M15 \Delta(lacZYA-argF)$ U169 <i>recA1 endA1 hsdR17</i> (rK ⁻ , mK ⁺) <i>phoA supE44 $\lambda^- thi-1 gyrA96 relA1$</i>	(Hanahan, 1983)
SM10	<i>thi thr leu tonA lacY supE recA::RP4-2-Tc::Mu Km λpir</i>	(Simon <i>et al.</i> , 1983)
<u>Plasmids</u>		
pAT04	TET ^R ; pMMB67EH with Rec _{Ab} system	(Tucker <i>et al.</i> , 2014)
pEX18Tc	TET ^R ; suicide vector	(Hoang <i>et al.</i> , 1998)
pEX_ <i>11155RR</i>	TET ^R , ERY ^R ; pEX18Tc with <i>11155</i> flanking regions and ERY resistance cassette cloned via <i>XbaI</i>	This study
pVA891	CHL ^R , ERY ^R ; source of ERY ^R cassette	(Macrina <i>et al.</i> , 1983)

^aCHL, chloramphenicol; ERY, erythromycin; ^R, resistant; TET, tetracycline

Table 3.2: Primers used in the study

Primer name/ purpose	Sequence (5' - 3')^a	Reference/ source
<u>Primers used for construction of $\Delta 11155$ via <i>sacB</i> strategy</u>		
<i>11155RR_UFR_F</i>	GAGATCTAGATTACCAGAACGTT GGGCTAGC	This study
<i>11155RR_UFR_R</i>	GAGAGGATCCCAATTGCACTTAA CCCATCGG	This study
<i>11155RR_DFR_F</i>	GAGAGGATCCAGACTCACTGCT AAAAATAGGC	This study
<i>11155RR_DFR_R</i>	GAGAGAGCTCCCAAACGAGATAA GG	This study
<i>ERY_F</i>	GAGAGGATCCCTTAAGAGTGTGT TGATAGTGC	This study
<i>ERY_R</i>	GAGAGGATCCCTCATAGAATTAT TTCCTCCG	This study
<u>Primers used for construction of $\Delta 11155$ via <i>Rec_{Ab}</i> strategy</u>		
<i>11155_NOL F</i>	GAACAGCTTGAACA	This study
<i>11155_NOL R</i>	AACAGCAATGGCACTCACC	This study
<u>Primers used for cloning and sequencing of <i>adeN</i></u>		
<i>adeN_F</i>	GAGAGGATCCGTGAACATACAGT TACATGATC	This study
<i>adeN_R</i>	GAGAGTCGACGTTTCATAACCTTTT GGTGATGC	This study
<i>adeN_checkseq1_R</i>	GCTCTGGTTGAAATGCAATG	This study
<i>adeN_checkseq2_F</i>	GTGTAGGTGACACATTCCAG	This study
<i>adeN_checkseq3_R</i>	CCCATCATGTGTGCAGCTTC	This study
<u>Primers used for qRT-PCR</u>		
<i>GAPDH_RT_F</i>	CAACACTGGTAAATGGCGTG	This study
<i>GAPDH_RT_R</i>	ACAACGTTTTTCATTTTCGCC	This study
<i>adeN_RT_F</i>	CATGCTGGTGGTTCAAAAAC	This study
<i>adeN_RT_R</i>	GCTCTGGTTGAAATGCAATG	This study
<i>adeI_RT_F</i>	AATTGTTTCAGGGCGTTGTTC	This study
<i>adeI_RT_R</i>	GTTTCAACAGGACGGCTCTC	This study
<i>craA_RT_F</i>	CGGCAGTTCCTTGGGTTA	This study

Primer name/ purpose	Sequence (5' - 3')^a	Reference/ source
<i>craA</i> _RT_R	AACCATATTGCACGCTCGT	This study
<i>csuC</i> _RT_F	GTGGATTAACCGAAGAAAGTCA	This study
<i>csuC</i> _RT_R	GGCTGGCCTTGTTGATTG	This study
<i>csuAB</i> _RT_F	GGTGAACGTACAGACCGCA	This study
<i>csuAB</i> _RT_R	AGTAGCTTGGCCACTTACTGTAGT	This study
<i>pgpB</i> _RT_F	CAACACTGGCTTGTCTGGC	This study
<i>pgpB</i> _RT_R	ATTCTTGAAAGCCCCATACAC	This study
ACX60_17010_RT_F	CAAAAGCAAAGCACCACAA	This study
ACX60_17010_RT_R	GAAGAAGAATCTGGCCATGC	This study
ACX60_14705_RT_F	TTGCCAAAATCTTGAACCAA	This study
ACX60_14705_RT_R	AGTCGCAATACCCCAGTCAT	This study
ACX60_11550_RT_F	CGTGATAATCAGGCGAACTG	This study
ACX60_11550_RT_R	GGTTGACCTGGAGCAACTTT	This study

^aNucleotides in bold-face type represent incorporated restriction sites, TCTAGA, *Xba*I; GGATTC, *Bam*HI; GTCGAC, *Sal*I; GAGCTC, *Sac*I; GCATGC, *Sph*I

(Tucker *et al.*, 2014). Recombinants were selected for on LB agar containing ERY and required 48 h incubation. Primers used for mutant construction are listed in Table 3.2.

3.4.3 Transcriptome profiling and qRT-PCR validation

Hi-seq RNA transcriptome profiling, subsequent bioinformatic analyses and qRT-PCR validation experiments using WT and $\Delta 11155 \Delta adeN::ISAbal2$ cells were performed as previously outlined in Sections 2.4.4, 2.4.5 and 2.4.6. RNA-seq data have been deposited in the gene expression omnibus database, accession number GSE134611. Primers used for validation experiments are listed in Table 3.2.

3.4.4 Bioinformatics

Nucleotide and protein sequence similarity searches used the basic local alignment search tool (Blast) against the national centre of biotechnology information non-redundant sequence (NCBI) database (Wheeler *et al.*, 2003). Domain annotation was based on outputs from the online tools, simple modular architecture research tool (SMART) (Letunic and Bork, 2018) (<http://smart.embl-heidelberg.de/>) and CD-Search from the NCBI conserved domain database (Marchler-Bauer *et al.*, 2017) (<https://www.ncbi.nlm.nih.gov/Structure/cdd/wrpsb.cgi>) (February, 2019). Secondary structures were predicted using Phobius as an integrated component of the Protter visualisation program (Omasits *et al.*, 2014). *E. coli*-derived $\sigma 70$ promoter sequences were determined using the Softberry BPROM tool (<http://www.softberry.com/berry.phtml?topic=bprom&group=programs&subgroup=gfi> [ndb](#)). Orthologues of 11160 were identified using the conserved domain architecture retrieval tool [CDART (Geer *et al.*, 2002)]. Upstream and downstream regions from 12 representative 11160 orthologues were chosen from CDART outputs and used to generate a tBlastx genetic map using Easyfig 2.2.2 (Sullivan *et al.*, 2011). Sequences and their GenBank accession numbers used in alignment are listed in Table 3.3.

3.5 Results

3.5.1 The ACX60_11155/60 genes encode a LuxR-type response regulator and a solute symporter family fused hybrid histidine kinase

To identify TCS that may regulate *A. baumannii* persistence and virulence characteristics, TCS comprised of adjacently orientated HK and RR genes present in the *A. baumannii* strain ATCC 17978, where both genes were absent from the avirulent isolate *A. baumannii* SDF (Fournier *et al.*, 2006), were identified. Six systems in ATCC 17978 fit these criteria; so far three have been experimentally examined (Chapter 2)

Table 3.3: Bacterial strains harbouring orthologues of 11160 used in gene alignments

Strain name	Accession number and reference
<i>A. baumannii</i> ATCC 17978	CP012004 (Weber <i>et al.</i> , 2015b)
<i>Pseudomonas fluorescens</i> PICF7	CP005975 (Martinez-Garcia <i>et al.</i> , 2015)
<i>Pseudomonas stutzeri</i> DSM4166	CP002622 (Yu <i>et al.</i> , 2011)
<i>Alteromonas mediterranea</i> U4	CP004849 (López-Pérez <i>et al.</i> , 2013)
<i>Vibrio natriegens</i> NBRC 15636	CP009977, unpublished
<i>Azoarcus communis</i> TSPY31	CP022187, unpublished
<i>Herbaspirillum seropedicae</i> SmR1	CP002039 (Pedrosa <i>et al.</i> , 2011)
<i>Bordetella pseudohinzii</i> HI4684	CP016440, unpublished
<i>Burkholderia gladioli</i> BSR3 chromosome 1	CP002599 (Seo <i>et al.</i> , 2011)
<i>Rhodopseudomonas palustris</i> DX1	CP002418 (Xing <i>et al.</i> , 2008)
<i>Bradyrhizobium lablabi</i> GAS499	LT670844, unpublished
<i>Acetobacter pasteurianus</i> 386B	HF677570 (Illegheems <i>et al.</i> , 2013)
<i>Rhizobium leguminosarum</i> ATCC 14479	CP030760, unpublished

(Beceiro *et al.*, 2011; Geisinger *et al.*, 2018). TCS encoded at the ACX60_11155/60 loci (subsequently referred to as *11155/11160*) was chosen for further examination.

Initially, the conserved domains of both proteins were identified using SMART software (Adebali *et al.*, 2015), revealing a REC domain (pfam00072; E value, 2.94e-35) and a LuxR-type helix-turn-helix (HTH) DNA-binding domain (pfam00196; E value, 3.14e-19) at the N- and C-termini of 11155, respectively (Figure 3.1). LuxR RRs are the second most common family within bacterial RRs, activating gene expression of target genes by binding to unique sequences within their promoter regions (Galperin, 2010). Using 11160 as a query, outputs identified the kinase core domains HisKA and HATPase_c and a REC domain at its C-terminus, where phosphoactive H and D residues could be identified within the HisKA and REC domains, respectively (Figure 3.1 A and B). Interestingly no conserved domain(s) were found across the N-terminal region of 11160. Thus, an additional platform, CD-Search, (Marchler-Bauer *et al.*, 2017) was employed and the N-terminal region (59-484) of 11160 was found to share significant homology to the SLC5 and 6-like solute binding domain (SLC5-6-like SBD) (Accession number: cl28304; E value, 2.23e-12). This superfamily, widely encountered in bacteria, archaea and higher eukaryotes, is comprised of the sodium-dependent glucose transporter (SLC5), sodium- and chlorine-dependent neurotransmitter transporter (SLC6), and nucleobase-cation-symport-1 (NCS1) transporter subfamilies, which share a similar structural core that functions to translocate small molecules across the membrane energised by sodium/proton gradients (Abramson and Wright, 2009; Patching, 2018). Both searches failed to identify an Hpt domain(s) or additional sensory or linker domains commonly identified in HKs, such as PAS (Wu *et al.*, 2013), GAF (Batchelor *et al.*, 2013) or HAMP (Ferris *et al.*, 2011) domains.

3.5.2 11155 and 11160 are co-transcribed in ATCC 17978

Examination of the *11155/11160* TCS genetic neighbourhood revealed genes encoding an acetyltransferase from the GCN5-related *N*-acetyltransferase (GNAT) family and a putative polar amino acid ABC transporter system comprised of five genes upstream of *11155* (Figure 3.1 C). The ABC transport system contained two genes encoding membrane-associated permeases both having amino acid HisM domains (ACX60_11145 and ACX60_11140), a gene for an amino acid ATP-binding protein with a glutamine transport domain (GlnQ; ACX60_11135), and two genes encoding substrate binding proteins from the Type 2 periplasmic binding-fold superfamily (ACX60_11130/11125)

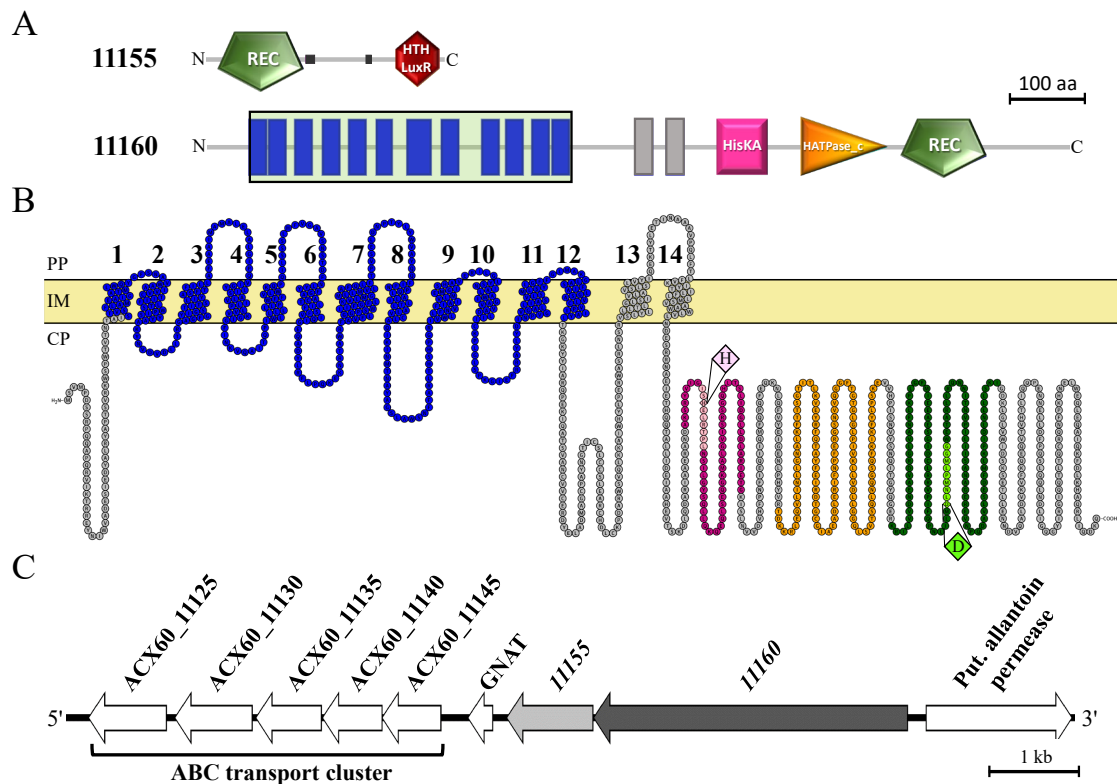


Figure 3.1: Overview of structural and genetic organisation of 11155 and 11160 present in *A. baumannii* ATCC 17978

(A) Conserved domains of 11155/11160 proteins determined by SMART (Letunic and Bork, 2018) with modifications. Sizes and positions of conserved domains are indicated by the coloured symbols; REC, receiver domain; HTH LuxR, LuxR-type DNA binding helix-turn-helix domain; HisKA, His kinase A domain; HATPase_c, histidine kinase, DNA gyrase B, and HSP90-like ATPase domain. Small unlabelled dark grey boxes represent low complexity regions. Blue and grey rectangles denote putative transmembrane segments (TM) localised within or outside of a conserved domain, respectively. The green box indicates the location of the SLC5-6-like SBD superfamily domain as identified by CD-Search (Marchler-Bauer *et al.*, 2017). **(B)** Topology of 11160 generated by Phobius as an integrated component of the Protter visualisation program (Omasits *et al.*, 2014). Coloured regions represent putative conserved domains as demonstrated in (A): blue, SLC5-6-like SBD; fuchsia, HisKA; orange, ATPase; green, REC. Pink and lime coloured residues indicate H- and D-boxes, with diamond markers highlighting the conserved phospho-active His and Asp residues, respectively. Putative TMs are numbered 1-14. PP; periplasm, IM; inner membrane, CP; cytoplasm. **(C)** Schematic representation of genetic loci surrounding 11155/11160 TCS genes on the *A. baumannii* ATCC 17978 chromosome. Downstream of the 11155/60 operon is a gene encoding an acetyltransferase from the GCN5-related *N*-acetyltransferase family (GNAT) and a putative polar amino acid ABC transport system (ACX60_11125-45) whilst a gene encoding a putative allantoin permease is located upstream and transcribed in the opposite direction. The sequence and neighbouring gene names/locus tags are derived from *A. baumannii* ATCC 17978 annotation (GenBank accession: CP012004.1) and visualised using the Easyfig 2.2.2 tool (Sullivan *et al.*, 2011).

with ACX60_11125 possessing a cysteine transporter domain. Divergently transcribed to 11160 was a gene encoding a putative allantoin permease (Figure 3.1 C).

The genes 11155 and 11160 appear to be co-transcribed as a 4-bp ATGA overlap motif could be identified between them. A putative ribosome binding site (AGGA) could also be identified six bp upstream of the start codon of 11155 indicating the protein products are probably not translationally linked. Additionally, putative -35 and -10 promoter sequences could be identified for the downstream GNAT acetyltransferase gene (data not shown) and transcript levels for this acetyltransferase were significantly higher when assessed in the AcinetoCom database (Kröger *et al.*, 2018).

3.5.3 Architecture of 11160 differs to characterised bacterial SLC fused histidine kinases

Both SMART and Protter (Omasits *et al.*, 2014) programs independently predicted 11160 to have 14 TMs of which TM 1-12 were localised within the SLC5-6-like SBD (Figure 3.1). The N-terminus was predicted to be located within the cytoplasm, with TM 13 separated from TM 12 by an 88 amino acid cytosolic loop and TM 14 positioned 46 amino acids upstream of the HisKA domain. The structural configuration of 11160 differs to the two characterised SLC5-fused HKs, CrbS and CbrA (Figure 3.2) which do not possess additional TMs outside of the symporter domain. Previous studies revealed both CrbS and CbrA harbour a STAC domain (Sepulveda and Lupas, 2017), however, this domain was not identified in the 11160 protein sequence (data not shown).

3.5.4 Absence of distinct Hpt proteins in *A. baumannii* genomes infers utilisation of multi-TCS signalling pathways for signal transfer

Typically, the phosphorelay mechanism of a HHK-containing TCS requires an Hpt domain to transfer the phosphoryl group from the HHK REC domain to that of its cognate RR (Casino *et al.*, 2010). Given the absence of an Hpt domain in 11160, Hpt-containing proteins were identified in the ATCC 17978 genome using the Hpt consensus sequence (pfam01627). Five Hpt domains within two multi-domain proteins were identified, one at the C-terminus of the unorthodox GacS orphan HK (Cerqueira *et al.*, 2014) and four across the N-terminus of the CheA chemosensory orphan HK homologue (Chen *et al.*, 2017). Comparison to the genomes of fully sequenced MDR clinical *A. baumannii* isolates revealed that Hpt domains were also restricted to these proteins, suggesting that inter-TCS interactions are required for the 11160/11155 TCS to effectively elicit a response to extracellular stimuli.

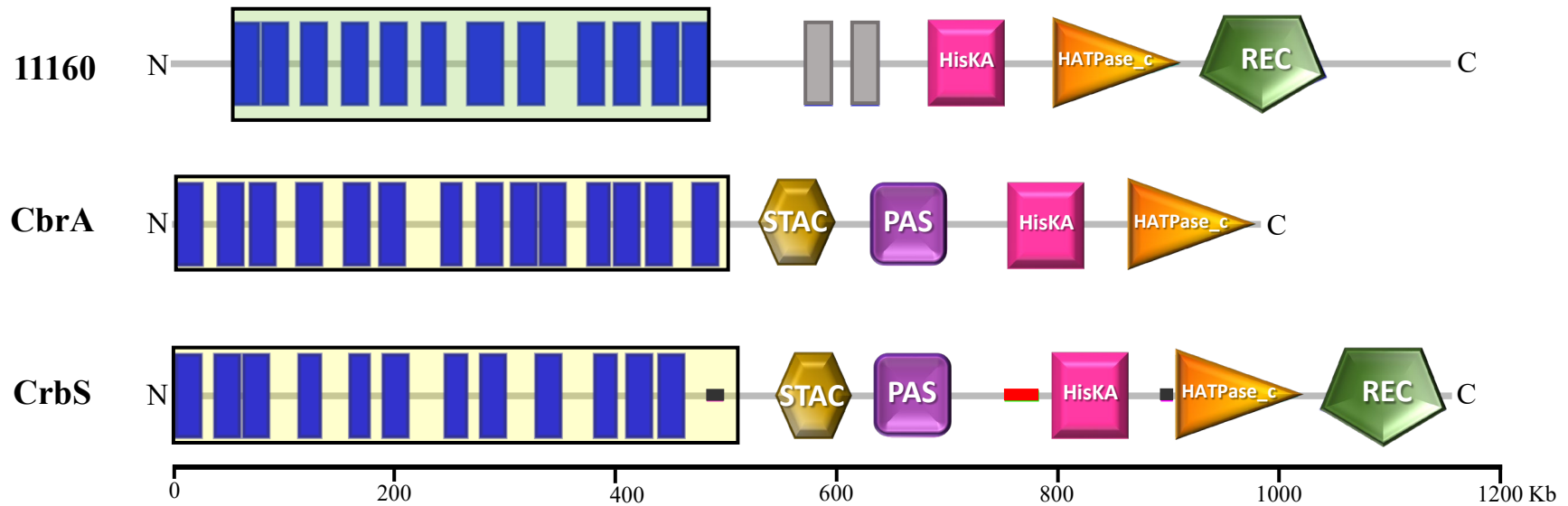


Figure 3.2: Comparison of structural domains of 11160 to CbrA and CbrS from *P. fluorescens* SBW25

Conserved domains were determined by SMART (Letunic and Bork, 2018) with modifications. Sizes and positions of conserved domains are indicated by the coloured symbols: HisKA, His kinase A domain (pink square); HATPase_c, histidine kinase-, DNA gyrase B- and HSP90-like ATPase domain (orange triangle); REC, receiver domain (green pentagon); PAS, Per-Arnt-Sim domain (purple square); STAC, SLC and TCS-associated component domain (gold hexagon). Horizontal rectangular boxes indicate the location of the SLC5-6-like SBD superfamily (light green) and PutP (light yellow) domains as identified by NCBI conserved domain searches (Marchler-Bauer *et al.*, 2017). Vertical bars denote putative TMs are localised within a conserved domain (blue) or outside of a conserved domain (grey). Unlabelled boxes represent low complexity (dark grey) and coiled coil (red) regions. The position of STAC domains (gold hexagon) were manually integrated into the figure based on results obtained from Supulveda and Lupas (2017). Scale bar and N and C termini are shown.

3.5.5 Deletion of *11155* from ATCC 17978 promoted selection for secondary loss-of-function mutations in the AdeN regulator.

To determine a functional role for the 11155/11160 TCS, *11155* was inactivated in *A. baumannii* ATCC 17978 using a *sacB*-based strategy. To ensure the introduced mutation did not significantly impact cell viability the growth rate of $\Delta 11155$ was examined. Only a slight growth delay for $\Delta 11155$ compared to WT cells during exponential phase of growth was observed (Figure 3.3).

The global transcriptional response from deletion of *11155* was investigated using RNA-seq. Significant alterations of the transcriptomic landscape occurred with 232 genes differentially expressed ≥ 2 -fold. Similar to the transcriptome of another ATCC 17978 TCS deletion strain (Figure 2.1, Appendix A), gene clusters involved in iron sequestration, and production of *csu-pili* were down-regulated and expression of *craA*, the chloramphenicol efflux pump and the ferric uptake regulator (*fur*) up-regulated (Figure 3.4 A, Appendix C). A number of unique genetic alterations were also identified, including down-regulation of the putative polar amino acid ABC transport cluster downstream of *11155/11160* (ACX60_11125-45; 5.5- to 2.5-fold), a gene cluster encoding components of a putative Dot/Icm Type IVB secretion system (ACX60_18410-18460; 3.2- to 9.8-fold) as well as the *adeN* TetR-family transcriptional regulator (ACX60_07895; 9-fold). Transcription levels of the *adeIJK* tripartite efflux system, a known target of AdeN were up-regulated (3.3- to 2-fold) and the gene encoded immediately upstream of *adeIJK* (ACX60_03840) encoding a phosphatidylglycerophosphatase thought to be involved in phospholipid production was up-regulated by 6.9-fold (Figure 3.4 A).

Given their importance in conferring multidrug resistance, the transcriptional changes identified for *adeN* and *adeIJK* were further explored. Since AdeN is not deemed self-regulatory (Rosenfeld *et al.*, 2012) it was hypothesised that the 11155/11160 TCS is an overarching regulator of this system. qRT-PCR analyses revealed similar expression changes to those determined by RNA-seq for eight of the nine differently-expressed genes chosen for examination (Figure 3.4 B). Transcriptional changes for *adeN* could not be validated for $\Delta 11155$ as subsequent examination by PCR across the *adeN* locus revealed an ~ 1 kb size increase compared to WT (Figure 3.4 C). Sequencing of this product identified the integration of the insertion sequence element *ISAbal2* within the *adeN* coding region (Figure 3.4 D). Similar to a previous finding, *ISAbal2* inserted into an AT-rich sequence and generated 9 bp target site duplications (Chapter 4). Subsequently, this

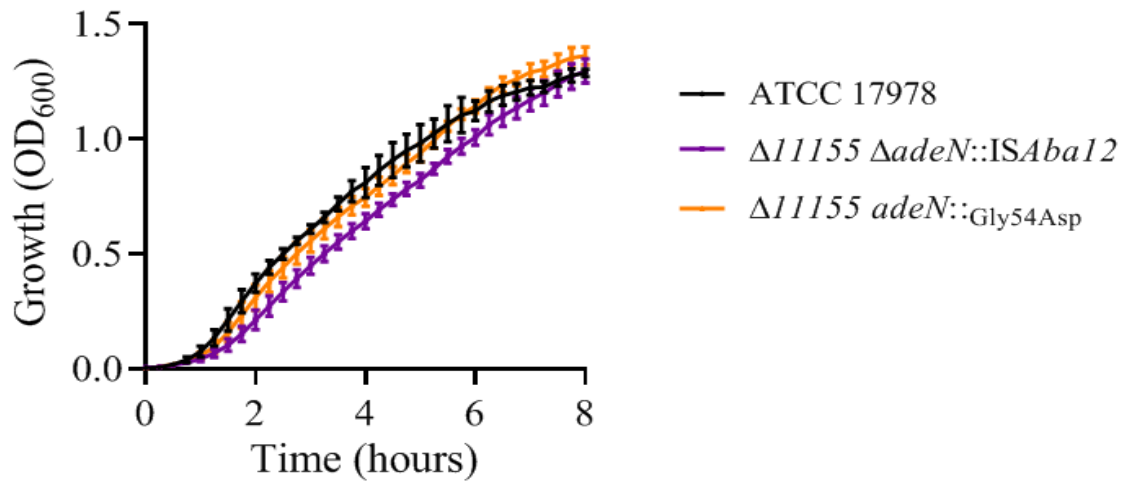
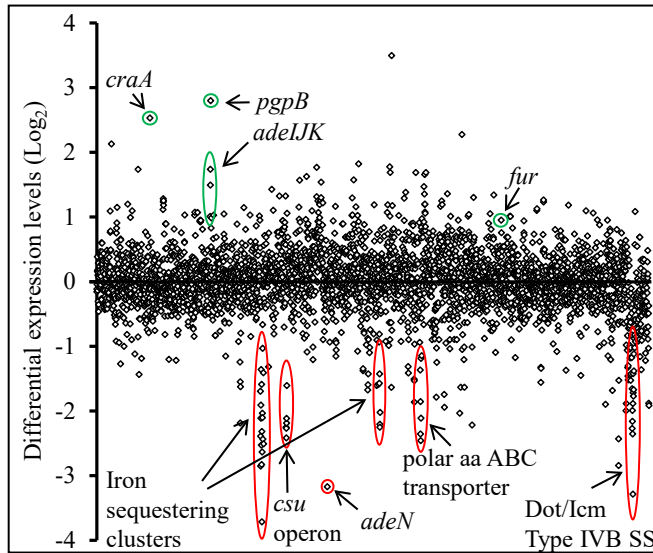


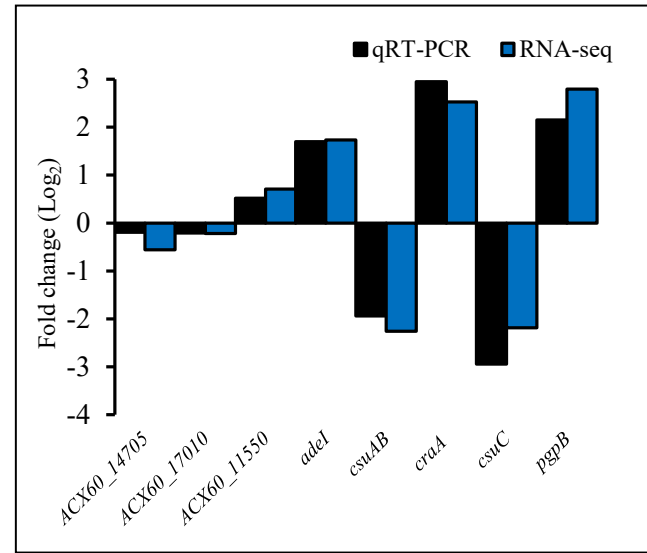
Figure 3.3: Growth kinetics of ATCC 17978, $\Delta 11155 \Delta adeN::ISAbA12$ and $\Delta 11155 adeN_{Gly54Asp}$

ATCC 17978 (WT; black circles), $\Delta 11155 \Delta adeN::ISAbA12$ (purple squares) and $\Delta 11155 adeN_{Gly54Asp}$ (orange triangles) cells were grown in LB medium at 37°C shaking at 100 rpm over eight hours. Cells were diluted to an OD₆₀₀ of 0.01 and measurements taken every 15 mins. Results displayed represent the mean \pm SD from biological quadruplicates.

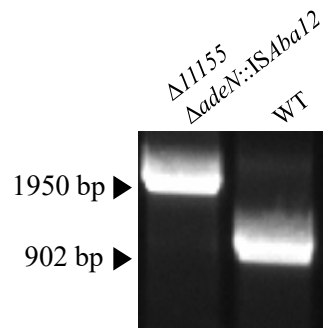
A



B



C



D

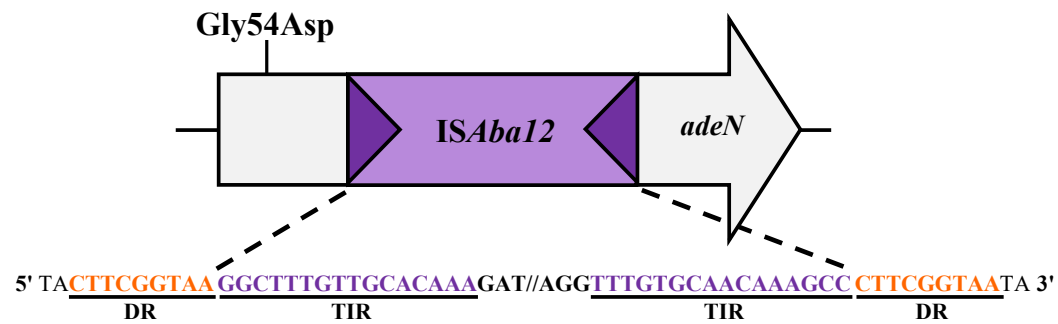


Figure 3.4: Identification of loss-of-function mutations in the global regulator AdeN from an 11155 deletion background

(A) Transcriptomic responses of *A. baumannii* ATCC 17978 compared to $\Delta 11155 \Delta adeN::ISAb12$. Each symbol signifies a predicted open reading frame, ordered on the X-axis according to locus tag with differential expression levels of WT against $\Delta 11155 \Delta adeN::ISAb12$ displayed as Log_2 -fold changes on the Y-axis. Genes up- and down-regulated upon deletion of $\Delta 11155$ in $\Delta adeN::ISAb12$ are displayed above and below the X-axis, respectively. Genes/gene clusters of interest that have been up- and down-regulated are circled in green and red, respectively. See Appendix C for the full list of genes that were differentially expressed $\geq 1 \text{ Log}_2$ fold. **(B)** Validation of RNA-seq results by qRT-PCR analysis. Nine genes were chosen for comparison, with eight displaying results comparable to those obtained by RNA-seq. Expression levels from qRT-PCR experiments for $\Delta 11155 \Delta adeN::ISAb12$ were corrected to that of *GAPDH* (ACX60_05065) prior to normalisation against values for WT cells. Black and blue columns represent values obtained from qRT-PCR and RNA-seq results, respectively. Differential expression levels are displayed in Log_2 values. **(C)** Amplicons generated from PCR across the *adeN* locus from $\Delta 11155 \Delta adeN::ISAb12$ compared to WT. The $\Delta 11155 \Delta adeN::ISAb12$ derived amplicon was ~ 1 kb larger than WT. **(D)** Position of loss-of-function *adeN* mutations identified in $\Delta 11155 \Delta adeN::ISAb12$ background. Open grey arrow depicts the *adeN* gene extents (ACX60_16755) and direction of transcription. The *ISAb12* element (1039 bp) contained a transposase gene flanked by 16 bp perfect terminal inverted repeat sequences (TIR; purple), // denotes break in DNA sequence. The novel direct repeat (DR) insertion sequence is displayed in orange. Location of the Gly54Asp mutation is also shown.

mutant derivative has been renamed $\Delta 11155 \Delta adeN::ISAbal2$.

Since stress conditions, such as growth in the presence of antibiotics, can facilitate movement of insertion sequences in *A. baumannii* (Wright *et al.*, 2017b), an alternative mutant construction method was adopted (Tucker *et al.*, 2014) to aid production of a $\Delta 11155$ derivative without any secondary mutations. Two independent attempts using a modified version of the Rec_{Ab} method failed to yield mutants (Section 2.4.3). However, after additional optimisation (see methods) deletion of *11155* was successful. From 20 potential mutant clones, 19 displayed TET resistance despite not using this antibiotic. It was believed that pAT04 (Tucker *et al.*, 2014), the TET-resistant plasmid required for mutant generation, was still present within these derivatives. Thus, to promote loss of pAT04 from these TET-resistant derivatives, serial passaging of two clones on non-selective LB agar over seven consecutive days was performed. Subsequent growth onto selective media revealed that all examined colonies displayed sensitivity to TET and also towards ERY, inferring that loss of pAT04 led to the reversal of the marked mutation in *11155*.

PCR across the *adeN* locus was performed on the remaining TET-sensitive, ERY-resistant mutant clone. No visible size differences in *adeN* could be seen (data not shown), however, sequencing of this product revealed a SNP (GGT to GAT) resulting in a missense mutation from glycine to aspartic acid at position 54 (Gly54Asp; Figure 3.4 D). This mutation was positioned within the second alpha helix of AdeN and most likely inhibits the ability of the protein to dimerise and repress target gene expression. Growth analyses of this mutant ($\Delta 11155 adeN_{Gly54Asp}$) revealed a slight growth delay compared to WT cells (Figure 3.3). Disk diffusion assays confirmed the novel point mutation also resulted in gene inactivation, as resistance levels towards norfloxacin and chloramphenicol, known AdeIJK substrates, were significantly increased compared to WT, mirroring results seen for $\Delta 11155 \Delta adeN::ISAbal2$ and $\Delta adeN$ (data not shown). Collectively, these results infer that deletion of *11155* could not occur unless secondary loss-of-function mutations in *adeN* were present.

3.5.6 11160 orthologues are present across different classes of the Proteobacteria phyla, frequently co-clustering with ABC transporter genes.

To examine whether orthologues of the 11155/11160 TCS could be identified in other bacterial sp., CDART searches (Geer *et al.*, 2002) were performed with the 11160 protein sequence. Similarity in domain architecture was chosen over traditional Blast searches

due to low primary sequence conservation. CDART searches identified 3261 bacterial sequences exhibiting a comparable domain organisation, with orthologues almost exclusively restricted to the proteobacteria phyla, enriched within alpha- (35.4%), beta- (24.4%) and gamma-proteobacteria (39.5%). From each of these taxonomic classes, four isolates from distinct sp. were further analysed using comparative alignments to identify any commonalities in the genetic region neighbouring the TCSs. Although only distantly related, a five ABC transporter gene cluster was located within close proximity to the TCS from all examined strains (Figure 3.5). In all sequences except *A. baumannii* ATCC 17978, the putative ABC transport system was divergently transcribed to the TCS genes and encoded proteins belonging to the UrtABCDE ABC transporter family responsible for urea uptake (Valladares *et al.*, 2002).

Interestingly, the alignment revealed significant shared identity between a putative allantoin permease (ACX60_11165) and the N-terminal region of the 11160 orthologue from *P. fluorescens* PICF7 (Figure 3.5). Additional analyses revealed that this ATCC 17978 protein possessed a SLC5-6-like SBD (E value, 1.97e-21) and shared 39-47% identity to the N-terminal regions (position ~20-540) of the 11160 orthologues listed in Table 3.3. Furthermore, the 2D topology of the putative allantoin permease also possessed 12 putative TMs.

3.6 Discussion

To gain a greater understanding into the regulatory circuitry that underpins the virulent phenotype of *A. baumannii* ATCC 17978, the putative TCS 11155/11160 was analysed. Conserved domain and genotypic analyses identified this system to contain a co-expressed secondary transporter fused HHK and a LuxR-type RR. Given that the RR component of a TCS is directly responsible for mediating a cellular response, 11155 was deleted from ATCC 17978. Using two different strategies, allelic exchange of 11155 for an Ery resistance cassette promoted two independent loss-of-function mutations in AdeN. From this process two novel AdeN mutations were identified; an insertional disruption by IS*Aba12* and a SNP leading to the missense mutation, Gly54Asp. Transcriptomic studies revealed alterations in expression of 232 genes, including up-regulation of *adeIJK* and downregulation of genes involved in production of a putative Type IVB secretion apparatus and an amino acid transport system. Since subsequent analyses found that the transcriptome was examined in a strain with a loss-of-function mutation in *A. baumannii* *adeN::ISAba12*, the regulon of 11155/11160 could not be ascertained.

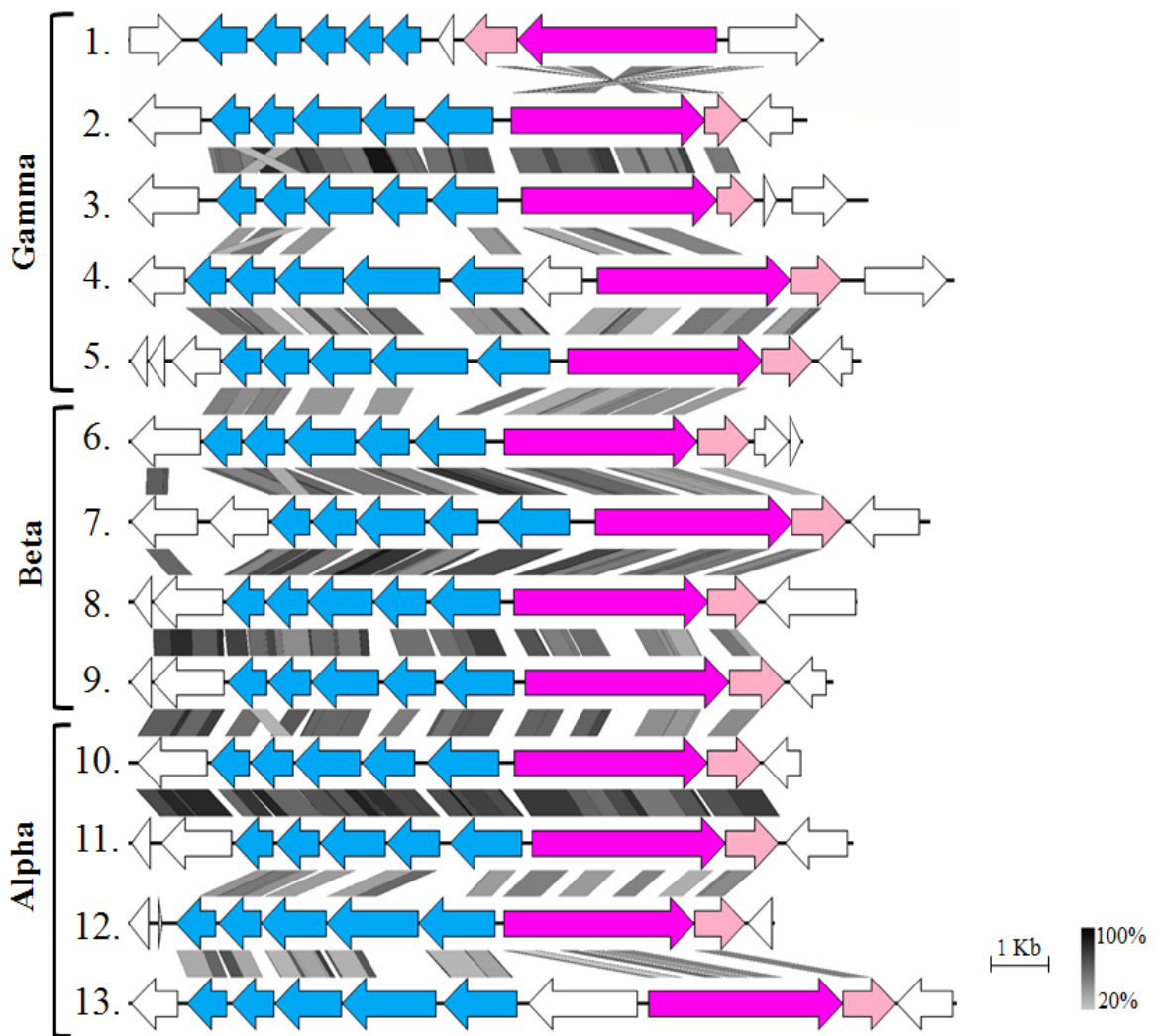


Figure 3.5: Alignment of the genetic region from different proteobacterial species carrying orthologues of the 11155/11160 TCS

Sequences were obtained from the NCBI database and a tBlastx genetic map was generated using the Easyfig 2.2.2 tool (Sullivan *et al.*, 2011). Blast parameters were set at minimum length of 100 bp and a threshold of $E = 0.001$. Arrows indicate the direction of transcription with blue, fuchsia and pink coloured arrows representing ABC transporter, 11160-like and 11155-like genes, respectively. Identity shared between regions is represented by a colour gradient. Sequences are organised by bacterial class; gamma-, beta- or alpha-proteobacteria. Numbers listed on the left represent the following strains: 1, *A. baumannii* ATCC 17978; 2, *P. fluorescens* PICF7; 3, *P. stutzeri* DSM4166; 4, *A. mediterranea* U4; 5, *V. natriegens* NBRC 15636; 6, *A. communis* TSPY31; 7, *H. seropedicae* SmR1; 8, *B. pseudohinzii* HI4684; 9, *B. gladioli* BSR3; 10, *R. palustris* DX1; 11, *B. lablabi* GAS499; 12, *A. pasteurianus* 386B; 13, *R. leguminosarum* ATCC 14479. See Table 3.3 for GenBank accession numbers.

HHKs have been proposed to be derived from canonical HKs that have laterally recruited a REC domain from co-operonic RRs (Zhang and Shi, 2005). This evolutionary step reduces cross-talk with other regulators, as the close spatial proximity and high local concentrations of a covalently bound REC domain can outcompete other soluble RRs for access to the phosphorylated histidine residue (Capra *et al.*, 2012). Given that nutrient transport can stimulate TCS activation, it would seem feasible that evolution would also converge solute symporter domains to their sensing counterparts, thus ensuring an accelerated and optimal response to external stimuli. Interestingly, the gene immediately downstream of *11160* encodes a putative allantoin permease that shares a topological structure and 44% protein identity to the N terminus of *11160*. Allantoin, also known as 5-ureidohydantoin, is a purine metabolite utilised by many organisms as an alternate source of carbon, nitrogen and energy. Transporters, including allantoin permeases such as PucI from *Bacillus subtilis*, import the metabolite from the external environment (Ma *et al.*, 2016), where, depending on the sp., it enters one of two purine degradation pathways (Izaguirre-Mayoral *et al.*, 2018). Acquisition of functional domains within a gene is known to increase upon the relative genetic distance between two genes (Cock and Whitworth, 2007). Given the close proximal location and conserved identity between the SLC5-6-like SBD domains from ACX60_11165 and *11160*, *11160* could have acquired this domain through duplication followed by terminal insertion. Interestingly, unlike other symporter fused HKs (Sepulveda and Lupas, 2017), from the architecture of *11160* the two original TMs of the HHK before acquisition of the N-terminal symporter domain can be identified. This finding raises questions as to whether TMs 13 and 14 and the adjoining extracellular loop still serve a functional role, putatively providing an additional avenue of stimulus sensing and/ or interaction with other regulatory proteins.

Conserved domain approaches identified 3261 orthologues of *11160*, with the vast majority found within sp. from the Proteobacteria phyla. Alignments of distantly related sp. carrying *11155/11160* TCS orthologues revealed co-localisation with an ABC transport system. Coevolution of two distinct protein families can be generated from different selection pressures, including direct interaction of both proteins to execute a given physiological process (Pazos and Valencia, 2008). A similar architecture can be seen with the BceAB ABC transporter and the BceRS TCS present across the Firmicutes phylum. In *B. subtilis*, these systems interact directly and are mutually indispensable for both sensing and resistance to antimicrobial peptides (Dintner *et al.*, 2014), leading to the proposition of coevolution. In the context of our findings, the observed co-occurrence

identified across sp. within the Proteobacteria phyla may also represent another example of a co-evolutionary relationship between TCS and ABC transporter proteins.

Hpt domains serve an integral role in TCS signalling, acting as histidine-phosphorylated intermediates during phosphotransfer. Our analyses revealed that GacS and CheA from *A. baumannii* contain Hpt domains. Since only two additional HHKs are encoded within the *A. baumannii* genome (11160 and ACX60_00940) it is not surprising that standalone Hpt proteins were not identified. Individual deletion mutants of *gacS* and *cheA* in *A. baumannii* ATCC 17978 can be constructed (Cerqueira *et al.*, 2014; Chen *et al.*, 2017) inferring that Hpt domains from either protein can be utilised for signal transfer. Transcriptomic profiling of a $\Delta gacA$ derivative revealed that GacA only regulated 75% of the GacS transcriptome, with the remaining transcriptional alterations hypothesised as TCS cross-talk (Cerqueira *et al.*, 2014). In light of our findings, these additional transcriptional variations could be a direct result of other TCS utilising the GacS Hpt domain to facilitate signal transfer. Multi-component TCS signalling has been reported in other bacterial pathogens including *Pseudomonas aeruginosa* and *Burkholderia cenocepacia* (Tomich and Mohr, 2004; Chambonnier *et al.*, 2016) but the full breadth of such interactions is yet to be elucidated in *A. baumannii*.

AdeN, a repressor of the tripartite multidrug efflux pump AdeIJK, is a renowned mutational hotspot in clinical isolates, with inactivation leading to increased *adeIJK* expression and subsequently decreased susceptibility to multiple antimicrobials in addition to other phenotypic changes (Rosenfeld *et al.*, 2012; Yoon *et al.*, 2015; Saranathan *et al.*, 2017). Diverse mechanisms can lead to AdeN inactivation, including integration of insertion sequences, SNPs and insertion/deletions resulting in missense mutations, frameshifts and premature protein termination (Valladares *et al.*, 2002; Fernando *et al.*, 2014; Saranathan *et al.*, 2017; Gerson *et al.*, 2018). Here, we identified two novel variants leading to *adeN* inactivation by means of IS*Aba12* insertion and the missense mutation, Gly54Asp. To our knowledge this is the first report where a targeted gene deletion has resulted in compensatory loss-of-function mutations in AdeN, raising the possibility that other clinical isolates carrying *adeN* mutations may have also occurred as a secondary effect from other gene insertion/deletion events, or from acquisition of new genetic material.

As Ery is a substrate of AdeIJK in other clinical isolates (Yoon *et al.*, 2015), it could be argued that Ery exposure during mutant construction may have promoted *adeN*

mutations, leading to AdeIJK over-expression. However, our laboratory has successfully generated over a dozen mutants in ATCC 17978, substituting genetic regions of interest including other TCS for an identical Ery resistance cassette (Sections 2.4.3 and 4.4.2). During these studies, no deletion derivatives carried additional mutations in *adeN*. Furthermore, the concurrent controls undertaken when generating all mutant derivatives within ATCC 17978 have not yielded spontaneous Ery resistant clones. It is therefore unlikely that exposure to Ery was the primary factor leading to AdeN inactivation. It is unclear whether the compensatory effects from *adeN* inactivation that promote deletion of 11155 resulted from *adeIJK* over-expression, de-repression of additional target genes, indirect transcriptional modifications, or combinations of the above. Further investigations are required to delineate the exact mechanism(s) responsible.

Targeted gene disruption has been instrumental in unravelling vital insights into the pathobiology of *A. baumannii* (Fitzsimons *et al.*, 2018; Tipton *et al.*, 2018). However, difficulties can arise when deleting essential genes, as in most cases they cannot be generated or if they can, they promote additional mutations at other loci in order to survive. One such example involves the essential TCS of *S. aureus*, WalKR, where single amino acid substitutions within the WalK PAS domain resulted in loss-of-function mutations in *saeRS* (Monk *et al.*, 2017), a TCS known to be under the regulatory control of WalKR. Conceivably the regulatory circuits of 11155/11160 and AdeN are linked, as seen with SaeRS and WalKR, however given that a publically available Δ *adeN* transcriptome is currently unavailable, inferences on possible interactions cannot be readily deduced. Interestingly, high throughput screens with ATCC 17978 cells found that only the OmpR-EnvZ TCS was essential for growth in rich media (Wang *et al.*, 2014). Whether inactivation of 11155 was compensated by secondary mutations in *adeN* as seen in this study is currently unknown and such limitations need to be considered when identifying the ‘true’ essential genome in these types of arrays.

In conclusion, *in silico* characterisation of a putative hybrid TCS encoded in *A. baumannii* has unveiled a HHK that adopts a novel domain architecture, with orthologues of the system shown to be conserved across the Proteobacteria phyla. This work also underscores the plastic nature of *A. baumannii* and its ability to readily mutate when faced with adverse selection pressures, in this case, deletion of an essential regulatory system. The study highlights the complex regulatory networks afforded by this formidable pathogen, unveiling a novel link between a TCS and the global TetR-type regulator, AdeN.

**CHAPTER 4: MITE_{Aba12}, a novel mobile
miniature inverted-repeat transposable
element identified in
Acinetobacter baumannii ATCC 17978
and its prevalence across the
Moraxellaceae family**

Declaration by candidate

In Chapter 4 the nature and extent of my contribution to the work was as follows:

Nature of contribution	Contribution extent (%)
Conceptualisation, methodology, performance of experiments, data curation, writing, editing and revision of the manuscript	90

The following co-authors contributed to the work

Name	Nature of contribution	Contribution extent (%)
Melissa Brown	Conceptualisation, editing and revision of the manuscript	10

The undersigned hereby certify the above declaration correctly reflects the nature and extent of the candidate and co-author contribution to this work.

Candidate signature		17.8.19
---------------------	--	---------

Supervisor signature		17.8.19
----------------------	--	---------

4.1 Preface

This chapter is closely based on the publication by Adams F.G. and Brown M.H. (2018) MITE_{Aba12}, a novel mobile miniature inverted-repeat transposable element identified in *Acinetobacter baumannii* ATCC 17978 and its prevalence across the *Moraxellaceae* family. mSphere 4, e00028-19 licensed under [Creative Commons Attribution 4.0](#). The printed version of this article can be found in Appendix E.

4.2 Abstract

Insertion sequences (IS) are fundamental mediators of genome plasticity with potential to generate phenotypic variation with significant evolutionary outcomes. Here, a recently active miniature inverted-repeat transposon element (MITE) was identified in a derivative of *Acinetobacter baumannii* ATCC 17978 after being subjected to stress conditions. Transposition of the novel element led to the disruption of the *hns* gene, resulting in a characteristic hyper-motile phenotype. DNA identity shared between the terminal inverted repeats of this MITE and co-resident IS_{Aba12} elements, together with the generation of nine bp target site duplications, provides strong evidence that IS_{Aba12} elements were responsible for mobilisation of the MITE (designated MITE_{Aba12}) within this strain. A wider genome-level survey identified MITE_{Aba12} in 30 additional *Acinetobacter* genomes at varying frequencies and one *Moraxella osloensis* genome. Ninety MITE_{Aba12} copies could be identified, of which 40% had target site duplications, indicating recent transposition events. Elements ranged between 111-114 bp; 90% were 113 bp in length. Using the MITE_{Aba12} consensus sequence, putative outward-facing *Escherichia coli* σ 70 promoter sequences in both orientations were identified. The identification of transcripts originating from the promoter in one direction supports the proposal that the element can influence neighboring host gene transcription. The location of MITE_{Aba12} varied significantly between and within genomes, preferentially integrating into AT-rich regions. Additionally, a copy of MITE_{Aba12} was identified in a novel 8.5 kb composite transposon, Tn6645, in the *M. osloensis* CCUG 350 chromosome. Overall, this study shows that MITE_{Aba12} is the most abundant non-autonomous element currently found in *Acinetobacter*.

4.2.1 Importance

One of the most important weapons in the armoury of *Acinetobacter* is its impressive genetic plasticity, facilitating rapid genetic mutations and rearrangements as well as integration of foreign determinants carried by mobile genetic elements. Of these, IS are

considered one of the key forces shaping bacterial genomes and ultimately evolution. We report the identification of a novel non-autonomous IS-derived element present in multiple bacterial sp. from the *Moraxellaceae* family, and its recent translocation into the *hns* locus in the *A. baumannii* ATCC 17978 genome. This latter finding adds new knowledge to only a limited number of documented examples of MITEs in the literature and underscores the plastic nature of the *hns* locus in *A. baumannii*. MITE_{Aba12}, and its predicted parent(s), may be a source of substantial adaptive evolution within environmental and clinically relevant bacterial pathogens and thus have broad implications for niche-specific adaptation.

4.3 Introduction

A. baumannii has been classed as one of the most predominant pathogens responsible for MDR nosocomial infections worldwide (Higgins *et al.*, 2010). Aside from its notorious MDR phenotype, *A. baumannii* also displays a remarkable capacity to persist on a variety of inanimate surfaces for extended periods, providing a reservoir for infection and facilitating transmission throughout clinical settings (Jawad *et al.*, 1998; Harding *et al.*, 2018). Significant work has been undertaken to identify and track the arsenal of genes that contribute to the impressive persistence and resistance strategies available to *A. baumannii* (Gayoso *et al.*, 2014; Harding *et al.*, 2015; Weber *et al.*, 2015b; Álvarez-Fraga *et al.*, 2016; Blackwell *et al.*, 2016b). This has identified a highly dynamic and plastic genome, dominated by numerous integration events as well as alterations in expression of intrinsic genes modulated through mutations and deletion and/ or insertion of mobile genetic elements (MGEs) (Wright *et al.*, 2014; Adams *et al.*, 2016; Wright *et al.*, 2017a). MGEs are present in nearly all prokaryote genomes and constitute the ‘mobilome’, a term which has gained significant traction in recent years driven by the increase in infections caused by MDR isolates. The mobilome itself is comprised of a number of genetic entities including plasmids, bacteriophages, gene cassettes in integrons and transposable elements, all capable of capturing and disseminating genetic material across bacterial genomes via horizontal gene transfer (HGT) (Toussaint and Chandler, 2012).

Of the above-mentioned entities, transposable elements are seen as a major contributor to niche-specific adaptive evolution. They are capable of moving from one position to another within a given genome and are often associated with the dissemination of antimicrobial resistance determinants (Zhang and Saier, 2011; Vandecraen *et al.*, 2017;

Partridge *et al.*, 2018). One of the simplest autonomous types of mobile elements is the insertion sequence (IS) consisting of a transposase gene(s) that is typically bordered by terminal inverted repeats (TIRs), designated left (IRL) and right (IRR) relative to the direction of the transposase gene. The TIRs contain multiple domains required for transposase binding, donor DNA cleavage and strand transfer, supporting the integration of the elements into host DNA via replicative or non-replicative mechanisms (Haren *et al.*, 1999). As a consequence of insertion, short direct repeat sequences of the target DNA are often generated (target site duplications; TSDs), which differ in length and degree of sequence specificity depending on the IS element being translocated (Siguier *et al.*, 2015). Movement of an IS to a new location within a genome offers a variety of possible integration sites. Although some IS display clear trends/preferences in target sites, the large majority of IS demonstrate low target specificity (Nagy and Chandler, 2004).

Small mobile elements can be further delineated based on their movement autonomy. A limited range of non-autonomous elements exist in bacteria, such as repetitive extragenic palindromic sequences, Tn3-derived inverted-repeat miniature elements (TIMEs), and miniature inverted-repeat transposable elements (MITEs) (Bertels and Rainey, 2011; Siguier *et al.*, 2014; Szuplewska *et al.*, 2014). Like eukaryotic MITEs (Fattash *et al.*, 2013), bacterial MITEs are small (~50–600 bp) AT rich sequences that have lost their cognate transposase gene and thus contain non-coding DNA that in most, but not all, cases is flanked by TIRs (Delihias, 2008). Based on their origins, MITEs can be categorised as Type I or Type II and are generated by internal deletion of parent transposable elements or by random convergence of TIR sequences, respectively (Brügger *et al.*, 2002). Movement of these elements is thought to be mediated by transposases of a co-resident parental element acting *in trans*. The site of integration and length of the TSDs of MITEs are generally identical or highly similar to that of the co-resident IS ‘parent’ (Delihias, 2008). Since their identification in bacteria (Correia *et al.*, 1988), a number of these elements have been documented from a diverse range of sp., where many have significantly influenced the evolutionary tempo of their host genomes (Siguier *et al.*, 2014). These elements are often overlooked due to the absence of a recognisable coding sequence (CDS) and their tendency to reside in intergenic regions. Thus, they represent a largely unexplored field in microbial genomics.

Through characterisation of a subset of morphologically distinct colonies isolated during desiccation stress analyses, we identified a novel MITE that transposed to a new location within the *A. baumannii* ATCC 17978 genome. Due to shared similarities in

TIRs and TSD sequence length, the 113 bp sequence is predicted to have proliferated through the activity of the transposase encoded by resident IS*Aba12* elements present in ATCC 17978 and thus was named, MITE_{Aba12}. The prevalence of this novel, non-autonomous MGE across all publicly available sequenced bacterial genomes was examined and insights gained in respect to its transposition activity as well as its overall function and evolution.

4.4 Materials and methods

4.4.1 Bacterial strains, plasmids, media and growth conditions

A. baumannii ATCC 17978 (Smith *et al.*, 2007) was obtained from the ATCC and is designed as wildtype (WT) in all analyses. Bacterial strains and plasmids are summarised in Table 4.1, and primers are listed in Table 4.2. All bacterial strains used in the study were grown in lysogeny broth (LB) or on LB agar plates and incubated under aerobic conditions overnight (16-20 h) at 37°C unless otherwise stated. Antibiotic concentrations used for selection purposes were ampicillin 100 mg/L and erythromycin 25 mg/L, unless otherwise stated and were purchased from AMRESCO and Sigma Aldrich, respectively.

4.4.2 Construction of deletion and complementation derivatives

A. baumannii ATCC 17978 *qseBC* (ACX60_06100/05) and *ygiW* (ACX60_06095) deletion strains were constructed using the RecET recombinase system (Tucker *et al.*, 2014) with modifications as outlined previously (Sections 2.4.3). Primers used to generate mutant strains are listed in Table 4.2. For complementation of insertionally-inactivated *hns* genes identified in this study, a previously generated pWH1266 shuttle vector carrying a WT copy of *hns* amplified from *A. baumannii* ATCC 17978 chromosomal DNA (pWH0268) was used to transform appropriate *A. baumannii* strains as previously described (Eijkelkamp *et al.*, 2013).

4.4.3 Desiccation survival assay

Desiccation survival assays followed the method outlined previously (Gayoso *et al.*, 2014) with modifications. Briefly, overnight (ON) cultures were diluted 1:25 in fresh LB broth and grown to late log phase (OD₆₀₀ = 0.8-1.0). Cells were subsequently washed three times in sterile dH₂O and diluted to OD₆₀₀ = 0.1. A total of 300 µl was pipetted into the centre of individual wells of 6-well culture plates and placed in a laminar-flow hood ON at 25°C to dry. All plates were incubated at 21°C with a relative humidity of 30 ± 2% maintained by the addition of saturated CaCl₂ within sealed plastic boxes. Humidity and

Table 4.1: Strains and plasmids used in this study

Strain or plasmid	Genotype or description ^a	Reference/ source
<u><i>A. baumannii</i> strains</u>		
ATCC 17978	Non-international type clone (wildtype)	ATCC (Smith <i>et al.</i> , 2007)
$\Delta qseBC$	ATCC 17978 with ERY ^R insertion disruption in <i>qseBC</i>	This study
$\Delta ygiW$	ATCC 17978 with ERY ^R insertion disruption in <i>ygiW</i>	This study
Δhns	ATCC 17978 with <i>hns</i> disrupted by <i>ISAbal2</i>	(Eijkelkamp <i>et al.</i> , 2013)
$\Delta hns::ISAbal2$	ATCC 17978 with <i>hns</i> disrupted by <i>ISAbal2</i>	This study
$\Delta qseBC \Delta hns::ISAbal2$	$\Delta qseBC$ with <i>hns</i> disrupted by <i>ISAbal2</i>	This study
$\Delta ygiW \Delta hns::ISAbal2$	$\Delta ygiW$ with <i>hns</i> disrupted by <i>ISAbal2</i>	This study
$\Delta ygiW \Delta hns::MITE_{Abal2}$	$\Delta ygiW$ with <i>hns</i> disrupted by <i>MITE_{Abal2}</i>	This study
Δhns pWH0268	Δhns with pWH0268	(Eijkelkamp <i>et al.</i> , 2013)
$\Delta hns::ISAbal2$ pWH0268	$\Delta hns::ISAbal2$ with pWH0268	This study
$\Delta qseBC \Delta hns::ISAbal2$ pWH0268	$\Delta qseBC \Delta hns::ISAbal2$ with pWH0268	This study
$\Delta ygiW \Delta hns::ISAbal2$ pWH0268	$\Delta ygiW \Delta hns::ISAbal2$ with pWH0268	This study
$\Delta ygiW \Delta hns::MITE_{Abal2}$ pWH0268	$\Delta ygiW \Delta hns::MITE_{Abal2}$ with pWH0268	This study
<u><i>E. coli</i> strains</u>		
DH5 α λpir	F- $\Phi 80lacZ\Delta M15 \Delta(lacZYA-argF)$ U169 <i>recA1 endA1 hsdR17</i> (rK, mK+) <i>phoA supE44</i> $\lambda-$ <i>thi-1 gyrA96 relA1</i> λpir , conjugative strain which can host $\lambda-pir$ -dependent plasmids	(Purins <i>et al.</i> , 2008)
<u>Plasmids</u>		
pAT04	TET ^R ; pMMB67EH with Rec _{Ab} system	(Tucker <i>et al.</i> , 2014)
pGEM-T Easy	AMP ^R ; T-overhang vector	Promega

Strain or plasmid	Genotype or description ^a	Reference/ source
pVA891	CML ^R ERY ^R ; Source of ERY ^R cassette	(Macrina <i>et al.</i> , 1983)
pWH0268	AMP ^R ; pWH1266 with <i>hns</i> cloned via <i>Bam</i> HI restriction site	(Eijkelkamp <i>et al.</i> , 2013)

^aAbbreviations; AMP, ampicillin; CML, chloramphenicol; ERY, erythromycin; ^R, resistant; TET, tetracycline

Table 4.2: Primers used in the study

Primer name/ purpose	Sequence (5' – 3') ^a	Reference/ source
<u>Primers used for cloning and sequencing of <i>hns</i> genes with integrated MGEs</u>		
<i>hns</i> _F	GAGACATATGATGCATCATCATCAT CATATAAATATTAAGAAAATATATTA	(Eijkelkamp <i>et al.</i> , 2013)
<i>hns</i> _R	TCTCGGATCCTTAGATTAAGAAATCTTC AAG	(Eijkelkamp <i>et al.</i> , 2013)
M13 F	GTAAAACGACGGCCAG	Promega
M13 R	CAGGAAACAGCTATGAC	Promega
<u>Primers used to identify presence of IS</u>		
ACX60_04650_F	CGTATTTGGGTCTTGGGGAA	This study
ACX60_04650_R	CCTTTGGTAAGTACTTTAT	This study
ACX60_18935_F	AGCAACTGAAGCTGAAATTTCG	(Eijkelkamp <i>et al.</i> , 2013)
ACX60_18935_R	TTGGTTCCGAATTAGACTTGC	(Eijkelkamp <i>et al.</i> , 2013)
ACX60_04795_F	CAGTCAGGTTCCGCAT	This study
ACX60_04795_R	GACCAGACAATACAATG	This study
<u>Primers used for construction of $\Delta qseBC$ and $\Delta ygiW$</u>		
<u>$\Delta qseBC$</u>		
$\Delta qseBC$ _UFR_F	CAATTCCGCGATAAGAGC	This study
$\Delta qseBC$ _UFR_R	CTATCAACACACTCTTAAGCCTGTTATA TCCTGAT	This study
$\Delta qseBC$ _DFR_F	CGGGAGGAAATAATTCTATTTGCAGTCA CAACTGG	This study
$\Delta qseBC$ _DFR_R	GTAGTAACCAGAACAGCAC	This study
$\Delta qseBC$ _NOL_F	GGCAAGGACGTCCTGTTT	This study
$\Delta qseBC$ _NOL_R	GGGCTGAAAACTTCAAC	This study
$\Delta qseBC$ _Ery_F	CTTAAGAGTGTGTTGATAG	This study
$\Delta qseBC$ _Ery_R	ATAGAATTATTCCTCCCG	This study
<u>$\Delta ygiW$</u>		
$\Delta ygiW$ _UFR_F	CAGTTGAAATGGCATCCATTAC	This study
$\Delta ygiW$ _UFR_R	CTCTTAAGGTATAGGAACTTCAAATTA CCCTCTGTTA	This study

Primer name/ purpose	Sequence (5' – 3')^a	Reference/ source
$\Delta ygiW$ _DFR_F	GAGGAAATAAGAAGTTCCTATACTAAA TTAATTTCTACATTTATTCC	This study
$\Delta ygiW$ _DFR_R	GAGAGCGGCCCGCCTCATTTTAAGTCTCC CATAAC	This study
$\Delta ygiW$ _NOL_F	CGGCATTTATGAGTTTATGCCAG	This study
$\Delta ygiW$ _NOL_R	GGCTTGCCCCCAACTGA	This study
$\Delta ygiW$ _Ery F	GAAGTTCCTATACCTTAAGAGTGTGTTG ATAG	This study
$\Delta ygiW$ _Ery R	GTATAGGAACTTCTTATTTCCCTCCCGTT AAATAATAGATAAC	This study

^aNucleotides in bold-face type represent incorporated restriction sites, *Nde*I; CATATG, *Bam*HI; GGATCC, *Not*I; GCGGCCGC

temperature were monitored over the 30-day time course using a thermohygrometer. CFU were assessed on days 0, 1, 3, 5, 7, 9, 15, 21 and 30. For viable cell quantification, desiccated cells were rehydrated in sterile PBS, scraped from their respective wells and serially diluted. Suspensions of diluted cells were plated on LB agar, incubated ON and desiccation survival calculated from the number of CFU/ml. Experiments were undertaken in two biological replicates from two independent experiments. Average CFU and standard error of the mean (SEM) were calculated and graphed.

4.4.4 Gene cloning and DNA sequencing

The upstream intergenic and coding regions of *hns* from hyper-motile variants obtained after desiccation stress experiments were PCR-amplified using Velocity DNA polymerase (Bioline, Australia) with *hns_F* and *hns_R* (Table 4.2) following the manufacturer's instructions. Adenosine treatment was undertaken on purified amplicons prior to T/A ligation with pGEMT Easy (Promega) and transformation into *E. coli* DH5 α λ pir. Transformants were screened by PCR, restriction digestion and DNA sequencing.

4.4.5 Stability of MITE_{Aba12} in *hns*

Five colonies were separately inoculated into 10 mL of LB broth and passaged over a five-day period using a dilution of 1:10,000. From the fifth passage, a loop of confluent bacterial suspension was streaked onto LB agar and incubated ON. A total of three well-isolated colonies from each of the five biological replicates was randomly selected and PCR-screened with *hns_F* and *hns_R* (Table 4.2) to identify maintenance of the MITE within the *hns* gene.

4.4.6 Motility assays

Motility assays for *A. baumannii* ATCC 17978 WT and mutant derivatives were undertaken as previously described (Giles *et al.*, 2015). Briefly, a colony was harvested from a LB agar plate grown overnight and used to inoculate the centre of LB agar (0.25%) plate. Motility was assessed by visual examination after ON incubation at 37°C. Experiments were performed in duplicate over at least three independent experiments. Images are an average representation of results obtained.

4.4.7 Comparative genomics, alignments and clustering

For generation of multiple DNA sequence alignments of all full length MITE_{Aba12} copies identified, sequences were obtained from NCBI GenBank and used as input data using Clustal Omega with default parameter settings applied

(<https://www.ebi.ac.uk/Tools/msa/clustalo/>) (Sievers and Higgins, 2018). Prior to alignment copies of MITE_{Aba12} identified in the opposite orientation (IRR to IRL) were reverse complemented. In strains with multiple copies of MITE_{Aba12} these were numbered (_#1, _#2, _3# etc) based on their order from NCBI Blastn (2.8.0+) outputs (Altschul *et al.*, 1990). Sub-groups in the alignment were defined based on the presence of two or more identical MITE_{Aba12} sequence arrangements, numbered from 1 to 10 and ordered according to abundance. To generate the MITE_{Aba12}(c) consensus sequence, all elements of 113 bp in length were used as input data and visualised using WebLogo software (Crooks *et al.*, 2004) with default settings applied.

The presence of the composite transposon in *M. osloensis* CCUG 350 was identified by manual examination of the sequence surrounding the MITE_{Aba12} element using the genome map tool from the Kyoto Encyclopaedia of Genes and Genomes database (<http://www.kegg.jp/>) (Kanehisa *et al.*, 2016). To identify this composite transposon in other genomes, nucleotide sequence spanning the gene locus tags AXE82_04585 to AXE82_04645 in *M. osloensis* CCUG 350 was used as a query in Blastn searches. Sequences from *M. osloensis* CCUG 350; AXE82_04585-04645 (15922 bp) and KSH (Lim *et al.*, 2018); KSH_08645-08655 (7446 bp) were used to generate a genetic map using the Easyfig 2.2.2 tool (Sullivan *et al.*, 2011). To identify the presence of the composite transposon across all sequenced genomes, nucleotide sequences located between the terminal ends of the composite transposon from *M. osloensis* CCUG 350 (AXE82_04595–AXE82_04625) were used as a query and comparative Blastn searches (Altschul *et al.*, 1990) performed. The alignment between *M. osloensis* CCUG 350 and *A. guillouiae* NBRC 110550 was generated using Easyfig 2.2.2 (Sullivan *et al.*, 2011) as described above. The composite transposon identified in this study was allocated the name Tn6645 by the transposon registry (<https://transposon.lstmed.ac.uk/tn-registry>).

Coding regions, *E. coli*-derived σ 70 consensus promoter sequences, RNA secondary structures, and Rho factor-independent terminators, were predicted using MITE_{Aba12}(c) as the input sequence using NCBI ORF finder (<https://www.ncbi.nlm.nih.gov/orffinder/>) (Wheeler *et al.*, 2003), Softberry BPROM tool (<http://www.softberry.com/berry.phtml?topic=bprom&group=programs&subgroup=gfnfdb>), RNA Mfold server (<http://unafold.rna.albany.edu/?q=mfold/rna-folding-form>) (Zuker, 2003) and ARNold, a Rho-independent transcription terminator finding tool (<http://rna.igmors.u-psud.fr/toolbox/arnold/>) (Naville *et al.*, 2011), respectively. Default settings were applied for all programs stated above.

4.4.8 Characterisation of MITE_{Aba12} target site duplications

A total of 20 bp upstream and downstream of each MITE_{Aba12} element from Blastn outputs were used to screen for the presence of TSDs. The AT ratio percentages was calculated based on the number of adenosine or thymidine nucleotides in each of the 9 bp integration sites and these percentages were plotted against the number of copies harbouring each ratio. To identify trends in MITE_{Aba12} integration sites, all identified TSD sequences were used as input data using WebLogo software (Crooks *et al.*, 2004) with default settings applied.

4.5 Results

4.5.1 Construction of *qseBC* and *ygiW* deletion derivatives in *A. baumannii* ATCC 17978

The regulatory mechanisms that co-ordinate the expression of many *A. baumannii* virulence factors remain largely unknown. One regulatory mechanism employed by bacteria, including *A. baumannii*, is two component signal transduction systems (TCS) (Kröger *et al.*, 2016). The TCS *qseBC* (ACX60_06100/05) and its upstream hypothesised target gene, which encodes the putative signal peptide *ygiW* (ACX60_06095), were deleted by allelic replacement in *A. baumannii* ATCC 17978 (GenBank accession: CP012004.1), generating the derivatives $\Delta qseBC$ and $\Delta ygiW$, respectively. To ensure the introduced mutations did not affect cell viability, growth curves assessing optical density at 600 nm (OD₆₀₀) were undertaken in LB medium and measured hourly over an 8 h period. No significant growth perturbations were identified for $\Delta qseBC$ or $\Delta ygiW$ compared to the wildtype (WT) ATCC 17978 parent cells under the tested conditions (data not shown).

4.5.2 Disruption of the *hns* gene after desiccation stress

To analyse the impact of deletion of the target genes in *A. baumannii* ATCC 17978, the constructed mutant strains were subjected to a number of *in vitro* assays, one of which was survival under desiccating conditions. No significant differences in survival compared to WT were seen over the 30-day test period (Figure 4.1 A). However, on day 5 a subset of morphologically-distinct colonies was identified during quantification of viable cells. These colonies displayed irregular edging reminiscent of a previously seen hyper-motile phenotype (Eijkelkamp *et al.*, 2013) (Figure 4.1 B). In total, seven hyper-motile isolates were identified; five from $\Delta ygiW$ and one each from the $\Delta qseBC$ and WT backgrounds.

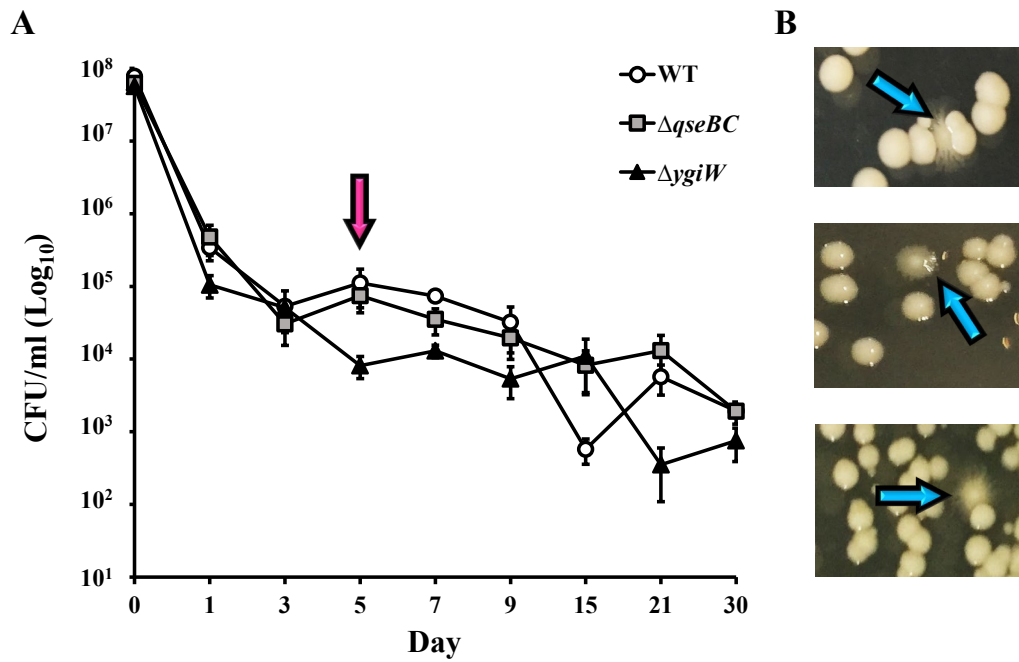


Figure 4.1: Identification of hyper-motile variants from *A. baumannii* ATCC 17978 wildtype, $\Delta qseBC$, and $\Delta ygiW$ strains after desiccation stress

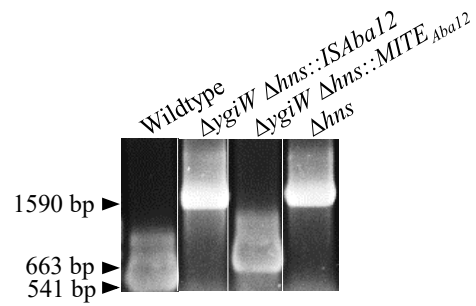
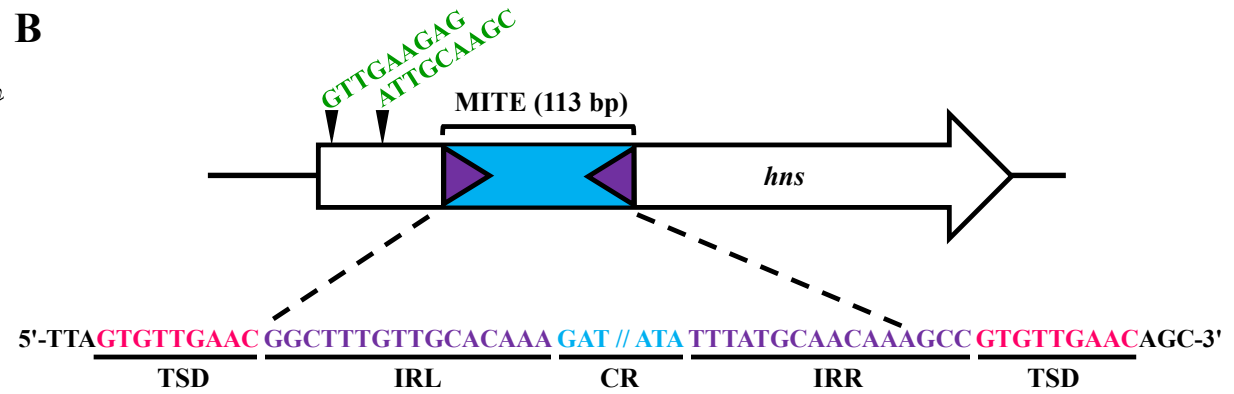
(A) Desiccation survival was determined by enumeration of viable cells (CFU/ml) over a 30-day period. Markers represent mean values of viable cells and error bars the SEM calculated on days 0, 1, 3, 5, 7, 9, 15, 21 and 30. Four biological replicates were undertaken over two independent experiments. Pink arrow indicates the day that hyper-motile variants were identified. **(B)** Images of hyper-motile variants (blue arrows) obtained from rehydrated desiccated cells after ON incubation at 37°C on 1% LB agar.

A previous study undertaken in *A. baumannii* ATCC 17978 showed that disruption of the histone-like nucleoid structuring (*hns*) gene by an IS (subsequently designated *ISAbal2* by ISfinder) (Siguier *et al.*, 2006) led to a number of phenotypic alterations, including hyper-motility (Eijkelkamp *et al.*, 2013). Given the similarity in colony morphology between the set of hyper-motile isolates identified after desiccation stress in this study and that previously seen for Δhns (Eijkelkamp, 2011), our investigations initially focused on this global regulator. PCR amplifications across the *hns* loci of the hyper-motile strains identified that all amplicons were larger than the WT control (Figure 4.2 A). DNA sequencing of these products revealed insertion of *ISAbal2* in three cases, originating from each of the different three background strains, which were located in two previously-identified integration sites (Eijkelkamp, 2011) (Figure 4.2 B). In the remaining four strains, all based on the $\Delta ygiW$ background, a shorter insertion in *hns* was detected and sequencing of one example revealed a 113 bp element integrated into a novel site (Figure 4.2 B). To determine if the integrated element was stably inserted in *hns* of the $\Delta ygiW$ strain, PCR screening after five consecutive passages in liquid culture from five biological replicates was undertaken. All samples maintained the element within *hns* (data not shown). To examine whether isolates with a disrupted *hns*, irrespective of the site/type of integration, still produced the distinctive hyper-motile phenotype, their motility phenotypes were assessed and found to be comparable to that seen for the previously identified *hns* mutant derivative (Eijkelkamp *et al.*, 2013; Giles *et al.*, 2015) (Figure 4.3). Complementation with a WT copy of *hns* (ACX60_16755) carried on the pWH1266 shuttle vector (Eijkelkamp *et al.*, 2013) restored all isolates to their parental non-motile phenotype (Figure 4.3).

4.5.3 Identification and characterisation of a novel active MITE in *A. baumannii* ATCC 17978

To characterise this novel 113 bp element found in the *A. baumannii* $\Delta ygiW$ strain, its DNA sequence and that of its insertion site in *hns* were analysed. This revealed that the 113 bp element carried 16 bp imperfect TIR sequences (1 nucleotide different), an 81 bp core region, and generated 9 bp TSDs on insertion into *hns* (Figure 4.2 B and C). The element is AT rich (78%) and does not contain any known CDS (Wheeler *et al.*, 2003). Taken together, these traits strongly suggested that this element is a MITE (Delihias, 2008).

To identify the abundance of the MITE within the *A. baumannii* ATCC 17978 genome, the 113 bp MITE sequence in *hns* from the $\Delta ygiW$ background was used as a

A**B****C****ACX60_04650**

E I T A L K N E F E D L L E S L K A L L H K Y V S I *

GAGATTACTGCTTTAAAAAATGAATTTGAAGATTTATTGGAATCTTTAAAGGCTTTGTTGCATAAAATATGTAAGCATCTGATTTAAATA

IRR

AATTTAATTTTGGATCAAAAAATAATCAAAACTTTTAAATCATATAGTTATGAAATCTTTGTGCAACAAAGCCGCTCAGATT

IRL

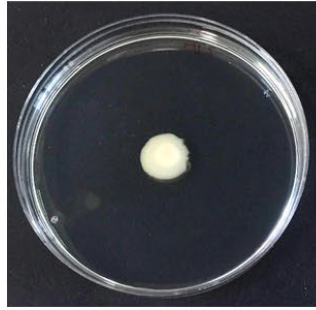
D

MITE _{Aba12} (<i>hns</i>)	TTA GTGTTGAAC GGCTTTGTTGCACAAA	TTTATGCAACAAAGCC GTGTTGAAC AGC
ISAbal12 (<i>hns</i>)	TTA ATTGCAAGC GGCTTTGTTGCACAAA	TTTGTGCAACAAAGCC ATTGCAAGC TGA
ISAbal12 ACX60_04793	GCT CTAAAAAAC GGCTTTGTTGCACAAA	TTTGTGCAACAAAGCC CTAAAAAAC TAA
ISAbal12 ACX60_12380	ACA GCTCAGTAA GGCTTTGTTGCACAAA	TTTATGCAACAAAGCC GCTCAGTAA TGA
ISAbal12 ACX60_18935 (pAB3)	TCAGATTCAACC <u>GGCTTTGTTGCACAAA</u>	<u>TTTGTGCAACAAAGCC</u> AATGAACGCTAA
	IRL	IRR

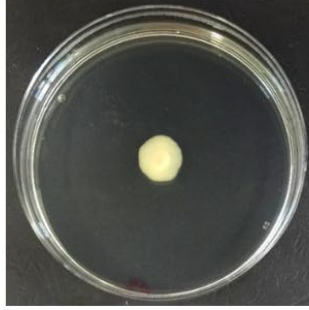
81-1008 bp

Figure 4.2: Insertions in the *hns* locus from hyper-motile variants and relationship between IS*Aba12* and MITE_{*Aba12*}

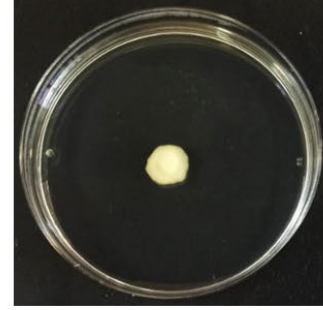
(A) Examples of amplicons generated from PCR across the *hns* locus from hyper-motile isolates compared to wildtype and the previously identified Δhns mutant (Eijkelkamp *et al.*, 2013). The amplicon from $\Delta ygiW \Delta hns::MITE_{Aba12}$ (663 bp) was 122 bp larger than that from the wildtype control (541 bp) whilst $\Delta ygiW \Delta hns::ISAb12$ yielded the same size product as the Δhns control (1590 bp). **(B)** Open white arrow depicts the *hns* gene (ACX60_16755) and direction of transcription, black triangles with green nucleotide sequences represent the TSD for the two integration sites identified previously (Eijkelkamp, 2011) as well as in this study. The 113 bp MITE is comprised of an 81 bp central region (CR, blue) flanked by 16 bp imperfect inverted repeat sequences (IRL and IRR; purple), // denotes break in DNA sequence. The novel insertion site/target site duplication (TSD) sequences are in pink. The figure is not drawn to scale. **(C)** Location of MITE_{*Aba12*} in the *A. baumannii* ATCC 17978 genome. The 3' end of ACX60_04650 is fused to MITE_{*Aba12*} leading to a truncation and the formation of a pseudogene. The deduced amino-acid sequence for the modified ACX60_04650 is designated by a single letter code above the underlined nucleotide sequence and the asterisk indicates the proposed stop codon. Purple and blue nucleotides represent TIR and CR of MITE_{*Aba12*}, respectively. **(D)** Nucleotide alignment of 12 bp up- and downstream of the MITE_{*Aba12*} element in *hns* of *A. baumannii* ATCC 17978 $\Delta ygiW$, IS*Aba12* elements present in ATCC 17978 and IS*Aba12* in *hns* (IS*Aba12* [*hns*]) (Eijkelkamp *et al.*, 2013). TIR and TSD are in purple and pink, respectively. Purple underlined nucleotides represent the mismatching base in IRR. Black bracket indicates the size of the region between IRL and IRR either 81 bp for MITE_{*Aba12*} or up to 1008 bp for IS*Aba12*.



WT



$\Delta qseBC$



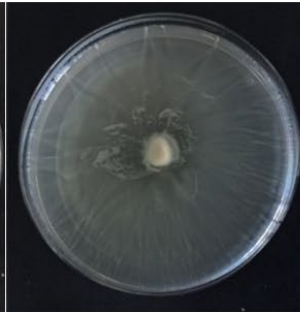
$\Delta ygiW$



Δhms (control)



$\Delta hms::ISAbal2$



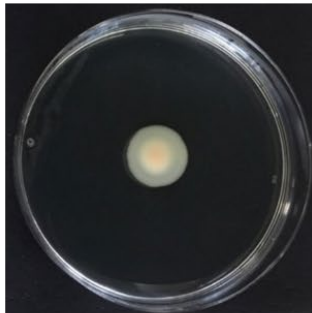
$\Delta qseBC \Delta hms::ISAbal2$



$\Delta ygiW \Delta hms::ISAbal2$



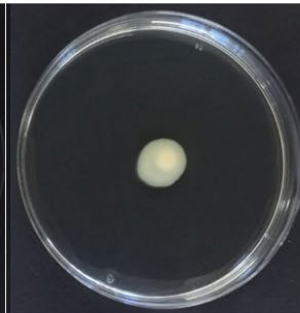
$\Delta ygiW \Delta hms::MITE_{Aba12}$



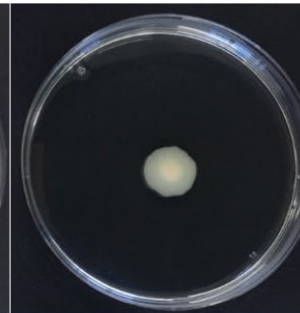
Δhms (control) + pWH0268



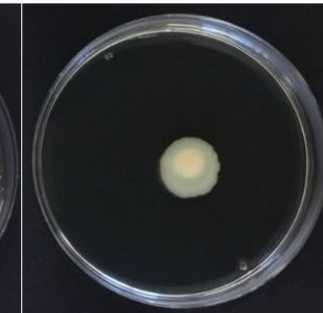
$\Delta hms::ISAbal2$ + pWH0268



$\Delta qseBC \Delta hms::ISAbal2$ + pWH0268



$\Delta ygiW \Delta hms::ISAbal2$ + pWH0268



$\Delta ygiW \Delta hms::MITE_{Aba12}$ + pWH0268

Figure 4.3: Motility of *A. baumannii* ATCC 17978 variants and complemented derivatives

Motility of *A. baumannii* ATCC 17978 variants and complemented derivatives. Cells grown overnight were used as the inoculum for motility assays on LB medium containing 0.25% agar. WT ATCC 17978, $\Delta qseBC$ and $\Delta ygiW$ cells displayed a non-motile phenotype. Derivatives of these strains with an *hns* gene interrupted by IS*Aba12* or MITE_{*Aba12*} and Δhns (Eijkelkamp *et al.*, 2013), displayed a hyper-motile phenotype, dispersing from the original inoculum site to cover the entire plate surface. Reintroduction of a WT copy of *hns* on the shuttle vector pWH1266 (pWH0268) returned strains to the parental non-motile phenotype. Images are a representative example of results obtained.

query for Blastn searches. Only one copy at the 3' end of the ACX60_04650 locus, encoding a hypothetical protein harbouring a partial KAP-family NTPase motif (Kanehisa *et al.*, 2016), was identified, fusing this gene with 31 bases from the MITE (Figure 4.2 C), generating a premature stop codon. Comparative analyses with *A. baumannii* D36 revealed that the protein was 398 amino acids shorter and is therefore likely to be non-functional (data not shown). Genes coding for KAP NTPases are known to be frequently disrupted leading to pseudogene formation (Aravind *et al.*, 2004). PCR with primers specific for the ACX60_04650 location (Table 4.2) identified that the MITE was maintained in this position in $\Delta ygiW \Delta hns::MITE$. Consequently, there are two MITE copies in the $\Delta ygiW$ background, one at the ACX60_04650 locus and the additional copy located in the *hns* gene, inferring duplication of the novel element (data not shown).

4.5.4 IS*Aba12* is the proposed autonomous parent of the novel MITE in *A. baumannii* ATCC 17978

To identify the potential parent element that may have aided in translocation of the MITE, IS present in the ATCC 17978 chromosome and pAB3 plasmid (GenBank accession numbers: CP012004.1 and CP012005.1, respectively), were first identified from results generated by ISseeker (Adams *et al.*, 2016). Subsequent manual examination of the length and sequence of their TIRs and TSD revealed that IS*Aba12* provided the best match to those of the MITE. IS*Aba12* harbours one single open reading frame coding for a transposase, with a characteristic DDE catalytic motif, between its 16 bp TIRs and generates 9 bp TSDs upon insertion (Siguier *et al.*, 2006) (Figure 4.2 D). Thus, the novel MITE was most likely translocated into *hns* by co-resident IS*Aba12* transposase present in ATCC 17978 and will be referred to as MITE_{*Aba12*}.

As MITE_{*Aba12*} does not contain a transposase gene it is not possible to define IRL and IRR relative to this gene. Two of the three copies of IS*Aba12* in ATCC 17978 (at loci ACX60_04795 and ACX60_18935) have identical TIR that perfectly match one TIR of MITE_{*Aba12*}. However, the non-identical TIR of the third copy of IS*Aba12* (ACX60_12380) each perfectly match one TIR of MITE_{*Aba12*}, allowing IRL and IRR of MITE_{*Aba12*} to be designated relative to this IS.

4.5.5 MITE_{*Aba12*} is present in a diverse range of species from the *Moraxellaceae* family

To identify whether MITE_{*Aba12*} is widespread or restricted to *A. baumannii* ATCC 17978, the sequence found within *hns* from $\Delta ygiW \Delta hns::MITE_{Aba12}$ was used as a query to search bacterial genomes present in publicly available databases (July 10th,

2018). Orthologs of MITE_{Aba12} were identified in both chromosomes and plasmids, with an additional 30 strains from the *Acinetobacter* genus and one from *Moraxella osloensis* harbouring the element at varying frequencies (Table 4.3). MITE_{Aba12} was found within a range of environmental *Acinetobacter* sp., with the greatest number of copies identified ($n = 22$) in *A. baumannii* DS002, isolated from soil in Anantapur India in 2005. A number of *Acinetobacter* strains isolated from patients and hospital sewage in multiple countries also carried copies of MITE_{Aba12}, inferring its presence and dissemination into clinically-relevant isolates worldwide. *Acinetobacter* sp. ACNIH2, SWBY1, *A. johnsonii* XBB1 and *A. junii* WCHAJ59 possessed MITE_{Aba12} on the chromosome as well as in plasmids (Table 4.3). An additional number of plasmid sequence(s) carrying MITE_{Aba12} were also identified (Table 4.3) but their corresponding chromosome sequences are not available. Copies of MITE_{Aba12} identified in the *A. baumannii* PR07 genome (GenBank accession number: CP012035.1) were not included in further analysis as the genome contained strings of undetermined bases and thus was not of a high enough quality.

Using ISseeker (Adams *et al.*, 2016), it was found that approximately 18.5% of the 1035 *A. baumannii* genomes examined harboured at least one copy of IS_{Aba12}, with an average of 5.6 copies per genome (data not shown). Using the ISfinder tool (Siguier *et al.*, 2006), four relatives of IS_{Aba12} were identified; IS_{Aba13}, IS_{Alw1}, IS_{Aha1} and IS_{Aha2} (Table 4.4). These elements are present at various frequencies in *Acinetobacter* genomes and the transposases encoded within the elements share between 92-94% amino acid identity with the transposase in IS_{Aba12}. Importantly, they have the same perfect 16 bp TIR sequence as the majority of IS_{Aba12} elements (Table 4.4). This led us to investigate whether other characterised IS contain similar TIR sequences to those in MITE_{Aba12} and thus could potentially translocate the non-autonomous element. An additional nine IS elements were found to have TIR sequences similar or identical to those of MITE_{Aba12} (Table 4.4). These IS elements are of a similar length to IS_{Aba12}, ranging between 1038-1053 bp, with the majority also generating 9 bp TSDs (Table 4.4). Comparisons of MITE_{Aba12} against the sequences of each IS listed in Table 4.4 revealed nucleotide identity was confined to only the TIR sequences and thus the origins of MITE_{Aba12} from an IS could not be readily deduced (data not shown).

4.5.6 MITE_{Aba12} is a highly conserved mobile element with potential to affect expression of neighbouring host genes

To examine sequence identity across all the identified MITE_{Aba12} copies a multiple sequence alignment using Clustal Omega (Sievers and Higgins, 2018) was performed.

Table 4.3: Bacterial strains that harbour full length MITE_{Aba12} elements

Strain name ^a	#MITE _{Aba12} / strain	Isolation source/ origin	Accession number and reference
<u>Chromosomes</u>			
<i>A. baumannii</i> DS002	22	Soil, India	CP027704.1, unpublished
<i>A. indicus</i> SGAir0564	10	Air, Singapore	CP024620.1 (Vettath <i>et al.</i> , 2018)
<i>A. johnsonii</i> XBB1 ^b	7	Hospital sewage, USA	CP010350.1 (Feng <i>et al.</i> , 2016)
<i>A. junii</i> 65	5	Limnetic water, Russia	CP019041 (Fomenkov <i>et al.</i> , 2017)
<i>Acinetobacter</i> sp. SWBY1 ^b	5	Hospital sewage, China	CP026616.1, unpublished
<i>A. baumannii</i> B8300	4	Human bloodstream, Southern India	LFYY00000000 (Vijaykumar <i>et al.</i> , 2015a)
<i>Acinetobacter</i> sp. ACNIH1	3	Hospital plumbing, USA	CP026420.1 (Weingarten <i>et al.</i> , 2018)
<i>A. baumannii</i> ABNIH28	3	Hospital plumbing, USA	CP026125 (Weingarten <i>et al.</i> , 2018)
<i>Acinetobacter</i> sp. TGL-Y2	2	Frozen soil, China	CP015110.1, unpublished
<i>A. baumannii</i> B8342	2	Human bloodstream, Southern India	LFYZ00000000 (Vijaykumar <i>et al.</i> , 2015b)
<i>M. osloensis</i> CCUG 350	1	Human cerebrospinal fluid, USA	CP014234.1, unpublished
<i>A. haemolyticus</i> TJS01	1	Human respiratory tract, China	CP018871.1, unpublished
<i>Acinetobacter</i> sp. NCu2D-2	1	Murine trachea, Germany	CP015594 (Blaschke and Wilharm, 2017)
<i>Acinetobacter</i> sp. ACNIH2 ^b	1	Hospital plumbing, USA	CP026412.1 (Weingarten <i>et al.</i> , 2018)
<i>A. baumannii</i> ATCC 17978	1	Human meninges, France	CP012004.1 (Weber <i>et al.</i> , 2015b)
<i>A. junii</i> WCHAJ59	1	Hospital sewage, China	CP028800.1, unpublished

Strain name ^a	#MITE _{Aba12} /strain	Isolation source/ origin	Accession number and reference
<i>A. baumannii</i> AR_0083	1	Unknown	CP027528.1, unpublished
<i>Acinetobacter</i> sp. WCHA45 ^b	1	Sewage, China	CP028561.1, unpublished
<i>A. baumannii</i> MAD ^c	1	Human skin, France	AY665723.1 (Poirel and Nordmann, 2006)
<u>Plasmids</u>			
<i>A. schindleri</i> SGAir0122, pSGAir0122	2	Air, Singapore	CP025619.1 (Kee <i>et al.</i> , 2018)
<i>A. baumannii</i> A297 (RUH875), pA297-3	1	Human urinary tract, Netherlands	KU744946 (Hamidian <i>et al.</i> , 2016a)
<i>A. johnsonii</i> XBB1, pXBB1-9	1	Hospital sewage, USA	CP010351.1 (Feng <i>et al.</i> , 2016)
<i>A. lwoffii</i> ED45-23, pALWED2.1	1	Permafrost, Russia	KX426229 (Mindlin <i>et al.</i> , 2016)
<i>A. baumannii</i> AbPK1, pAbPK1a	1	Ovine respiratory tract, Pakistan	CP024577 (Linz <i>et al.</i> , 2018)
<i>Acinetobacter</i> sp. DUT-2, unnamed 1	1	Marine sediment, China	CP014652, unpublished
<i>Acinetobacter</i> sp. BW3, pKLH207	1	Stream water, USA	AJ486856 (Kholodii <i>et al.</i> , 2004)
<i>A. towneri</i> strain G165, pNDM-GJ01	1	Human stool, China	KT965092 (Zou <i>et al.</i> , 2017)
<i>A. baumannii</i> D46, pD46-4	1	Human urine, Australia	MF399199 (Nigro and Hall, 2017)
<i>Acinetobacter</i> sp. ACNIH2, pACI-3569	1	Hospital plumbing, USA	CP026416.1 (Weingarten <i>et al.</i> , 2018)
<i>Acinetobacter</i> sp. WCHA45, pNDM1_100045	1	Hospital sewage, China	CP028560.1, unpublished

Strain name ^a	#MITE _{Aba12} /strain	Isolation source/ origin	Accession number and reference
<i>A. baumannii</i> CHI-32, pNDM-32	1	Human bloodstream, India	LN833432.1, unpublished
<i>A. defluvi</i> WCHA30, pOXA58_010030	1	Hospital sewage, China	CP029396.1, unpublished
<i>A. pittii</i> WCHAP005069, pOXA58_005069	1	Clinical isolate, China	CP026086.1, unpublished
<i>A. pittii</i> WCHAP100004, pOXA58_100004	1	Clinical isolate, China	CP027249.1, unpublished
<i>A. pittii</i> WCHAP005046, pOXA58_005046	1	Clinical isolate, China	CP028573.1, unpublished
<i>Acinetobacter</i> sp. SWBY1, pSWBY1	1	Hospital sewage, China	CP026617.1, unpublished

^asp.; species

^bStrains where MITE_{Aba12} is present on both chromosomal and plasmid DNA

^cIn *A. baumannii* MAD MITE_{Aba12} was found on a 7.8 kb stretch of sequenced DNA rather than a full length chromosome (Poirel and Nordmann, 2006)

Table 4.4: IS with TIR closely related to those of IS*Aba12* and MITE*Aba12*

IS name ^a	IRL sequence	IRR sequence	Size (bp)	TSD (bp)
MITE _{<i>Aba12</i>}	GGCTTTGTTGCACAAA	GGCTTTGTTGCATAAAA	113	9
IS <i>Aba12</i>	GGCTTTGTTGCACAAA	GGCTTTGTTGCACAAA	1039	9
IS <i>I7</i>	GGCTTTGTTGCACAAA	GGCTTTGTTGCACAAA	1040	9
IS <i>Aba5</i> ^b	GGCTTTGTTGCACAAA	GGCTTTGTTGCATAAAA	1044	ND
IS <i>Aba7</i>	GGCTTTGTTGCATAAAA	GGCTTTGTTGCACAAA	1039	9
IS <i>Aba10</i>	GGCTTTGTTGCATAAATA	GGCTTTGTTGCACAAATA	1023	9
IS <i>Aba13</i>	GGCTTTGTTGCACAAA	GGCTTTGTTGCACAAA	1039	9
IS <i>Aba40</i>	GGCTTTGTTGCACAAA	GGCTTTGTTGCACAAA	1039	9
IS <i>Aha1</i>	GGCTTTGTTGCACAAAC	GGCTTTGTTGCACAAAC	1039	4
IS <i>Aha2</i>	GGCTTTGTTGCACAAA	GGCTTTGTTGCACAAA	1040	ND
IS <i>Aha3</i>	GGCTTTGTTGCACAAA	GGCTTTGTTGCATAAAA	1039	ND
IS <i>Ajo1</i>	GGCTTTGTTGCACAAA	GGCTTTGTTGCATAAAA	1039	3
IS <i>Alw1</i>	GGCTTTGTTGCACAAAG	GGCTTTGTTGCACAAAG	1038	ND
IS <i>Ecl7</i>	GGCTTTGTTGCACAAA	GGCTTTGTTGCATAAAA	1052	9
IS <i>Nov2</i>	GGCTTTGTTGCGCAAAT	GGCTTTGTTGCATAAAT	1048	9

^aAbbreviations; IS, insertion sequence; IRL, inverted repeat left; IRR, inverted repeat right; TSD, target site duplication; ND, not determined

^bThe transposase of IS*Aba5* is thought to be inactive (Siguier *et al.*, 2006)

From the analysis of 90 MITE_{Aba12} copies it was found that 10% of MITE_{Aba12} copies diverged from the 113 bp consensus (Figure 4.4). Three of the ten MITE_{Aba12} copies present in *A. indicus* SGAir0564 are atypical; two were 112 bp sharing 100% identity with each other whilst the other is 114 bp. Similarly, in *Acinetobacter* sp. SWBY1, three of the five MITE_{Aba12} copies differed from the consensus length, which included the smallest identified element at 111 bp and two at 114 bp. A further three atypical 112 bp MITE_{Aba12} sequences were identified in the genomes of *A. baumannii* DS002, *Acinetobacter* sp. TGL-Y2, and ACNIH1 (Figure 4.4). Thus, a total of 34 different MITE_{Aba12} sequences were identified, leading to the assignment of 10 Sub-groups. MITE_{Aba12} sequence arrangements that harboured two copies, or more were segregated into Sub-groups that were ordered from one to ten based on the most to least abundant (Figure 4.4 and Table 4.5). Significant variation existed across the central region of the element as only 10 bases were conserved across all 90 identified copies (Figure 4.4; it is possible that some nucleotide differences identified across MITE_{Aba12} copies could be attributed to sequencing errors). The MITE_{Aba12} TIR sequences were the most conserved, as eight and nine of the 16 bp IRL and IRR sequences, respectively, were identical across all MITE_{Aba12} copies analysed (Figure 4.4). Overall, no preference in the orientation of MITE_{Aba12} in the genomes could be identified (data not shown).

MITEs generally insert into AT-rich regions (Delilhas, 2008). Of the 90 identified MITE_{Aba12} copies, 36 from 13 different genomes had 9 bp TSDs. From the 22 MITE_{Aba12} copies in *A. baumannii* DS002, TSDs could be identified for 17, which could infer a burst of recent activity. Interestingly, all MITE_{Aba12} elements from Sub-group 4 were found in the same site and flanked by identical TSD of eight, rather than nine bp (TTTTTGTT). These elements were on large plasmids (~62–112.5 kb) and Blastn analyses using the MITE_{Aba12} element together with ~700 bp left and right of the sequence from pNDM-32 of *A. baumannii* CHI-32 identified they were all located in an identical position, sharing 100 % identity across this ~1.5 kb region (data not shown). Overall, MITE_{Aba12} appeared to favour inserting into sequences with an AT ratio $\geq 55.5\%$, as demonstrated by the skewed distribution of the columns to the right (Figure 4.5 A), although no identifiable trends in nucleotide sequence arrangements could be identified (Figure 4.5 B).

To assess how MITE_{Aba12} could influence host gene expression a consensus sequence MITE_{Aba12}(c) was generated using WebLogo (Crooks *et al.*, 2004) from all 113 bp MITE_{Aba12} elements ($n = 81$) (Figure 4.4). At least two stop codons in all six reading frames can be identified after translation of the MITE_{Aba12}(c) DNA sequence. Start codons

Subgroup

MITE_{Abu12}(c)

GGCTTTGTTGCACAAAGATTTCACTAATATATGATTTTAAAAGTTTTGATTATTTTTTGATCCAAAATTTAAATTTTAAATCAGATGCTTACATATTTATGCAACAAAGCC

Acinetobacter sp. TGL-Y2_#1	GGCTTTGTTGCACAAATATTTAAAC TAC---TGATTTATAGTGATTAGTTT TAGATTAAAA-ATTAATAAAACCCACTAAAATCAATTCTTTACAAAAATTTATGCAACAAAGTC	113
Acinetobacter sp. TGL-Y2_#2	GGCTTTGTTGCACAAACATTTAAAC TAC---TGATTTGTAATGATTATTTTTTACATTA AAAA-ATTAATAAG-CCTATTA AAAATCAATGATTTAAAAAATTTATGCAACAAAGTC	112
Acinetobacter sp. ACNIH1_#3	GGCTTTGTTGCATAAAATAT TAA GACTA---TGATTTTTTAATTCATTTT--TGGATTAAAAATCAAAAAATCTTTAAGCAATCAGCATCTTGAAGCAATGTTTATGCAACAAAGGCC	112
Acinetobacter sp. ACNIH1_#2	GGCTTTGTTGTATAAATACATAAACC AAC---TGATTTTGTTCATTTAATTTTTAGGTTGAAA-TTCATACAAACCTATTTAAATCAGAA GCTTACAAAATCTTTATGCAACAAAGGCC	113
Acinetobacter sp. SWBY1_#5	GGCTTTGTTGCATTAATATGTAAAGCATC---TGATTTAAATAAATTTAATTTTGGATCAAAAAATAAATAAAACTTTTAAATCATGTAGTTATGAAATCTTTATGCAACAAAGGCC	114
Acinetobacter sp. WCHA45	GGCTTTGTTGCATAAAATATGTAAAGCAAC---TGATTTAAATAAATTTAATTTTGGATTA AAAA-AAATAATCAAAACTTTTAAATCATATAGTTATGAAATCTTTATGCAAAAAAGGCC	113
8. A. indicus SGAir0564_#9 (2)	GGCTTTGTTGCACAAAGATTT CATAACTATATGATTTTAAAGATTTTGA--TTATTTATGATCCAAAATTA---AATACATTTAAATCAGATGCTTACATATTTATGCAACAAAGGCC	112
Acinetobacter sp. SWBY1_#4	GGCTTTGTTGCATAAAGATTT CATAACTATATGATTTTAAAAATTTTGGATTATTTTTTTGATCCAAAATTA---AATTTATTTAAATCAGATGCTTACATATTTATGCAACAAAGGCC	114
Acinetobacter sp. SWBY1_#3	GGCTTTGTTGCACAAAGATTT CATAACTATATGATTTTAAAA-CTTTTGGATTATTTTTT-GATACAAAATTA---AATTTATTTAAATCAGATGCTTACATATTTATGCAACAAAG-C	111
A. indicus SGAir0564_#8	GGCTTTGTTGCACAAAGATTT CATAACTATATGATTTTAAAAATTTTGGATTATTTTTTAAATCCAAAATTA---AATTTATTTAAATCAGATGCTTACATATTTATGCAACAAAGGCC	114
Acinetobacter sp. SWBY1 pSWBY1	GGCTTTGTTGCACAAAGATTTTATAACTATATGATTTTAAACATTTTGGATTGTTTTT-TGATCTAAAATTA---AATCTATTTAAATCAGATGCTTACATATTTATGCAACAAAGGCC	113
A. junii 65_#5	TGATTTGTTGCACAAAATTT CATAACTATATGATTTTAAAAATTTTGGATTATTTTTT-TGATCCAAAATTA---AATTTATTTAAATCAGATGCTTACATATTTATGCAACAAAGGCC	113
7. Acinetobacter sp. ABNIH28_#3 (2)	GGCTTTGTTGCACAAAGATTT CATAACTATATGATTTTAAAAATTTTGGATTATTTTTT-TAATCCAAAATTA---AATTTATTTAAATCAGTTGCTTACATATTTATGCAACAAAGGCC	113
A. johnsonii XBB1_#7	GGCTTTGTTGCACAAAGATTT CATAACTATATGATTTTAAAAATTTTGGATTATTTTTT-TGATCTAAAATTA---AATTTATTTAAATCAGATGCTTACATATTTATGCAACAAAGGCC	113
6. A. johnsonii XBB1_#4 (3)	GGCTTTGTTGCACAAAGATTT CATAACTATATGATTTTAAAAATTTTGGATTATTTTTT-TAATCCAAAATTA---AATTTATTTAAATCAGATGCTTACATATTTATGCAACAAAGGCC	113
A. baumannii AbPK1 pAbPK1a	GGCTTTGTTGCACAAAGATTT CATAACTATATGATTTTAAAAATTTTGGATTGTTTTT-TGATCCAAAATTA---AATCTATTTAAATCAATGCTTACATATTTATGCAACAAAGGCC	113
A. indicus SGAir0564_#7	GGCTTTGTTGCACAAAGATTT CATAACTATATGATTTTAAAAATTTTGGATTATTTTTT-TGATCCAAAATTA---AATCTATTTAAATCAAAATGCTTACATATTTATGCAACAAAGGCC	113
Acinetobacter sp. SWBY1_#2	GGCTTTGTTGCGCAAAGTTTT CATAACTATATGATTTTAAAAATTTTGGATTATTTTTT-TGATCCAAAATTA---AATTTATTTAAATCAGATGCTTACATATTTATGCAACAAAGGCC	113
3. Acinetobacter sp. DUT-2 (5)	GGCTTTGTTGCACAAAGATTT CATAACTATATGATTTTAAAAATTTTGGATTGTTTTT-TGATCCAAAATTA---AATTTATTTAAATCAGATGCTTACATATTTATGCAACAAAGGCC	113
9. Acinetobacter sp. SWBY1_#1 (2)	GGCTTTGTTGCACAAAGATTT CATAACTATATGATTTTAAAAATTTTGGATTGTTTTT-TGATCCAAAATTA---AATTTATTTAAATCAGATGCTTACATATTTATGCAACAAAGGCC	113
A. townneri G165 pNDM-GJ01	GGCTTTGTTGCACAAAGATAT CATAACTATATGATTTTAAAAATTTTGGATTATTTTTT-TGATCCAAAATTA---AATTTATTTAAATCAGATGCTTACATATTTATGCAACAAAGGCC	113
A. baumannii ABNIH28_#2	GGCTTTGTTGCACAAAGATTT CATAACTATTTGATTTTAAAAATTTTGGATTATTTTTT-TGATCCAAAATTA---AATTTATTTAAATCAGATGCTTACATATTTATGCAACAAAGGCC	113
A. junii 65_#3	GGCTTTGTTGCACAAAATATTT CATAACTATATGATTTTAAAAATTTTGGATTATTTTTT-TGATCCAAAATTA---AATTTATTTAAATCAGATGCTTACATATTTATGCAACAAAGGCC	113
Acinetobacter sp. pNDM_010045	GGCTTTGTTGCACAAAGATTT CATAACTATATGATTTTAAAAATTTTGGATTATTTTTT-TGATCCAAAATTA---AATTTATTTAAATCAGATGCTTACATATTTATGCAACAAAACC	113
1. A. baumannii DS002_#1 (27)	GGCTTTGTTGCACAAAGATTT CATAACTATATGATTTTAAAAATTTTGGATTATTTTTT-TGATCCAAAATTA---AATTTATTTAAATCAGTTGCTTACATATTTATGCAACAAAGGCC	113
A. baumannii DS002_#19	GGCTTTGTTGCACAAAGATTT CATAACTATATGATTTTAAAAATTTTGGATTATTTTTT-TGATCCAAAATTA---AATTTATTTAAATCAGTTGCTTACATATTTATGCAACAAAG-C	112
A. haemolyticus TJS01	GGCTTTGTTGCACAAAGATTT CATAACTATATGATTTTAAAAATTTTGGATTATTTTTT-TGATCCAAAATTA---AATTTATTTAAATCAGATGCTTACATATTTATGCAACAAAGGCC	113
Acinetobacter sp. Ncu2D-2	GGCTTTGTTGCACAAAGATTT CATAACTATATGATTTTAAAAATTTTGGATTATTTTTT-TAATCCAAAATTA---AATTTATTTAAATCAGATGCTTACATATTTATGCAACAAAGGCC	113
A. baumannii ABNIH28_#1	GGCTTTGTTGCACAAAGATTT CATAACTATATGATTTTAAAAATTTTGGATTATTTTTT-GATCCAAAATTA---AATTTATTTAAATCAGATGCTTACATATTTATGCAACAAAGGCC	113
5. A. indicus SGAir0564_#4 (4)	GGCTTTGTTGCACAAAGATTT CATAACTATATGATTTTAAAAATTTTGGATTATTTTTT-TGATCCAAAATTA---AATTTATTTAAATCAGATGCTTACATATTTATGCAACAAAGGCC	113
2. A. baumannii ATCC 17978 (17)	GGCTTTGTTGCACAAAGATTT CATAACTATATGATTTTAAAAATTTTGGATTATTTTTT-TGATCCAAAATTA---AATTTATTTAAATCAGATGCTTACATATTTATGCAACAAAGGCC	113
A. baumannii MAD	GGCTTTGTTGCATAAAGATTTTGTAAAGCTTGTGATTTAAATAGGTTTGTATGAAATTT-AAACCTAAAATTT---AAATGAAAGAAAATCAGTTGGTTATGTATTTATGCAACAAAGGCC	113
10. A. johnsonii XBB1 pXBB1-9 (2)	GGCTTTGTTGTATAAACATT TTTCAAGATACTGATTTTAAAGGATTTGTTTAAATTT-TAATCCAAAATTA---AATTTAAACAAAATCATAGTCTTAGATATTTATGCAACAAAGGCC	113
4. A. pittii pOXA58_005046 (4)	GGTTTTGTTGCATAAAGATTTTGTAAAGGTA CTGATTTTAAAGGTTTGGGAAAATTT-CAACCTAAGAAATA---AATTTAAATAAAATCATATTCTTAGGTATTTATGCAACAAAGGCC	113

* * * * * *
IRL

* * * * * *
IRR

Figure 4.4: Nucleotide alignment of all MITE_{Aba12} elements identified in this study

The nucleotide sequence above the alignment (black box) denotes the consensus sequence, MITE_{Aba12}(c), derived using WebLogo software (Crooks *et al.*, 2004). MITE_{Aba12} sequences with nucleotide variations are displayed. Sub-group representatives are numbered and in bold-face type with numbers in parentheses indicating the total number of MITE_{Aba12} copies with that sequence. A, T, G and C nucleotides are denoted in blue, yellow, purple and green boxes, respectively. Black lines and asterisks represent the terminal inverted repeats (IRL and IRR) and conserved bases, respectively. See Table 4.5 for full list of MITE_{Aba12} elements included in each Sub-group and Table 4.3 for strain accession numbers.

Table 4.5: List of MITE_{Aba12} elements and their corresponding strain names that formulate MITE_{Aba12} Sub-groups 1-10

Subgroup number	Copies of MITE _{Aba12}	Representative MITE _{Aba12} element	Additional MITE _{Aba12} elements
1	27	<i>A. baumannii</i> DS002_#1	<i>A. baumannii</i> DS002_#2-18, 20-22 <i>A. baumannii</i> B8300_#1-4 <i>A. baumannii</i> B8342_#1 <i>A. junii</i> 65_#2
2	17	<i>A. baumannii</i> ATCC 17978	<i>A. indicus</i> SGAir0564_#1-3 <i>A. johnsonii</i> XBB1_#1-3 <i>A. schindleri</i> SGAir, pSGAir0122_#1-2 <i>A. baumannii</i> ATCC 17978 Δ ysiW Δ hns::MITE _{Aba12} _#1-2 <i>A. junii</i> 65_#1 <i>Acinetobacter</i> sp. BW3 <i>M. osloensis</i> CCUG 350 <i>A. lwoffii</i> ED45-23, pALWED2.1 <i>A. junii</i> WCHAJ59 <i>Acinetobacter</i> sp. ACNIH1_#1
3	5	<i>Acinetobacter</i> sp. DUT-2, unnamed 1	<i>Acinetobacter</i> sp. ACNIH2 <i>Acinetobacter</i> sp. ACNIH2, pACI-3569 <i>A. baumannii</i> D46, pD46-4 <i>A. baumannii</i> A297, pA297-3
4	4	<i>A. pittii</i> WCHAP005046, pOXA58_005046	<i>A. pittii</i> WCHAP100004, pOXA58_100004 <i>A. pittii</i> WCHAP005069, pOXA58_005069 <i>A. baumannii</i> CHI-32, pNDM-32
5	4	<i>A. indicus</i> SGAir0564_#4	<i>A. indicus</i> SGAir0564_#5-6 <i>A. baumannii</i> AR_0083
6	3	<i>A. johnsonii</i> XBB1_#4	<i>A. johnsonii</i> XBB1_#5-6
7	2	<i>Acinetobacter</i> sp. ABNIH28_#3	<i>A. baumannii</i> B8342_#2
8	2	<i>A. indicus</i> SGAir0564_#9	<i>A. indicus</i> SGAir0564_#10
9	2	<i>Acinetobacter</i> sp. SWBY1_#1	<i>A. junii</i> 65_#4
10	2	<i>A. johnsonii</i> XBB1 pXBB1-9	<i>A. defluvii</i> WCHA30 pOXA58_010030

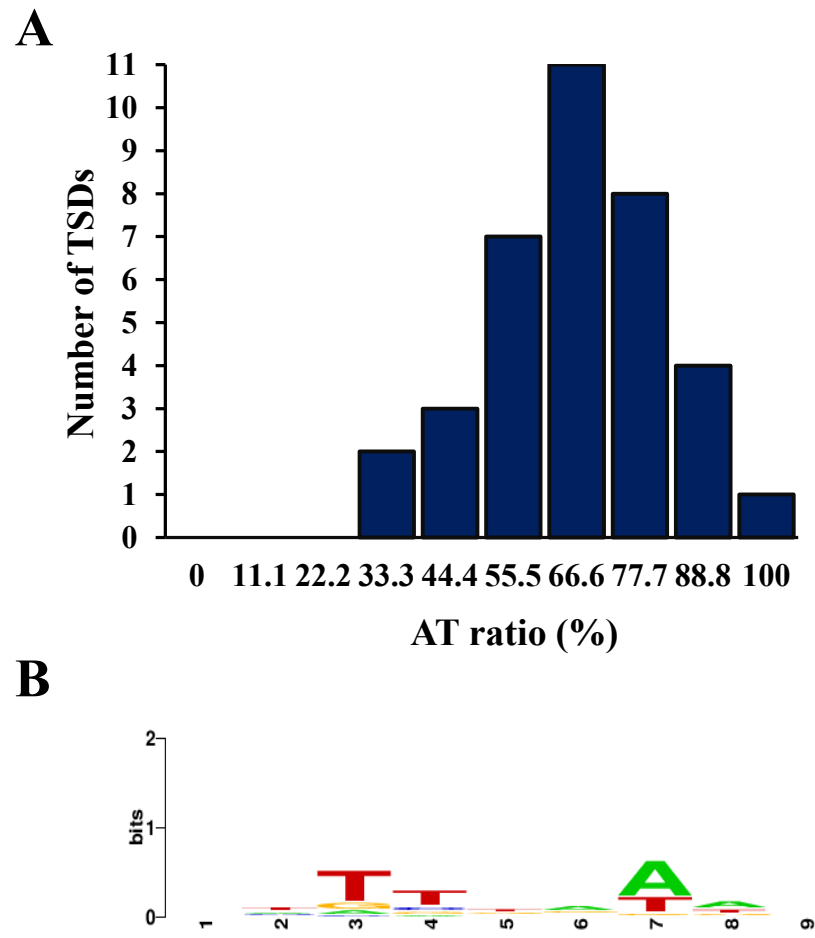


Figure 4.5: Characterisation of target site duplications flanking MITE_{Aba12}

(A) Graphical representation of AT-richness (%) identified from all target site duplications flanking MITE_{Aba12} elements. **(B)** Nucleotide logo generated from all target site duplication events using WebLogo software (Crooks *et al.*, 2004).

followed by three, seven or eight amino acids at the terminal ends of the element were identified in three of the reading frames (data not shown). Depending on the integration site in a given genome these characteristics could allow for fusion with neighboring CDSs. Mfold (Zuker, 2003) predicted weak secondary structures of $\Delta G = -23.99$ or -26.94 kcal/mol; in the two orientations of MITE_{Aba12}(c), (IRL to IRR or IRR to IRL, respectively), (data not shown). Using the ARNold tool (Naville *et al.*, 2011), no predicted Rho-independent transcriptional terminators were identified. The Softberry program, BPPROM, predicted two outward-facing promoter sequences based on the -35 and -10 *Escherichia coli* $\sigma 70$ promoter consensus sequences (Figure 4.6). These sequences were also compared with the strong outward-facing promoter found in IS_{Aba1} coupled with flanking sequence associated with overexpression of the *bla_{ampC}* gene in *A. baumannii* CLA-1 (Héritier *et al.*, 2006) (Figure 4.6 B). To verify whether the two putative outward-facing promoters identified within MITE_{Aba12}(c) could drive the production of mRNA transcripts, three previously published *A. baumannii* ATCC 17978-derived RNA-seq transcriptomes (Giles *et al.*, 2015) and from Chapter 2 were aligned to the reference ATCC 17978 genome (GenBank accession number: CP012004.1) using the integrative genomics viewer program (Robinson *et al.*, 2011). Transcripts originating within the MITE_{Aba12} sequence that could be attributed to the P_{out} IRR putative promoter were identified across all three transcriptomes. However, transcripts reading out from P_{out} IRL were limited (data not shown). Thus, it appears in ATCC 17978 that the P_{out} IRR putative promoter within MITE_{Aba12}(c) has the potential to influence host gene transcription.

The fusion of small mobile elements with neighboring genes can affect gene function and in some cases lead to improved host fitness or formation of new proteins (Abergel *et al.*, 2006; Delihias, 2007). The exhaustive analysis conducted on MITE_{Aba12} in publicly available GenBank entries, revealed that some insertions of MITE_{Aba12} interrupted host genes and in some cases the encoded protein could be fused with up to 19 amino acids encoded by MITE_{Aba12} sequences (data not shown). MITE_{Aba12} elements located in pAbPK1a from *A. baumannii* AbPK1 and in the chromosomes of *A. baumannii* B8300 and *Acinetobacter* sp. ACNIH1_#2 could create fusions to the 5' end of adjacent genes. Each had incorporated nucleotides reading outwards from the TIR of MITE_{Aba12} to generate the first four amino acids (MQQS) of the neighboring CDS. These particular arrangements also placed the host gene in proximal distance to the P_{out} IRR promoter sequences and given its activity in ATCC 17978, the element could also influence the expression of fused genes.

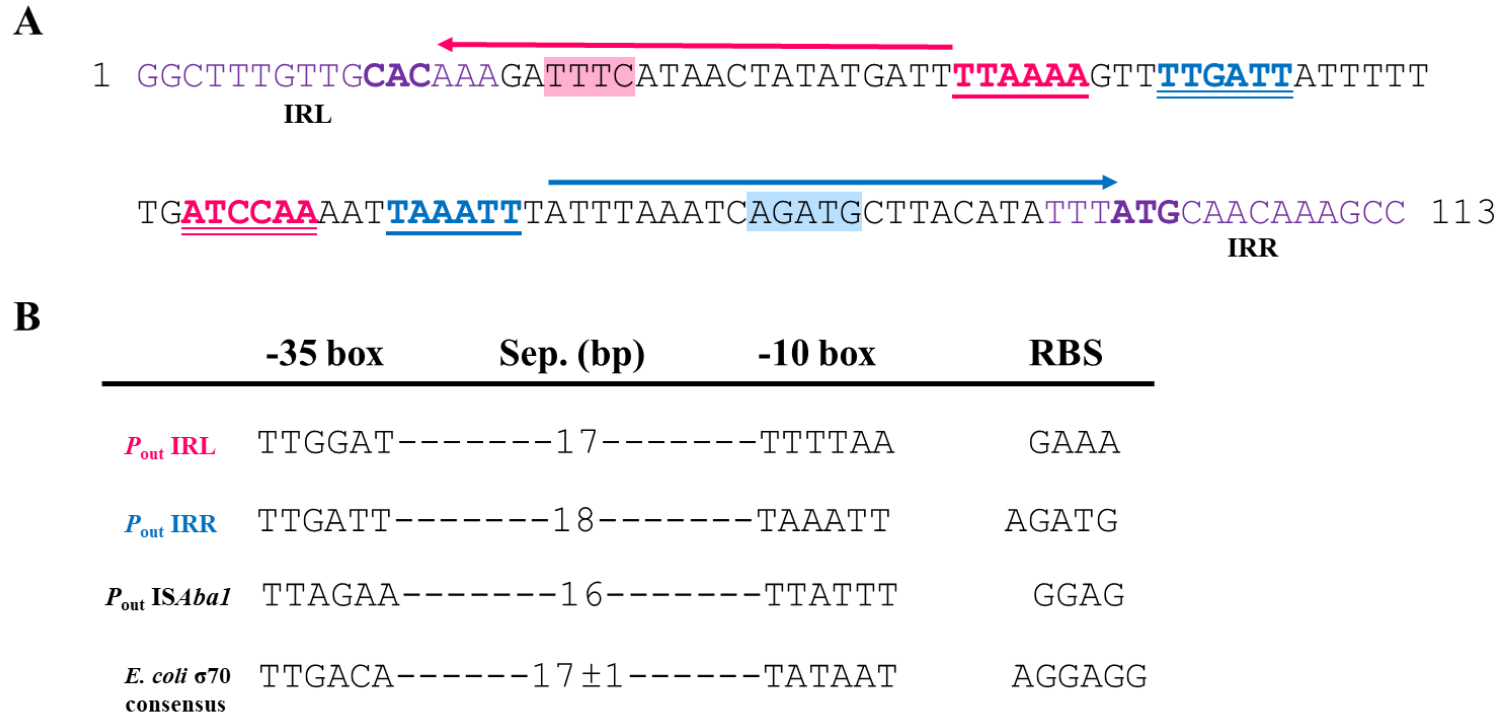


Figure 4.6: Putative σ 70 promoter sequences identified in MITE_{Aba12}(c)

The σ 70 promoter sequences were predicted using the Softberry BPROM tool. **(A)** Pink and blue nucleotide sequences represent outward-facing promoters, reading out through the IRL and IRR sequences (*P_{out} IRL* and *P_{out} IRR*, respectively) and the orientation of transcription is shown by arrows. Nucleotides underlined and double underlined denote -10 box and -35 box sequences, respectively. Purple nucleotides denote IRL and IRR, with putative translational start codons in bold-face type with their corresponding putative ribosome binding sites (RBS) shaded in pink and blue, respectively. **(B)** Alignment of the putative *P_{out} IRL* and *P_{out} IRR* and RBSs in MITE_{Aba12}(c) against the *E. coli* σ 70 promoter and RBS consensus and *P_{out}* of *ISAbal* coupled with the adjacent region and RBS in the *ISAbal*-activated *bla_{ampC}* gene of *A. baumannii* CLA-1 (Héritier *et al.*, 2006). The nucleotide length between the -10 and -35 boxes (Sep. [bp]) is indicated.

4.5.7 MITE_{Aba12} in *M. osloensis* CCUG 350 is located within a novel composite transposon.

As previously stated, *M. osloensis* CCUG 350 carries one copy of MITE_{Aba12} (Table 4.3). It lies within an 8.5 kb region absent from five closely related *M. osloensis* genome sequences, (see alignment in Figure 4.7 A). IS were found at the terminal ends of the novel insert and shared highest identity with the IS_I-family member IS_{Aba3} (81% identity, *E*-value; 5e-55) (Siguier *et al.*, 2006). Both terminal IS carried 24 bp TIR sequences (5'-GGTGGTGTTCAAAAAGTATGCTG-3') and TSDs of eight bp were identified at each end of the 8.5 kb insert (Figure 4.7 B). These features make this sequence synonymous to a composite transposon (Siguier *et al.*, 2015) now named Tn6645. In *M. osloensis* CCUG 350 the MITE_{Aba12} element was located between the IS_{Aba3} element and a gene of unknown function containing a DUF 2789 motif (*E*-value; 4.2e-27) (Kanehisa *et al.*, 2016). Additionally, an IS_{Aba11}-like element, an alkylsulfatase gene, a TetR-family transcriptional regulator gene and a partial gene encoding a major facilitator superfamily transporter were identified within the composite transposon (Figure 4.7). The insertion of IS_{Aba3} truncated the 3' end of the transporter gene by 540 bp, and therefore is likely to be non-functional (a pseudogene).

Blastn searches were used to search for Tn6645 in other bacterial genomes but no additional full length copies were identified (data not shown). However, approximately 4.3 kb of the 8.5 kb sequence aligned (96% identity) to a region in the chromosome of *Acinetobacter guillouiae* NBRC 110550 (Yee *et al.*, 2014) (Figure 4.7 B). This region harboured the alkylsulfatase, TetR-family regulator and the truncated transporter genes and thus may represent a potential source for this portion of the Tn6645 cargo.

4.6 Discussion

Since their identification in bacteria 30 years ago, MITEs have been reported in a multitude of sp., displaying significant diversity in their nucleotide sequence and functional properties (Delihias, 2011). In this study, a novel MITE was identified in environmental and clinical isolates of *Acinetobacter* sp. including *A. baumannii*, one of the leading bacterial organisms threatening human health (Harding *et al.*, 2018). This novel element lacked any CDS that could produce a functional transposase, inferring that like other MITEs MITE_{Aba12} is *trans*-activated. Given the high similarity between the TIR sequence of MITE_{Aba12} and those of IS_{Aba12} (Figure 4.2 D), we propose the transposase from IS_{Aba12} elements were responsible for MITE_{Aba12} mobilisation in the *A. baumannii*

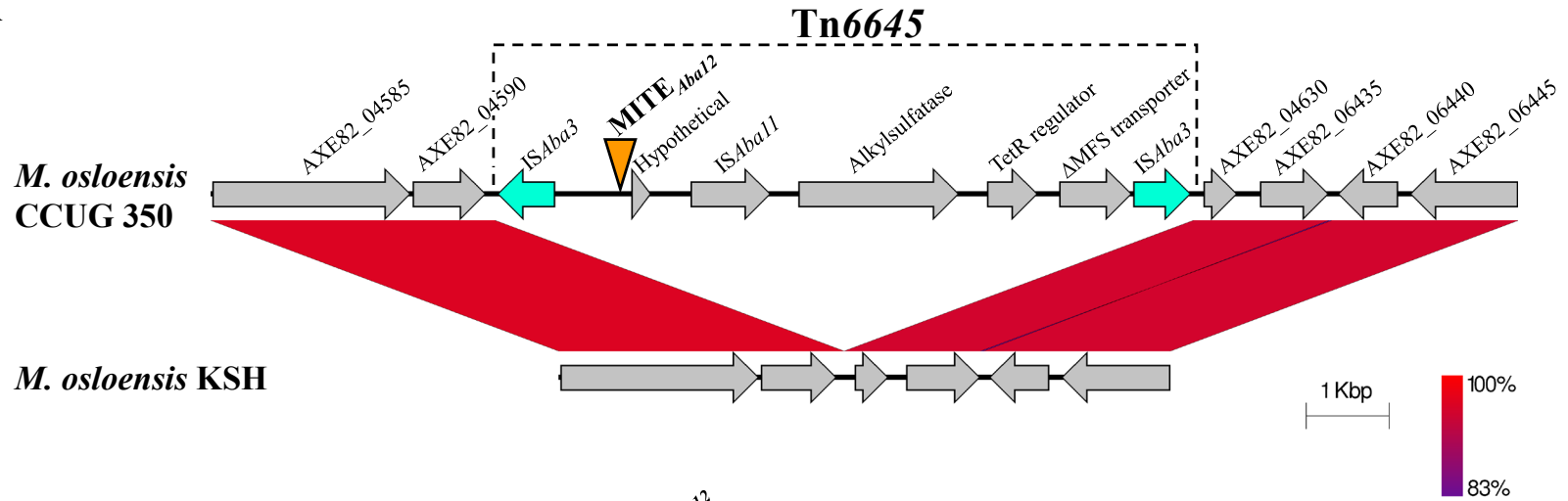
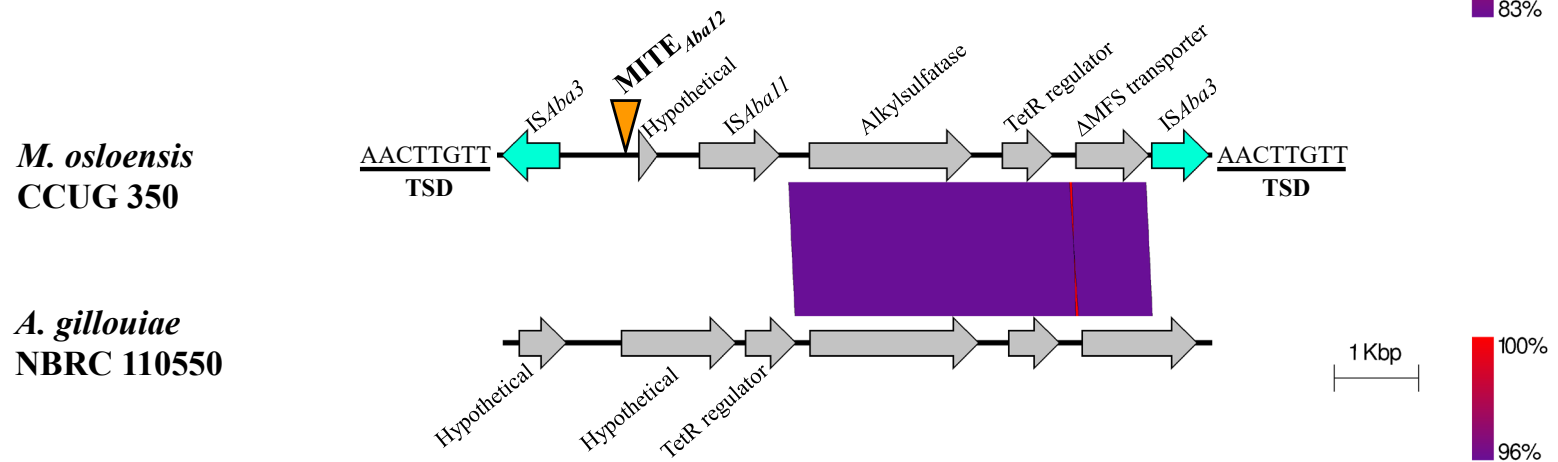
A**B**

Figure 4.7: MITE_{Aba12} is located within Tn6645 in *Moraexella osloensis* CCUG 350

Grey arrows indicate direction of transcription and blue arrows represent IS_{Aba3} elements forming the boundaries of Tn6645. Identity between regions is indicated by the colour gradient. **(A)** Alignment of nucleotide sequence from AXE82_04585-AXE82_06445 in *M. osloensis* CCUG 350 and the corresponding region in KSH (Lim *et al.*, 2018) (GenBank accession numbers: CP014234.1 and CP024180.2, respectively). Gene names and locus tags are derived from *M. osloensis* CCUG 350 annotation. **(B)** Alignment of Tn6645 from *M. osloensis* CCUG 350 and part of the *A. guillouiae* NBRC 110550 chromosome (GenBank accession number: AP014630.1), (Yee *et al.*, 2014). Identity between Tn6645 and *A. guillouiae* NBRC 110550 starts 80 bp downstream from TIR of IS_{Aba11}. The eight bp TSD flanking Tn6645 are shown. The location of MITE_{Aba12} is indicated by the orange triangle. Sequences were obtained from the NCBI database and aligned and visualised using the Easyfig 2.2.2 tool (Sullivan *et al.*, 2011).

ΔygiW strain but whether IS*Aba12*, or other ISs with similar TIR to MITE_{*Aba12*} (Table 4.4) can mobilise MITE_{*Aba12*} will need to be experimentally examined.

With the addition of MITE_{*Aba12*} the list of non-autonomous elements reported in *Acinetobacter* grows to three. Like most prokaryotic MITEs, the two previously characterised MITEs from *Acinetobacter* isolates are flanked by TIRs and generate TSDs upon insertion (Gillings *et al.*, 2009; Hamidian *et al.*, 2016a). In comparison to MITE_{*Aba12*}, both elements have only been identified on plasmid sequences and are approximately four times larger in size (439 and 502 bp, respectively) (Gillings *et al.*, 2009; Hamidian *et al.*, 2016a). Identical copies of the MITE originally identified in *Acinetobacter* sp. NFM2 flank class 1 integrons carrying different resistance determinants in a number of *Acinetobacter* strains, forming a structure comparable to a composite transposon (Gillings *et al.*, 2009; Domingues *et al.*, 2011; Domingues *et al.*, 2013; Zong, 2014; Gallagher *et al.*, 2015; Wibberg *et al.*, 2018). MITE-297 is found on the large conjugative plasmid pA297-3 present in the *A. baumannii* Global Clone (GC) 1 reference strain A297 (RUH875) (Hamidian *et al.*, 2016a). In pA297-3, two copies of MITE-297 flank a 76 kb region carrying numerous IS and a *mer* module which confers resistance to mercury (Hamidian *et al.*, 2016a). Interestingly, within pA297-3 MITE_{*Aba12*} is also present in the intergenic region between the *merD* and 5-hydroxyisourate hydrolase precursor genes (data not shown). MITE_{*Aba12*} is also found in an identical position in the ~208 kb pD46-4 plasmid from *A. baumannii* D46 (Nigro and Hall, 2017) and a 141 kb plasmid from *Acinetobacter* sp. DUT-2 strains. Given the position of the element within these plasmids, it could be suggested that MITE_{*Aba12*} has travelled with this *mer* operon, which may partly explain its distribution throughout these bacterial genomes. Our analyses also identified a copy of MITE_{*Aba12*} flanked by two IS on the large non-conjugative plasmid pALWED2.1 from the *Acinetobacter lwoffii* strain ED45-23, isolated from uncontaminated Russian permafrost sediments dated to be 20-40, 000 years old (Mindlin *et al.*, 2016). To our knowledge, this is the most primitive strain that has been sequenced and shown to carry a copy of MITE_{*Aba12*}. Interestingly, heavy metal resistance operons identified on pALWED2.1 share identity with sequences from two additional *Acinetobacter* strains that also carry copies of MITE_{*Aba12*} (Mindlin *et al.*, 2016). Our data, which provides another example of MITE_{*Aba12*} ‘hitchhiking’ alongside resistance genes, supports the idea that HGT has played an important role in the evolution of heavy metal resistance to confer a selective advantage to the organism (Mindlin *et al.*, 2016).

Bacterial MITEs can possess various motifs that affect their own regulation and/ or modulate expression of other genes within the residing genome (Siddique *et al.*, 2011; Klein *et al.*, 2015; Wachter *et al.*, 2018). Using the MITE_{Aba12(c)} consensus sequence identified as part of this study, putative outward-facing *E. coli* σ 70 promoters could be identified in both orientations (Figure 4.6). IS_{Aba1} is present in high copy numbers across a number of *A. baumannii* genomes and has been shown to have a significant impact on host gene expression and genome architecture (Adams *et al.*, 2016). Additionally, IS_{Aba1} is frequently implicated in increased antibiotic resistance, achieved by insertion upstream of resistance genes, namely those encoding cephalosporinases or carbapenamases (Héritier *et al.*, 2006; Turton *et al.*, 2006; Lopes and Amyes, 2012). Despite the putative promoter sequences not being maintained across all MITE_{Aba12} elements, the two Sub-groups which exhibited the greatest number of conserved arrangements (Sub-groups 1 and 2 with 27 and 17 elements, respectively) have promoter sequences that exactly match the MITE_{Aba12(c)} consensus (Figure 4.4). Elements within these Sub-groups were derived from a variety of sp. from the *Moraxellaceae* family and isolated from geographically distinct locations (Table 4.3), suggesting that a selective pressure to maintain these nucleotides may exist.

Analysis of the 90 MITE_{Aba12} copies revealed that sequence conservation was mainly confined to their TIRs and they only deviated in length from the MITE_{Aba12(c)} consensus by a maximum of two nucleotides (Figure 4.4). This is in contrast with significant size differences seen between variants of other types of bacterial MITEs (Liu *et al.*, 2002; Zhou *et al.*, 2008; Siddique *et al.*, 2011). However, the lack of significant divergence seen within MITE_{Aba12} copies may indicate that the element was generated from a single event and dispersed through bacterial genomes via HGT.

Shared identity of IS_{Aba12} and the additional 13 IS harbouring similar TIR to those of MITE_{Aba12} was restricted to the TIR sequences (Table 4.3). Nevertheless, this finding significantly broadens the range of potential parental IS that could be capable of translocating MITE_{Aba12}. However, further experimental evidence is required to confirm whether these IS can translocate MITE_{Aba12}.

The observation of a MITE translocation within a prokaryote genome in ‘real-time’ is generally considered to be a rare event, as only a few examples have been documented in the literature (Delihias, 2011). Remarkably, four separate instances where MITE_{Aba12} underwent translocation into *hns*, all of which were observed within the *A. baumannii*

$\Delta ygiW$ ATCC 17978 background were identified. YgiW is known as a stress-induced protein in many Gram-negative bacterial sp. (Lee *et al.*, 2010a; Steele *et al.*, 2012; Juárez-Rodríguez *et al.*, 2013; Moreira *et al.*, 2013). For instance, in *Salmonella enterica* serovar Typhimurium, YgiW (renamed VisP for virulence induced stress protein) was shown to be critical in stress resistance *in vitro* and virulence (Moreira *et al.*, 2013). Similar to *S. enterica* and other bacteria, the *ygiW* homologue found in *A. baumannii* also contains the characteristic bacterial oligonucleotide/oligosaccharide-binding fold domain (DUF388) (Ginalski *et al.*, 2004) and is located immediately upstream of the *qseBC* TCS genes (data not shown). As transposition of IS are strongly controlled, most likely to reduce potential deleterious effects within the cell, we question whether the deletion of a protein involved in the stress response influenced the transposition and/ or properties that regulate expression and subsequent movement of IS*Aba12*/MITE_{*Aba12*} elements within the ATCC 17978 genome. Furthermore, as isolates displaying hyper-motility were only identified once during desiccation analyses, we speculate that these events might represent a ‘transposition burst’ (Wu *et al.*, 2015). This new phenomenon offers a substitute to the ‘selfish DNA’ hypothesis, where these intermittent bursts of IS transposition can increase copy numbers and therefore assist in their maintenance within bacterial genomes.

H-NS is defined as a DNA architectural protein, known to play multiple fundamental roles across a number of Gram-negative pathogens, including regulation of AT-rich horizontally acquired genes, many of which are involved in multiple stress responses (Dorman, 2007; Elgaml and Miyoshi, 2015). Two distinct locations for IS*Aba12* insertions in the *hns* locus were previously identified in *A. baumannii* (Eijkelkamp, 2011; Eijkelkamp *et al.*, 2013). These were also the target sites for the IS*Aba12* insertions in this study, inferring these sequences may be favoured integration hotspots. MITE_{*Aba12*} inserted into a novel location within *hns*; 151 bp from the start codon and upstream of the characterised DNA-binding domain (Eijkelkamp *et al.*, 2013). Two additional examples of IS-mediated disruption of *hns* in *A. baumannii* have been recently identified (Wright *et al.*, 2017a; Deveson Lucas *et al.*, 2018). IS*Aba125* was shown to be responsible in both studies, integrating into the intergenic region downstream of *hns* (ACICU_00289). In one case the last two amino acids of H-NS are altered and the protein extended for an additional three amino acids by the integration of complete and partial copies of IS*Aba125* element (Deveson Lucas *et al.*, 2018). Collectively, these results infer that H-NS is a

hotspot for disruption in *A. baumannii*, where a number of different integration sites have now been identified.

Transposable elements are a key driving force in the worrying increase in MDR isolates across many bacterial sp., particularly within the *Acinetobacter* genus. Despite their small size, MITEs have been shown to be a significant contributor to genetic variation in a number of pathogens. In conclusion, this work has identified and characterised a new MGE, MITE_{Aba12}, and determined its prevalence across the *Moraexellaceae* family. This also led to the identification of a novel composite transposon in *M. osloensis* CCUG 350, Tn6645. Due to the relatively small number of MITE_{Aba12} copies identified in sequenced genomes, the element may be maintained neutrally or under tight regulatory control from yet to be identified host and/ or environmental factor(s). The full effects of MITE_{Aba12} on genetic variation and thus evolution of bacterial genomes, in addition to transcriptional and translational influences, are yet to be experimentally examined, opening a new and exciting avenue of research. The overall findings of this study not only illustrate the fluidity of the *Acinetobacter* pan-genome but highlight the importance of mobile sequences as vehicles for niche-specific adaptive evolution in a number of clinically and environmentally relevant bacterial pathogens.

CHAPTER 5: Final discussion

The opportunistic nosocomial pathogen *A. baumannii* is the causative agent of a variety of infections in susceptible individuals. In recent years, *A. baumannii* has been propelled to the forefront of scientific attention due to its ability to readily persist across a number of abiotic and biotic niches and accrue resistance to the current suite of therapeutic treatments. Considerable efforts by multiple research groups worldwide have unveiled important virulence factors that contribute to the pathobiology of this organism. However, information detailing the mechanisms involved in their regulation still remains ill defined. TCSs are one strategy bacteria including *A. baumannii* utilise to sense changes in the extracellular environment and respond by modifying gene expression levels accordingly. This thesis sought to examine the role of three different TCS encoded in the *A. baumannii* genome. These systems were independently deleted and phenotypically analysed using a range of different genetic approaches. Results presented in this thesis reveal new knowledge about the TCSs under examination. Additionally, during the study other avenues were pursued that identified novel mechanisms impacting on the lifestyle and evolution of this bacterium.

5.1 *A. baumannii* ATCC 17978, a good model organism?

In this work, the *A. baumannii* ATCC 17978 isolate was used for all investigations. Although some questions have been raised as to the clinical relevance of this ‘lab-adapted’ strain (Jacobs *et al.*, 2014), its frequent use in mutational analyses, largely owing to its sensitivity to most antibiotics used in laboratories and ability to be genetically manipulated has made it the best studied *A. baumannii* isolate to date (Boll *et al.*, 2015; Murray *et al.*, 2017; Álvarez-Fraga *et al.*, 2018; Gil-Marqués *et al.*; Knauf *et al.*, 2018; Leus *et al.*, 2018; Wood *et al.*, 2018; Pérez-Varela *et al.*, 2019). *A. baumannii* ATCC 17978 is also a strain that does not display the phase-variable phenotype (Tipton *et al.*, 2015) (Sections 1.4.6 and 1.6.1.7.4). As the virulence potential between opaque and translucent isolates significantly varies, working with a strain that does not possess this trait is beneficial. Furthermore, a recent study have used ATCC 17978 for defining the transcriptome architecture of *A. baumannii*, providing a wealth of knowledge pertaining to gene expression levels, transcriptional start sites and presence of small RNAs; information that is readily available to researchers via the Acinetocom resource (<http://bioinf.gen.tcd.ie/acinetocom/>) (Kröger *et al.*, 2018).

5.1.1 Strain to strain variation, a cause for concern?

Despite the aforementioned attributes of ATCC 17978 as a model organism for phenotypic analyses, strain specific phenotypes, even amongst phylogenetically similar *A. baumannii* strains have been reported (Eijkelkamp *et al.*, 2011b; Eijkelkamp *et al.*, 2014; Richmond *et al.*, 2016; Murray *et al.*, 2017). This strain-to-strain variation poses a major concern for the development of novel broad-spectrum antimicrobial therapies. It could now be proposed that researchers need to validate novel phenotypes and findings using a panel of genetically distinct *A. baumannii* strains, omitting the need to define a model organism. Factors previously preventing such analyses were often associated with difficulties in genetic manipulation of MDR and hyper-virulent isolates. However, in recent years, novel genetic tools have been developed that overcome some of these drawbacks, including streamlined methods to generate targeted genetic mutations (Tucker *et al.*, 2014) and the availability of resistance cassettes which can be used as selection markers against multi- and extensively-drug resistant isolates (Kalivoda *et al.*, 2011; Lucidi *et al.*, 2018; Ducus-Mowchun *et al.*, 2019). Furthermore, Tn-derived mutant banks or individual mutants generated within a highly virulent, extensively-resistant isolate such as *A. baumannii* 5075 are commercially available (Gallagher *et al.*, 2015). Although it should be noted that phenotypes even amongst the same clinical isolate cannot always be reciprocated across different laboratories. For example, mutant variants may be isolated from a different phase-variant background and unless assessed on a selective type of media can go undetected confounding subsequent phenotypic analyses and conclusions (Chin *et al.*, 2018). Furthermore, the presence or absence of transmissible plasmids, which can affect expression of virulence factors, such as the chromosomally encoded T6SS and resistance profiles of isolates carrying this MGE (Weber *et al.*, 2015b) (Sections 1.4.7 and 1.5.5). These recent findings highlight the significant diversity of *A. baumannii* strains, helping to explain its naturally occurring variability and some of the hurdles clinicians face when treating infections caused by this pathogen.

5.2 New genetic tools to analyse *A. baumannii* pathogenesis

The original strategy adopted for generation of targeted gene deletions in *A. baumannii* (Section 2.4.3 and 3.4.2) was through a *sacB*-based strategy. This method was found to be labour intensive, requiring a series of cloning and transformation steps prior to introduction into *A. baumannii* cells. This was then followed by counter-selection on a defined medium to simultaneously promote allelic exchange through double homologous recombination and plasmid loss. A study by Tucker *et al.*, (2014) introduced a new

streamlined recombineering protocol to generate targeted gene deletions in *A. baumannii* (Tucker *et al.*, 2014). This procedure was further optimised in the course of this study to decrease the associated costs with synthesis of long primers (≥ 150 bp) which acted as flanking regions for homologous recombination. Additionally, using polymerases with proof reading ability, the likelihood of incorporating errors within the flanking region sequences was reduced when compared to chemically synthesised nucleotide sequences. These drawbacks were overcome by designing primers that could be used in a nested overlap extension PCR to generate the linear product required for subsequent electroporation into *A. baumannii* cells. Proof of concept was achieved by the successful generation of a number of deletion derivatives (Sections 2.4.3, 3.4.2 and 4.4.2).

Complementation assays are important to confirm phenotypic observations in genetically-modified strains. However, ambiguous results can often arise, particularly when complementing phenotypes that are sensitive to copy number effects. This can hold particularly true for regulatory genes, as the fine-tuned balance which may be required to modify target gene expression is generally not reciprocated, often leading to unanticipated results. The most commonly used vector for *A. baumannii* complementation studies is the *E. coli/A. baumannii* shuttle vector pWH1266, which was initially constructed through the fusion of the natural cryptic plasmid pWH1277 from *A. calcoaceticus* BD413 and pBR322 from *E. coli* (Hunger *et al.*, 1990). Although useful, a number of studies have shown that phenotypes were not always complemented back to WT levels (Saroj *et al.*, 2012; Liou *et al.*, 2014; Li *et al.*, 2016c; Wang *et al.*, 2018). In order to overcome some of the drawbacks associated with pWH1266, new complementation shuttle vectors using a pWH1277 backbone have been generated (Lucidi *et al.*, 2018) which have already been adopted (Breisch *et al.*, 2019; Pérez-Varela *et al.*, 2019). One particularly useful feature is the addition of an arabinose-inducible expression system, providing a means to fine-tune gene expression through the supplementation of arabinose into the growth medium. An alternate method using mini-Tn7 transposon-based plasmids was recently optimised to assist in genetic complementation in MDR *A. baumannii* backgrounds (Ducus-Mowchun *et al.*, 2019). These plasmids assist in the integration of gene(s) of interest at a highly conserved site in the *A. baumannii* genome and thus enables single-copy gene complementation. Chromosomal integration to complement mutant phenotypes has many benefits over plasmid-based gene complementation systems including bypassing the requirement for continual antibiotic selection and eliminates aberrant results often caused by “multicopy effects”. Both methods offer more flexibility and control when

complementing difficult and/ or complex phenotypes, such as those involving regulatory systems.

5.3 MGEs play a role in the genetic plasticity of *A. baumannii* ATCC 17978

The success of a clone is often associated with increased genetic plasticity, providing a bacterial cell with a means to rapidly alter its genetic content when placed under adverse conditions. Whilst mostly being seen as advantageous, this trait can also be deleterious, as an increased frequency of mutations would also increase the likelihood of disrupting genes that are essential for survival (Doolittle *et al.*, 1984).

As described in Chapters 3 and 4, targeted deletion of the *11155* RR gene and desiccation stress, independently promoted translocation of *ISAbal2*. Analysis of these translocation events revealed that *ISAbal2* elements preferentially integrated into AT-rich regions, generating nine bp DRs upon insertion (Figure 3.4 and 4.2). *ISAbal2* is the most abundant IS encoded in the ATCC 17978 genome; there are three copies. Despite this being only a small number in comparison to some other *A. baumannii* strains (Adams *et al.*, 2016), results from Chapter 3 and 4 in conjunction with previous reports (Eijkelkamp *et al.*, 2013; Trebosc *et al.*, 2016), label *ISAbal2* as the primary vehicle driving genetic alternations in ATCC 17978. Whether specific stress conditions accelerate transposition of *ISAbal2* is not currently known.

5.3.1 Does disruption of H-NS enhance survival under desiccation stress in ATCC 17978?

Stress induced by desiccation can have profound impacts on cell survival. The loss of water from a bacterial cell leads to a decrease in turgor pressure which can have significant ramifications on a number of vital processes (Potts, 1994). In response, bacteria have evolved mechanisms to combat the damage imposed by desiccation. Although, many *A. baumannii* isolates are well adapted to desiccation stress, only a small number of genetic determinants that contribute to this have been identified. These include; production of hepta-acylated lipid A (Boll *et al.*, 2015), the RecA DNA repair protein (Aranda *et al.*, 2011), the KatE catalase regulated by the BfmRS TCS (Farrow *et al.*, 2018) and an ability to form a robust biofilm (Espinal *et al.*, 2012) (Section 1.4.5).

H-NS is defined as a transcriptional regulator belonging to the bacterial nucleoid-associated protein superfamily which functions by binding and silencing horizontally or vertically acquired AT-rich DNA (Ali *et al.*, 2012). In other bacteria, physiochemical

changes such as temperature and osmolarity are known to modulate H-NS repression (Owen-Hughes *et al.*, 1992; Madrid *et al.*, 2002). In *A. baumannii* ATCC 17978, inactivation of H-NS by an IS_{Aba12} element was had a profound effect on the global transcriptome, leading to significant transcriptional changes to numerous virulence factors including genes encoding the Ata autotransporter, the Csu type I pilus cluster, and a T6SS (Eijkelkamp *et al.*, 2013).

During desiccation stress experiments (Chapter 4), seven motile derivatives were identified, all had a disruption in the chromosomally-encoded *hns* gene through the insertion of MGEs. Whether the sudden change in growth conditions, such as an increase in temperature, promoted mutations in H-NS cannot be excluded. However, as this motile phenotype was not again seen throughout the 30-day experiment, it was hypothesised that this burst of IS-mediated activity was random. Translocation of additional MGEs to alternative genetic regions is indeed possible, but went undetected due to the lack of a visibly distinct phenotype. Although no direct link to desiccation tolerance has been previously defined for H-NS, it would be of interest to examine whether the *hns*-disrupted mutants isolated within this study differ in their potential to survive desiccation stress. Furthermore, future studies could employ ISseeker, a computational method developed to track IS movement under a given condition/stress (Wright *et al.*, 2017b). Application of this methodology would determine if H-NS is a common mutational hotspot and/ or identify novel genetic loci that promote desiccation resistance in this pathogen.

5.3.2 Insights and implications of MITE_{Aba12} elements in host genome evolution

MITEs belong to a small group of non-autonomous elements that are present not only in prokaryotes but in all domains of life (Feng, 2003; Fattash *et al.*, 2013). Despite their small size, these often termed ‘hidden elements’ can have a profound impact on shaping host genome architecture. Although significant work has been undertaken to track the movement and evolution of MGEs in *A. baumannii* strains, particularly in the context of antimicrobial resistance (Lopes and Amyes, 2012; Adams *et al.*, 2016; Nigro and Hall, 2016a; Pagano *et al.*, 2016), non-autonomous elements are a largely understudied area of research. As described in Chapter 4, a series of fortuitous events led to the identification of a MITE, termed MITE_{Aba12}, where the non-autonomous element translocated into a known global regulator (Eijkelkamp *et al.*, 2013) during desiccation stress experiments that was readily detected due to a visibly altered motility phenotype (Figure 4.1).

MITEs are multifaceted elements that have the potential to influence novel phenotypes and/ or regulation of virulence traits in bacteria (Delihias, 2011). A well-documented example is the Correia elements of *Neisseria* (also termed CREE, for Correia repeat enclosed element or NEMIS, for *Neisseria* miniature insertion sequence). Considerable efforts have tracked their evolution since their initial identification in 1986 (Correia *et al.*, 1986), revealing significant diversity within and between isolates shaped by selective pressures (Buisine *et al.*, 2002; Liu *et al.*, 2002; Siddique *et al.*, 2011). Siddique and colleagues (2011) categorised these elements from three distinct *Neisseria meningitidis* isolates into eight subtypes; two subtypes carried strong outward-facing promoter sequences, impacting on downstream genes and the potential to generate short non-coding regulatory RNAs (Siddique *et al.*, 2011).

Characterisation of the MITE_{Aba12(c)} consensus sequence led to the identification of two potential outward-facing σ 70 promoter sequences (Figure 4.6). Using pre-existing ATCC 17978 RNA-seq data from our laboratory including those from Chapter 2, gene transcripts reading out from the MITE_{Aba12} sequence that could be attributed to the putative P_{out} IRR promoter sequence were found (Section 4.5.6). At this time, ATCC 17978 was the only isolate carrying a copy of MITE_{Aba12} that had RNA-transcriptomic data publically available and thus other isolates carrying this element could not be examined using this methodology. Similar to Correia elements of *Neisseria* (Siddique *et al.*, 2011), whether selective pressures or random events drive mutations in MITE_{Aba12} elements that could enhance promoter activity is possible and should be tracked closely. Such changes could have significant consequences reminiscent of IS_{Aba1} insertions, where the strong outward-facing promoter within this MGE has had a profound impact on the generation of multidrug resistance across phylogenetically distinct *A. baumannii* isolates (Héritier *et al.*, 2006; Turton *et al.*, 2006; Lopes and Amyes, 2012; Nigro and Hall, 2016b).

In this work, a total of 30 genomes carried copies of MITE_{Aba12} at varying frequencies (Table 4.3). Of these, the *Acinetobacter* sp. DS002 from pesticide-polluted agricultural soil contained the highest number of copies (n=22). A recent comparison of this genome to that of previously published *A. baumannii* genome sequences revealed that DS002 clustered with the avirulent *A. baumannii* SDF strain, a genome enriched with IS_{Aba6} and IS_{Aba7} (Yakkala *et al.*, 2019). These elements have contributed to extensive genome rearrangements, resulting in a reduced genome size compared to other *A. baumannii* strains (Fournier *et al.*, 2006). Despite its reported similarities to the IS-rich SDF genome

and the presence of 22 copies of MITE_{Aba12}, the role that MGEs play on the genetic architecture of *Acinetobacter* sp. DS002 was not examined (Yakkala *et al.*, 2019). Thus, it would be of great interest to see if MGEs including that of MITE_{Aba12} have influenced the adaptive evolution of this environmental strain.

MITE_{Aba12} elements were shown to share similar TIR sequences with not only IS_{Aba12} but an additional 13 different IS, including IS derived from bacterial Sp. other than *A. baumannii* (Table 4.4). Further experimental studies could assess the ability of these IS to transpose MITE_{Aba12} using the previously described antibiotic-coupling mobility assay, which was adopted to demonstrate translocation of E622, a MITE identified in *Pseudomonas syringae* (Stavrinos *et al.*, 2012). Findings from such analyses may reveal trends and/ or preferences for parent elements of MITE_{Aba12} and explain the higher abundance of this element in some isolates compared to others.

Only a small number of nucleotides located within TIR sequences of ISs are required for transposase binding, cleavage and strand transfer reactions (Nagy and Chandler, 2004). Thus, additional MITE_{Aba12}-derived or evolutionary distinct elements could still be awaiting identification. More robust studies using computational methods tailored to repeat sequence identification such as detectMITE (Ye *et al.*, 2016) may overcome limitations of the methodology used in this study. Moreover, partial sequences and remnants of these elements within genomes were not explored. Collectively, this work has opened up a new direction in MGE research where further studies are necessary to determine the full breadth of how MITE_{Aba12} elements have influenced niche-specific adaptation, genome organisation and ultimately evolution.

5.4 The contribution of the AdeRS/AdeAB(C) cluster in the pathogenic success of *A. baumannii*

AdeRS is a prototypical TCS that is comprised of adjacent HK and RR proteins. The AdeS HK contains two TM helices linked by an extracellular loop at its N terminus; a HAMP domain is present as an immediate extension of the C-terminal TM helix which links to the two kinase core domains. The AdeR RR contains a C-terminal REC domain and an N-terminal OmpR/PhoB output domain with a winged HTH DNA-binding domain (Figure 1.6). The binding mechanism of AdeR differs to most OmpR/PhoB type RRs. Instead of binding to the promoter region of their target genes, AdeR binds to a 10 bp perfect DR DNA sequence located within the intercistronic region between *adeRS* and *adeAB(C)* (Chang *et al.*, 2016; Wen *et al.*, 2017). Interestingly, only one repeat sequence

could be identified within a number of *A. baumannii* genomes, including ATCC 17978, revealing a restricted regulon for this TCS.

It is very rare to identify the activating stimulus of a HK; thus only a handful have been identified to date (García Véscovi *et al.*, 1996; Wosten *et al.*, 2000; Mike *et al.*, 2013; Ainsaar *et al.*, 2014; Kreamer *et al.*, 2015; Li *et al.*, 2016b). In Chapter 2, it was shown that shock treatment with sub-MIC levels of the antimicrobial pentamidine increased *adeAB* expression approximately 30-fold (Figure 2.4). In a separate study, shock treatment with another intrinsic substrate identified in this work, CHX, also increased *adeAB* expression to similar levels (Hassan *et al.*, 2013). Treatment with benzylkonium, a quaternary ammonium compound, increased *adeAB* expression 62.5- and 19-fold, respectively, despite it not being identified as a substrate for AdeAB in this study. Furthermore, shock treatment with the monovalent cation, NaCl also increased *adeA* expression, albeit to a lesser extent (~17-fold). Although the stimulus of AdeS is yet to be determined, the aforementioned studies reveal that a number of membrane stressors result in increased expression of *adeAB* genes.

As expression of *adeAB* is increased under a variety of different conditions, it seems more likely that AdeS may respond to these stressors indirectly, e.g., through stress-induced molecular cues or membrane associated changes. An example of the latter involves the osmo-sensing HK EnvZ from *E. coli*, which similar to AdeS has a periplasmic sensing domain. Interestingly, removal of this domain did not affect the osmo-sensing ability of EnvZ, indicating that the activating stimulus was independent of small molecule binding (Leonardo and Forst, 1996). The periplasmic sensing domain of AdeS is approximately half the length of the EnvZ homologue in *A. baumannii* (Figure 1.6), which raises the question as to whether this domain plays a functional role in kinase activation.

Future studies should examine whether deletion of the periplasmic domain from AdeS affects the ability of this protein to phosphorylate AdeR and as a result alter expression levels of *adeAB(C)*. Given the number of conditions in which *adeAB(C)* expression is significantly increased, independent treatment with compounds including pentamidine could be used as a useful readout system for such analyses. This would provide new knowledge into the activating mechanism of the AdeS HK, which may assist in the development of novel inhibitors against a TCS which directly impacts the MDR phenotype of *A. baumannii*.

5.4.1 Does BaeSR communicate with AdeRS?

It has been previously shown that the BaeSR TCS modulates expression of *adeAB* in ATCC 17978 (Lin *et al.*, 2014). Although results from RNA-seq of ATCC 17978 cells grown in a rich medium within this thesis showed that *adeAB* is expressed at very low levels, Lin and colleagues (2014) revealed deletion of *baeR* in the same background further reduced *adeAB* expression by more than 50% (Lin *et al.*, 2014). It was speculated that this decrease in expression was responsible for a 2-fold decrease in tigecycline resistance observed in $\Delta baeR$ (Lin *et al.*, 2014). The study also revealed over-expression of *baeR* on a multi-copy plasmid increased both expression of *adeAB* and tigecycline resistance by 2-fold. Resistance levels to tigecycline were not found to differ within the $\Delta adeAB$ derivative in this study (Table 2.3), nor by Leus and colleagues (2018) who also investigated resistance profiles of a ATCC 17978 $\Delta adeAB$ derivative (Leus *et al.*, 2018). These findings would suggest that changes in expression of *adeAB* observed by Lin *et al.*, (2014) are most likely not linked to tigecycline resistance, although variation amongst ATCC 17978 isolates between these laboratories cannot be excluded.

As BaeR did not bind to the promoter region of the *adeAB* operon (Lin *et al.*, 2015), it could be hypothesised that BaeR communicates with AdeRS to modulate expression levels of *adeAB*. Whether this communication is intentional, a form of regulatory-based redundancy, or a result of inappropriate phosphorylation of AdeR by BaeS, remains to be determined. Expression levels of *baeSR* genes are differentially expressed under membrane-associated stress conditions, including exposure to colistin (Henry *et al.*, 2015; Boinett *et al.*, 2019). In the study by Boinett and colleagues (2019), WGS of laboratory-induced colistin resistant strains identified IS-mediated disruptions in *baeR* or *baeS* amongst other mutations. RNA-seq of these strains under colistin stress revealed a 5-fold increase in *adeABC* expression (Boinett *et al.*, 2019), strengthening the hypothesis of communication between these regulatory systems. As it cannot be ruled out that the additional mutations within these isolates may also influence *adeABC* expression, future studies should repeat these experiments using targeted individual deletion derivatives of *baeR* and/ or *baeS* genes to confirm this hypothesis. If increased *adeABC* expression levels are maintained in these mutants, experimental approaches that could confirm interactions and/ or phosphotransfer between BaeS and AdeR proteins include bacterial two-hybrid analyses and *in vitro* phosphorylation assays using radiolabelled ATP (Cerqueira *et al.*, 2014; Chambonnier *et al.*, 2016).

5.4.2 AdeA and AdeB function together to confer intrinsic resistance in *A. baumannii* ATCC 17978

A key strategy *A. baumannii* utilises to confer multidrug resistance is through adaptive mutations mediated in regulatory systems that results in overexpression of multidrug efflux pumps (Vila *et al.*, 2007) (Sections 1.4.9.1.1 and 1.4.9.1.2). Although speculated to confer no intrinsic resistance (Yoon *et al.*, 2015), findings presented in this study demonstrate that AdeAB can confer intrinsic resistance to a limited number of dicationic compounds (Table 2.3). Dicationic compounds are defined as compounds that harbour two positively charged moieties separated by short/long, symmetric/asymmetric carbon linkers as demonstrated by the identified substrates of AdeAB. The cationic nitrogenous groups are separated by a long carbon chain forming symmetrical compounds for pentamidine and CHX, whilst DAPI lacks this long linker and is asymmetric (Figure 2.3). The length of linkers separating the cationic pharmacophores of dicationic compounds is an important factor in substrate specificity of the *E. coli* MdfA efflux protein (Fluman *et al.*, 2014). Given AdeAB provides resistance to dicationic compounds which significantly differ in the length between the charged groups, it suggests that the mechanism of action of AdeB differs to the findings for MdfA. Resistance levels to other dicationic compounds were also examined in this study (methyl viologen and dequalinium), however, the MICs to these compounds for $\Delta adeRS/\Delta adeAB$ were indistinguishable to WT cells. These results indicate that the substrate specificity of AdeAB does not extend to all dicationic compounds. However, it cannot be ruled out that changes in MIC levels towards methyl viologen and dequalinium were not observed in $\Delta adeRS/\Delta adeAB$ derivatives due to overlapping substrate profiles with other efflux proteins present in *A. baumannii*. This limitation could be overcome by assessing resistance profiles of AdeAB in a different host background where the major efflux pumps have been deleted (Fernando *et al.*, 2014).

Recently, the first structure of AdeB was determined using single-particle cryo-electron microscopy reconstituted in lipidic nanodiscs (Su *et al.*, 2019). Comparable to other RND efflux proteins, the AdeB structure forms a homotrimer, with each protomer comprised of transmembrane and periplasmic domains. The confirmation of each AdeB subunit represented the protein in its resting state, and was proposed to remain in this state in the absence of its substrates. Key residues involved in substrate recognition and translocation were determined, sharing both similarities and differences to other solved RND transporter structures. To understand the potential drug binding modes of AdeB, a panel of structurally distinct substrates was computationally docked to the AdeB structure, revealing key residues involved in the drug-binding (Su *et al.*, 2019). However,

the substrates examined did not extend to any of the intrinsic substrates of the AdeAB system identified in this thesis. Su *et al.*, (2019) identified that only eight of 1035 residues differ across AdeB proteins encoded within different *A. baumannii* strains and these non-conserved residues are distally located from the multidrug binding sites (Su *et al.*, 2019). Although the dicationic compounds identified as substrates of AdeB in this study have only been examined in ATCC 17978, the finding that the AdeB protein sequence is highly conserved would suggest that the intrinsic substrates recognised by AdeB of ATCC 17978 would most likely extend to AdeB proteins encoded in other strains. It would be of interest to expand upon the substrate range for docking analyses and examine whether differences exist between the entry and binding modes and the predicted binding affinities of intrinsic substrates such as pentamidine to the non-intrinsic substrates presented by Su *et al.*, (2019).

The work in Chapter 2 also addressed whether AdeB, the membrane bound transport protein can function with other MFPs aside from AdeA. Through the generation of a deletion strain targeting *adeA*, MIC values found for $\Delta adeA$ were indistinguishable to that of $\Delta adeB$ and $\Delta adeAB$ (Table 2.3), providing direct evidence that AdeB could not function with other MFPs. Work by Lues *et al.*, (2018) confirmed in *A. baumannii* ATCC 17978 that AdeAB can form a functional tripartite complex with AdeK, the OMP from the AdeIJK RND efflux pump (Leus *et al.*, 2018). Although not tested here, it is speculated that the presence of AdeK would also be required for expulsion of the dicationic substrates identified within this study.

Although not all published work employs complementation studies (Richmond *et al.*, 2016; De Silva and Kumar, 2017), complementation assays were performed in Chapter 2 to confirm the role of the deleted genes in the observed resistance profile alterations (Table 2.3). These showed that the resistance profiles of the respective mutant strains analysed were not always restored back to WT levels. Whether this was a limitation of the complementation vector used has not been ascertained. Therefore it would be of interest to assess whether resistance profiles from complemented strains presented in Table 2.3 may be fully restored to WT levels using either of the new *A. baumannii* complementation methods outlined in Section 5.2 (Lucidi *et al.*, 2018; Ducus-Mowchun *et al.*, 2019).

5.4.3 Does strain specific phenotypes affect pentamidine efficacy against *A. baumannii*?

Recently, pentamidine was found to display synergy with antibiotics typically restricted to Gram-positive bacteria, resulting in novel treatment combinations against a variety of distinct Gram-negative pathogens, including colistin sensitive and resistant *A. baumannii* strains (Stokes *et al.*, 2017). Despite Stokes and colleagues (2017) detailing the adjuvant activity of pentamidine across an array of distinct Gram-negative pathogens, gain of resistance experiments were restricted to *E. coli* and one type of media. These findings prompted examination into whether alternate pentamidine resistance mechanisms independent of AdeAB could be identified in *A. baumannii*. Different carbon sources and the bioavailability of iron in the growth medium had drastic effects on the level of pentamidine resistance conferred by *A. baumannii* (Tables 2.4 and 2.5, Figures 2.5 and 2.6).

Thus, it is clear that different growth media can have far reaching implications on pentamidine efficacy. Subsequently, it would be of interest to extend this work and examine how growth conditions, which more accurately reflect host niches, may impact pentamidine resistance across different Gram-negative bacterial species. Once again, these findings highlight the individuality of isolates and their varying effects in different growth environments, which further complicates analyses and the ultimate goal of generating novel broad-spectrum agents to treat infections caused by MDR bacteria.

5.5 The role of the 11155/60 TCS in *A. baumannii* ATCC 17978

In Chapter 3, a TCS harbouring a HHK with a unique domain architecture not previously reported in the literature was identified. Comparative genomic analyses revealed the absence of the 11155/11160 TCS from the avirulent SDF *A. baumannii* isolate (Figure 1.6), leading to the hypothesis that this system may be involved in regulating virulence associated phenotypes. In order to address this research question, the 11155 RR was deleted by allelic exchange, and RNA-seq employed as a tool to define the full set of genes directly or indirectly affected. From this manipulation a loss-of-function mutation in the distal regulator AdeN was identified (Figure 3.4).

AdeN is a typical TetR-family transcriptional repressor (Rosenfeld *et al.*, 2012). Proteins belonging to this family possess a N-terminal DNA binding domain and a larger C-terminal domain and function through ligands binding to the C-terminal domain. This interaction consequently affects their ability to bind to DNA, leading to derepression of

target gene expression (Cuthbertson and Nodwell, 2013). AdeN is defined as a mutational hotspot across clinical *A. baumannii* isolates (Saranathan *et al.*, 2017; Gerson *et al.*, 2018). Its inactivation promotes derepression of the *adeIJK* MDR efflux pump resulting in increased resistance to a diverse set of antimicrobial agents. Selective pressures such as continual antimicrobial exposure in laboratory settings can promote mutations in *adeN* leading to its inactivation (Fernando *et al.*, 2014; Yoon *et al.*, 2015), however, the direct stimuli and target binding sequence motif of AdeN are yet to be identified. Analysis of the global transcriptome of the $\Delta 11155 \Delta adeN::ISAbal2$ ATCC 17978 derivative undertaken in this study revealed that *pgpB*, the gene immediately upstream of *adeIJK* was also significantly upregulated (Figure 3.4). These genes are transcribed in the same direction, separated by less than 30 bp, and do not contain additional transcription start sites. This supports the likelihood of co-transcription and expression jointly regulated by AdeN. Future work should verify whether the AdeN regulon extends beyond that of the *adeIJK/pgpB* operon. Experiments could compare the global transcriptomes of an $\Delta adeN$ derivative to its respective WT parent to identify potential gene targets of this regulator. As AdeN is known to function as a transcriptional repressor (Rosenfeld *et al.*, 2012), genes upregulated within the array could then be further examined using *in silico* approaches to identify commonalities in nucleotide sequences upstream of differentially expressed CDS. From this, a putative binding consensus sequence logo could be generated, which may assist in identification of additional genes under the regulatory control of AdeN not first identified through RNA-seq methodologies. The findings obtained from such studies would determine if AdeN is in fact a global regulator of *A. baumannii* and may reveal why loss-of-function mutations in *adeN* were a prerequisite for the deletion of the 11155 RR from the ATCC 17978 chromosome. Additional studies to elucidate the connection between these distinct regulatory systems could be achieved by WGS of the mutant variants identified in Chapter 3. Subsequent characterisation of these strains would readily identify if other genetic mutations aside from those found within *adeN* are present.

Given that targeted mutation of 11155 could not be achieved without secondary loss-of-function mutations, different approaches should be adopted to define the regulon of the 11155/60 TCS in ATCC 17978. Deletion of 11160 could help to determine the biological role of this TCS, however, it is currently unknown if 11160 is also essential for survival in ATCC 17978. If target deletions can be generated without the introduction of additional mutations, caution still needs to be taken as analyses may be confounded by

inappropriate phosphorylation of 11155 by other HK proteins. Despite TCS evolving molecular mechanisms to insulate TCS pathways (Section 1.6.1.5), the observation that a Hpt domain present within either GacS or CheA proteins would be required for efficient signal flow of the 11155/60 system increases the likelihood of cross-talk with non-cognate HKs. Similar to characterisation of other essential proteins, introduction of point mutations in 11160 and/ or 11155 that lead to reduced protein function but do not induce lethality could be performed. However, this approach is not always successful, as introduced point mutations in the PAS domain of the WalK HK from the essential WalKR TCS promoted secondary mutations in other genetic loci, confounding subsequent analyses (Monk *et al.*, 2017).

To determine if 11155/60 is truly an essential TCS, experiments will also need to be undertaken in other *A. baumannii* clinical isolates. Analyses into the transposon library of AB5075 using the transposon mutant library browser (www.tools.uwgenomics.org/tn_mutants/) revealed two independent insertional disruptions in the *11155* homologue, with only one confirmed (Gallagher *et al.*, 2015). Whether secondary loss-of-function mutations are also present in *adeN* or other genes is possible and will need to be determined by WGS. If this is a strain specific phenomenon, an alternative hypothesis is that the acquisition of additional regulatory genes present in recently isolated MDR strains, such as those found in AB5075 (Casella *et al.*, 2017), negate the essentiality of the 11155/60 TCS. Given the MDR nature of *A. baumannii* isolates and the lack of new antimicrobial agents in the pipeline, research into TCSs deemed essential for bacterial survival is of high relevance and thus further investigations into the 11155/60 system are of significant interest.

5.6 How to define the regulatory role of the QseBC TCS in *A. baumannii*

The original research aim of this thesis was to characterise the role of three distinct TCS in modulating genes involved in resistance and/ or persistence strategies afforded by *A. baumannii*. One of the TCS examined in this thesis was an orthologue of the QseBC system found in other Gram-negative pathogens. However, the serendipitous finding of a novel element during analyses of this regulatory system changed the course of this chapter, leaving detailed characterisation of this TCS requiring further exploration.

Orthologues of the QseBC system are found in a range of Gram-negative bacteria, where the genetic organisation of the TCS present in *A. baumannii* shares similarities to

a number of previously characterised systems. In these, the *qseBC* genes are adjacently orientated with a gene encoding a putative periplasmic protein belonging to the oligonucleotide/oligosaccharide binding (OB-fold) family of proteins separated by an attenuating stem loop structure (Steele *et al.*, 2012; Juárez-Rodríguez *et al.*, 2013). Despite these genetic commonalities, a number of diverse functions have been attributed to characterised orthologues (Wang *et al.*, 2011a; Steele *et al.*, 2012; Weigel *et al.*, 2015; Weigel and Demuth, 2016), making clear predictions of its role in *A. baumannii* challenging.

Given the difficulties associated with defining phenotypic roles for regulatory proteins (Section 5.7), future work should prioritise analysis of previously published *A. baumannii* global array datasets such as those generated from RNA-seq or transposon insertion site sequencing to determine conditions where the *qseBC/ygiW* gene cluster is differentially expressed and/ or required for survival. For example, global transcriptomics and WGS of *A. baumannii* strains revealed direct links between colistin resistance and the BaeSR TCS (Henry *et al.*, 2015; Boinett *et al.*, 2019). These findings have thus identified a condition in which the TCS is active and the molecular mechanisms involved in this association can be pursued in greater detail. Although not guaranteed to yield definitive answers, this approach may help to narrow down potential avenues for further investigation.

5.7 Challenges associated with defining phenotypes for bacterial TCSs

Bacteria employ a number of different mechanisms to adapt and survive across a number of environmental conditions. One particularly important molecular mechanism promoting such robustness is through genetic buffering, where phenotypic consequences of mutations are masked (Hartman *et al.*, 2001). The most commonly identified form of genetic buffering is functional redundancy, defined by two proteins having overlapping functions which allow each one to compensate in the absence of the other (Ghosh and O'Connor, 2017). For a pathogen, the more choices available to achieve a specific goal, the greater the likelihood of its success.

Whilst seen as beneficial for the bacteria, these layers of redundancy are a major obstacle preventing the identification of discernible phenotypes for genes of interest. Redundancy can be a significant burden when defining roles for regulatory systems such as TCSs, as multiple paralogous systems that share highly conserved core functional domains are often present in the genome and may regulate and/ or manipulate the same

or complementary pathway(s). Not only does this phenomenon occur between paralogues such as TCSs but has also been found to exist between unrelated proteins. Whether inactivation of AdeN was a form of genetic buffering to mitigate the deleterious effect of *11155* inactivation will require further examination.

Another hurdle in assigning phenotypes to TCS is because the environment in which the system is activate is not reciprocated under laboratory conditions. This can be seen for the PhoP-PhoQ and PhoR-PhoB TCSs which are only activated when cells are grown in magnesium- and phosphate-limited environments, respectively (García Véscovi *et al.*, 1996). Before *A. baumannii* was designated as a nosocomial pathogen, the bacterium was defined as a nutritionally versatile organism isolated from soil and water environments (Baumann, 1968). In light of its origins, whether a number of the regulatory systems in *A. baumannii* may have evolved to sense and respond to physical and/ or chemical insults originally present in these environments. As most *in vitro* experiments are undertaken in rich media, testing conditions which more accurately reflect such stressors using methodologies such as Biolog Phenotype Microarrays (Mackie *et al.*, 2014) may help to identify activating conditions of different TCSs. Such knowledge could subsequently be applied to answering if and how these systems promote persistence and enhance disease potential within host niches.

5.8 Deciphering interactions between TCS in *A. baumannii*

In silico comparisons of TCS from three *A. baumannii* isolates revealed a number of structurally diverse systems, harbouring an array of different functional domains and topologies (Figure 1.6). To date, the characterised TCS systems present in *A. baumannii* have been found to promote survival across a number of distinct environmental niches including those within the human host (Section 1.6.1.7). However, unlike closely related bacterial pathogens such as *P. aeruginosa* (Chambonnier *et al.*, 2016; Francis *et al.*, 2018), little to no information pertaining to multicomponent TCS cascades have been defined for this organism.

A total of four HHK were identified in the *A. baumannii* ATCC 17978 genome, where the experimentally characterised proteins, CheA (Chen *et al.*, 2017) and GacS (Cerqueira *et al.*, 2014), were found to possess Hpt domains (Figure 1.6). Further examination revealed that no additional Hpt domains were present in a number of clinically isolated *A. baumannii* genomes (Section 3.5.4). This led to the hypothesis that the Hpt domains

encoded by CheA and/ or GacS act as signalling hubs, promoting signal transfer for not only their respective system but also for the HHKs lacking this domain.

Phosphotransfer profiling experiments could be employed to investigate this hypothesis, as exemplified by works from Biondi and colleagues who used this method to identify the cognate partners of an Hpt domain from *Caulobacter crescentus* (Biondi *et al.*, 2006). This method was also adopted to define the complete interactome of *Mycobacterium tuberculosis* detailing novel interactions between proteins from various TCS revealing a complex signalling landscape (Agrawal *et al.*, 2015). Another approach using ‘bait and prey’ reporter assays in a yeast two-hybrid system detailed the interactome of TCS from plant species (Dortay *et al.*, 2008; Sharan *et al.*, 2017). Given the complexity and difficulties in defining phenotypes for TCS, it would be of great interest to adopt either of the aforementioned methodologies to generate a TCS interactome map of *A. baumannii*. This could reveal valuable information pertaining to the interactions between TCS members including those involving Hpt domains and determine whether TCSs of *A. baumannii* adopt insulated or promiscuous forms of signalling.

5.9 Conclusions

Overall, the findings presented within this thesis have shed light on the role of TCSs in modulating expression of genes involved in resistance and persistence phenotypes of *A. baumannii*. Additionally the versatility and robustness of this pathogen exemplifies the importance of autonomous and nonautonomous MGEs in stress adaptation and genome architecture. As we enter the post-antibiotic era, defining the intricacies of regulatory cascades such as those afforded by TCS could prove to be vital, as identifying weaknesses in these networks may offer new targets for the development of novel therapeutic strategies to treat infections caused by this formidable pathogen.

CHAPTER 6: Appendices

Appendix A - Genes significantly down- and up-regulated (≥ 2 -fold) in $\Delta adeRS$ compared against ATCC 17978 (CP012004) by RNA-seq

Gene ID	Gene Annotation	FC(Log ₂) ^a
Genes significantly down-regulated		
ACX60_05645	isochorismatase	-3.86
ACX60_05640	enterobactin synthase subunit E	-3.77
ACX60_05605	iron ABC transporter permease	-3.46
ACX60_09665	siderophore 1 biosynthesis protein	-2.68
ACX60_05630	RhbE rhizobactin siderophore biosynthesis protein	-2.65
ACX60_05600	acinetobactin biosynthesis protein	-2.62
ACX60_09120	AdeR response regulator protein	-2.55
ACX60_05655	hypothetical protein	-2.51
ACX60_09720	siderophore 1 biosynthesis protein	-2.48
ACX60_05680	isochorismate synthase	-2.47
ACX60_05615	iron ABC transporter ATP-binding protein	-2.40
ACX60_09710	RND transporter	-2.33
ACX60_05650	histidine decarboxylase	-2.33
ACX60_05710	beta-lactamase	-2.17
ACX60_05665	ABC transporter	-2.06
ACX60_09715	ornithine monooxygenase	-1.97
ACX60_05610	iron ABC transporter permease	-1.96
ACX60_05660	ABC transporter	-1.95
ACX60_00325	4-hydroxyphenylpyruvate dioxygenase	-1.94
ACX60_17945	alkanesulphonate monooxygenase	-1.91
ACX60_06600	C4-dicarboxylate transporter	-1.85
ACX60_17950	ABC transporter permease	-1.80
ACX60_11680	type VI secretion protein	-1.80
ACX60_11955	ATP-binding protein	-1.78
ACX60_05620	ferric anguibactin-binding protein	-1.75
ACX60_06480	CsuA/B protein	-1.66
ACX60_16650	DNA transfer protein p32	-1.62
ACX60_14710	hypothetical protein	-1.57
ACX60_09200	transporter	-1.56
ACX60_11455	2,2 C3-dehydroadipyl-CoA hydratase	-1.56
ACX60_09250	acetyl-CoA acetyltransferase	-1.53
ACX60_11685	hypothetical protein	-1.53

Gene ID	Gene Annotation	FC(Log₂)^a
ACX60_07755	hypothetical protein	-1.51
ACX60_05635	peptide synthetase	-1.50
ACX60_06500	CsuD protein	-1.47
ACX60_17735	L-lactate permease	-1.47
ACX60_17955	aliphatic sulphonates transport ATP-binding subunit	-1.42
ACX60_14705	5-methyltetrahydropteroyltriglutamate--homocysteine methyltransferase	-1.42
ACX60_05595	peptide synthetase	-1.41
ACX60_06705	30S ribosomal protein S18	-1.38
ACX60_09240	succinyl-CoA:3-ketoacid-CoA transferase	-1.35
ACX60_07070	alcohol dehydrogenase	-1.34
ACX60_11450	enoyl-CoA hydratase	-1.33
ACX60_06710	30S ribosomal protein S6	-1.31
ACX60_09115	AdeS histidine kinase protein	-1.31
ACX60_09315	4Fe-4S ferredoxin	-1.30
ACX60_17240	TonB-dependent receptor	-1.30
ACX60_09685	ligand-gated channel protein	-1.27
ACX60_00345	fumarylacetoacetase	-1.25
ACX60_00340	maleylacetoacetate isomerase	-1.23
ACX60_09605	hypothetical protein	-1.22
ACX60_06505	CsuE protein	-1.21
ACX60_06700	50S ribosomal protein L9	-1.21
ACX60_00750	ligand-gated channel protein	-1.20
ACX60_10725	ABC transporter permease	-1.20
ACX60_11715	ABC transporter	-1.17
ACX60_07055	aldehyde dehydrogenase	-1.16
ACX60_12900	arginine N-succinyltransferase	-1.16
ACX60_10705	monooxygenase	-1.16
ACX60_09700	siderophore 1 biosynthesis protein	-1.13
ACX60_11475	phenylacetate-CoA oxygenase	-1.13
ACX60_09235	succinyl-CoA:3-ketoacid-CoA transferase	-1.11
ACX60_00335	glyoxalase	-1.09
ACX60_09690	dimethylmenaquinone methyltransferase	-1.07
ACX60_11675	EvpB family type VI secretion protein	-1.07
ACX60_09245	short chain fatty acid transporter	-1.07

Gene ID	Gene Annotation	FC(Log₂)^a
ACX60_17290	glutathione peroxidase	-1.06
ACX60_00950	acetate permease	-1.06
ACX60_09705	AcsC siderophore 1 achromobactin biosynthesis protein	-1.06
ACX60_11950	secretion protein HlyD	-1.05
ACX60_02525	50S ribosomal protein L13	-1.04
ACX60_11665	type VI secretion protein	-1.03
ACX60_06495	CsuC protein	-1.03
ACX60_02110	50S ribosomal protein L2	-1.03
ACX60_15730	ligand-gated channel protein	-1.02
ACX60_07195	porin	-1.02
ACX60_00935	hypothetical protein	-1.01
ACX60_10810	Na ⁺ :H ⁺ dicarboxylate symporter	-1.01
ACX60_02115	30S ribosomal protein S19	-1.00
ACX60_02105	50S ribosomal protein L23	-1.00
Genes significantly up-regulated		
ACX60_01760	CraA multidrug transporter protein	2.83
ACX60_03300	hypothetical protein	2.54
ACX60_10085	hypothetical protein	2.28
ACX60_08970	hypothetical protein	2.24
ACX60_12490	hypothetical protein	2.08
ACX60_11320	threonine transporter RhtB	2.03
ACX60_05985	tRNA-Arg	1.95
ACX60_17005	sulphate transporter	1.94
ACX60_18810	sulphate transporter	1.94
ACX60_17010	universal stress protein	1.94
ACX60_18815	universal stress protein	1.94
ACX60_10140	hypothetical protein	1.88
ACX60_03305	Fis family transcriptional regulator protein	1.87
ACX60_08745	hypothetical protein	1.83
ACX60_09475	hypothetical protein	1.81
ACX60_18655	replication protein C	1.74
ACX60_08795	hypothetical protein	1.70
ACX60_18230	hypothetical protein	1.68
ACX60_07175	hypothetical protein	1.66

Gene ID	Gene Annotation	FC(Log₂)^a
ACX60_07230	hypothetical protein	1.66
ACX60_10065	hypothetical protein	1.66
ACX60_12555	hypothetical protein	1.66
ACX60_18670	hypothetical protein	1.66
ACX60_18515	hypothetical protein	1.63
ACX60_17015	hypothetical protein	1.63
ACX60_18820	hypothetical protein	1.63
ACX60_00635	hypothetical protein	1.62
ACX60_18075	dual-action HEIGH metallo-peptidase	1.60
ACX60_08515	polyketide cyclase	1.59
ACX60_09520	energy transducer TonB	1.53
ACX60_11880	hypothetical protein	1.52
ACX60_08875	fumarylacetoacetate hydrolase	1.46
ACX60_17020	hypothetical protein	1.46
ACX60_18825	hypothetical protein	1.46
ACX60_18585	hypothetical protein	1.44
ACX60_01135	TetR family transcriptional regulator	1.40
ACX60_08665	ThiJ thiamine biosynthesis protein	1.40
ACX60_12390	hypothetical protein	1.40
ACX60_12550	hypothetical protein	1.40
ACX60_06960	hypothetical protein	1.37
ACX60_08965	hypothetical protein	1.37
ACX60_10870	ArsR family transcriptional regulator	1.36
ACX60_07215	ABC transporter ATPase	1.35
ACX60_07685	lysozyme	1.35
ACX60_15380	TetR family transcriptional regulator	1.35
ACX60_06435	membrane protein	1.34
ACX60_00085	tRNA-Ala	1.34
ACX60_02440	tRNA-Ala	1.34
ACX60_02605	tRNA-Ala	1.34
ACX60_14995	tRNA-Ala	1.34
ACX60_17210	tRNA-Ala	1.34
ACX60_18015	tRNA-Ala	1.34
ACX60_12795	p-hydroxycinnamoyl CoA hydratase/lyase	1.33
ACX60_09040	TetR family transcriptional regulator	1.33

Gene ID	Gene Annotation	FC(Log₂)^a
ACX60_09125	AdeA membrane protein	1.33
ACX60_12765	MFS transporter	1.32
ACX60_08740	bile acid:sodium symporter	1.32
ACX60_10155	hypothetical protein	1.32
ACX60_00080	tRNA-Ile	1.31
ACX60_02435	tRNA-Ile	1.31
ACX60_02600	tRNA-Ile	1.31
ACX60_15000	tRNA-Ile	1.31
ACX60_17215	tRNA-Ile	1.31
ACX60_18020	tRNA-Ile	1.31
ACX60_02950	hypothetical protein	1.30
ACX60_07185	hypothetical protein	1.30
ACX60_07695	hypothetical protein	1.30
ACX60_06535	TetR family transcriptional regulator	1.30
ACX60_12085	transposase	1.30
ACX60_07865	hypothetical protein	1.29
ACX60_05560	hypothetical protein	1.28
ACX60_04305	molecular chaperone Tir	1.28
ACX60_08180	acetyltransferase	1.28
ACX60_10175	hypothetical protein	1.27
ACX60_04275	GCN5 family acetyltransferase	1.27
ACX60_11730	transcriptional regulator	1.27
ACX60_17650	hypothetical protein	1.26
ACX60_07530	hypothetical protein	1.26
ACX60_09725	hypothetical protein	1.25
ACX60_12055	cold-shock protein	1.25
ACX60_07860	hypothetical protein	1.25
ACX60_00615	hypothetical protein	1.25
ACX60_08150	hypothetical protein	1.25
ACX60_09980	hypothetical protein	1.25
ACX60_10070	DNase	1.25
ACX60_10170	hypothetical protein	1.25
ACX60_16000	translation initiation factor IF-1	1.24
ACX60_13910	Ferric uptake regulator (Fur) protein	1.24
ACX60_16755	DNA-binding protein	1.24

Gene ID	Gene Annotation	FC(Log₂)^a
ACX60_02290	tRNA-Arg	1.23
ACX60_02295	tRNA-Arg	1.23
ACX60_02310	tRNA-Arg	1.23
ACX60_07750	histidine kinase	1.23
ACX60_18150	hypoxanthine phosphoribosyltransferase	1.22
ACX60_12430	hypothetical protein	1.22
ACX60_09525	hypothetical protein	1.21
ACX60_10225	orotidine 5'-phosphate decarboxylase	1.20
ACX60_08710	3-oxoacyl-ACP reductase	1.20
ACX60_09945	hypothetical protein	1.20
ACX60_06940	membrane protein	1.20
ACX60_18235	hypothetical protein	1.20
ACX60_08510	IacB protein	1.19
ACX60_11825	hypothetical protein	1.19
ACX60_13405	rubredoxin	1.19
ACX60_08040	sulphate transporter	1.19
ACX60_08755	hypothetical protein	1.18
ACX60_12955	hypothetical protein	1.18
ACX60_03395	alkylphosphonate utilisation protein	1.18
ACX60_16225	hypothetical protein	1.17
ACX60_07150	hypothetical protein	1.17
ACX60_11405	reverse transcriptase	1.17
ACX60_10160	hypothetical protein	1.17
ACX60_08760	membrane protein	1.16
ACX60_08630	FAH family protein	1.16
ACX60_11230	hypothetical protein	1.16
ACX60_11550	hemolysin	1.16
ACX60_03630	hypothetical protein	1.16
ACX60_09055	hypothetical protein	1.15
ACX60_07690	hypothetical protein	1.15
ACX60_02580	membrane protein	1.15
ACX60_01640	fimbrial protein	1.15
ACX60_18225	hypothetical protein	1.15
ACX60_10005	hypothetical protein	1.15
ACX60_03480	tRNA-Val	1.14

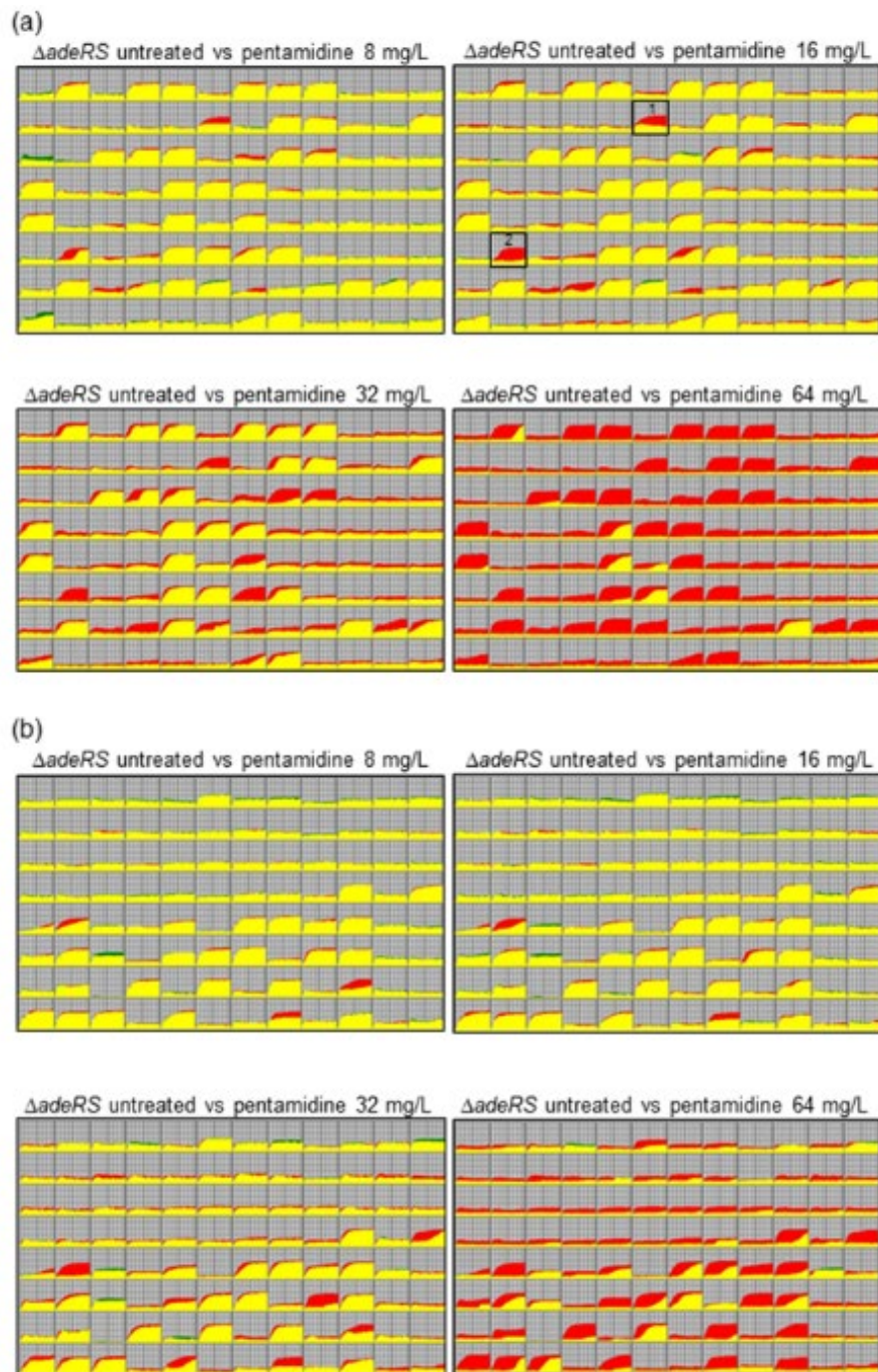
Gene ID	Gene Annotation	FC(Log₂)^a
ACX60_03495	tRNA-Val	1.14
ACX60_03505	tRNA-Val	1.14
ACX60_11170	AsnC family transcriptional regulator	1.14
ACX60_06565	acetyltransferase	1.14
ACX60_14685	Darcynin 1	1.13
ACX60_02700	hypothetical protein	1.13
ACX60_01625	DNA-directed RNA polymerase subunit	1.13
ACX60_09855	30S ribosomal protein S20	1.12
ACX60_08125	hypothetical protein	1.12
ACX60_09990	hypothetical protein	1.12
ACX60_14670	Darcynin 1	1.11
ACX60_10130	DNA helicase	1.11
ACX60_06925	hypothetical protein	1.11
ACX60_07515	hypothetical protein	1.11
ACX60_07210	DNA breaking-rejoining protein	1.11
ACX60_09765	HU transcriptional regulator α subunit	1.10
ACX60_04280	hypothetical protein	1.10
ACX60_02940	hypothetical protein	1.09
ACX60_06915	hypothetical protein	1.09
ACX60_06360	tRNA-Leu	1.09
ACX60_06370	tRNA-Leu	1.09
ACX60_08065	hypothetical protein	1.09
ACX60_12360	hypothetical protein	1.08
ACX60_02945	hypothetical protein	1.08
ACX60_10525	FxsA cytoplasmic membrane protein	1.08
ACX60_18560	hypothetical protein	1.08
ACX60_01150	hypothetical protein	1.08
ACX60_06250	cold-shock protein	1.08
ACX60_05480	tRNA-Val	1.08
ACX60_10025	HK97 gp10 family phage protein	1.08
ACX60_10090	hypothetical protein	1.08
ACX60_10970	hypothetical protein	1.08
ACX60_11185	hypothetical protein	1.08
ACX60_11765	urea carboxylase	1.08
ACX60_12535	hypothetical protein	1.08

Gene ID	Gene Annotation	FC(Log₂)^a
ACX60_12960	TetR family transcriptional regulator	1.08
ACX60_01975	hypothetical protein	1.07
ACX60_06430	blue light sensor protein	1.07
ACX60_16110	tRNA-Lys	1.06
ACX60_16115	tRNA-Lys	1.06
ACX60_18780	recombinase	1.06
ACX60_12835	GntR family transcriptional regulator	1.06
ACX60_15560	acyl carrier protein	1.06
ACX60_07380	hypothetical protein	1.06
ACX60_07670	hypothetical protein	1.05
ACX60_10405	TetR family transcriptional regulator	1.05
ACX60_12450	hypothetical protein	1.04
ACX60_18730	phosphoglucosamine mutase	1.04
ACX60_12485	phage-like protein	1.04
ACX60_10750	hypothetical protein	1.04
ACX60_03935	hypothetical protein	1.04
ACX60_04120	hypothetical protein	1.04
ACX60_12685	hypothetical protein	1.04
ACX60_12090	tRNA-Met	1.04
ACX60_10570	hypothetical protein	1.03
ACX60_12965	hypothetical protein	1.03
ACX60_00730	arsenate reductase	1.03
ACX60_10660	transcriptional regulator	1.03
ACX60_18775	hypothetical protein	1.03
ACX60_14690	hypothetical protein	1.03
ACX60_18725	transposase	1.02
ACX60_18580	hypothetical protein	1.02
ACX60_11010	malonate decarboxylase subunit beta	1.02
ACX60_04295	HIT family hydrolase	1.02
ACX60_07275	AceI efflux protein	1.02
ACX60_08785	hypothetical protein	1.02
ACX60_03485	tRNA-Asp	1.02
ACX60_03490	tRNA-Asp	1.02
ACX60_03500	tRNA-Asp	1.02
ACX60_16820	transcriptional regulator	1.02

Gene ID	Gene Annotation	FC(Log₂)^a
ACX60_06470	hypothetical protein	1.01
ACX60_07650	lipoprotein	1.01
ACX60_18565	hypothetical protein	1.01
ACX60_18250	hypothetical protein	1.01
ACX60_18220	hypothetical protein	1.01
ACX60_12655	carbon storage regulator	1.01
ACX60_13365	hypothetical protein	1.01
ACX60_06365	tRNA-Trp	1.01
ACX60_06375	tRNA-Trp	1.01
ACX60_08800	hypothetical protein	1.01
ACX60_15375	hypothetical protein	1.00
ACX60_07575	stress-responsive nuclear envelope protein	1.00
ACX60_02830	hypothetical protein	1.00
ACX60_12355	hypothetical protein	1.00
ACX60_10595	hypothetical protein	1.00
ACX60_07630	hypothetical protein	1.00

^aFC; fold-change

Appendix B - Comparative analysis of kinetic response curves obtained from Biolog PM plates for $\Delta adeRS$ cells untreated and subjected to increasing concentrations of pentamidine



Appendix C - Genes significantly down- and up-regulated (≥ 2 -fold) in $\Delta 11155 \Delta adeN::ISAbal2$ compared against WT ATCC 17978 (CP012004) by RNA-seq

Gene ID	Gene Annotation	FC(Log ₂) ^a
Genes significantly down-regulated		
ACX60_05645	isochorismatase	-3.71
ACX60_18435	hypothetical protein	-3.29
ACX60_07895	TetR family transcriptional regulator	-3.17
ACX60_05605	iron ABC transporter permease	-2.85
ACX60_17950	ABC transporter permease	-2.85
ACX60_05640	enterobactin synthase subunit E	-2.83
ACX60_05655	hypothetical protein	-2.63
ACX60_05630	RhbE rhizobactin siderophore biosynthesis protein	-2.53
ACX60_05710	beta-lactamase	-2.51
ACX60_11140	amino acid ABC transporter permease	-2.46
ACX60_05680	isochorismate synthase	-2.44
ACX60_17945	alkanesulfonate monooxygenase	-2.43
ACX60_06490	protein CsuB	-2.42
ACX60_05600	acinetobactin biosynthesis protein	-2.39
ACX60_18430	type VI secretion protein	-2.36
ACX60_11130	glutamine-binding protein	-2.36
ACX60_05650	histidine decarboxylase	-2.32
ACX60_18415	hypothetical protein	-2.27
ACX60_06485	protein CsuA	-2.27
ACX60_09715	ornithine monooxygenase	-2.25
ACX60_06480	protein CsuA/B	-2.25
ACX60_12900	arginine N-succinyltransferase	-2.22
ACX60_09710	RND transporter	-2.21
ACX60_04890	sulfate/thiosulfate transporter permease subunit	-2.19
ACX60_06495	protein CsuC	-2.19
ACX60_18425	hypothetical protein	-2.16
ACX60_06500	protein CsuD	-2.11
ACX60_05610	iron ABC transporter permease	-2.11
ACX60_11145	amino acid ABC transporter	-2.11
ACX60_05665	ABC transporter	-2.10

Gene ID	Gene Annotation	FC(Log₂)^a
ACX60_05660	ABC transporter	-2.04
ACX60_12480	hypothetical protein	-2.04
ACX60_09720	siderophore biosynthesis protein	-2.02
ACX60_18205	hypothetical protein	-2.00
ACX60_18420	conjugal transfer protein TrbI	-2.00
ACX60_11955	ATP-binding protein	-1.94
ACX60_18990	hypothetical protein	-1.92
ACX60_05615	iron (Fe) ABC transporter ATP-binding protein	-1.91
ACX60_17505	acyl carrier protein	-1.90
ACX60_18210	hypothetical protein	-1.89
ACX60_18440	type VI secretion protein	-1.89
ACX60_18985	hypothetical protein	-1.88
ACX60_10915	taurine dioxygenase	-1.86
ACX60_11135	glutamine ABC transporter ATP-binding protein	-1.86
ACX60_11665	type VI secretion protein	-1.79
ACX60_18455	hypothetical protein	-1.77
ACX60_11950	secretion protein HlyD	-1.74
ACX60_18450	type IV secretion protein IcmB	-1.72
ACX60_05595	peptide synthetase	-1.70
ACX60_17735	L-lactate permease	-1.69
ACX60_09300	sulfonate ABC transporter ATP-binding protein	-1.68
ACX60_18460	hypothetical protein	-1.67
ACX60_18410	conjugal transfer protein	-1.66
ACX60_10125	hypothetical protein	-1.63
ACX60_12520	hypothetical protein	-1.63
ACX60_12645	hypothetical protein	-1.63
ACX60_04895	sulfate transporter	-1.63
ACX60_06505	protein CsuE	-1.61
ACX60_09605	hypothetical protein	-1.61
ACX60_09310	nitrate ABC transporter substrate-binding protein	-1.60
ACX60_09665	siderophore biosynthesis protein	-1.59
ACX60_05635	peptide synthetase	-1.59

Gene ID	Gene Annotation	FC(Log₂)^a
ACX60_09700	siderophore biosynthesis protein%2C IucA/IucC family	-1.57
ACX60_15280	NAD synthetase	-1.56
ACX60_04885	sulfate ABC transporter ATP-binding protein	-1.55
ACX60_10920	taurine transporter subunit	-1.53
ACX60_18365	hypothetical protein	-1.53
ACX60_17955	aliphatic sulfonates transport ATP-binding subunit	-1.53
ACX60_18275	hypothetical protein	-1.52
ACX60_10910	Asp/Glu/hydantoin racemase	-1.51
ACX60_18270	hypothetical protein	-1.46
ACX60_16645	DNA transfer protein p32	-1.45
ACX60_18350	hypothetical protein	-1.44
ACX60_01390	Sell repeat protein	-1.43
ACX60_09705	siderophore achromobactin biosynthesis protein AcsC	-1.43
ACX60_18370	hypothetical protein	-1.43
ACX60_09315	4Fe-4S ferredoxin	-1.43
ACX60_18445	hypothetical protein	-1.42
ACX60_10710	methionine transporter	-1.41
ACX60_05705	hypothetical protein	-1.41
ACX60_18475	hypothetical protein	-1.38
ACX60_09125	membrane protein	-1.38
ACX60_16145	monooxygenase	-1.37
ACX60_11125	ABC transporter substrate-binding protein	-1.37
ACX60_18725	transposase	-1.36
ACX60_05620	ferric anguibactin-binding protein	-1.36
ACX60_09130	acriflavine resistance protein B	-1.35
ACX60_15290	NAD(P) transhydrogenase subunit alpha	-1.34
ACX60_18265	peptidase M23	-1.33
ACX60_15285	NAD(P) transhydrogenase subunit alpha	-1.33
ACX60_05875	acyl-CoA dehydrogenase	-1.32
ACX60_10705	monooxygenase	-1.31
ACX60_18280	hypothetical protein	-1.30
ACX60_00750	ligand-gated channel protein	-1.27
ACX60_11685	hypothetical protein	-1.25

Gene ID	Gene Annotation	FC(Log₂)^a
ACX60_04880	CysB family transcriptional regulator	-1.25
ACX60_18875	hypothetical protein	-1.22
ACX60_02650	hypothetical protein	-1.22
ACX60_07400	hypothetical protein	-1.21
ACX60_12625	hypothetical protein	-1.21
ACX60_17675	3-oxoacyl-ACP synthase	-1.21
ACX60_02405	hypothetical protein	-1.20
ACX60_11150	GNAT family acetyltransferase	-1.19
ACX60_01475	ABC transporter permease	-1.19
ACX60_16510	hypothetical protein	-1.19
ACX60_18345	hypothetical protein	-1.18
ACX60_14390	membrane protein	-1.18
ACX60_18395	hypothetical protein	-1.18
ACX60_18685	toxin of toxin-antitoxin system	-1.16
ACX60_04360	formate dehydrogenase	-1.16
ACX60_08195	cytochrome d ubiquinol oxidase subunit 2	-1.15
ACX60_17585	endoribonuclease L-PSP	-1.15
ACX60_11175	lysine transporter LysE	-1.15
ACX60_01250	hypothetical protein	-1.12
ACX60_18470	hypothetical protein	-1.12
ACX60_18870	hypothetical protein	-1.11
ACX60_09365	NAD(FAD)-dependent dehydrogenase	-1.10
ACX60_13715	hypothetical protein	-1.10
ACX60_07195	porin	-1.09
ACX60_15830	methionine sulfoxide reductase A	-1.08
ACX60_08935	permease	-1.08
ACX60_18245	hypothetical protein	-1.06
ACX60_08200	cytochrome d terminal oxidase subunit 1	-1.06
ACX60_12565	hypothetical protein	-1.05
ACX60_18335	hypothetical protein	-1.04
ACX60_12140	ATPase	-1.04
ACX60_18970	DNA repair protein	-1.03
ACX60_05670	thioesterase	-1.03
ACX60_11680	type VI secretion protein	-1.03
ACX60_18495	hypothetical protein	-1.02

Gene ID	Gene Annotation	FC(Log₂)^a
ACX60_18360	type II/IV secretion system domain protein	-1.02
ACX60_09370	Zn-dependent hydrolase	-1.02
ACX60_12905	acetylornithine aminotransferase	-1.01
ACX60_07395	hypothetical protein	-1.01
ACX60_12630	hypothetical protein	-1.01
ACX60_17290	glutathione peroxidase	-1.01
ACX60_00865	membrane protein	-1.00
Genes significantly up-regulated		
ACX60_10140	hypothetical protein	3.49
ACX60_03840	phosphatidylglycerophosphatase	2.79
ACX60_01760	multidrug transporter	2.53
ACX60_12555	hypothetical protein	2.27
ACX60_00425	hypothetical protein	2.13
ACX60_08970	hypothetical protein	1.82
ACX60_10065	hypothetical protein	1.77
ACX60_07530	hypothetical protein	1.77
ACX60_03835	haemolysin D	1.74
ACX60_01360	fatty acyl-CoA reductase	1.73
ACX60_10085	hypothetical protein	1.69
ACX60_10970	hypothetical protein	1.69
ACX60_11320	threonine transporter RhtB	1.69
ACX60_11275	TetR family transcriptional regulator	1.65
ACX60_07175	hypothetical protein	1.63
ACX60_08795	hypothetical protein	1.57
ACX60_06940	membrane protein	1.57
ACX60_07680	holin	1.54
ACX60_03830	multidrug transporter	1.49
ACX60_11245	hypothetical protein	1.47
ACX60_05985	tRNA-Arg	1.42
ACX60_10620	membrane protein	1.38
ACX60_12060	amino acid transporter LysE	1.36
ACX60_11265	SAM-dependent methyltransferase	1.35
ACX60_13650	hypothetical protein	1.34
ACX60_06250	cold-shock protein	1.32
ACX60_06460	ATPase AAA	1.32

Gene ID	Gene Annotation	FC(Log ₂) ^a
ACX60_07535	phage terminase%2C large subunit	1.31
ACX60_12955	hypothetical protein	1.30
ACX60_07685	lysozyme	1.30
ACX60_08745	hypothetical protein	1.29
ACX60_10575	ferrous iron transporter B	1.29
ACX60_02215	30S ribosomal protein S4	1.28
ACX60_15380	TetR family transcriptional regulator	1.26
ACX60_07670	hypothetical protein	1.26
ACX60_02225	50S ribosomal protein L17	1.25
ACX60_11865	hypothetical protein	1.25
ACX60_07575	stress-responsive nuclear envelope protein	1.25
ACX60_02210	30S ribosomal protein S11	1.23
ACX60_15375	hypothetical protein	1.23
ACX60_07625	hypothetical protein	1.22
ACX60_07750	histidine kinase	1.22
ACX60_11280	isovaleryl-CoA dehydrogenase	1.20
ACX60_00990	hypothetical protein	1.20
ACX60_11270	fatty acid--CoA ligase	1.19
ACX60_11880	hypothetical protein	1.19
ACX60_07630	hypothetical protein	1.19
ACX60_09990	hypothetical protein	1.18
ACX60_09520	energy transducer TonB	1.18
ACX60_02220	DNA-directed RNA polymerase subunit alpha	1.18
ACX60_16225	hypothetical protein	1.18
ACX60_10160	hypothetical protein	1.17
ACX60_08180	acetyltransferase	1.16
ACX60_11825	hypothetical protein	1.16
ACX60_08875	fumarylacetoacetate hydrolase	1.16
ACX60_06915	hypothetical protein	1.15
ACX60_00635	hypothetical protein	1.15
ACX60_05015	S-(hydroxymethyl)glutathione synthase	1.14
ACX60_15145	50S ribosomal protein L35	1.12
ACX60_02205	30S ribosomal protein S13	1.11
ACX60_06035	histidine ABC transporter permease	1.10
ACX60_15140	50S ribosomal protein L20	1.10

Gene ID	Gene Annotation	FC(Log₂)^a
ACX60_01145	HxlR family transcriptional regulator	1.10
ACX60_07365	TetR family transcriptional regulator	1.10
ACX60_16820	transcriptional regulator	1.09
ACX60_00380	urocanate hydratase	1.09
ACX60_18515	hypothetical protein	1.08
ACX60_11285	methylcrotonoyl-CoA carboxylase	1.07
ACX60_03305	Fis family transcriptional regulator	1.07
ACX60_07590	hypothetical protein	1.07
ACX60_03395	alkylphosphonate utilisation protein	1.07
ACX60_09980	hypothetical protein	1.07
ACX60_17080	membrane protein	1.06
ACX60_06515	glycine/betaine ABC transporter	1.06
ACX60_11290	enoyl-CoA hydratase	1.05
ACX60_13525	transketolase	1.05
ACX60_04305	molecular chaperone Tir	1.04
ACX60_12790	MFS transporter	1.04
ACX60_08755	hypothetical protein	1.03
ACX60_05225	hypothetical protein	1.03
ACX60_02950	hypothetical protein	1.03
ACX60_03300	hypothetical protein	1.03
ACX60_03945	hypothetical protein	1.02
ACX60_08930	AraC family transcriptional regulator	1.02
ACX60_10385	phosphoglycerate kinase	1.02
ACX60_08740	bile acid:sodium symporter	1.02
ACX60_05560	hypothetical protein	1.02
ACX60_10070	DNase	1.01
ACX60_12165	NADH oxidase	1.01
ACX60_12765	MFS transporter	1.01
ACX60_14205	tRNA-Gln	1.00
ACX60_14210	tRNA-Gln	1.00
ACX60_14215	tRNA-Gln	1.00
ACX60_14220	tRNA-Gln	1.00
ACX60_03825	adenine deaminase	1.00

^aFC; fold-change

Appendix D - Adams *et al.*, 2018; *PLoS ONE*

RESEARCH ARTICLE

Resistance to pentamidine is mediated by AdeAB, regulated by AdeRS, and influenced by growth conditions in *Acinetobacter baumannii* ATCC 17978

Felise G. Adams¹, Uwe H. Stroehrer¹, Karl A. Hassan^{2*}, Shashikanth Marri³, Melissa H. Brown^{1*}

1 College of Science and Engineering, Flinders University, Adelaide, SA, Australia, **2** Department of Chemistry and Biomolecular Sciences, Macquarie University, Sydney, NSW, Australia, **3** College of Medicine and Public Health, Flinders University, Adelaide, SA, Australia

* Current address: School of Environmental and Life Science, University of Newcastle, Callaghan, NSW, Australia

* melissa.brown@flinders.edu.au



OPEN ACCESS

Citation: Adams FG, Stroehrer UH, Hassan KA, Marri S, Brown MH (2018) Resistance to pentamidine is mediated by AdeAB, regulated by AdeRS, and influenced by growth conditions in *Acinetobacter baumannii* ATCC 17978. *PLoS ONE* 13(5): e0197412. <https://doi.org/10.1371/journal.pone.0197412>

Editor: Eric Cascales, Centre National de la Recherche Scientifique, Aix-Marseille Université, FRANCE

Received: February 16, 2018

Accepted: May 1, 2018

Published: May 11, 2018

Copyright: © 2018 Adams *et al.* This is an open access article distributed under the terms of the [Creative Commons Attribution License](https://creativecommons.org/licenses/by/4.0/), which permits unrestricted use, distribution, and reproduction in any medium, provided the original author and source are credited.

Data Availability Statement: Relevant data are within the paper and its Supporting Information files. Additionally, RNA-seq data have been deposited in the gene expression omnibus database, accession number GSE102711.

Funding: This work was supported by the Australian National Health and Medical Research Council (Project Grant 1047509) and a Flinders Medical Research Foundation Grant to MHB and

Abstract

In recent years, effective treatment of infections caused by *Acinetobacter baumannii* has become challenging due to the ability of the bacterium to acquire or up-regulate antimicrobial resistance determinants. Two component signal transduction systems are known to regulate expression of virulence factors including multidrug efflux pumps. Here, we investigated the role of the AdeRS two component signal transduction system in regulating the AdeAB efflux system, determined whether AdeA and/or AdeB can individually confer antimicrobial resistance, and explored the interplay between pentamidine resistance and growth conditions in *A. baumannii* ATCC 17978. Results identified that deletion of *adeRS* affected resistance towards chlorhexidine and 4',6-diamidino-2-phenylindole dihydrochloride, two previously defined AdeABC substrates, and also identified an 8-fold decrease in resistance to pentamidine. Examination of Δ *adeA*, Δ *adeB* and Δ *adeAB* cells augmented results seen for Δ *adeRS* and identified a set of dicationic AdeAB substrates. RNA-sequencing of Δ *adeRS* revealed transcription of 290 genes were ≥ 2 -fold altered compared to the wildtype. Pentamidine shock significantly increased *adeA* expression in the wildtype, but decreased it in Δ *adeRS*, implying that AdeRS activates *adeAB* transcription in ATCC 17978. Investigation under multiple growth conditions, including the use of Biolog phenotypic microarrays, revealed resistance to pentamidine in ATCC 17978 and mutants could be altered by bio-availability of iron or utilization of different carbon sources. In conclusion, the results of this study provide evidence that AdeAB in ATCC 17978 can confer intrinsic resistance to a subset of dicationic compounds and in particular, resistance to pentamidine can be significantly altered depending on the growth conditions.

UHS. FGA was supported by AJ and IM Naylon and Playford Trust Ph.D. Scholarships. The funders had no role in study design, data collection and analysis, decision to publish, or preparation of the manuscript.

Competing interests: The authors have declared that no competing interests exist.

Introduction

Acinetobacter baumannii causes a range of disease states including hospital-acquired pneumonia, blood stream, urinary, wound and bone infections, and is responsible for epidemic outbreaks of infection worldwide [1]. Such infections are often very difficult to treat due to the multidrug resistant (MDR) character of isolates displayed by this organism [2, 3]. In addition to the impressive propensity of the organism to acquire genetic elements carrying resistance determinants [2, 3, 4], up-regulation resulting in overproduction of resistance modulation cell-division (RND) drug efflux systems through integration of insertion sequence elements or mutations in regulatory genes, has also been deemed a major contributor to the MDR phenotype [6–9]. The best studied RND efflux systems in *A. baumannii* include AdeABC [10], AdeFGH [11] and AdeIJK [12]. Of particular interest is the AdeABC system which affords resistance to diverse antibiotics, biocides and dyes [10, 13–15], and has gained attention due to its high incidence of over-expression across many MDR *A. baumannii* clinical isolates, primarily from incorporation of point mutations in the genes encoding its positive regulator, AdeRS [6, 8, 13, 16]. Typically RND pumps consist of three proteins that form a complex; the absence of any of these components renders the entire complex non-functional [12]. Interestingly, deletion of *adeC* in the *A. baumannii* strain BM4454 did not affect resistance towards two substrates of the pump suggesting that AdeAB can utilize an alternative outer membrane protein (OMP) to efflux antimicrobial compounds [13].

The genetic arrangement of the AdeABC system places *adeABC* in an operon that is divergently transcribed to the regulatory *adeRS* two component signal transduction system (TCSTS). Expression of *adeABC* occurs by binding of AdeR to a ten base-pair direct repeat motif found within the intercistronic region separating these operons [18, 19]. Many clinical *A. baumannii* isolates harbor different genetic arrangements of the *adeRS* and *adeABC* operons [20], and whether regulation via AdeRS is conserved in these strains is not completely understood.

With an increase in infections caused by MDR isolates across many bacterial species, including *A. baumannii*, understanding mechanisms of resistance and how resistance to and evasion of treatments has evolved over time has become a key research topic. Furthermore, determining the impact of expression of resistance determinants within the host environment and its effect on the efficacy of therapeutic treatments has gained attention. For example, when *Pseudomonas aeruginosa* is grown using L-glutamate as the sole carbon source, resistance to the related compounds polymyxin B and colistin increased ≥ 25 - and 9-fold, respectively [21]. Other studies have shown that the bioavailability of cations such as iron can have a drastic effect towards the resistance of a number of antimicrobials across a range of pathogenic bacterial species [22]. Despite *A. baumannii* being recognized as a major human pathogen, these types of studies are limited for this organism.

This study aimed to determine the regulatory role of the AdeRS TCSTS in *A. baumannii* ATCC 17978, a clinical isolate which only encodes the *adeAB* subunits and identify whether AdeA and/or AdeB alone can confer antimicrobial resistance in the ATCC 17978 background. Phenotypic characterization of a constructed panel of deletion strains identified that alterations to the *adeRS* and *adeAB* operons of ATCC 17978 reduced resistance to a subset of dicationic compounds, including pentamidine. As a recent study highlighted the effectiveness of pentamidine in combination therapy to treat infections caused by Gram-negative pathogens [23], we sought to further examine alternative mechanisms of pentamidine resistance in *A. baumannii*. The type of carbon source and availability of iron were identified as affecting pentamidine resistance, thereby revealing interconnectedness between metabolic and resistance strategies within this formidable pathogen.

sequence flanking the region of interest and the ERY resistance cassette from pVA891 [27] were PCR amplified, purified and subsequently cloned into a modified pBluescript SK⁺ II vector that had the *Bam*HI site removed by end-filling, generating pBl_{adeRS}. Confirmed clones were re-cloned into *Xba*I-digested pEX18Tc [28]. The resulting pEX18Tc_{adeRS} vector was introduced into ATCC 17978 cells via electroporation, as previously described [29]. Transformants were selected on LB agar supplemented with ERY. Counter-selection was undertaken on M9 minimal agar containing ERY and 5% sucrose. The second method used to generate Δ *adeA*, Δ *adeB* and Δ *adeAB* strains utilized the RecET recombinase system with modifications [30]. Briefly, 400–600 bp of sequence flanking the gene(s) were used as templates in a nested overlap extension PCR with the ERY resistance cassette from pVA891 [27]. Approximately, 3.5–5 μ g of the purified linear PCR product was electroporated into ATCC 17978 cells harboring the vector pAT04 and recovered as previously described [30]. Recombinants were selected on LB agar supplemented with ERY. All mutants generated in this study were confirmed by PCR amplification and Sanger sequencing. Primers utilized to generate mutant strains are listed in S2 Table.

For genetic complementation of mutant strains, WT copies of *adeRS* and *adeAB* were cloned into pWH1266 [31] where transcription was driven by the tetracycline promoter. Resulting plasmids denoted pWH_{adeRS} and pWH_{adeAB}, respectively were confirmed by Sanger sequencing. The GEN resistance cassette from pUCGM [32] was PCR amplified and cloned into *Bam*HI digested pWH_{adeAB} generating pWHgent_{adeAB} thus abrogating transcription from the pWH1266 tetracycline promoter. Plasmids were introduced into appropriate *A. baumannii* cells as previously described [33]. Primers used to generate complementation vectors are listed in S2 Table.

Cell treatments and RNA isolation

RNA was isolated from WT and Δ *adeRS* cells and Hiseq RNA transcriptome analysis performed following methodologies as outlined previously [34].

For pentamidine stress assays, WT and Δ *adeRS* strains were grown overnight in MH broth, sub-cultured 1:100 in fresh medium and grown to OD₆₀₀ = 0.6; they were subsequently split into two 10 mL cultures. One 10 mL sample was treated with 7.8 mg/L of pentamidine (0.5 \times MIC for Δ *adeRS*), whilst the other remained untreated. Cultures were grown for an additional 30 min before total RNA was extracted as outlined previously [34].

Bioinformatic analysis

Bioinformatic analysis of RNA-seq data was undertaken as described previously [34], with the modification that obtained reads were mapped to the recently re-sequenced *A. baumannii* ATCC 17978 genome (GenBank: CP012004). RNA-seq data have been deposited in the gene expression omnibus database, accession number GSE102711 (<https://www.ncbi.nlm.nih.gov/geo/query/acc.cgi?acc=GSE102711>).

Quantitative Real-Time PCR

Pentamidine stress and RNA-seq validation experiments were achieved using a two-step qRT-PCR method. RNA samples were first purified as previously described [34], subsequently DNaseI treated (Promega) and then converted to cDNA using an iScriptTM cDNA synthesis kit (Biorad), following the manufacturer's instructions. The cDNA generated was used as a template for qRT-PCR using the SYBR[®] Green JumpStart[™] Taq readymix[™] (Sigma) in a 20 μ l final volume. Either a Rotor-Gene Q (Qiagen, Australia) or RG-3000 (Corbett Life Science, Australia) instrument was used for quantification of cDNA using the following protocol; 1

sequence flanking the region of interest and the ERY resistance cassette from pVA891 [27] were PCR amplified, purified and subsequently cloned into a modified pBluescript SK⁺ II vector that had the *Bam*HI site removed by end-filling, generating pBl_{adeRS}. Confirmed clones were re-cloned into *Xba*I-digested pEX18Tc [28]. The resulting pEX18Tc_{adeRS} vector was introduced into ATCC 17978 cells via electroporation, as previously described [29]. Transformants were selected on LB agar supplemented with ERY. Counter-selection was undertaken on M9 minimal agar containing ERY and 5% sucrose. The second method used to generate *ΔadeA*, *ΔadeB* and *ΔadeAB* strains utilized the RecET recombinase system with modifications [30]. Briefly, 400–600 bp of sequence flanking the gene(s) were used as templates in a nested overlap extension PCR with the ERY resistance cassette from pVA891 [27]. Approximately, 3.5–5 μg of the purified linear PCR product was electroporated into ATCC 17978 cells harboring the vector pAT04 and recovered as previously described [30]. Recombinants were selected on LB agar supplemented with ERY. All mutants generated in this study were confirmed by PCR amplification and Sanger sequencing. Primers utilized to generate mutant strains are listed in S2 Table.

For genetic complementation of mutant strains, WT copies of *adeRS* and *adeAB* were cloned into pWH1266 [31] where transcription was driven by the tetracycline promoter. Resulting plasmids denoted pWH::*adeRS* and pWH::*adeAB*, respectively were confirmed by Sanger sequencing. The GEN resistance cassette from pUCGM [32] was PCR amplified and cloned into *Bam*HI digested pWH::*adeAB* generating pWHgent::*adeAB* thus abrogating transcription from the pWH1266 tetracycline promoter. Plasmids were introduced into appropriate *A. baumannii* cells as previously described [33]. Primers used to generate complementation vectors are listed in S2 Table.

Cell treatments and RNA isolation

RNA was isolated from WT and *ΔadeRS* cells and HiSeq RNA transcriptome analysis performed following methodologies as outlined previously [34].

For pentamidine stress assays, WT and *ΔadeRS* strains were grown overnight in MH broth, sub-cultured 1:100 in fresh medium and grown to OD₆₀₀ = 0.6; they were subsequently split into two 10 mL cultures. One 10 mL sample was treated with 7.8 mg/L of pentamidine (0.5 × MIC for *ΔadeRS*), whilst the other remained untreated. Cultures were grown for an additional 30 min before total RNA was extracted as outlined previously [34].

Bioinformatic analysis

Bioinformatic analysis of RNA-seq data was undertaken as described previously [34], with the modification that obtained reads were mapped to the recently re-sequenced *A. baumannii* ATCC 17978 genome (GenBank: CP012004). RNA-seq data have been deposited in the gene expression omnibus database, accession number GSE102711 (<https://www.ncbi.nlm.nih.gov/geo/query/acc.cgi?acc=GSE102711>).

Quantitative Real-Time PCR

Pentamidine stress and RNA-seq validation experiments were achieved using a two-step qRT-PCR method. RNA samples were first purified as previously described [34], subsequently DNaseI treated (Promega) and then converted to cDNA using an iScriptTM cDNA synthesis kit (BioRad), following the manufacturer's instructions. The cDNA generated was used as a template for qRT-PCR using the SYBR[®] Green JumpStart[™] Taq readymix[™] (Sigma) in a 20 μl final volume. Either a Rotor-Gene Q (Qiagen, Australia) or RG-3000 (Corbett Life Science, Australia) instrument was used for quantification of cDNA using the following protocol; 1

min at 95°C, followed by 40 cycles of 10 sec at 95°C, 15 sec at 57°C and 20 sec at 72°C. Melt curve analyses were undertaken to ensure only the desired amplicon was generated. Primers used (S2 Table) for amplification of cDNA transcripts were designed using NetPrimer (www.premiersoft.com). Transcriptional levels for RNA-seq validation experiments were corrected to GAPDH levels prior to normalization to the ATCC 17978 WT. For pentamidine stress experiments, transcriptional levels of *adeA* were corrected to 16S rDNA levels prior to being normalized to their respective untreated *A. baumannii* cultures. Transcriptional variations were calculated using the $2^{-\Delta\Delta CT}$ method [35]. Results for pentamidine stress experiments display the mean Log₂ fold change (\pm SEM) of three biological replicates each undertaken in triplicate. Statistical analyses were performed by Student's *t*-test, two-tailed, unpaired; ** = $P < 0.01$ and *** = $P < 0.001$.

Phenotypic microarray analysis

A. baumannii $\Delta adeRS$ cells were cultured on LB agar overnight at 37°C. A suspension of cells was made from a single colony in Biolog IF-0 inoculation fluid (Biolog, Inc.) to 85% transmittance and was subsequently diluted 1:200 in Biolog IF-0 containing dye A (Biolog, Inc.) and 0, 8, 16, 32 or 64 mg/L pentamidine. One hundred μ L of each dilution was added to each well of the Biolog PM01 and PM02A MicroPlates and placed in an OmniLog automatic plate reader (Biolog, Inc.) for 72 h at 37°C. Color formation from the redox active dye (Biolog dye A) was monitored every 15 min. Data obtained from respiration of $\Delta adeRS$ under different pentamidine conditions were individually overlaid against the untreated control using the OmniLog File Management/Kinetic Analysis software v1.20.02, and analyzed using OmniLog Parametric Analysis software v1.20.02 (Biolog, Inc.).

Results

Generation of $\Delta adeRS$ and complemented strains

The *adeRS* operon of *A. baumannii* ATCC 17978 was disrupted through the introduction of an ERY resistance cassette to produce a $\Delta adeRS$ strain. Complementation of $\Delta adeRS$ was achieved via reintroduction of a WT copy of *adeRS* *in trans* on the pWH1266 shuttle vector, generating $\Delta adeRS$ pWH::*adeRS* and comparisons were made to cells carrying the empty vector control ($\Delta adeRS$ pWH1266). To ensure deletion of *adeRS* did not affect viability, growth was monitored by OD₆₀₀ readings in MH broth over an 8 h period; results identified no significant perturbations in the growth rate in laboratory media compared to WT cells (data not shown).

Transcriptomic profiling of $\Delta adeRS$

Transcriptome profiling by RNA-sequencing (RNA-seq) of RNA isolated from $\Delta adeRS$ compared to that from WT ATCC 17978 identified 290 differentially expressed (≥ 2 -fold) genes; 210 up-regulated and 80 down-regulated (Fig 1 and S1 Table). RNA-seq results were confirmed by quantitative Real-Time PCR (qRT-PCR) for nine genes that displayed different levels of expression in $\Delta adeRS$ compared to WT; a good correlation between methods was observed (S1 Fig).

Expression of a number of efflux proteins was affected by inactivation of *adeRS*. For example, the *crxA* major facilitator superfamily transporter (ACX60_01760) shown to confer resistance to chloramphenicol and recently chlorhexidine efflux [26] was the highest up-regulated gene (7.1-fold; Fig 1) and *adeA* (ACX60_09125), *adeB* (ACX60_09130) and *aceI* (ACX60_07275)

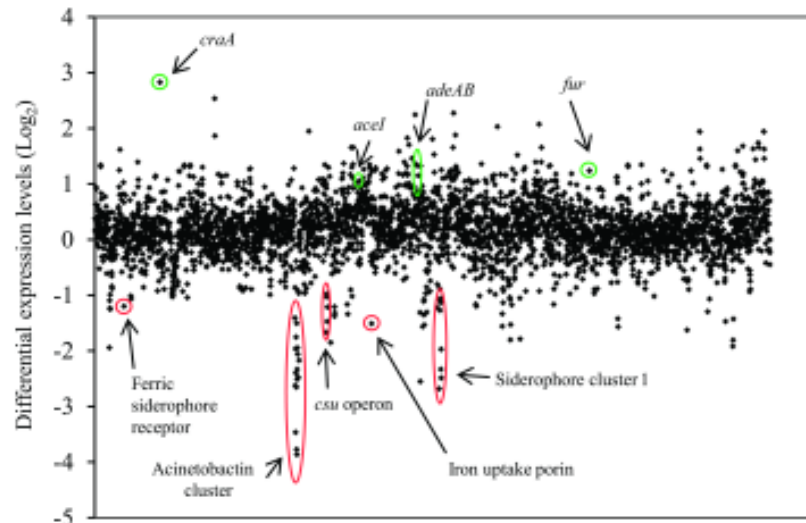


Fig 1. Global transcriptomic response differences of *A. baumannii* ATCC 17978 after deletion of *adeRS*. Each diamond marker represents a predicted gene within the genome ordered according to locus tag along the X-axis and differential expression generated from normalized reads per kilobase mapped of WT against $\Delta adeRS$ are displayed on the Y-axis (Log_2). Positive and negative Log_2 -values correlate to up- and down-regulated genes, respectively. Green and red circles highlight genes/gene clusters of interest that have been up- and down-regulated, respectively. See [S3 Table](#) for the full list of genes that were differentially expressed $\geq 1 \text{ Log}_2$ fold.

<https://doi.org/10.1371/journal.pone.0197412.g001>

which encode the AdeAB and the AceI efflux pumps, were up-regulated by 2.5-, 1.43-, and 2-fold, respectively, following deletion of *adeRS*.

Expression of multiple genes involved in virulence were down-regulated in the $\Delta adeRS$ strain, including the type 1 pilus operon *craA/BABCDE* (ACX60_06480–06505) (3.2- to 2-fold) and the siderophore-mediated iron-acquisition systems acinetobactin (ACX60_05590–05680) and siderophore 1 (ACX60_09665–09720) clusters (7.7- to 1.1-fold and 5.4- to 0.3-fold, respectively). In contrast, the ferric uptake regulator gene (*fur*) (ACX60_13910) was up-regulated 2.4-fold. Despite these alterations in expression levels of iron siderophore clusters and their regulator, no significant growth defects were identified when $\Delta adeRS$ was grown in the presence of 200 μM of DIP (data not shown).

Deletion of *adeRS* in ATCC 17978 reduced susceptibility to a limited number of antimicrobial agents

To assess if changes in expression of the *adeAB* and *craA* drug efflux genes identified in the transcriptome of the $\Delta adeRS$ derivative translated to an alteration in resistance profile, antibiogram analyses were undertaken. Resistance to a number of antibiotics including those that are known substrates of the CraA and AdeABC pumps were assessed. Surprisingly, despite *craA* being the highest up-regulated gene, no change in resistance to the primary substrate of CraA, chloramphenicol [36], was seen (data not shown). Previous studies examining the level of antimicrobial resistance conferred by AdeABC indicate that only when deletions are generated in strains which overexpress AdeABC is there a significant impact on the antibiogram [10, 13, 15,

[16, 32], implying that AdeABC confers only minimal to no intrinsic resistance. This was supported in our analysis as the MIC for tetracycline, tigecycline, GEN, kanamycin, nalidixic acid, ampicillin, streptomycin and amikacin, all previously identified AdeABC substrates, remained unchanged, whilst resistance to norfloxacin and ciprofloxacin increased 2-fold (data not shown) and chlorhexidine decreased 2-fold for the $\Delta adeRS$ mutant compared to WT (Table 1).

A variety of additional compounds were tested, primarily focusing on substrates of other multidrug efflux pumps and/or clinically relevant compounds, these included; colistin, polymyxin B, rifampicin, triclosan, novobiocin, benzalkonium, methyl viologen, pentamidine, DAPI and dequalinium. Of these, significant differences in the MICs of $\Delta adeRS$ versus WT were observed only for the diamidine compounds, pentamidine and DAPI, where an 8- and 4-fold reduction in resistance was identified, respectively (Table 1). Thus, taken together the $\Delta adeRS$ strain showed reduced resistance to the bisbiguanide chlorhexidine, and the diamidines pentamidine and DAPI which display structural similarities [38] (S2 Fig). Resistance to these substrates was partially or fully restored by complementation using $\Delta adeRS$ pWH::adeRS (Table 1).

Both AdeA and AdeB are required for intrinsic antimicrobial resistance in ATCC 17978

Since the 10-bp direct repeat where AdeR has been demonstrated to bind in other *A. baumannii* strains [18, 19] is also present in the ATCC 17978 *adeA-adeR* intercistronic region (data not shown), we hypothesized that the decreased resistance towards the subgroup of dicationic

Table 1. Antibiotic susceptibility of *A. baumannii* ATCC 17978, deletion mutants and complemented strains.

Strain	MIC (mg/L) ^{a,b}		
	PENT	DAPI	CHX
WT	125	4	8
$\Delta adeA$	15.6	1	4
$\Delta adeB$	15.6	1	4
$\Delta adeAB$ ^c	15.6	1	4
$\Delta adeRS$ ^d	15.6	1	4
$\Delta adeRS$ pWH::adeRS	125	1	8
$\Delta adeRS$ pWH1266	15.6	0.5	4/2
$\Delta adeRS$ pWH::adeAB	31.3	4	4
$\Delta adeRS$ pWHgent::adeAB	15.6	1	4
$\Delta adeRS$ pWHgent	7.8	0.5	4
$\Delta adeA$ pWHgent::adeAB	62.5	2	8/4
$\Delta adeA$ pWHgent	7.8	0.5	4
$\Delta adeB$ pWHgent::adeAB	62.5	4	4
$\Delta adeB$ pWHgent	7.8	1	2
$\Delta adeAB$ pWHgent::adeAB	62.5	4	4
$\Delta adeAB$ pWHgent	7.8	1	2

^aPENT, pentamidine; DAPI, 4',6-diamidino-2-phenylindole; CHX, chlorhexidine.

^bValues highlighted in bold indicate MIC values altered two-fold or greater compared to WT ATCC 17978.

^cAntimicrobials that did not significantly differ from WT susceptibility levels included gentamicin, kanamycin, norfloxacin, ciprofloxacin, ampicillin, colistin, polymyxin B, dequalinium, tigecycline, triclosan and methyl viologen.

^dAntimicrobials tested that did not significantly differ from WT susceptibility levels included rifampicin, benzylalkonium, streptomycin, amikacin and novobiocin as well as antimicrobials listed above in ^c with the exception of ciprofloxacin and norfloxacin.

<https://doi.org/10.1371/journal.pone.0197412.t001>

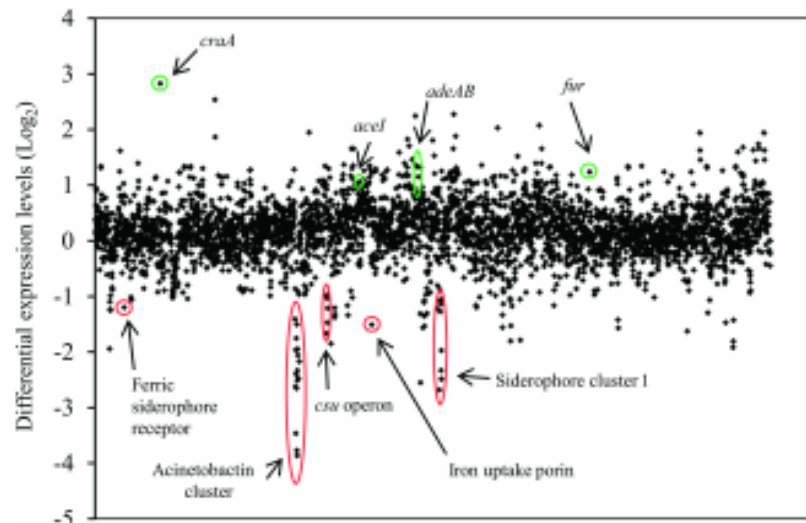


Fig 1. Global transcriptomic response differences of *A. baumannii* ATCC 17978 after deletion of *adeRS*. Each diamond marker represents a predicted gene within the genome ordered according to locus tag along the X-axis and differential expression generated from normalized reads per kilobase mapped of WT against $\Delta adeRS$ are displayed on the Y-axis (Log_2). Positive and negative Log_2 -values correlate to up- and down-regulated genes, respectively. Green and red circles highlight genes/gene clusters of interest that have been up- and down-regulated, respectively. See [S3 Table](#) for the full list of genes that were differentially expressed $\geq 1 \text{ Log}_2$ fold.

<https://doi.org/10.1371/journal.pone.0197412.g001>

which encode the AdeAB and the AceI efflux pumps, were up-regulated by 2.5-, 1.43-, and 2-fold, respectively, following deletion of *adeRS*.

Expression of multiple genes involved in virulence were down-regulated in the $\Delta adeRS$ strain, including the type 1 pilus operon *cuaA/BABCDE* (ACX60_06480–06505) (3.2- to 2-fold) and the siderophore-mediated iron-acquisition systems acinetobactin (ACX60_05590–05680) and siderophore 1 (ACX60_09665–09720) clusters (7.7- to 1.1-fold and 5.4- to 0.3-fold, respectively). In contrast, the ferric uptake regulator gene (*fur*) (ACX60_13910) was up-regulated 2.4-fold. Despite these alterations in expression levels of iron siderophore clusters and their regulator, no significant growth defects were identified when $\Delta adeRS$ was grown in the presence of 200 μM of DIP (data not shown).

Deletion of *adeRS* in ATCC 17978 reduced susceptibility to a limited number of antimicrobial agents

To assess if changes in expression of the *adeAB* and *craA* drug efflux genes identified in the transcriptome of the $\Delta adeRS$ derivative translated to an alteration in resistance profile, antibiogram analyses were undertaken. Resistance to a number of antibiotics including those that are known substrates of the CraA and AdeABC pumps were assessed. Surprisingly, despite *craA* being the highest up-regulated gene, no change in resistance to the primary substrate of CraA, chloramphenicol [36], was seen (data not shown). Previous studies examining the level of antimicrobial resistance conferred by AdeABC indicate that only when deletions are generated in strains which overexpress AdeABC is there a significant impact on the antibiogram [10, 13, 15,

[16, 37], implying that AdeABC confers only minimal to no intrinsic resistance. This was supported in our analysis as the MIC for tetracycline, tigecycline, GEN, kanamycin, nalidixic acid, ampicillin, streptomycin and amikacin, all previously identified AdeABC substrates, remained unchanged, whilst resistance to norfloxacin and ciprofloxacin increased 2-fold (data not shown) and chlorhexidine decreased 2-fold for the $\Delta adeRS$ mutant compared to WT (Table 1).

A variety of additional compounds were tested, primarily focusing on substrates of other multidrug efflux pumps and/or clinically relevant compounds, these included colistin, polymyxin B, rifampicin, triclosan, novobiocin, benzalkonium, methyl viologen, pentamidine, DAPI and dequalinium. Of these, significant differences in the MICs of $\Delta adeRS$ versus WT were observed only for the diamidine compounds, pentamidine and DAPI, where an 8- and 4-fold reduction in resistance was identified, respectively (Table 1). Thus, taken together the $\Delta adeRS$ strain showed reduced resistance to the bisguanide chlorhexidine, and the diamidines pentamidine and DAPI which display structural similarities [38] (S2 Fig). Resistance to these substrates was partially or fully restored by complementation using $\Delta adeRS$ pWHE-*adeRS* (Table 1).

Both AdeA and AdeB are required for intrinsic antimicrobial resistance in ATCC 17978

Since the 10-bp direct repeat where AdeR has been demonstrated to bind in other *A. baumannii* strains [18, 19] is also present in the ATCC 17978 *adeA-adeR* intergenic region (data not shown), we hypothesized that the decreased resistance towards the subgroup of dicationic

Table 1. Antibiotic susceptibility of *A. baumannii* ATCC 17978, deletion mutants and complemented strains.

Strain	MIC (mg/L) ^{ab}		
	PENT	DAPI	CHX
WT	125	4	8
$\Delta adeA$	15.6	1	4
$\Delta adeB$	15.6	1	4
$\Delta adeAB^c$	15.6	1	4
$\Delta adeRS^d$	15.6	1	4
$\Delta adeRS$ pWHE- <i>adeRS</i>	125	1	8
$\Delta adeRS$ pWH1266	15.6	0.5	4/2
$\Delta adeRS$ pWHE- <i>adeAB</i>	31.3	4	4
$\Delta adeRS$ pWHgent- <i>adeAB</i>	15.6	1	4
$\Delta adeRS$ pWHgent	7.8	0.5	4
$\Delta adeA$ pWHgent- <i>adeAB</i>	62.5	2	8/4
$\Delta adeA$ pWHgent	7.8	0.5	4
$\Delta adeB$ pWHgent- <i>adeAB</i>	62.5	4	4
$\Delta adeB$ pWHgent	7.8	1	2
$\Delta adeAB$ pWHgent- <i>adeAB</i>	62.5	4	4
$\Delta adeAB$ pWHgent	7.8	1	2

^aPENT, pentamidine; DAPI, 4',6-diamidino-2-phenylindole; CHX, chlorhexidine.

^bValues highlighted in bold indicate MIC values altered two-fold or greater compared to WT ATCC 17978.

^cAntimicrobials that did not significantly differ from WT susceptibility levels included gentamicin, kanamycin, norfloxacin, ciprofloxacin, ampicillin, colistin, polymyxin B, dequalinium, tigecycline, triclosan and methyl viologen.

^dAntimicrobials tested that did not significantly differ from WT susceptibility levels included rifampicin, benzalkonium, streptomycin, amikacin and novobiocin as well as antimicrobials listed above in ^c with the exception of ciprofloxacin and norfloxacin.

<https://doi.org/10.1371/journal.pone.0197412.t001>

compounds seen in $\Delta adeRS$ resulted from changes in *adeAB* expression. To test this, deletion strains targeting *adeAB*, as well as individual *adeA* and *adeB* mutations were generated in ATCC 17978.

Using $\Delta adeAB$, MIC analyses verified that deletion of the pump resulted in negligible changes in resistance to a subset of the antimicrobials tested for $\Delta adeRS$ (data not shown). However, an identical resistance pattern for the dicationic compounds as that afforded by $\Delta adeRS$ was observed (Table 1). Complementation of the inactivated genes partially restored resistance to all compounds, validating that AdeAB plays a direct role in resistance to these dicationic compounds (Table 1).

AdeRS is critical for increased expression of *adeAB* following pentamidine exposure

From MIC analysis of the ATCC 17978 derivatives, it was proposed that the presence of the AdeRS TCSTS increased *adeAB* expression consequently providing resistance to pentamidine, chlorhexidine and DAPI (Table 1). To confirm this, the level of *adeA* transcription was assessed by qRT-PCR of RNA isolated from WT and $\Delta adeRS$ strains after addition of a sub-inhibitory concentration of pentamidine. Transcription of the *adeAB* operon was significantly up-regulated in WT and down-regulated in $\Delta adeRS$ following pentamidine stress (Fig 2). Additionally, qRT-PCR was used to determine if *adeS* expression levels altered after pentamidine stress in WT cells. It was found that *adeS* expression increased less than <2-fold compared to untreated WT cells (data not shown). To phenotypically support the transcriptional evidence that *adeRS* initiates transcription of the ATCC 17978 *adeAB* operon, additional antibiograms were determined. Using the shuttle vector pWH1266, two clones were constructed; pWH-*adeAB* and pWHgent-*adeAB*, where the GEN resistance cartridge cloned in the latter vector inhibited transcription of *adeAB* from the tetracycline promoter naturally present in pWH1266. MIC analyses determined that the carriage of pWHgent-*adeAB* in $\Delta adeRS$ did not differ from results obtained for $\Delta adeRS$. Conversely, $\Delta adeRS$ cells with pWH-*adeAB* displayed a 4- and 8-fold increase in pentamidine and DAPI resistance, respectively (Table 1). Collectively, these results suggest that expression of *adeAB* and subsequent resistance to the dicationic compounds in ATCC 17978 can only occur when AdeRS is present.

Carbon source utilization alters resistance to pentamidine

Pentamidine, a drug known to be effective in the treatment of fungal and protozoan infections has gained recent attention in a bacterial context. Pentamidine has shown synergy with Gram-positive antibiotics, potentiating their activity towards Gram-negative bacteria [23]. As such, pentamidine has been proposed to be utilized as an adjunct therapy for MDR bacteria, including *A. baumannii* [22]. To identify additional pentamidine resistance mechanisms employed by *A. baumannii*, growth in different media was assessed. Disk diffusion assays identified that in *A. baumannii*, resistance to pentamidine was affected by the carbon source provided in M9 minimal medium (S4 Table), whilst for chlorhexidine and DAPI this pattern was not conserved indicating a pentamidine-specific response (data not shown). To determine the MIC levels for pentamidine, plate dilution experiments were undertaken for WT, $\Delta adeRS$ and $\Delta adeAB$ strains provided with varied carbon sources (Fig 3). Growth of $\Delta adeRS$ and $\Delta adeAB$ cells on MH agar were significantly perturbed at 32 mg/L of pentamidine. This MIC drastically differs when succinic acid was utilized as the sole carbon source, as growth was maintained up to 512 mg/L of pentamidine for all strains tested (Fig 3). Fumaric, α -ketoglutaric and oxaloacetic acids also increased pentamidine resistance by 8-fold for $\Delta adeRS$ and $\Delta adeAB$ strains when compared to the MIC obtained for MH agar. Growth of $\Delta adeRS$ and $\Delta adeAB$ mutants was inhibited at a higher dilution factor in the presence of oxaloacetic acid compared to fumaric

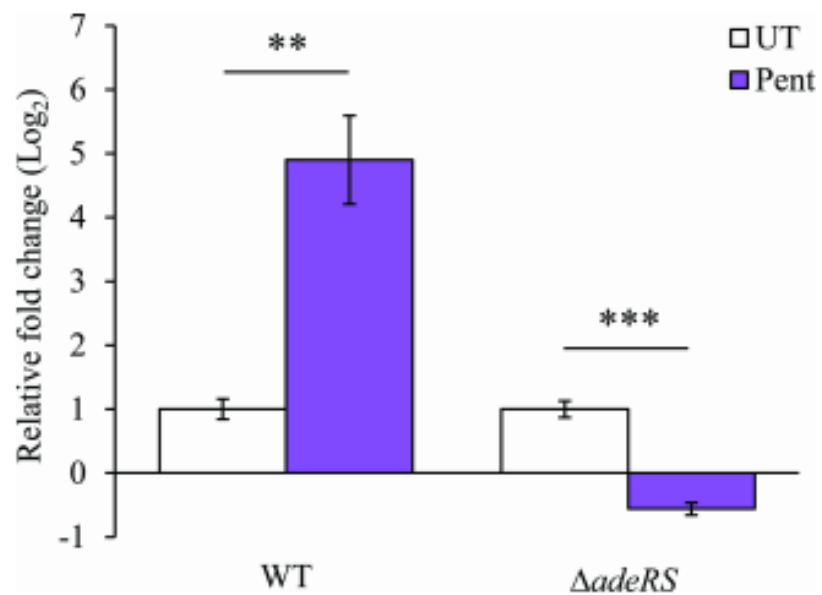


Fig 2. Increased expression of *adeA* following pentamidine stress is dependent on the presence of *AdeRS* in ATCC 17978. Transcriptional levels of *adeA* (ACX60_09125) from WT and $\Delta adeRS$ were determined by qRT-PCR after 30 min shock with 7.8 mg/L of pentamidine (Pent) (0.5 \times MIC of $\Delta adeRS$) and corrected to untreated cells (UT) after normalization to 16S. Bars represent the mean fold change (Log_2) of three biological replicates undertaken in triplicate, and error bars represent \pm SEM. Statistical analysis was performed by Student's *t*-test, two-tailed, unpaired; ** = $P < 0.01$ and *** = $P < 0.001$.

<https://doi.org/10.1371/journal.pone.0197412.g002>

and α -ketoglutaric acids whilst growth using citrate as the sole carbon source negatively affected resistance to WT cells, decreasing resistance 2-fold.

Biolog phenotypic arrays were undertaken to identify additional synergistic or antagonistic relationships between carbon sources and pentamidine resistance. Respiration of $\Delta adeRS$ cells for a total of 190 carbon compounds was assessed at various pentamidine concentrations (S3 Fig). From this, an additional ten compounds were identified that increased resistance to pentamidine in $\Delta adeRS$ at 64 mg/L (Fig 4). Despite minimal changes in pentamidine resistance in the presence of citric acid for $\Delta adeRS$ (Fig 3), this compound negatively affected respiration at lower pentamidine concentrations (S3 Fig). Surprisingly, succinic, α -ketoglutaric and fumaric acids failed to restore respiration at 64 mg/L of pentamidine for $\Delta adeRS$ (S3 Fig). By extending the incubation period for another 72 h, respiration in the presence of succinic or fumaric acids was restored to levels similar to the untreated control (data not shown). This may indicate that succinic and fumaric acids significantly lag in their ability to recover the cells from pentamidine in the IF-0 medium (Biolog Inc.) whilst α -ketoglutaric acid recovery is dependent on growth medium.

Bioavailability of iron correlates with pentamidine resistance

Iron has been shown to influence pentamidine resistance in protozoan species [39], thus we assessed if it plays a similar role in *A. baumannii*. The addition of ferrous sulphate to the growth

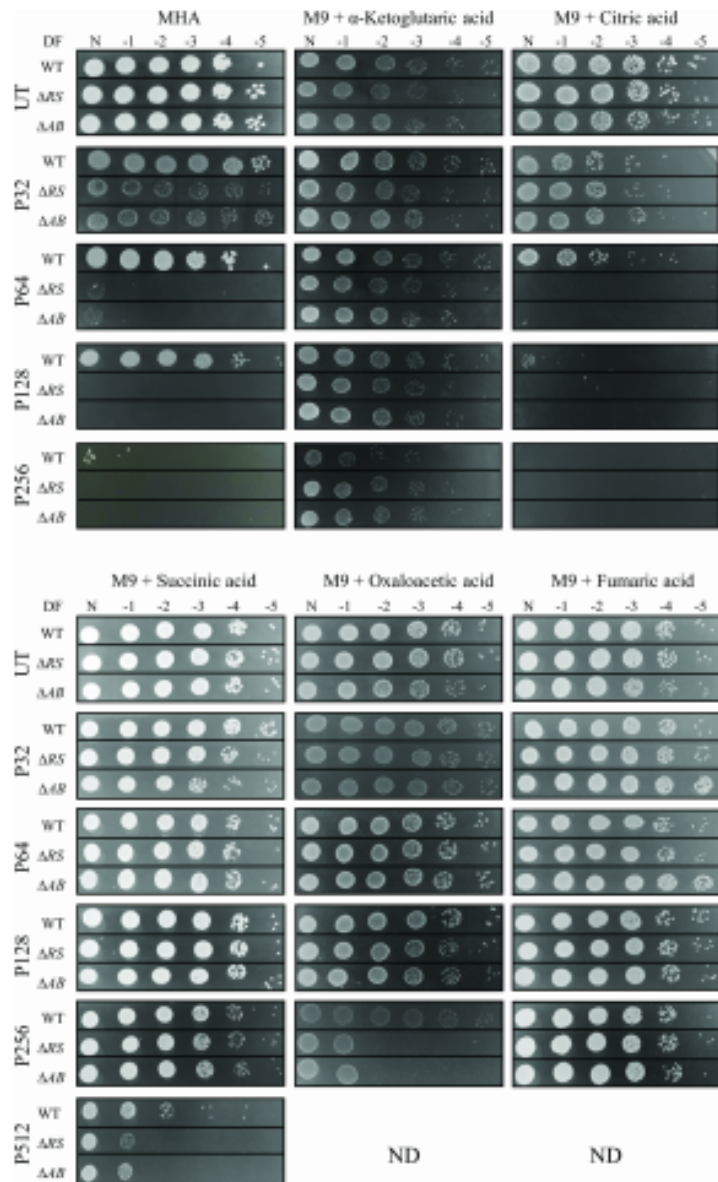


Fig 3. Resistance to pentamidine is modulated by carbon sources available in the growth medium. Ten-fold serial dilutions of *A. baumannii* ATCC 17978 (WT), *ΔadeRS* (*ΔRS*) and *ΔadeABC* (*ΔAB*) cells were used to compare the concentration of pentamidine that inhibits growth in different media. Mueller-Hinton agar (MHA) was used as a comparative control. Images display serial 1:10 dilutions after overnight incubation at 37°C, where DF is abbreviated for dilution factor and N represents undiluted cells. Strains were grown in the absence of pentamidine (UT) or presence of 32, 64, 128, 256 and 512 mg/L of pentamidine (P32, P64, P128, P256, and P512, respectively). Carbon sources tested in M9 minimal medium were used at a final concentration of 0.4% (w/v). ND, not done due to precipitation of pentamidine once added into the molten medium. Figures are representative examples of results obtained.

<https://doi.org/10.1371/journal.pone.0197412.g003>

medium significantly reduced the zone of clearing from pentamidine in a dose-dependent manner up to a final concentration of 5 mM for WT and mutant strains (Table 2 and S4 Fig). Furthermore, chelation of iron using DIP resulted in WT cells becoming more susceptible to pentamidine compared to the untreated control (Table 2). This modified pentamidine susceptibility is iron specific as inclusion of other cations in the growth medium (zinc, copper, manganese, cobalt, nickel) did not significantly affect the zones of clearing (data not shown). Using inductively-coupled plasma mass spectrometry the internal iron concentration in WT and *ΔadeRS* cells was determined in the absence/presence of a sub-inhibitory concentration of pentamidine. Internal iron concentrations remained essentially unchanged in both strains under the different conditions tested (data not shown), indicating that iron/pentamidine interactions may occur outside of the cell and the observed response was not due to a reduced capacity to store iron.

Discussion

The *adeRS* and *adeABC* operons of *A. baumannii* have gained considerable attention due to their role in regulating and conferring multidrug resistance, respectively [8, 13, 16, 40]. Multiple genetic arrangements of the *adeABC* operon in *A. baumannii* clinical isolates exist, where

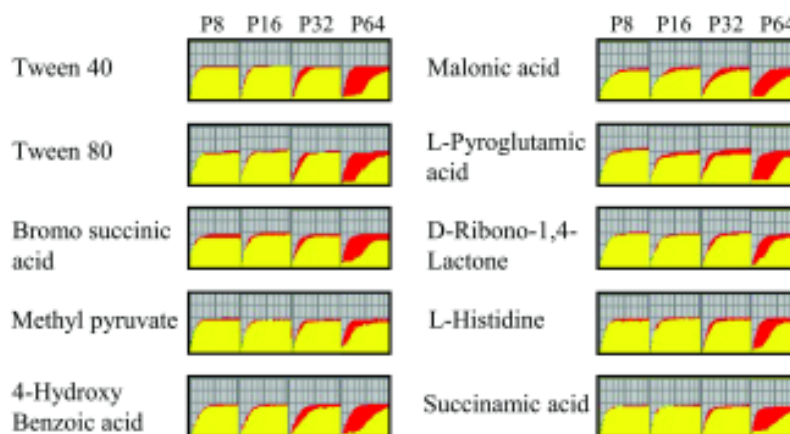


Fig 4. Kinetic response curves paralleling bacterial growth from Biolog PM01 and PM2A plates identify ten carbon sources that increase pentamidine resistance in *ΔadeRS*. P8, P16, P32 and P64 represent kinetic response curves at 8, 16, 32, or 64 mg/L of pentamidine compared to the untreated control, respectively. Red curves represent respiration of untreated *ΔadeRS*, while yellow curves represent respiration of the sample in the different experimental conditions. Only carbon compounds that promote at least 50% maximal respiration and induce a recovery response by 36 h are shown. See S3 Fig for respiration curves for all tested treatments.

<https://doi.org/10.1371/journal.pone.0197412.g004>

Table 2. Zones of clearing for *A. baumannii* ATCC 17978 and deletion mutants grown on Mueller-Hinton agar with the addition or chelation of iron after pentamidine exposure.

Strain	Zone of clearing (mm) ^{ab}				
	WT	Δ adeRS	Δ adeAB	Δ adeA	Δ adeB
MHA control	1.4 ± 0.3	6.9 ± 0.5	6.9 ± 0.3	6.9 ± 0.4	7.2 ± 0.4
+ 2.5 mM FeSO ₄	0.8 ± 0.1	5.4 ± 0.2	5.6 ± 0.3	5.4 ± 0.1	5.6 ± 0.1
+ 5 mM FeSO ₄	0.7 ± 0.2	2.5 ± 0.8	2.8 ± 0.3	3.2 ± 0.3	2.9 ± 0.6
+ 7.5 mM FeSO ₄	NG	NG	NG	NG	NG
+ 100 μ M DIP	1.7 ± 0.1	6.7 ± 0.2	6.9 ± 0.1	6.2 ± 0.2	6.6 ± 0.2
+ 200 μ M DIP	5 ± 0.3	6.7 ± 0.4	6.6 ± 0.4	6.1 ± 0.1	6.4 ± 0.1

^aAveraged values are displayed ± SD. Statistical analysis were performed by Student's *t*-test, two-tailed, unpaired

^b * = *P* < 0.0005 and

*** = *P* < 0.000001.

^cValues given in bold indicate a significant difference between a strain grown under iron-rich or iron-limited conditions versus its respective MHA control.

^dMHA, Mueller-Hinton agar; FeSO₄, ferrous sulphate; DIP, 2,2'-dipyridyl; NG, no growth due to iron toxicity.

<https://doi.org/10.1371/journal.pone.0197412.t002>

35% of 116 diverse isolates lack the *adeC* OMP component [20]. This is also the case for the clinical isolate *A. baumannii* ATCC 17978, which was chosen for further analysis in this study. It is not uncommon for RND pumps to recruit an alternative OMP to form a functional complex [41–43]. This may also be the situation for *AdeAB* in *A. baumannii* ATCC 17978, since in an *Escherichia coli* background, *adeAB* can be co-expressed with *adeK*, an OMP belonging to the *A. baumannii* *AdeIJK* RND complex to confer resistance [44]. However, whether *AdeB* can work alone or function with alternative membrane fusion proteins such as *adeJ* or *adeF* is not known. As the resistance profile of Δ adeA was indistinguishable from the Δ adeAB and Δ adeB strains, it provides confirmatory evidence that both *adeA* and *adeB* are required for efficient efflux to only a subset of dicationic compounds in ATCC 17978. Further assessments will be required to verify if this phenotype is maintained across other *A. baumannii* isolates and extends to other structurally-similar compounds.

It has been found previously, that the introduction of shuttle vectors expressing WT copies of genes *in trans* do not restore resistance profiles back to WT levels as also seen in this study [45–48]. Using qRT-PCR, *adeS* was expressed at low levels in WT cells even after pentamidine shock (data not shown). Complementation studies with *adeRS* thus could be influenced by copy number effects, which may perturb the native expression levels of these proteins within the cell. Additionally, the differing modes of action of the dicationic compounds may have influenced the MIC results, as fold-shifts in resistance were observed even when the empty pWH1266 vector was being expressed (Table 1).

The transcriptomic analysis of ATCC 17978 Δ adeRS revealed changes in gene expression were not limited to *adeAB* but included many genes, some of which have been shown to be important in *A. baumannii* pathogenesis [49, 50] and virulence *in vivo* [51]. Although this had been seen before in an *adeRS* mutant generated in the MDR *A. baumannii* isolate AYE [16], here the transcriptional changes were to a largely different subset of genes. Previously, deletion of *adeRS* in AYE resulted in decreased expression of *adeABC* by 128-, 91-, and 28-fold, respectively [16]. This decreased gene expression was expected as AYE naturally contains a point mutation in *AdeS* (producing an Ala 94 to Val substitution in *AdeS*) resulting in constitutive expression of *adeABC* and contributing to its MDR phenotype [2, 16]. Richmond *et al.*, (2016) [16] proposed that the high similarities in phenotypic changes between their *adeRS* and *adeB* AYE deletion derivatives were largely due to downstream effects caused by reduced expression

of *adeABC*. We cannot rule out the possibility that some of the changes in gene expression in our study have resulted from the slight increase seen in expression of *adeAB*, most likely caused by polar effects exerted by the ERY resistance cassette. However, our transcriptome data indicated *adeAB* were expressed at low levels and thus represent basal levels of expression; results consistent with ATCC 17978 being labelled as a 'drug susceptible' isolate [24].

Currently, the environmental signal(s) that interact with the periplasmic sensing domain of AdeS are not known. Antimicrobial compounds can directly stimulate autophosphorylation of specific TCSTS which in turn directly regulate the expression of genes providing resistance to that compound [52, 53]. It is unlikely that pentamidine is the environmental stimulus that is sensed by AdeS, as a number of conditions, including chlorhexidine shock, can also up-regulate *adeAB* expression in ATCC 17978 [54–57]. Instead, AdeS may respond to stimuli such as solutes that are excreted and accumulate in the periplasm when cells are subjected to various stressors including AdeAB substrates.

This study revealed unique interactions between pentamidine and a number of carbon sources which significantly alter the resistance profile to pentamidine for *A. baumannii* ATCC 17978 and derivatives. Biolog phenotypic arrays identified a number of succinic acid derivatives that also allowed respiration in the presence of a lethal concentration of pentamidine (Fig 4). Interestingly, when AdeRS utilized malonic acid as the sole carbon source, a potent inhibitor of the succinate dehydrogenase complex, cells were also able to respire at increased pentamidine concentrations (Fig 4). In Gram-negative bacteria, the mechanism of action for pentamidine is thought to primarily occur via binding to the lipid-A component of the outer membrane and not through inhibition of an intracellular target [23, 58]. Therefore, it seems unlikely that pentamidine interferes with enzymatic functions like that of succinate dehydrogenase, and instead the compounds which showed an increase in pentamidine resistance may contribute to either chelation of the compound or provide protective mechanisms that reduce binding to the lipid-A target. Interestingly, a 1956 study [59] identified that in the presence of α -ketoglutaric or glutamic acid, resistance to a lethal concentration of pentamidine could be achieved in *E. coli*, leading to the proposition that pentamidine interferes with the transaminase reaction in glutamic acid production. However, our study shows that glutamic acid does not affect pentamidine resistance (S4 Table), inferring that a different mechanism might be responsible for the increase in pentamidine resistance in *A. baumannii*.

Iron is an essential metal serving as a co-factor in numerous proteins involved in redox chemistry and electron transport. It is generally a limited resource for pathogenic bacteria such as *A. baumannii* where it is important for virulence and disease progression [6, 50]. Our studies showed that altering iron levels also had a marked effect on resistance to pentamidine. This is in agreement with the observation that citric and gluconic acids can act as iron-chelating agents [60, 61] and respiration activity in the presence of these compounds at the pentamidine concentrations tested were significantly altered (S3 Fig). Many clinically relevant antimicrobials have shown to be affected by the presence of iron, including compounds belonging to tetracycline, aminoglycoside and quinolone classes [22]. Activity of these compounds can be altered by numerous factors, including the formation of stable complexes which can affect drug efficacy or have unfavourable effects on patient health. Understanding the metabolic flux in *A. baumannii* and other MDR bacteria has the potential to lead to more effective therapeutic interventions thus reducing infection rates, knowledge critical to slow the progress towards our re-entry into a pre-antibiotic era.

Conclusions

Overall, this is the first study which has demonstrated that the AdeAB system in *A. baumannii* ATCC 17978 provides intrinsic resistance to a subset of dicationic compounds, and efflux of

these compounds via AdeAB is directly regulated by the AdeRS TCSTS. RNA-seq identified that deletion of *adeRS* produced significant changes in the transcriptome. These results support the notion that strain specific variations are apparent [16]. We have provided evidence that in ATCC 17978, AdeRS is directly responsible for the activation of *adeAB* gene expression, as Δ *adeRS* failed to increase expression upon subjection to one of the pumps newly identified intrinsic substrates, pentamidine. It will be of interest to assess whether these dicationic compounds also extend as substrates towards AdeAB(C) pumps present in other *A. baumannii* isolates and if expression levels of *adeAB(C)* upon exposure to these substrates and other potential stressors also occur. This information may help to identify the stimulus that activates the AdeRS TCSTS. We have also demonstrated for the first time that for pentamidine to exert its antibacterial effect in *A. baumannii*, a dependence on the availability of iron is required, and that growth in the presence of selected carbon sources has a profound effect on its resistance.

Supporting information

S1 Fig. Validation of RNA-sequencing results. The transcriptomic results obtained by RNA-sequencing were validated by qRT-PCR analysis. The level of nine genes that displayed differential expression or remained essentially unchanged between Δ *adeRS* and WT ATCC 17978 were chosen for comparison. Expression levels for qRT-PCR experiments were corrected to those obtained for *GAPDH* (*ACC60_05065*) prior to normalisation against WT ATCC 17978 transcriptional levels. Grey and black bars represent values obtained from RNA-seq and qRT-PCR results, respectively. Differential expression between Δ *adeRS* and WT ATCC 17978 are given in Log₂-values.
(TIF)

S2 Fig. Structures of dicationic antimicrobial compounds to which Δ *adeRS*, Δ *adeA*, Δ *adeB* and Δ *adeAB* deletion mutant derivatives showed a decrease in resistance when compared to WT ATCC 17978. Compounds include (a) pentamidine, (b) DAPI and (c) chlorhexidine. For pentamidine and chlorhexidine, the cationic nitrogenous groups are separated by a long carbon chain, forming symmetrical compounds, whereas, DAPI lacks this long linker and is asymmetric.
(TIF)

S3 Fig. Comparative analysis of kinetic response curves obtained from Biolog PM plates for Δ *adeRS* cells untreated and subjected to increasing concentrations of pentamidine. Respiration of ATCC 17978 Δ *adeRS* cells in the presence of pentamidine (8, 16, 32, or 64 mg/L) against untreated control cells are shown for (a) Biolog PM01 plates and (b) Biolog PM02A plates. Respiration activity for both plates were monitored in IF-0 (Biolog, Inc.) liquid medium for 72 h at 37°C. The curve in each well represents the colour intensity of a redox-active dye (*y* axis) over time (*x* axis: 72 h). Respiration of Δ *adeRS* cells are shown in red (control), green (under different concentrations of pentamidine), and yellow (depicts the regions of respiratory overlap). Black numbered squares represent carbon sources which decreased resistance to pentamidine (1, D-gluconic acid; 2, citric acid).
(TIF)

S4 Fig. Pentamidine resistance is affected by the concentration of iron within the growth medium. Resistance to pentamidine was assessed by disc diffusion assays in Mueller-Hinton agar (MHA) for ATCC 17978 and Δ *adeRS*, Δ *adeA*, Δ *adeB* and Δ *adeAB* deletion derivatives. Zones of clearing were compared to iron rich conditions from the addition of ferrous sulphate (FeSO_4) at the final concentrations of 2.5 and 5 mM and iron-chelated conditions obtained by the addition of 2',2'-dipyridyl (DIP) at the final concentrations of 100 and 200 μM

in MHA. Images displayed are a representative of the typical results obtained.
(TIF)

S1 Table. Strains and plasmids used in the study.
(DOCX)

S2 Table. Primers used in this study.
(DOCX)

S3 Table. Genes significantly up- and down-regulated (≥ 2 -fold) in $\Delta adeRS$ compared against the parent ATCC 17978 (CP012004) by RNA-seq methodologies.
(DOCX)

S4 Table. Zones of clearing obtained from growth on M9 minimal medium with the addition of different carbon sources after exposure to pentamidine.
(DOCX)

Acknowledgments

We would like to thank Professor Bryan Davies from the Department of Molecular Biosciences at the University of Texas for providing the plasmid pAT04.

Author Contributions

Conceptualization: Felise G. Adams, Uwe H. Stroecher, Melissa H. Brown.

Data curation: Felise G. Adams, Uwe H. Stroecher, Karl A. Hassan, Shashikanth Marri, Melissa H. Brown.

Formal analysis: Felise G. Adams, Shashikanth Marri.

Funding acquisition: Uwe H. Stroecher, Melissa H. Brown.

Investigation: Felise G. Adams, Shashikanth Marri.

Methodology: Felise G. Adams, Karl A. Hassan.

Supervision: Uwe H. Stroecher, Melissa H. Brown.

Writing – original draft: Felise G. Adams, Uwe H. Stroecher, Karl A. Hassan, Melissa H. Brown.

Writing – review & editing: Felise G. Adams, Karl A. Hassan, Melissa H. Brown.

References

1. Peleg AY, Seifert H, Paterson DL. *Acinetobacter baumannii*: emergence of a successful pathogen. *Clin Microbiol Rev.* 2008; 21(3):538–82. <https://doi.org/10.1128/CMR.00058-07> PMID: 18625687
2. Fournier PE, Vallienet D, Barbe V, Audic S, Ogata H, Point L, et al. Comparative genomics of multidrug resistance in *Acinetobacter baumannii*. *PLoS Genet.* 2006; 2(1):e7. <https://doi.org/10.1371/journal.pgen.0020007> PMID: 16414994
3. Adams MD, Chan ER, Molyneux ND, Bonomo RA. Genomewide analysis of divergence of antibiotic resistance determinants in closely related isolates of *Acinetobacter baumannii*. *Antimicrob Agents Chemother.* 2010; 54(9):3569–77. <https://doi.org/10.1128/AAC.00057-10> PMID: 20530228
4. Stackwell GA, Hamidian M, Hall RM. IncM plasmid R1215 is the source of chromosomally located regions containing multiple antibiotic resistance genes in the globally disseminated *Acinetobacter baumannii* GC1 and GC2 clones. *mSphere.* 2016; 1(3):e00117–16. <https://doi.org/10.1128/mSphere.00117-16> PMID: 27203751

5. Hamidian M, Kenyon JJ, Holt KE, Pickard D, Hall RM. A conjugative plasmid carrying the carbapenem resistance gene bla_{OXA-23} in *AbaR*H in an extensively resistant GC1 *Acinetobacter baumannii* isolate. *J Antimicrob Chemother*. 2014; 69(10):2625–8. <https://doi.org/10.1093/ac/cku188> PMID: 24907141
6. Wright MS, Jacobs MR, Bonomo RA, Adams MD. Transcriptome remodeling of *Acinetobacter baumannii* during infection and treatment. *MBio*. 2017; 8(2):e02193–16. <https://doi.org/10.1128/mBio.02193-16> PMID: 28270585
7. Saranathan R, Pragal S, Sawant AR, Tomar A, Madhavi M, Sah S, et al. Disruption of TetR type regulator *adeN* by mobile genetic element confers elevated virulence in *Acinetobacter baumannii*. *Virulence*. 2017;1–19.
8. Yoon EJ, Courvalin P, Grillot-Courvalin C. RND-type efflux pumps in multidrug-resistant clinical isolates of *Acinetobacter baumannii*: major role for AdeABC overexpression and AdeRS mutations. *Antimicrob Agents Chemother*. 2013; 57(7):2989–95. <https://doi.org/10.1128/AAC.02556-12> PMID: 23587930
9. Coyne S, Courvalin P, Perichon B. Efflux-mediated antibiotic resistance in *Acinetobacter* spp. *Antimicrob Agents Chemother*. 2011; 55(3):947–53. <https://doi.org/10.1128/AAC.01388-10> PMID: 21173183
10. Magnat S, Courvalin P, Lambert T. Resistance-nodulation-cell division-type efflux pump involved in aminoglycoside resistance in *Acinetobacter baumannii* strain BM4454. *Antimicrob Agents Chemother*. 2001; 45(12):3375–80. <https://doi.org/10.1128/AAC.45.12.3375-3380.2001> PMID: 11709311
11. Coyne S, Rosenfeld N, Lambert T, Courvalin P, Perichon B. Overexpression of resistance-nodulation-cell division pump AdeFGH confers multidrug resistance in *Acinetobacter baumannii*. *Antimicrob Agents Chemother*. 2010; 54(10):4389–93. <https://doi.org/10.1128/AAC.00145-10> PMID: 20898809
12. Damier-Piolle L, Magnat S, Bremont S, Lambert T, Courvalin P, AdeLJK, a resistance-nodulation-cell division pump effluxing multiple antibiotics in *Acinetobacter baumannii*. *Antimicrob Agents Chemother*. 2008; 52(2):557–62. <https://doi.org/10.1128/AAC.00732-07> PMID: 18088832
13. Marchand I, Damier-Piolle L, Courvalin P, Lambert T. Expression of the RND-type efflux pump AdeABC in *Acinetobacter baumannii* is regulated by the AdeRS two-component system. *Antimicrob Agents Chemother*. 2004; 48(9):3298–304. <https://doi.org/10.1128/AAC.48.9.3298-3304.2004> PMID: 15378989
14. Pelleg AY, Adams J, Paterson DL. Tetracycline efflux as a mechanism for nonsusceptibility in *Acinetobacter baumannii*. *Antimicrob Agents Chemother*. 2007; 51(6):2065–9. <https://doi.org/10.1128/AAC.01198-06> PMID: 17420217
15. Rajamohan G, Srinivasan VB, Gebreyes WA. Novel role of *Acinetobacter baumannii* RND efflux transporters in mediating decreased susceptibility to biocides. *J Antimicrob Chemother*. 2010; 65(2):228–32. <https://doi.org/10.1093/ac/cku427> PMID: 20008046
16. Richmond GE, Evans LP, Anderson MJ, Ward ME, Bonney LC, Ivans A, et al. The *Acinetobacter baumannii* two-component system AdeRS regulates genes required for multidrug efflux, biofilm formation, and virulence in a strain-specific manner. *MBio*. 2016; 7(2):e00430–16. <https://doi.org/10.1128/mBio.00430-16> PMID: 27094331
17. Nikaido H, Takatsuka Y. Mechanisms of RND multidrug efflux pumps. *Biochim Biophys Acta*. 2009; 1794(5):769–81. <https://doi.org/10.1016/j.bbabap.2008.10.004> PMID: 19026770
18. Chang TY, Huang BJ, Sun JR, Peng CL, Chan MC, Yu CP, et al. AdeR protein regulates adeABC expression by binding to a direct-repeat motif in the intercatronic spacer. *Microbiol Res*. 2016; 183:60–7. <https://doi.org/10.1016/j.micres.2015.11.010> PMID: 26805619
19. Wen YQ, Z, Yu Y, Zhou X, Pei YD, B., Higgins P, Zheng F. Mechanistic insight into how multidrug resistant *Acinetobacter baumannii* response regulator AdeR recognizes an intercatronic region. *Nucleic Acids Res*. 2017; 45(16):9773–87. <https://doi.org/10.1093/nar/gkx524> PMID: 28904482
20. Nemecek A, Malinzerova M, van der Reijden TJ, van den Broek PJ, Dijkshoorn L. Relationship between the AdeABC efflux system gene content, netilmicin susceptibility and multidrug resistance in a genotypically diverse collection of *Acinetobacter baumannii* strains. *J Antimicrob Chemother*. 2007; 60(3):483–9. <https://doi.org/10.1093/ac/ckm201> PMID: 17426288
21. Conrad RS, Wulf RG, Clay DL. Effects of carbon sources on antibiotic resistance in *Pseudomonas aeruginosa*. *Antimicrob Agents Chemother*. 1979; 15(1):59–66. PMID: 106771
22. Ematy B, Barma F. The 'laissez faire' between iron and antibiotics. *FEMS Microbiol Rev*. 2016; 40(3):418–35. <https://doi.org/10.1093/femsre/fuw004> PMID: 26945776
23. Stokes JM, MacNair CR, Ilyas B, French S, Cote JP, Boussman C, et al. Pentamidine sensitizes Gram-negative pathogens to antibiotics and overcomes acquired colistin resistance. *Nat Microbiol*. 2017; 2:17028. <https://doi.org/10.1038/nmicrobiol.2017.28> PMID: 28283303
24. Smith MG, Gianoulis TA, Pukatzki S, Melikalans JJ, Ormston LN, Gerstein M, et al. New insights into *Acinetobacter baumannii* pathogenesis revealed by high-density pyrosequencing and transposon mutagenesis. *Genes Dev*. 2007; 21(5):601–14. <https://doi.org/10.1101/gad.1510307> PMID: 17344419

25. Wegand I, Hilpert K, Hancock RE. Agar and broth dilution methods to determine the minimal inhibitory concentration (MIC) of antimicrobial substances. *Nat Protoc*. 2008; 3(2):163–75. <https://doi.org/10.1038/nprot.2007.521> PMID: 18274517
26. Kariga K, Delor I, Cornella GR. A wide-host-range suicide vector for improving reverse genetics in Gram-negative bacteria: inactivation of the blaA gene of *Yersinia enterocolitica*. *Gene*. 1991; 109(1):137–41. PMID: 1758974
27. Macrina FL, Evans RP, Tobian JA, Hartley DL, Clewell DB, Jones KR. Novel shuttle plasmid vehicles for *Escherichia-Shigella* transgeneric cloning. *Gene*. 1983; 25(1):145–50. PMID: 6319229
28. Hoang TT, Karkhoff-Schweizer RR, Kutchma AJ, Schweizer HP. A broad-host-range Flp-FRT recombination system for site-specific excision of chromosomally-located DNA sequences: application for isolation of unmarked *Pseudomonas aeruginosa* mutants. *Gene*. 1998; 212(1):77–86. PMID: 9661666
29. Dorsey CW, Tomarski AP, Actis LA. Genetic and phenotypic analysis of *Acinetobacter baumannii* insertion derivatives generated with a transposome system. *Appl Environ Microbiol*. 2002; 68(12):6353–60. <https://doi.org/10.1128/AEM.68.12.6353-6360.2002> PMID: 12450860
30. Tucker AT, Nowicki EM, Boff JM, Knauf GA, Burda NC, Trent MS, et al. Defining gene-phenotype relationships in *Acinetobacter baumannii* through one-step chromosomal gene inactivation. *MBio*. 2014; 5(4):e01313–14. <https://doi.org/10.1128/mBio.01313-14> PMID: 25096877
31. Hunger M, Schmucker R, Kahlan V, Hillen W. Analysis and nucleotide sequence of an origin of DNA replication in *Acinetobacter calcoaceticus* and its use for *Escherichia coli* shuttle plasmids. *Gene*. 1990; 87(1):45–51. PMID: 2185139
32. Schweizer HD. Small broad-host-range gentamycin resistance gene cassettes for site-specific insertion and deletion mutagenesis. *Biotechniques*. 1993; 15(5):831–4. PMID: 8207974
33. Eijkelkamp BA, Strother UH, Hassan KA, Elbourne LD, Paulsen IT, Brown MH. H-NS plays a role in expression of *Acinetobacter baumannii* virulence features. *Infect Immun*. 2013; 81(7):2574–83. <https://doi.org/10.1128/IAI.00065-13> PMID: 23649094
34. Giles SK, Strother UH, Eijkelkamp BA, Brown MH. Identification of genes essential for pellicle formation in *Acinetobacter baumannii*. *BMC Microbiol*. 2015; 15:116. <https://doi.org/10.1186/s12866-015-0440-6> PMID: 26047264
35. Livak KJ, Schmittgen TD. Analysis of relative gene expression data using real-time quantitative PCR and the 2^{-ΔΔC_T} method. *Methods*. 2001; 25(4):402–8. <https://doi.org/10.1006/meth.2001.1262> PMID: 11846629
36. Li L, Hassan KA, Brown MH, Paulsen IT. Rapid multiplexed phenotypic screening identifies drug resistance functions for three novel efflux pumps in *Acinetobacter baumannii*. *J Antimicrob Chemother*. 2016; 71(5):1223–32. <https://doi.org/10.1093/jac/dkv460> PMID: 26832750
37. Yoon EJ, Chabane YN, Goussard S, Smeared E, Courvalin P, De E, et al. Contribution of resistance-modulation-cell division efflux systems to antibiotic resistance and biofilm formation in *Acinetobacter baumannii*. *MBio*. 2015; 6(2):e00309–15. <https://doi.org/10.1128/mBio.00309-15> PMID: 26826730
38. Brown MH, Skumay RA. Staphylococcal multidrug efflux protein QacA. *J Mol Microbiol Biotechnol*. 2001; 3(2):163–70. PMID: 11321569
39. Wong IL, Chow LM. The role of *Leishmania enrietti* multidrug resistance protein 1 (LeMDR1) in mediating drug resistance is iron-dependent. *Mol Biochem Parasitol*. 2006; 150(2):278–87. <https://doi.org/10.1016/j.molbiopara.2006.06.014> PMID: 17018238
40. Nowak J, Schneiders T, Seifert H, Higgins PG. The Asp20-to-Asn substitution in the response regulator AdeR leads to enhanced efflux activity of AdeB in *Acinetobacter baumannii*. *Antimicrob Agents Chemother*. 2016; 60(2):1085–90. <https://doi.org/10.1128/AAC.02413-15> PMID: 26643347
41. Chuanchuen R, Narasaki CT, Schweizer HP. The MexJK efflux pump of *Pseudomonas aeruginosa* requires OprM for antibiotic efflux but not for efflux of triclosan. *J Bacteriol*. 2002; 184(18):5036–44. <https://doi.org/10.1128/JB.184.18.5036-5044.2002> PMID: 12193619
42. Mine T, Morita Y, Kataoka A, Mizushima T, Tsuchiya T. Expression in *Escherichia coli* of a new multidrug efflux pump, MexXY, from *Pseudomonas aeruginosa*. *Antimicrob Agents Chemother*. 1999; 43(2):415–7. PMID: 9925549
43. Fralick JA. Evidence that TolC is required for functioning of the Mex/AcrAB efflux pump of *Escherichia coli*. *J Bacteriol*. 1996; 178(15):5803–5. PMID: 8824631
44. Sugawara E, Nikaide H. Properties of AdeABC and AdeJK efflux systems of *Acinetobacter baumannii* compared with those of AcrAB-TolC system of *Escherichia coli*. *Antimicrob Agents Chemother*. 2014; 58:7250–7. <https://doi.org/10.1128/AAC.03278-14> PMID: 25246400
45. Li X, Quan J, Yang Y, Ji J, Liu L, Fu Y, et al. Abrp, a new gene, confers reduced susceptibility to tetracycline, glycylcine, chloramphenicol and fosfomycin classes in *Acinetobacter baumannii*. *Eur J Clin Microbiol Infect Dis*. 2016; 35(8):1371–5. <https://doi.org/10.1007/s10096-016-2674-0> PMID: 27220329

46. Liu ML, Soo PC, Ling SR, Kuo HY, Tang CY, Chang KC. The sensor kinase BfmS mediates virulence in *Acinetobacter baumannii*. *J Microbiol Immunol Infect*. 2014; 47(4):275–81. <https://doi.org/10.1016/j.jmii.2012.12.004> PMID: 23453126
47. Saroj SD, Clemmer KM, Bonomo RA, Rather PN. Novel mechanism for fluoroquinolone resistance in *Acinetobacter baumannii*. *Antimicrob Agents Chemother*. 2012; 56(9):4955–7. <https://doi.org/10.1128/AAC.00739-12> PMID: 22733072
48. Wang J, Zhou Z, He F, Ruan Z, Jiang Y, Hua X, et al. The role of the type VI secretion system *vgrG* gene in the virulence and antimicrobial resistance of *Acinetobacter baumannii* ATCC 19606. *PLoS One*. 2018; 13(2):e0192288. <https://doi.org/10.1371/journal.pone.0192288> PMID: 29394284
49. Tomaras AP, Dorsey CW, Edelmann RE, Actis LA. Attachment to and biofilm formation on abiotic surfaces by *Acinetobacter baumannii*: involvement of a novel chaperone-usher pil assembly system. *Microbiology*. 2003; 149(Pt 12):3473–84. <https://doi.org/10.1099/mic-0-26541-0> PMID: 14953080
50. Gaddy JA, Arivett BA, McConnell MJ, Lopez-Rojas R, Pachon J, Actis LA. Role of acinetobactin-mediated iron acquisition functions in the interaction of *Acinetobacter baumannii* strain ATCC 19606T with human lung epithelial cells, *Galleria mellonella* caterpillars, and mice. *Infect Immun*. 2012; 80(3):1015–24. <https://doi.org/10.1128/IAI.06279-11> PMID: 22232180
51. Murray GL, Tsyanov K, Kostoulas XP, Bulach DM, Powell D, Creek DJ, et al. Global gene expression profile of *Acinetobacter baumannii* during bacteremia. *J Infect Dis*. 2017; 215(suppl_1):S52–7. <https://doi.org/10.1093/infdis/jw529> PMID: 28372520
52. Koteva K, Hong HJ, Wang XD, Nazzari, Hughes D, Naldrett MJ, et al. A vancomycin photoprobe identifies the histidine kinase VanS_{ac} as a vancomycin receptor. *Nat Chem Biol*. 2010; 6(5):327–9. <https://doi.org/10.1038/nchembio.350> PMID: 20383152
53. Li L, Wang Q, Zhang H, Yang M, Khan MI, Zhou X. Sensor histidine kinase is a β -lactam receptor and induces resistance to β -lactam antibiotics. *Proc Natl Acad Sci USA*. 2016; 113(6):1648–53. <https://doi.org/10.1073/pnas.1520000113> PMID: 26851117
54. Hassan KA, Jackson SM, Penevian A, Patching SG, Teto SG, Eijkelkamp BA, et al. Transcriptomic and biochemical analyses identify a family of chlorhexidine efflux proteins. *Proc Natl Acad Sci USA*. 2013; 110(50):20254–9. <https://doi.org/10.1073/pnas.1317052110> PMID: 24277845
55. Eijkelkamp BA, Hassan KA, Paulsen IT, Brown MH. Investigation of the human pathogen *Acinetobacter baumannii* under iron limiting conditions. *BMC Genomics*. 2011; 12:126. <https://doi.org/10.1186/1471-2164-12-126> PMID: 21342532
56. Lin MF, Lin YY, Lan CY. The role of the two-component system BaeSR in disposing chemicals through regulating transporter systems in *Acinetobacter baumannii*. *PLoS One*. 2015; 10(7):e0132843. <https://doi.org/10.1371/journal.pone.0132843> PMID: 26161744
57. Camarena L, Bruno V, Euskirchen G, Poggio S, Snyder M. Molecular mechanisms of ethanol-induced pathogenesis revealed by RNA-sequencing. *PLoS Pathog*. 2010; 6(4):e1000834. <https://doi.org/10.1371/journal.ppat.1000834> PMID: 20298292
58. David SA, Bechtel B, Annaiah C, Mathan VI, Balarim P. Interaction of cationic amphiphilic drugs with lipid A: implications for development of endotoxin antagonists. *Biochim Biophys Acta*. 1994; 1212(2):167–75. PMID: 8180242
59. Amos H, Vollmayer E. Effect of pentamidine on the growth of *Escherichia coli*. *J Bacteriol*. 1957; 73(2):172–7. PMID: 13416166
60. Hamm RE, Shull CM Jr., Grant DM. Citrate complexes with iron(II) and iron(III). *J Am Chem Soc* 1953; 75:2111–4.
61. Pacock RL, Sanders J. The gluconate complexes. II. The ferric-gluconate system. *J Am Chem Soc*. 1955; 77(6):1489–94.

Appendix E - Adams and Brown, 2019; *mSphere*RESEARCH ARTICLE
Molecular Biology and Physiology

MITE_{Aba12r}, a Novel Mobile Miniature Inverted-Repeat Transposable Element Identified in *Acinetobacter baumannii* ATCC 17978 and Its Prevalence across the *Moraxellaceae* Family

Felise G. Adams,* Melissa H. Brown*

*College of Science and Engineering, Flinders University, Bedford Park, South Australia, Australia

ABSTRACT Insertion sequences (IS) are fundamental mediators of genome plasticity with the potential to generate phenotypic variation with significant evolutionary outcomes. Here, a recently active miniature inverted-repeat transposon element (MITE) was identified in a derivative of *Acinetobacter baumannii* ATCC 17978 after being subjected to stress conditions. Transposition of the novel element led to the disruption of the *hns* gene, resulting in a characteristic hypermotile phenotype. DNA identity shared between the terminal inverted repeats of this MITE and coresident IS_{Aba12} elements, together with the generation of 9-bp target site duplications, provides strong evidence that IS_{Aba12} elements were responsible for mobilization of the MITE (designated MITE_{Aba12r}) within this strain. A wider genome-level survey identified MITE_{Aba12r} in 30 additional *Acinetobacter* genomes at various frequencies and one *Moraxella osloensis* genome. Ninety MITE_{Aba12r} copies could be identified, of which 40% had target site duplications, indicating recent transposition events. Elements ranged between 111 and 114 bp; 90% were 113 bp in length. Using the MITE_{Aba12r} consensus sequence, putative outward-facing *Escherichia coli* σ 70 promoter sequences in both orientations were identified. The identification of transcripts originating from the promoter in one direction supports the proposal that the element can influence neighboring host gene transcription. The location of MITE_{Aba12r} varied significantly between and within genomes, preferentially integrating into AT-rich regions. Additionally, a copy of MITE_{Aba12r} was identified in a novel 8.5-kb composite transposon, Tn6645, in the *M. osloensis* CCUG 350 chromosome. Overall, this study shows that MITE_{Aba12r} is the most abundant nonautonomous element currently found in *Acinetobacter*.

IMPORTANCE One of the most important weapons in the armory of *Acinetobacter* is its impressive genetic plasticity, facilitating rapid genetic mutations and rearrangements as well as integration of foreign determinants carried by mobile genetic elements. Of these, IS are considered one of the key forces shaping bacterial genomes and ultimately evolution. We report the identification of a novel nonautonomous IS-derived element present in multiple bacterial species from the *Moraxellaceae* family and its recent translocation into the *hns* locus in the *A. baumannii* ATCC 17978 genome. The latter finding adds new knowledge to only a limited number of documented examples of MITEs in the literature and underscores the plastic nature of the *hns* locus in *A. baumannii*. MITE_{Aba12r} and its predicted parent(s), may be a source of substantial adaptive evolution within environmental and clinically relevant bacterial pathogens and, thus, have broad implications for niche-specific adaptation.

KEYWORDS *Acinetobacter*, genetic evolution, insertion sequences, nonautonomous elements, transposons

January/February 2019 Volume 4 Issue 1 e00028-19

Citation Adams FG, Brown MH. 2019. MITE_{Aba12r}, a novel mobile miniature inverted-repeat transposable element identified in *Acinetobacter baumannii* ATCC 17978 and its prevalence across the *Moraxellaceae* family. *mSphere* 4:e00028-19. <https://doi.org/10.1128/mSphereDirect.00028-19>.

Editor Craig D. Ellensiek, University of Iowa
Copyright © 2019 Adams and Brown. This is an open-access article distributed under the terms of the [Creative Commons Attribution 4.0 International license](https://creativecommons.org/licenses/by/4.0/).

Address correspondence to Melissa H. Brown, melissa.brown@flinders.edu.au.

Solicited external reviewers: Sally Partridge, University of Sydney; John Boyce, Monash University.

This paper was submitted via the [mSphereDirect™](https://mSphereDirect.com) pathway.

Received 31 January 2019

Accepted 4 February 2019

Published 20 February 2019

[mSphere™](https://mSphereDirect.com) mSphereDirect.com 1

Acinetobacter baumannii has been classed as one of the most predominant pathogens responsible for multidrug-resistant (MDR) nosocomial infections worldwide (1). Aside from its notorious MDR phenotype, *A. baumannii* also displays a remarkable capacity to persist on a variety of inanimate surfaces for extended periods, providing a reservoir for infection and facilitating transmission throughout clinical settings (2, 3). Significant work has been undertaken to identify and track the arsenal of genes that contribute to the impressive persistence and resistance strategies available to *A. baumannii* (4–8). This has identified a highly dynamic and plastic genome, dominated by numerous integration events as well as alterations in expression of intrinsic genes modulated through mutations and deletion and/or insertion of mobile genetic elements (MGEs) (9–11). MGEs are present in nearly all prokaryote genomes and constitute the “mobilome,” a term which has gained significant traction in recent years, driven by the increase in infections caused by MDR isolates. The mobilome itself is comprised of a number of genetic entities, including plasmids, bacteriophages, gene cassettes in integrons, and transposable elements, all capable of capturing and disseminating genetic material across bacterial genomes via horizontal gene transfer (HGT) (12).

Of the above-mentioned entities, transposable elements are seen as a major contributor to niche-specific adaptive evolution. They are capable of moving from one position to another within a given genome and are often associated with the dissemination of antimicrobial resistance determinants (13–15). One of the simplest autonomous types of mobile elements is the insertion sequence (IS), consisting of a transposase gene(s) that is typically bordered by terminal inverted repeats (TIRs), designated left (IRL) and right (IRR) relative to the direction of the transposase gene. The TIRs contain multiple domains required for transposase binding, donor DNA cleavage, and strand transfer, supporting the integration of the elements into host DNA via replicative or nonreplicative mechanisms (16). As a consequence of insertion, short direct repeat sequences of the target DNA are often generated (target site duplications, or TSDs), which differ in length and degree of sequence specificity depending on the IS element being translocated (17). Movement of an IS to a new location within a genome offers a variety of possible integration sites. Although some IS display clear trends/preferences in target sites, the large majority of IS demonstrate low target specificity (18).

Small mobile elements can be further delineated based on their movement autonomy. A limited range of nonautonomous elements exist in bacteria, such as repetitive extragenic palindromic sequences, Tn3-derived inverted-repeat miniature elements (TIMEs), and miniature inverted-repeat transposable elements (MITEs) (19–21). Like eukaryotic MITEs (22), bacterial MITEs are small (–50 to 600 bp) AT-rich sequences that have lost their cognate transposase gene and, thus, contain noncoding DNA that in most, but not all, cases are flanked by TIRs (23). Based on their origins, MITEs can be categorized as type I or type II and are generated by internal deletion of parent transposable elements or by random convergence of TIR sequences, respectively (24). Movement of these elements is thought to be mediated by transposases of a coresident parental element acting in trans. The site of integration and length of the TSDs of MITEs are generally identical or highly similar to that of the coresident IS parent (23). Since their identification in bacteria (25), a number of these elements have been documented from a diverse range of species, where many have significantly influenced the evolutionary tempo of their host genomes (20). These elements are often overlooked due to the absence of a recognizable coding sequence (CDS) and their tendency to reside in intergenic regions. Thus, they represent a largely unexplored field in microbial genomics.

Through characterization of a subset of morphologically distinct colonies isolated during desiccation stress analyses, we identified a novel MITE that transposed to a new location within the *A. baumannii* ATCC 17978 genome. Due to shared similarities in TIRs and TSD sequence length, the 113-bp sequence is predicted to have proliferated through the activity of the transposase encoded by resident ISAbal2 elements present in ATCC 17978 and, thus, was named MITE_{Abal2}. The prevalence of this novel, nonautonomous MGE across all publicly available sequenced bacterial genomes was exam-

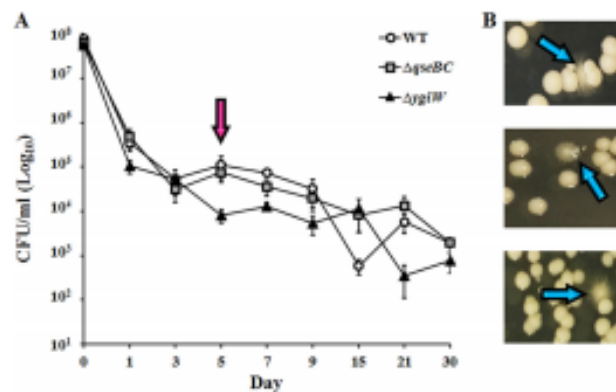


FIG 1 Identification of hypermotile variants from *A. baumannii* ATCC 17978 WT, Δ qseBC, and Δ ygiW strains after desiccation stress. (A) Desiccation survival was determined by enumeration of viable cells (CFU/ml) over a 30-day period. Markers represent mean values of viable cells and error bars the standard errors of the means calculated on days 0, 1, 3, 5, 7, 9, 15, 21, and 30. Four biological replicates were undertaken over two independent experiments. The pink arrow indicates the day that hypermotile variants were identified. (B) Images of hypermotile variants (blue arrows) obtained from rehydrated desiccated cells after 30-day incubation at 37°C on 1% LB agar.

ined and insights gained with respect to its transposition activity as well as its overall function and evolution.

RESULTS

Construction of qseBC and ygiW deletion derivatives in *A. baumannii* ATCC 17978. The regulatory mechanisms that coordinate the expression of many *A. baumannii* virulence factors remain largely unknown. One regulatory mechanism employed by bacteria, including *A. baumannii*, is two-component signal transduction systems (TCS) (26). The TCS qseBC (ACX60_06100/05) and its upstream hypothesized target gene, which encodes the putative signal peptide ygiW (ACX60_06095), were deleted by allelic replacement in *A. baumannii* ATCC 17978 (GenBank accession no. CP012004.1), generating the Δ qseBC and Δ ygiW derivatives, respectively. To ensure the introduced mutations did not affect cell viability, growth curves assessing optical density at 600 nm (OD₆₀₀) were undertaken in lysogeny broth (LB) medium and measured hourly over an 8-h period. No significant growth perturbations were identified for the Δ qseBC or Δ ygiW strain compared to growth of wild-type (WT) ATCC 17978 parent cells under the tested conditions (data not shown).

Disruption of the hns gene after desiccation stress. To analyze the impact of deletion of the target genes in *A. baumannii* ATCC 17978, the constructed mutant strains were subjected to a number of *in vitro* assays, one of which was survival under desiccating conditions. No significant differences in survival compared to that of the WT were seen over the 30-day test period (Fig. 1A). However, on day 5 a subset of morphologically distinct colonies was identified during quantification of viable cells. These colonies displayed irregular edging reminiscent of a previously seen hypermotile phenotype (27) (Fig. 1B). In total, seven hypermotile isolates were identified, five from the Δ ygiW strain and one each from the Δ qseBC and WT backgrounds.

A previous study undertaken in *A. baumannii* ATCC 17978 showed that disruption of the histone-like nucleoid structuring (hns) gene by an IS (subsequently designated ISAbn72 by ISfinder) (28) led to a number of phenotypic alterations, including hypermotility (27). Given the similarity in colony morphology between the set of hypermotile isolates identified after desiccation stress in this study and that previously seen for the Δ hns strain (29), our investigations initially focused on this global regulator. PCR

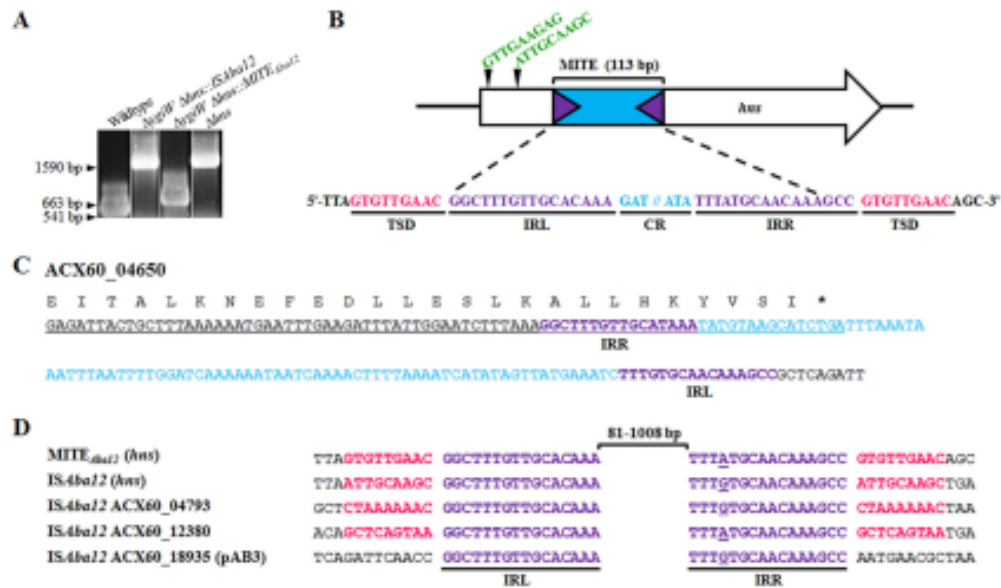


FIG 2 Insertions in the *hns* locus from hypermotile variants and relationship between ISAbal2 and MITE_{Δba12}. (A) Examples of amplicons generated from PCR across the *hns* locus from hypermotile isolates compared to the wild type and the previously identified *Δhns* mutant (27). The amplicon from the *ΔygiW Δhns:MITE_{Δba12}* strain (663 bp) was 122 bp larger than that from the wild-type control (541 bp), while the *ΔygiW Δhns:ISAbal2* strain yielded the same size product as the *Δhns* control (1,590 bp). (B) The open white arrow depicts the *hns* gene (ACX60_16755) and direction of transcription, and black triangles with green nucleotide sequences represent the TSD for the two integration sites identified previously (29) as well as in this study. The 113-bp MITE is comprised of an 81-bp central region (CR; blue) flanked by 16-bp imperfect inverted repeat sequences (IRL and IRR; purple). //, break in DNA sequence. The novel insertion site/TSD sequences are in pink. The figure is not drawn to scale. (C) Location of MITE_{Δba12} in the *A. baumannii* ATCC 17978 genome. The 3' end of ACX60_04650 is fused to MITE_{Δba12}, leading to a truncation and the formation of a pseudogene. The deduced amino acid sequence for the modified ACX60_04650 is designated by a single letter code above the underlined nucleotide sequence, and the asterisk indicates the proposed stop codon. Purple and blue nucleotides represent TIR and CR, respectively, of MITE_{Δba12}. (D) Nucleotide alignment of 12 bp up- and downstream of the MITE_{Δba12} element in *hns* of the *A. baumannii* ATCC 17978 *ΔygiW* strain, ISAbal2 elements present in ATCC 17978, and ISAbal2 in *hns* [ISAbal2 (*hns*)] (27). TIR and TSD are in purple and pink, respectively. Purple underlined nucleotides represent the mismatching base in IRR. The black bracket indicates the size of the region between IRL and IRR, either 81 bp for MITE_{Δba12} or up to 1,008 bp for ISAbal2.

amplifications across the *hns* loci of the hypermotile strains identified that all amplicons were larger than the WT control (Fig. 2A). DNA sequencing of these products revealed insertion of ISAbal2 in three cases, originating from each of the three different background strains, which were located in two previously identified integration sites (29) (Fig. 2B). In the remaining four strains, all based on the *ΔygiW* background, a shorter insertion in *hns* was detected, and sequencing of one example revealed a 113-bp element integrated into a novel site (Fig. 2B). To determine if the integrated element was stably inserted in *hns* of the *ΔygiW* strain, PCR screening after five consecutive passages in liquid culture from five biological replicates was undertaken. All samples maintained the element within *hns* (data not shown). To examine whether isolates with a disrupted *hns*, irrespective of the site/type of integration, still produced the distinctive hypermotile phenotype, their motility phenotypes were assessed and found to be comparable to that seen for the previously identified *hns* mutant derivative (27, 30) (see Fig. S1 in the supplemental material). Complementation with a WT copy of *hns* (ACX60_16755) carried on the pWH1266 shuttle vector (27) restored all isolates to their parental nonmotile phenotype (Fig. S1).

Identification and characterization of a novel active MITE in *A. baumannii* ATCC 17978. To characterize this novel 113-bp element found in the *A. baumannii* *ΔygiW* strain, its DNA sequence and that of its insertion site in *hns* were analyzed. This revealed that the 113-bp element carried 16-bp imperfect TIR sequences (different in 1 nucle-

otide) and an 81-bp core region and generated 9-bp TSDs on insertion into *hns* (Fig. 2). The element is AT rich (78%) and does not contain any known CDS (31). Taken together, these traits strongly suggested that this element is a MITE (23).

To identify the abundance of the MITE within the *A. baumannii* ATCC 17978 genome, the 113-bp MITE sequence in *hns* from the $\Delta ygiW$ background was used as a query for BLASTN searches. Only one copy at the 3' end of the ACX60_04650 locus, encoding a hypothetical protein harboring a partial KAP-family NTPase motif (32), was identified, fusing this gene with 31 bases from the MITE (Fig. 2C) and generating a premature stop codon. Comparative analyses with *A. baumannii* D36 revealed that the protein was 398 amino acids shorter and is therefore likely to be nonfunctional (data not shown). Genes coding for KAP NTPases are known to be frequently disrupted, leading to pseudogene formation (33). PCR with primers specific for the ACX60_04650 location (see Table 4) identified that the MITE was maintained in this position in the $\Delta ygiW \Delta hns$:MITE strain. Consequently, there are two MITE copies in the $\Delta ygiW$ background, one at the ACX60_04650 locus and an additional copy located in the *hns* gene, inferring duplication of the novel element (data not shown).

ISAb₁₂ is the proposed autonomous parent of the novel MITE in *A. baumannii* ATCC 17978. To identify the potential parent element that may have aided in translocation of the MITE, IS present in the ATCC 17978 chromosome and pAB3 plasmid (GenBank accession numbers CP012004.1 and CP012005.1, respectively) were first identified from results generated by ISseeker (11). Subsequent manual examination of the length and sequence of their TIRs and TSDs revealed that ISAb₁₂ provided the best match to those of the MITE. ISAb₁₂ harbors a single open reading frame coding for a transposase, with a characteristic DDE catalytic motif, between its 16-bp TIRs and generates 9-bp TSDs upon insertion (28). Thus, the novel MITE was most likely translocated into *hns* by a co-resident ISAb₁₂ transposase present in ATCC 17978 and will be referred to as MITE_{Ab₁₂}.

As MITE_{Ab₁₂} does not contain a transposase gene, it is not possible to define IRL and IRR sequences relative to this gene. Two of the three copies of ISAb₁₂ in ATCC 17978 (at loci ACX60_04795 and ACX60_18935) have identical TIRs that perfectly match one TIR of MITE_{Ab₁₂}. However, the nonidentical TIRs of the third copy of ISAb₁₂ (ACX60_12380) each perfectly match one TIR of MITE_{Ab₁₂}, allowing IRL and IRR of MITE_{Ab₁₂} to be designated relative to this IS.

MITE_{Ab₁₂} is present in a diverse range of species from the Moraxellaceae family. To identify whether MITE_{Ab₁₂} is widespread or restricted to *A. baumannii* ATCC 17978, the sequence found within *hns* from the $\Delta ygiW \Delta hns$:MITE_{Ab₁₂} strain was used as a query to search bacterial genomes present in publicly available databases (10 July 2018). Orthologs of MITE_{Ab₁₂} were identified in both chromosomes and plasmids, with an additional 30 strains from the *Acinetobacter* genus and one from *Moraxella osloensis* harboring the element at various frequencies (Table 1). MITE_{Ab₁₂} was found within a range of environmental *Acinetobacter* species, with the greatest number of copies identified ($n = 22$) in *A. baumannii* D5002, isolated from soil in Anantapur, India, in 2005. A number of *Acinetobacter* strains isolated from patients and hospital sewage in multiple countries also carried copies of MITE_{Ab₁₂}, inferring its presence and dissemination into clinically relevant isolates worldwide. *Acinetobacter* sp. strains ACNH2, SWBY1, and WCHA45 and *A. johnsonii* XBB1 possessed MITE_{Ab₁₂} on the chromosome as well as in plasmids (Table 1). An additional number of plasmid sequences carrying MITE_{Ab₁₂} were also identified (Table 1), but their corresponding chromosome sequences are not available. Copies of MITE_{Ab₁₂} identified in the *A. baumannii* PR07 genome (GenBank accession number CP012035.1) were not included in further analyses as the genome contained strings of undetermined bases and was not of a high enough quality.

Using ISseeker (11), it was found that approximately 18.5% of the 1,035 *A. baumannii* genomes examined harbored at least one copy of ISAb₁₂, with an average of 5.6 copies per genome (data not shown). Using the ISfinder tool (28), four relatives of ISAb₁₂ were identified: ISAb₁₃, ISAlw1, ISAha1, and ISAha2 (Table 2). These elements

TABLE 1 Bacterial strains that harbor full-length MITE_{ISAb012} elements

Strain or plasmid	No. of MITE _{ISAb012} elements per strain	Isolation source/origin	Accession no. and reference or source
Strain			
<i>A. baumannii</i> DS002	22	Soil, India	CP027704.1, unpublished
<i>A. indicus</i> SGAir0564	10	Air, Singapore	CP024620.1 (75)
<i>A. johnsonii</i> XBB1*	7	Hospital sewage, USA	CP010350.1 (76)
<i>A. junii</i> 65	5	Limnetic water, Russia	CP019041 (77)
<i>Acinetobacter</i> sp. strain SWBY1*	5	Hospital sewage, China	CP026616.1, unpublished
<i>A. baumannii</i> B8300	4	Human bloodstream, southern India	LFY0000000.1 (78)
<i>Acinetobacter</i> sp. strain ACNH1	3	Hospital plumbing, USA	CP026420.1 (79)
<i>A. baumannii</i> ABNH28	3	Hospital plumbing, USA	CP026125 (79)
<i>Acinetobacter</i> sp. strain TGL-Y2	2	Frozen soil, China	CP015110.1, unpublished
<i>A. baumannii</i> B8342	2	Human bloodstream, southern India	LFY20000000.1 (80)
<i>M. osloensis</i> CCLG 350	1	Human cerebrospinal fluid, USA	CP014234.1, unpublished
<i>A. haemolyticus</i> TJS01	1	Human respiratory tract, China	CP018871.1, unpublished
<i>Acinetobacter</i> sp. strain NCu2D-2	1	Murine trachea, Germany	CP015594 (81)
<i>Acinetobacter</i> sp. strain ACNH2*	1	Hospital plumbing, USA	CP026412.1 (79)
<i>A. baumannii</i> ATCC 17978	1	Human meningitis, France	CP012004.1 (5)
<i>A. junii</i> WCHAJ59	1	Hospital sewage, China	CP028800.1, unpublished
<i>A. baumannii</i> AR_0083	1	Unknown	CP027528.1, unpublished
<i>Acinetobacter</i> sp. strain WCHA45*	1	Sewage, China	CP028561.1, unpublished
<i>A. baumannii</i> MAD*	1	Human skin, France	AY665723.1 (82)
Plasmids			
<i>A. schindleri</i> SGAir0122, pSGAir0122	2	Air, Singapore	CP025619.1 (83)
<i>A. baumannii</i> A297 (RLH875), pA297-3	1	Human urinary tract, Netherlands	KU744946 (46)
<i>A. johnsonii</i> XBB1, pXBB1-9	1	Hospital sewage, USA	CP010351.1 (76)
<i>A. Iwoffii</i> ED45-23, pALWED2.1	1	Permafrost, Russia	KX426329 (53)
<i>A. baumannii</i> AbPK1, pAbPK1a	1	Ovine respiratory tract, Pakistan	CP024577 (84)
<i>Acinetobacter</i> sp. strain DUT-2, unnamed 1	1	Marine sediment, China	CP014652, unpublished
<i>Acinetobacter</i> sp. strain BW3, pKLH207	1	Stream water, USA	AJ486856 (85)
<i>A. towneri</i> strain G165, pNDM-GJ01	1	Human stool, China	KT965092 (86)
<i>A. baumannii</i> D46, pD46-4	1	Human urine, Australia	MF399199 (52)
<i>Acinetobacter</i> sp. strain ACNH2, pACI-3569	1	Hospital plumbing, USA	CP026416.1 (79)
<i>Acinetobacter</i> sp. strain WCHA45, pNDM1_100045	1	Hospital sewage, China	CP028560.1, unpublished
<i>A. baumannii</i> CHI-32, pNDM-32	1	Human bloodstream, India	LN833432.1, unpublished
<i>A. defluxii</i> WCHA30, pOXA58_010030	1	Hospital sewage, China	CP029396.1, unpublished
<i>A. pittii</i> WCHAP005069, pOXA58_005069	1	Clinical isolate, China	CP026086.1, unpublished
<i>A. pittii</i> WCHAP100004, pOXA58_100004	1	Clinical isolate, China	CP027249.1, unpublished
<i>A. pittii</i> WCHAP005046, pOXA58_005046	1	Clinical isolate, China	CP028573.1, unpublished
<i>Acinetobacter</i> sp. strain SWBY1, pSWBY1	1	Hospital sewage, China	CP026617.1, unpublished

*Strains where MITE_{ISAb012} is present on both chromosomal and plasmid DNA.

*In *A. baumannii* MAD, MITE_{ISAb012} was found on a 7.8-kb stretch of sequenced DNA rather than a full-length chromosome (82).

are present at various frequencies in *Acinetobacter* genomes, and the transposases encoded within the elements share between 92 and 94% amino acid identity with the transposase in ISAb012. Importantly, they have the same perfect 16-bp TIR sequence as the majority of ISAb012 elements (Table 2). This led us to investigate whether other characterized IS contain TIR sequences similar to those in MITE_{ISAb012} and thereby could translocate the nonautonomous element. An additional nine IS elements were found to have TIR sequences similar or identical to those of MITE_{ISAb012} (Table 2). These IS elements are of a length similar to that of ISAb012, ranging from 1,023 to 1,052 bp, with the majority also generating 9-bp TSDs (Table 2). Comparisons of MITE_{ISAb012} against the sequences of each IS listed in Table 2 revealed nucleotide identity was confined to only the TIR sequences; thus, the origins of MITE_{ISAb012} from an IS could not be readily deduced (data not shown).

MITE_{ISAb012} is a highly conserved mobile element with potential to affect expression of neighboring host genes. To examine sequence identity across all the identified MITE_{ISAb012} copies, a multiple-sequence alignment using Clustal Omega (34) was performed. From the analysis of 90 MITE_{ISAb012} copies it was found that 10% of

TABLE 2 IS with TIR closely related to those of ISAbol2 and MITE_{Abol2}

IS name*	IRL sequence	IRR sequence	Length (bp)	TSD (bp)
MITE _{Abol2}	GGCTTTGTTGCACAAA	GGCTTTGTTGCATAAA	113	9
ISAbol2	GGCTTTGTTGCACAAA	GGCTTTGTTGCACAAA	1,039	9
IS17	GGCTTTGTTGCACAAA	GGCTTTGTTGCACAAA	1,040	9
ISAbol5 ^b	GGCTTTGTTGCACAAA	GGCTTTGTTGCATAAA	1,044	ND
ISAbol7	GGCTTTGTTGCATAAA	GGCTTTGTTGCACAAA	1,039	9
ISAbol10	GGCTTTGTTGCATAAATA	GGCTTTGTTGCACAAATA	1,023	9
ISAbol13	GGCTTTGTTGCACAAA	GGCTTTGTTGCACAAA	1,039	9
ISAbol40	GGCTTTGTTGCACAAA	GGCTTTGTTGCACAAA	1,039	9
ISAbol1	GGCTTTGTTGCACAAAC	GGCTTTGTTGCACAAAC	1,039	4
ISAbol2	GGCTTTGTTGCACAAA	GGCTTTGTTGCACAAA	1,040	ND
ISAbol3	GGCTTTGTTGCACAAA	GGCTTTGTTGCATAAA	1,039	ND
ISAbol1	GGCTTTGTTGCACAAA	GGCTTTGTTGCATAAA	1,039	3
ISAbol1	GGCTTTGTTGCACAAAG	GGCTTTGTTGCACAAAG	1,038	ND
ISEcl7	GGCTTTGTTGCACAAA	GGCTTTGTTGCATAAA	1,052	9
ISNov2	GGCTTTGTTGCACAAAT	GGCTTTGTTGCATAAAT	1,048	9

*Abbreviations: IS, insertion sequence; IRL, inverted repeat left; IRR, inverted repeat right; TSD, target site duplication; ND, not determined.

^bThe transpose of ISAbol5 is thought to be inactive (28).

MITE_{Abol2} copies diverged from the 113-bp consensus (Fig. 3). Three of the 10 MITE_{Abol2} copies present in *Acinetobacter indicus* SGAir0564 are atypical; two were 112 bp, sharing 100% identity with each other, while the other is 114 bp. Similarly, in *Acinetobacter* sp. strain SWBY1, three of the five MITE_{Abol2} copies differed from the consensus length, which included the smallest identified element at 111 bp and two at 114 bp. A further three atypical 112-bp MITE_{Abol2} sequences were identified in the genomes of *A. baumannii* D5002 and *Acinetobacter* sp. strains TGL-Y2 and ACNIH1 (Fig. 3). Thus, a total of 34 different MITE_{Abol2} sequences were identified, leading to the assignment of 10 subgroups. MITE_{Abol2} sequence arrangements that harbored two copies or more were

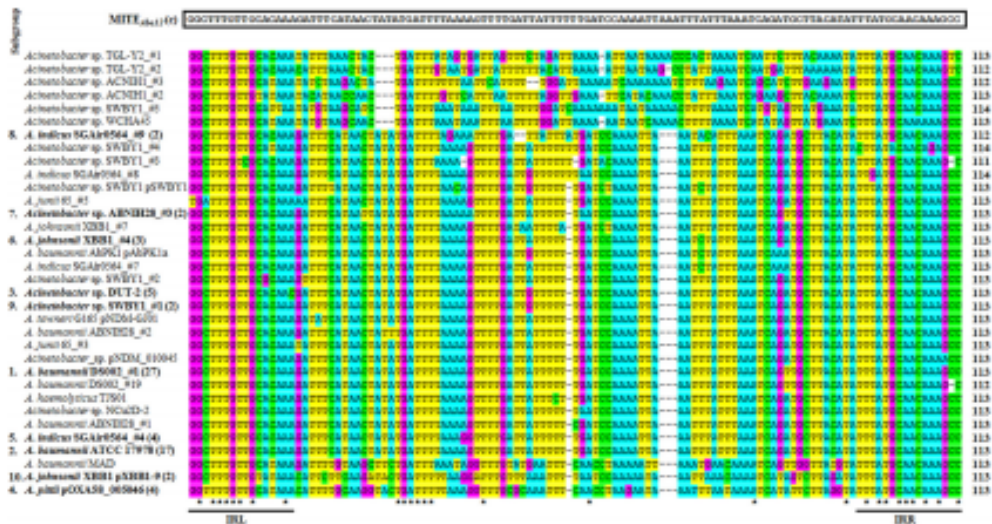


FIG 3 Nucleotide alignment of all MITE_{Abol2} elements identified in this study. The nucleotide sequence above the alignment (black box) denotes the consensus sequence, MITE_{Abol2}(C), derived using WebLogo software (35). MITE_{Abol2} sequences with nucleotide variations are displayed. Subgroup representatives are numbered and in boldface type with numbers in parentheses indicating the total number of MITE_{Abol2} copies with that sequence. A, T, G, and C nucleotides are denoted in blue, yellow, purple, and green boxes, respectively. Black lines and asterisks represent the terminal inverted repeats (IRL and IRR) and conserved bases, respectively. See Table S1 for a full list of MITE_{Abol2} elements included in each subgroup and Table 1 for strain accession numbers.

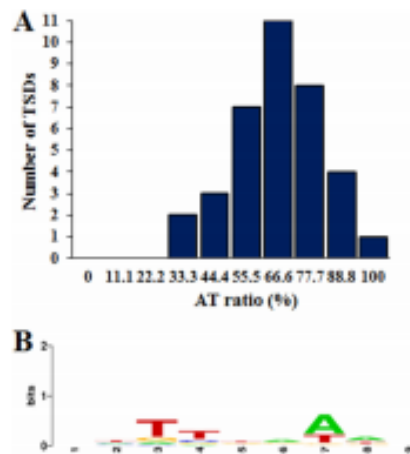


FIG 4 Characterization of target site duplications flanking MITE_{Aba12}. (A) Graphical representation of AT richness (%) identified from all target site duplications flanking MITE_{Aba12} elements. (B) Nucleotide logo generated from all target site duplication events using WebLogo software (35).

segregated into subgroups that were ordered from 1 to 10 based on the most to least abundant (Fig. 3 and Table S1). Significant variation existed across the central region of the element, as only 10 bases were conserved across all 90 identified copies (Fig. 3) (it is possible that some nucleotide differences identified across MITE_{Aba12} copies can be attributed to sequencing errors). The MITE_{Aba12} TIR sequences were the most conserved, as eight and nine of the 16-bp IRL and IRR sequences, respectively, were identical across all MITE_{Aba12} copies analyzed (Fig. 3). Overall, no preference in the orientation of MITE_{Aba12} in the genomes could be identified (data not shown).

MITEs generally insert into AT-rich regions (23). Of the 90 identified MITE_{Aba12} copies, 36 from 13 different genomes had 9-bp TSDs. From the 22 MITE_{Aba12} copies in *A. baumannii* D5002, TSDs could be identified for 17, which could infer a burst of recent activity. Interestingly, all MITE_{Aba12} elements from subgroup 4 were found in the same site and flanked by identical TSDs of 8 rather than 9 bp (TTTTGTGTT). These elements were on large plasmids (−62 to 112.5 kb), and BLASTN analyses using the MITE_{Aba12} element together with −700 bp left and right of the sequence from pNDM-32 of *A. baumannii* CHI-32 identified they were all located in an identical position, sharing 100% identity across this −1.5-kb region (data not shown). Overall, MITE_{Aba12} appeared to favor insertion into sequences with an AT ratio of $\geq 55.5\%$, as demonstrated by the skewed distribution of the columns to the right (Fig. 4A), although no identifiable trends in nucleotide sequence arrangements could be identified (Fig. 4B).

To assess how MITE_{Aba12} could influence host gene expression, a consensus sequence, MITE_{Aba12}(c), was generated using WebLogo (35) from all 113-bp MITE_{Aba12} elements ($n = 81$) (Fig. 3). At least two stop codons in all six reading frames can be identified after translation of the MITE_{Aba12}(c) DNA sequence. Start codons followed by three, seven, or eight amino acids at the terminal ends of the element were identified in three of the reading frames (data not shown). Depending on the integration site in a given genome, these characteristics could allow for fusion with neighboring CDSs. Mfold (36) predicted weak secondary structures with ΔG of -23.99 or -26.94 kcal/mol in the two orientations of MITE_{Aba12}(c) (IRL to IRR or IRR to IRL, respectively) (data not shown). Using the ARNold tool (37), no predicted Rho-independent transcriptional terminators were identified. The Softberry program BPRCM predicted two outward-facing promoter sequences based on the -35 and -10 *Escherichia coli* $\sigma 70$ promoter

consensus sequences (Fig. 52). These sequences were also compared with the strong outward-facing promoter found in ISAb₇ coupled with flanking sequence associated with overexpression of the *bla*_{TEM-5C} gene in *A. baumannii* CLA-1 (38) (Fig. 52B). To verify whether the two putative outward-facing promoters identified within MITE_{Ab₁₂}(c) could drive the production of mRNA transcripts, three previously published *A. baumannii* ATCC 17978-derived RNA-sequencing transcriptomes (30, 39) were aligned to the reference ATCC 17978 genome (GenBank accession number CP012004.1) using the Integrative Genomics Viewer program (40). Transcripts originating within the MITE_{Ab₁₂} sequence that could be attributed to the P_{out} IRR putative promoter were identified across all three transcriptomes. However, transcripts reading out from P_{out} IRL were limited (data not shown). Thus, it appears in ATCC 17978 that the P_{out} IRR putative promoter within MITE_{Ab₁₂}(c) has the potential to influence host gene transcription.

The fusion of small mobile elements with neighboring genes can affect gene function and in some cases lead to improved host fitness or formation of new proteins (41, 42). The exhaustive analysis conducted on MITE_{Ab₁₂} in publicly available GenBank entries revealed that some insertions of MITE_{Ab₁₂} interrupted host genes, and in some cases the encoded protein could be fused with up to 19 amino acids encoded by MITE_{Ab₁₂} sequences (data not shown). MITE_{Ab₁₂} elements located in pAbPK1a from *A. baumannii* AbPK1 and in the chromosomes of *A. baumannii* B8300 and *Acinetobacter* sp. strain ACNH1_#2 could create fusions to the 5' end of adjacent genes. Each had incorporated nucleotides reading outwards from the TIR of MITE_{Ab₁₂} to generate the first four amino acids (MQQ5) of the neighboring CDS. These particular arrangements also placed the host gene in proximal distance to the P_{out} IRR promoter sequences, and given its activity in ATCC 17978, the element could also influence the expression of fused genes.

MITE_{Ab₁₂} in *M. osloensis* CCUG 350 is located within a novel composite transposon. As previously stated, *M. osloensis* CCUG 350 carries one copy of MITE_{Ab₁₂} (Table 1). It lies within an 8.5-kb region absent from five closely related *M. osloensis* genome sequences (Fig. 5A shows the sequence alignment). IS were found at the terminal ends of the novel insert and shared highest identity with the IS1 family member ISAb₃ (81% identity; E value, 5e-55) (28). Both terminal IS carried 24-bp TIR sequences (5'-GGTGGTGTTCAAAAAGTATGCTG-3'), and TSDs of 8 bp were identified at each end of the 8.5-kb insert (Fig. 5B). These features make this sequence synonymous with a composite transposon (17) now named Tn6645. In *M. osloensis* CCUG 350, the MITE_{Ab₁₂} element was located between the ISAb₃ element and a gene of unknown function containing a DUF 2789 motif (E value, 4.2e-27) (32). Additionally, an ISAb₁₇-like element, an alkylsulfatase gene, a TetR-family transcriptional regulator gene, and a partial gene encoding a major facilitator superfamily transporter were identified within the composite transposon (Fig. 5). The insertion of ISAb₃ truncated the 3' end of the transporter gene by 540 bp and therefore is likely nonfunctional (a pseudogene).

BLASTN searches were used to search for Tn6645 in other bacterial genomes, but no additional full-length copies were identified (data not shown). However, approximately 4.3 kb of the 8.5-kb sequence aligned (96% identity) to a region in the chromosome of *Acinetobacter guillouiae* NBRC 110550 (43) (Fig. 5B). This region harbored the alkylsulfatase, TetR-family regulator, and the truncated transporter genes and may represent a source for this portion of the Tn6645 cargo.

DISCUSSION

Since their identification in bacteria 30 years ago, MITEs have been reported in a multitude of species, displaying significant diversity in their nucleotide sequence and functional properties (44). In this study, a novel MITE was identified in environmental and clinical isolates of *Acinetobacter* species, including *A. baumannii*, one of the leading bacterial organisms threatening human health (2). This novel element lacked any CDS that could produce a functional transposase, inferring that like other MITEs, MITE_{Ab₁₂} is activated in trans. Given the high similarity between the TIR sequences of MITE_{Ab₁₂} and those of ISAb₁₂ (Fig. 2D), we propose the transposase from ISAb₁₂ elements

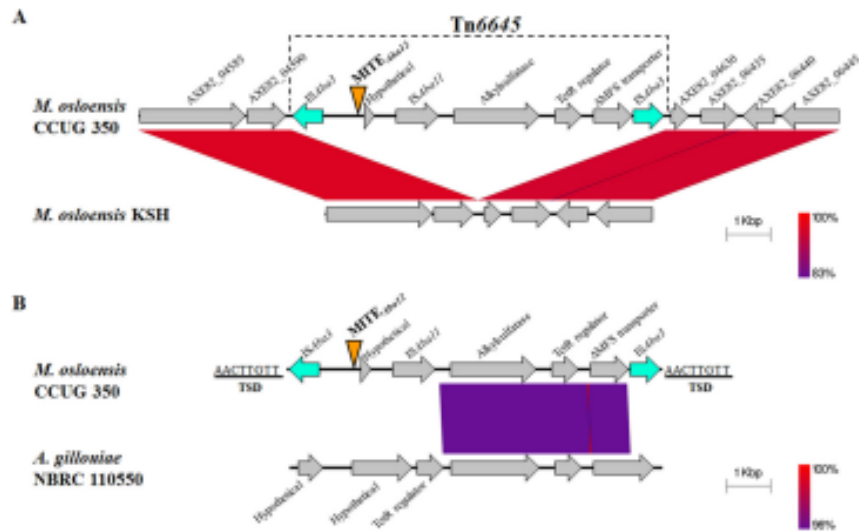


FIG 5 MITE_{Aba12} is located within Tn6645 in *Moraxella osloensis* CCUG 350. Gray arrows indicate the direction of transcription, and blue arrows represent ISAbal elements forming the boundaries of Tn6645. Identity between regions is indicated by the color gradient. (A) Alignment of nucleotide sequence from AXE82_04585 to AXE82_06445 in *M. osloensis* CCUG 350 and the corresponding region in strain KSH (73) (GenBank accession numbers CP014234.1 and CP024180.2, respectively). Gene names and locus tags are derived from *M. osloensis* CCUG 350 annotation. (B) Alignment of Tn6645 from *M. osloensis* CCUG 350 and part of the *A. gillouiae* NBRC 110550 chromosome (GenBank accession number AP014630.1 [43]). Identity between Tn6645 and *A. gillouiae* NBRC 110550 starts 80 bp downstream from the TIR of ISAbal11. The 8-bp TSDs flanking Tn6645 are shown. The location of MITE_{Aba12} is indicated by the orange triangle. Sequences were obtained from the NCBI database and aligned and visualized using the Easyfig 2.2.2 tool (74).

were responsible for MITE_{Aba12} mobilization in the *A. baumannii* DygiW strain. Whether ISAbal2, or another IS with a TIR similar to that of MITE_{Aba12} (Table 2), can mobilize MITE_{Aba12} will need to be experimentally examined.

With the addition of MITE_{Aba12}, the list of nonautonomous elements reported in *Acinetobacter* grows to three. Like most prokaryotic MITEs, the two previously characterized MITEs from *Acinetobacter* isolates are flanked by TIRs and generate TSDs upon insertion (45, 46). Compared to MITE_{Aba12}, both elements have been identified only on plasmid sequences and are approximately four times larger in size (439 and 502 bp, respectively) (45, 46). Identical copies of the MITE originally identified in *Acinetobacter* sp. strain NFM2 flank class 1 integrons carrying different resistance determinants in a number of *Acinetobacter* strains, forming a structure comparable to that of a composite transposon (45, 47–51). MITE-297 is found on the large conjugative plasmid pA297-3 present in the *A. baumannii* global clone 1 reference strain A297 (RUH875) (46). In pA297-3, two copies of MITE-297 flank a 76-kb region carrying numerous IS and a *mer* module which confers resistance to mercury (46). Interestingly, within pA297-3, MITE_{Aba12} is also present in the intergenic region between the *merD* and 5-hydroxysourate hydrolase precursor genes (data not shown). MITE_{Aba12} is also found in an identical position in the ~208-kb pD46-4 plasmid from *A. baumannii* D46 (52) and a 141-kb plasmid from *Acinetobacter* sp. strain DUT-2. Given the position of the element within these plasmids, we suggest that MITE_{Aba12} has travelled with this *mer* operon, which may partly explain its distribution throughout these bacterial genomes. Our analyses also identified a copy of MITE_{Aba12} flanked by two IS on the large nonconjugative plasmid pALWED2.1 from the *Acinetobacter* *lwoffi* strain ED45-23, isolated from uncontaminated Russian permafrost sediments dated to be 20,000 to 40,000 years old (53). To our knowledge, this is the most primitive strain that has been sequenced and

shown to carry a copy of MITE_{Aba12}. Interestingly, heavy-metal resistance operons identified on pALWED2.1 share identity with sequences from two additional *Acinetobacter* strains that also carry copies of MITE_{Aba12} (53). Our data, which provide another example of MITE_{Aba12} hitchhiking alongside resistance genes, supports the idea that HGT has played an important role in the evolution of heavy-metal resistance to confer a selective advantage to the organism (53).

Bacterial MITEs can possess various motifs that affect their own regulation and/or modulate expression of other genes within the residing genome (54–56). Using the MITE_{Aba12}(c) consensus sequence identified as part of this study, putative outward-facing *E. coli* σ 70 promoters could be identified in both orientations (see Fig. S2 in the supplemental material). ISAba1 is present in high copy numbers across a number of *A. baumannii* genomes and has been shown to have a significant impact on host gene expression and genome architecture (11). Additionally, ISAba1 is frequently implicated in increased antibiotic resistance, achieved by insertion upstream of resistance genes, namely, those encoding cephalosporinases or carbapenemases (38, 57, 58). Despite the putative promoter sequences not being maintained across all MITE_{Aba12} elements, the two subgroups which exhibited the greatest number of conserved arrangements (subgroups 1 and 2, with 27 and 17 elements, respectively) have promoter sequences that exactly match the MITE_{Aba12}(c) consensus (Fig. 3). Elements within these subgroups were derived from a variety of species from the *Moraxellaceae* family and isolated from geographically distinct locations (Table 1), suggesting that a selective pressure to maintain these nucleotides exists.

Analysis of the 90 MITE_{Aba12} copies revealed that sequence conservation was mainly confined to their TIRs, and they only deviated in length from the MITE_{Aba12}(c) consensus by a maximum of two nucleotides (Fig. 3). This is in contrast to significant size differences seen between variants of other types of bacterial MITEs (55, 59, 60). However, the lack of significant divergence seen within MITE_{Aba12} copies indicates that the element was generated from a single event and dispersed through bacterial genomes via HGT.

Shared identity of ISAba12 and the additional 13 IS harboring TIRs similar to those of MITE_{Aba12} was restricted to the TIR sequences (Table 2). Nevertheless, this finding significantly broadens the range of potential parental IS that could be capable of translocating MITE_{Aba12}. However, further experimental evidence is required to confirm whether these IS can translocate MITE_{Aba12}.

The observation of a MITE translocation within a prokaryote genome in real time is generally considered to be a rare event, as only a few examples have been documented in the literature (44). Remarkably, four separate instances where MITE_{Aba12} underwent translocation into *hns*, all of which were observed within the *A. baumannii* Δ YgiW ATCC 17978 background, were identified. YgiW is known as a stress-induced protein in many Gram-negative bacterial species (61–64). For instance, in *Salmonella enterica* serovar Typhimurium, YgiW (renamed VisP, for virulence-induced stress protein) was shown to be critical in stress resistance *in vitro* and in virulence (64). Similar to that of *S. enterica* and other bacteria, the ygiW homolog found in *A. baumannii* also contains the characteristic bacterial oligonucleotide/oligosaccharide-binding fold domain (DUF388) (65) and is located immediately upstream of the *qseBC* TCS genes (data not shown). As transposition of IS is strongly controlled, most likely to reduce potential deleterious effects within the cell, we question whether the deletion of a protein involved in the stress response influenced the transposition and/or properties that regulate expression and subsequent movement of ISAba12/MITE_{Aba12} elements within the ATCC 17978 genome. Furthermore, as isolates displaying hypermotility were only identified once during desiccation analyses, we speculate that these events represent a transposition burst (66). This new phenomenon offers a substitute for the selfish DNA hypothesis, where these intermittent bursts of IS transposition can increase copy numbers and therefore assist in their maintenance within bacterial genomes.

H-NS is defined as a DNA architectural protein known to play multiple fundamental roles across a number of Gram-negative pathogens, including regulation of AT-rich

horizontally acquired genes, many of which are involved in multiple stress responses (67, 68). Two distinct locations for ISAb₁₂ insertions in the *hns* locus were previously identified in *A. baumannii* (27, 29). These were also the target sites for the ISAb₁₂ insertions in this study, inferring these sequences are favored integration hotspots. MITE_{Ab₁₂} inserted into a novel location within *hns*, 151 bp from the start codon and upstream of the characterized DNA-binding domain (27). Two additional examples of IS-mediated disruption of *hns* in *A. baumannii* have been recently identified (9, 69). ISAb_{12S} was shown to be responsible in both studies, integrating into the intergenic region downstream of *hns* (ACXU_00289). In one case, the last two amino acids of H-NS are altered and the protein extended for an additional three amino acids by the integration of complete and partial copies of the ISAb_{12S} element (69). Collectively, these results infer that H-NS is a hot spot for disruption in *A. baumannii*, where a number of different integration sites have now been identified.

Transposable elements are a key driving force in the worrying increase in MDR isolates across many bacterial species, particularly within the *Acinetobacter* genus. Despite their small size, MITEs have been shown to be a significant contributor to genetic variation in a number of pathogens. In conclusion, this work has identified and characterized a new MGE, MITE_{Ab₁₂}, and determined its prevalence across the Moraxellaceae family. This also led to the identification of a novel composite transposon in *M. osloensis* CCUG 350, Tn6645. Due to the relatively small number of MITE_{Ab₁₂} copies identified in sequenced genomes, the element may be maintained neutrally or under tight regulatory control from a yet-to-be-identified host and/or environmental factor(s). The full effects of MITE_{Ab₁₂} on genetic variation and, thus, evolution of bacterial genomes, in addition to transcriptional and translational influences, have yet to be experimentally examined, opening a new and exciting avenue of research. The overall findings of this study not only illustrate the fluidity of the *Acinetobacter* pangenome but also highlight the importance of mobile sequences as vehicles for niche-specific adaptive evolution in a number of clinically and environmentally relevant bacterial pathogens.

MATERIALS AND METHODS

Bacterial strains, plasmids, media, and growth conditions. *A. baumannii* ATCC 17978 (70) was obtained from the American Type Culture Collection (ATCC) and is designated the WT strain in all analyses. Bacterial strains and plasmids are summarized in Table 3, and primers are listed in Table 4. All bacterial strains used in the study were grown in LB broth or on LB agar plates and incubated under aerobic conditions overnight (ON) (16 to 20 h) at 37°C unless otherwise stated. Antibiotic concentrations used for selection purposes were 100 µg/ml ampicillin and 25 µg/ml erythromycin, unless otherwise stated, and were purchased from AMRESCO and Sigma-Aldrich, respectively.

Construction of deletion and complementation derivatives. *A. baumannii* ATCC 17978 *qseB* (ACX60_06100/05) and *ygiW* (ACX60_06095) deletion strains were constructed using the RecET recombinase system (71), with modifications as outlined previously (30). Primers used to generate mutant strains are listed in Table 4. For complementation of insertionally inactivated *hns* genes identified in this study, a previously generated pWH1266 shuttle vector carrying a WT copy of *hns* amplified from *A. baumannii* ATCC 17978 chromosomal DNA (pWH0268) was used to transform appropriate *A. baumannii* strains as previously described (27).

Desiccation survival assay. Desiccation survival assays followed the method outlined previously (8), with modifications. Briefly, ON cultures were diluted 1:25 in fresh LB broth and grown to late log phase (OD₆₀₀ of 0.8 to 1.0). Cells were subsequently washed three times in sterile distilled water and diluted to an OD₆₀₀ of 0.1. A total of 300 µl was pipetted into the center of individual wells of 6-well culture plates and placed in a laminar-flow hood ON at 25°C to dry. All plates were incubated at 21°C with a relative humidity of 30% ± 2%, maintained by the addition of saturated CaCl₂ within sealed plastic boxes. Humidity and temperature were monitored over the 30-day time course using a thermohygrometer. CFU were assessed on days 0, 1, 3, 5, 7, 9, 15, 21, and 30. For viable cell quantification, desiccated cells were rehydrated in sterile phosphate-buffered saline, scraped from their respective wells, and serially diluted. Suspensions of diluted cells were plated on LB agar and incubated ON, and desiccation survival was calculated from the number of CFU/ml. Experiments were undertaken in two biological replicates from two independent experiments. Average CFU and standard errors of the means were calculated and graphed.

Gene cloning and DNA sequencing. The upstream intergenic and coding regions of *hns* from hypermotile variants obtained after desiccation stress experiments were PCR amplified using Velocity DNA polymerase (BioLase, Australia) with *hns_F* and *hns_R* (Table 4) by following the manufacturer's instructions. Adenosine treatment was undertaken on purified amplicons prior to T/A ligation with

TABLE 3 Strains and plasmids used in this study

Strain or plasmid	Genotype or description ^a	Reference or source
Strains		
<i>A. baumannii</i>		
ATCC 17978	Noninternational type clone (wild type)	ATCC (70)
Δ qseBC	ATCC 17978 with Ery ^r insertion disruption in qseBC	This study
Δ ygiW	ATCC 17978 with Ery ^r insertion disruption in ygiW	This study
Δ hns	ATCC 17978 with hns disrupted by ISAbot2	27
Δ hns-ISAbot2	ATCC 17978 with hns disrupted by ISAbot2	This study
Δ qseBC Δ hns-ISAbot2	Δ qseBC with hns disrupted by ISAbot2	This study
Δ ygiW Δ hns-ISAbot2	Δ ygiW with hns disrupted by ISAbot2	This study
Δ ygiW Δ hns-MITE _{hns12}	Δ ygiW with hns disrupted by MITE _{hns12}	This study
Δ hns pWH0268	Δ hns with pWH0268	27
Δ hns-ISAbot2 pWH0268	Δ hns-ISAbot2 with pWH0268	This study
Δ qseBC Δ hns-ISAbot2 pWH0268	Δ qseBC Δ hns-ISAbot2 with pWH0268	This study
Δ ygiW Δ hns-ISAbot2 pWH0268	Δ ygiW Δ hns-ISAbot2 with pWH0268	This study
Δ ygiW Δ hns-MITE _{hns12} pWH0268	Δ ygiW Δ hns-MITE _{hns12} with pWH0268	This study
<i>E. coli</i>		
DH5 α Δ pir	F ⁺ Φ 80lacZ Δ M15 Δ (lacZ Δ Y Δ -argF)U169 recA1 endA1 hsdR170 ₃ m _g ⁺ phoA supE44 Δ thi-1 gyrA96 relA1 Δ pir, conjugative strain which can host λ -pir-dependent plasmids	87
Plasmids		
pAT04	Tet ^r ; pMMB67EH with Rec _{ts} system	71
pGEM-T Easy	Amp ^r ; T-overhang cloning vector	Promega
pVAB01	Cm ^r Ery ^r ; Source of Ery ^r cassette	88
pWH0268	Amp ^r ; pWH1266 with hns cloned via BamHI restriction site	27

^aAbbreviations: Amp, ampicillin; Cm^r, chloramphenicol; Ery^r, erythromycin; Tet^r, tetracycline.

pGEMT Easy (Promega) and transformation into *E. coli* DH5 α Δ pir. Transformants were screened by PCR, restriction digestion, and DNA sequencing.

Stability of MITE_{hns12} in hns. Five colonies were separately inoculated into 10 ml of LB broth and passaged over a 5-day period using a dilution of 1:10,000. From the fifth passage, a loop of confluent bacterial suspension was streaked onto LB agar and incubated ON. A total of three well-isolated colonies from each of the five biological replicates were randomly selected and PCR screened with hns_F and hns_R (Table 3) to identify maintenance of the MITE within the hns gene.

Motility assays. Motility assays for *A. baumannii* ATCC 17978 WT and mutant derivatives were undertaken as previously described (30). Briefly, a colony was harvested from an LB agar plate grown ON and used to inoculate the center of an LB agar (0.25%) plate. Motility was assessed by visual examination after ON incubation at 37°C. Experiments were performed in duplicate over at least three independent experiments. Images are average representations of results obtained.

Comparative genomics, alignments, and clustering. For generation of multiple DNA sequence alignments of all full-length MITE_{hns12} copies identified, sequences were obtained from NCBI GenBank and used as input data using Clustal Omega with default parameter settings applied (<https://www.ebi.ac.uk/Tools/msa/clustalo/>) (34). Prior to alignment, copies of MITE_{hns12} identified in the opposite orientation (IRL to IRL) were reverse complemented. In strains with multiple copies of MITE_{hns12}, these were numbered (_#1, _#2, _#3, etc.) based on their order from NCBI BLASTN (2.8.0+) outputs (72). Subgroups in the alignment were defined based on the presence of two or more identical MITE_{hns12} sequence arrangements, numbered from 1 to 10 and ordered according to abundance. To generate the MITE_{hns12}(c) consensus sequence, all elements of 113 bp in length were used as input data and visualized using WebLogo software (35) with default settings applied.

The presence of the composite transposon in *M. osloensis* CCLUG 350 was identified by manual examination of the sequence surrounding the MITE_{hns12} element using the genome map tool from the Kyoto Encyclopedia of Genes and Genomes database (<http://www.kegg.jp/>) (32). To identify this composite transposon in other genomes, nucleotide sequence spanning the gene locus tags AXE82_04585-AXE82_04645 in *M. osloensis* CCLUG 350 was used as a query in BLASTN searches. Sequences from *M. osloensis* CCLUG 350, AXE82_04585-04645 (15,922 bp), and R5H (73), R5H_08645-08655 (7,446 bp), were used to generate a genetic map using the Easyfig 2.2.2 tool (74). To identify the presence of the composite transposon across all sequenced genomes, nucleotide sequences located between the terminal ends of the composite transposon from *M. osloensis* CCLUG 350 (AXE82_04585-AXE82_04625) were used as a query, and comparative BLASTN searches (72) were performed. The alignment between *M. osloensis* CCLUG 350 and *A. gyllouzei* NBRC 110550 was generated using Easyfig 2.2.2 (74) as described above. The composite transposon identified in this study was allocated the name Tn6645 by the transposon registry (<https://transposon.ltmcd.ac.uk/tn-registry/>).

Coding regions, *E. coli*-derived σ 70 consensus promoter sequences, RNA secondary structures, and Rho factor-independent terminators were predicted with MITE_{hns12}(c) as the input sequence using NCBI ORF finder (<https://www.ncbi.nlm.nih.gov/orffinder/>) (31), the Softberry BPROM tool (<http://www.softberry.com/berry.php?tool=bprom&group=program&subgroup=gfindb>), the RNA Fold server

TABLE 4 Primers used in this study

Primer function and name	Sequence* (5'-3')	Reference or source
Cloning and sequencing of <i>hns</i> genes with integrated mobile genetic elements		
<i>hns</i> _F	GAGACATATGATGCATCATCATCATATAAATTAAGAAAATATATTA	27
<i>hns</i> _R	TCTCGGATCCITAGATTAAGAAATCTTCAAG	27
M13 F	GTAAAACGACGGCCAG	Promega
M13 R	CAGGAACAGCTATGAC	Promega
Identification of presence of IS		
ACX60_04650_F	CGTATTGGGTCTTGGGGAA	This study
ACX60_04650_R	CCITGGTAAGTACTTTAT	This study
ACX60_18935_F	AGCAACTGAAGCTGAAATTCG	27
ACX60_18935_R	TTGGTCCGAATTAGACTTGC	27
ACX60_04795_F	CAGTCAGGTTCCGCAT	This study
ACX60_04795_R	GACCAGACAATACAATG	This study
Construction of Δ qseBC and Δ ygiW		
Δ qseBC		
Δ qseBC_UFR_F	CAATCCGCGATAAGAGC	This study
Δ qseBC_UFR_R	CTATCAACACACTCTAAGCCTGTATATCTCTGAT	This study
Δ qseBC_DFR_F	CGGGAGGAAATAATTCTATTTCAGTCAAACTGG	This study
Δ qseBC_DFR_R	GTAGTAACCCAGAACAGCAC	This study
Δ qseBC_NDL_F	GGCAAGGACCTCTGTTT	This study
Δ qseBC_NDL_R	GGGCTGAAAACTTCAAC	This study
Δ qseBC_Ery_F	CTTAAGAGTGTGTGATAG	39
Δ qseBC_Ery_R	ATAGAATTATTTCTCCCG	39
Δ ygiW		
Δ ygiW_UFR_F	CAGTTGAAATGGCATCCATTAC	This study
Δ ygiW_UFR_R	CTCTTAAGGTATAGGAACCTCAAATACCTCTGTTA	This study
Δ ygiW_DFR_F	GAGGAAATAAGAAGTCTCTATACTAAATTAATTTCTACATTTATCC	This study
Δ ygiW_DFR_R	GAGAGCGGCCCTCATTAAAGTCTCCCATAC	This study
Δ ygiW_NDL_F	CGGCATTATGAGTTATGCCAG	This study
Δ ygiW_NDL_R	GGCTTGCCCAACTGA	This study
Δ ygiW_Ery_F	GAAGTTCTATACCTTAAGAGTGTGTGATAG	This study
Δ ygiW_Ery_R	GTATAGGAACCTTCTATTCTCCCGTAAATAATAGATAAC	This study

*Nucleotides in boldface represent incorporated restriction sites: NdeI, CATATG; BamHI, GGATCC; NotI, GGGCCGCG.

(<http://unafold.mauflary.edu/?q=mfold/mfolding-form>) (36), and ARNold, a *rho*-independent transcription terminator finding tool (<http://maigmors.u-psud.fr/toolbox/arnold/>) (37), respectively. Default settings were applied for all programs mentioned above.

Characterization of MITE_{Acet12} TSDs. A total of 20 bp upstream and downstream of each MITE_{Acet12} element from BLASTN outputs were used to screen for the presence of TSDs. The AT ratio percentages were calculated based on the number of adenosine or thymidine nucleotides in each of the 9-bp integration sites, and these percentages were plotted against the number of copies harboring each ratio. To identify trends in MITE_{Acet12} integration sites, all identified TSD sequences were used as input data using WebLogo software (35) with default settings applied.

SUPPLEMENTAL MATERIAL

Supplemental material for this article may be found at <https://doi.org/10.1128/mSphereDirect.00028-19>.

FIG S1, TIF file, 1.9 MB.

FIG S2, TIF file, 1.5 MB.

TABLE S1, DOCX file, 0.01 MB.

ACKNOWLEDGMENTS

This work was supported by the Australian National Health and Medical Research Council (project grant 1047509) and a Flinders Medical Research Foundation Grant. F.G.A. was supported by A. J. and I. M. Naylor and Playford Trust Ph.D. scholarships.

REFERENCES

- Higgins PG, Dammhayn C, Hackel M, Seifert H. 2010. Global spread of carbapenem-resistant *Acinetobacter baumannii*. *J Antimicrob Chemother* 65:233–238. <https://doi.org/10.1093/jac/dkp428>.
- Harding CM, Hennon SW, Feldman MF. 2018. Uncovering the mechanisms of *Acinetobacter baumannii* virulence. *Nat Rev Microbiol* 16: 91–102. <https://doi.org/10.1038/nrmicro.2017.148>.

3. Jawad A, Seifert H, Snelling AM, Heritage J, Hawkey PM. 1998. Survival of *Acinetobacter baumannii* on dry surfaces: comparison of outbreak and sporadic isolates. *J Clin Microbiol* 36:1938–1941.
4. Blackwell GA, Negro SJ, Hall RM. 2016. Evolution of AbGRII-0, the progenitor of the AbGRII resistance island in global clone 2 of *Acinetobacter baumannii*. *Antimicrob Agents Chemother* 60:1421–1429. <https://doi.org/10.1128/AAC.02662-15>.
5. Weber BS, Ly PM, Irwin JN, Pakatzki S, Feldman MF. 2015. A multidrug resistance plasmid contains the molecular switch for type VI secretion in *Acinetobacter baumannii*. *Proc Natl Acad Sci U S A* 112:9442–9447. <https://doi.org/10.1073/pnas.1502966112>.
6. Harding CM, Nasir MA, Kinsella RL, Scott NE, Foster LJ, Weber BS, Piester SE, Actis LA, Tracy EN, Mason RS, Jr, Feldman MF. 2015. *Acinetobacter* strains carry two functional oligosaccharyltransferases, one devoted exclusively to type IV pilin, and the other one dedicated to O-glycosylation of multiple proteins. *Mol Microbiol* 96:1023–1041. <https://doi.org/10.1111/mmi.12986>.
7. Álvarez-Fraga L, Pérez A, Rumbo-Feal S, Merino M, Vallejo JA, Ohneck EJ, Edelmann RE, Becerra A, Vázquez-Ucha JC, Valle J, Actis LA, Bou G, Poza M. 2016. Analysis of the role of the LH92_11085 gene of a biofilm hyper-producing *Acinetobacter baumannii* strain on biofilm formation and attachment to eukaryotic cells. *Virulence* 7:443–455. <https://doi.org/10.1080/21505594.2016.1145335>.
8. Gayoso CM, Mateos J, Méndez JA, Fernández-Puente P, Rumbo C, Tomás M, Martínez de Ilarduya O, Bou G. 2014. Molecular mechanisms involved in the response to desiccation stress and persistence in *Acinetobacter baumannii*. *J Proteome Res* 13:460–476. <https://doi.org/10.1021/pr400603f>.
9. Wright MS, Jacobs MR, Bonomo RA, Adams MD. 2017. Transcriptome remodeling of *Acinetobacter baumannii* during infection and treatment. *mBio* 8:e02193-16. <https://doi.org/10.1128/mBio.02193-16>.
10. Wright MS, Haft DH, Harkins DM, Perez F, Hujer KM, Bajaksouzian S, Benard MF, Jacobs MR, Bonomo RA, Adams MD. 2014. New insights into dissemination and variation of the health care-associated pathogen *Acinetobacter baumannii* from genomic analysis. *mBio* 5:e00963-13. <https://doi.org/10.1128/mBio.00963-13>.
11. Adams MD, Bishop B, Wright MS. 2016. Quantitative assessment of insertion sequence impact on bacterial genome architecture. *Microb Genom* 2:e00062. <https://doi.org/10.1099/mgen.0.00062>.
12. Toussaint A, Chandler M. 2012. Prokaryote genome fluidity: toward a systems approach of the mobilome. *Methods Mol Biol* 804:57–80. https://doi.org/10.1007/978-1-61779-361-5_4.
13. Vandecasteele J, Chandler M, Aertsen A, Van Houdt R. 2017. The impact of insertion sequences on bacterial genome plasticity and adaptability. *Crit Rev Microbiol* 43:709–730. <https://doi.org/10.1080/1040841X.2017.1303661>.
14. Zhang Z, Sailer MH, Jr. 2011. Transposon-mediated adaptive and directed mutations and their potential evolutionary benefits. *J Mol Microbiol Biotechnol* 21:59–70. <https://doi.org/10.1159/000333106>.
15. Partridge SR, Kwong SM, Firth N, Jensen SO. 2018. Mobile genetic elements associated with antimicrobial resistance. *Clin Microbiol Rev* 31:e00088-17. <https://doi.org/10.1128/CMR.00088-17>.
16. Haren L, Ton-Huang B, Chandler M. 1999. Integrating DNA: transposases and retroviral integrases. *Annu Rev Microbiol* 53:245–281. <https://doi.org/10.1146/annurev.micro.53.1.245>.
17. Siguler P, Goubeyre E, Varani A, Ton-Huang B, Chandler M. 2015. Everyman's guide to bacterial insertion sequences. *Microbiol Spectr* 3:MDNA3-0030-2014. <https://doi.org/10.1128/microbiolspec.MDNA3-0030-2014>.
18. Nagy Z, Chandler M. 2004. Regulation of transposition in bacteria. *Res Microbiol* 155:387–398. <https://doi.org/10.1016/j.resmic.2004.01.008>.
19. Szuplińska M, Łudziński M, Lyszka K, Czamecki J, Bartosik D. 2014. Mobility and generation of mosaic non-autonomous transposons by *TrnJ*-derived inverted-repeat miniature elements (TIMEs). *PLoS One* 9:e105010. <https://doi.org/10.1371/journal.pone.0105010>.
20. Siguler P, Goubeyre E, Chandler M. 2014. Bacterial insertion sequences: their genomic impact and diversity. *FEMS Microbiol Rev* 38:865–891. <https://doi.org/10.1111/1574-6975.12067>.
21. Bertels F, Rainey PB. 2011. Within-genome evolution of REPINs: a new family of miniature mobile DNA in bacteria. *PLoS Genet* 7:e1002152. <https://doi.org/10.1371/journal.pgen.1002152>.
22. Fattah L, Rooker R, Wong A, Hui C, Luo T, Bhardwaj P, Yang G. 2013. Miniature inverted-repeat transposable elements: discovery, distribution, and activity. *Genome* 56:475–486. <https://doi.org/10.1139/gen-2012-0174>.
23. Delhas N. 2008. Small mobile sequences in bacteria display diverse structure/function motifs. *Mol Microbiol* 67:475–481. <https://doi.org/10.1111/j.1365-2958.2007.06068.x>.
24. Brügger K, Redder P, She Q, Confalonieri F, Zhanovic Y, Garrett RA. 2002. Mobile elements in archaeal genomes. *FEMS Microbiol Lett* 206:131–141. <https://doi.org/10.1111/j.1574-6968.2002.tb10999.x>.
25. Comela FF, Inouye S, Inouye M. 1988. A family of small repeated elements with some transposon-like properties in the genome of *Neisseria gonorrhoeae*. *J Biol Chem* 263:12194–12198.
26. Kröger C, Kary SC, Schauer K, Cameron AD. 2016. Genetic regulation of virulence and antibiotic resistance in *Acinetobacter baumannii*. *Genes* 8:12. <https://doi.org/10.3390/genes8010012>.
27. Eijkalkamp BA, Stroehrer UH, Hassan KA, Elbourne LD, Paulsen IT, Brown MH. 2013. H-NS plays a role in expression of *Acinetobacter baumannii* virulence features. *Infect Immun* 81:2574–2583. <https://doi.org/10.1128/IAI.00065-13>.
28. Siguler P, Perochon J, Lestrade L, Mahillon J, Chandler M. 2006. ISfinder: the reference centre for bacterial insertion sequences. *Nucleic Acids Res* 34:D32–D36. <https://doi.org/10.1093/nar/gkj014>.
29. Eijkalkamp BA. 2011. Factors contributing to the success of *Acinetobacter baumannii* as a human pathogen. Ph.D. thesis. Flinders University of South Australia, Adelaide, Australia.
30. Giles SK, Stroehrer UH, Eijkalkamp BA, Brown MH. 2015. Identification of genes essential for pellicle formation in *Acinetobacter baumannii*. *BMC Microbiol* 15:116. <https://doi.org/10.1186/s12866-015-0440-6>.
31. Wheeler DL, Church DM, Federhen S, Lash AE, Madden TL, Pontius JU, Schuler GD, Schriml LM, Sequoia E, Tatusova TA, Wagner L. 2003. Database resources of the National Center for Biotechnology. *Nucleic Acids Res* 31:28–33. <https://doi.org/10.1093/nar/gkg033>.
32. Kanehisa M, Sato Y, Kawashima M, Furumichi M, Tanabe M. 2016. KEGG as a reference resource for gene and protein annotation. *Nucleic Acids Res* 44:D457–D462. <https://doi.org/10.1093/nar/gkv1070>.
33. Aravind L, Iyer LM, Leipe DD, Koonin EV. 2004. A novel family of P-loop NTPases with an unusual phyletic distribution and transmembrane segments inserted within the NTPase domain. *Genome Biol* 5:R30. <https://doi.org/10.1186/gb-2004-5-5-r30>.
34. Sievers F, Higgins DG. 2018. Clustal Omega for making accurate alignments of many protein sequences. *Protein Sci* 27:135–145. <https://doi.org/10.1002/pro.3290>.
35. Crooks GE, Hon G, Chandonia JM, Brenner SE. 2004. WebLogo: a sequence logo generator. *Genome Res* 14:1188–1190. <https://doi.org/10.1101/gr.849004>.
36. Zuker M. 2003. Mfold web server for nucleic acid folding and hybridization prediction. *Nucleic Acids Res* 31:3406–3415. <https://doi.org/10.1093/nar/gkg595>.
37. Naville M, Ghullot-Gaudeffroy A, Marchais A, Gautheret D. 2011. ARNold: a web tool for the prediction of *rho*-independent transcription terminators. *RNA Biol* 8:11–13. <https://doi.org/10.4161/rna.8.1.13346>.
38. Héritier C, Poinel L, Nordmann P. 2008. Cephalosporinase overexpression resulting from insertion of ISAbo1 in *Acinetobacter baumannii*. *Clin Microbiol Infect* 12:123–130. <https://doi.org/10.1111/j.1469-0691.2005.01320.x>.
39. Adams FG, Stroehrer UH, Hassan KA, Mari S, Brown MH. 2018. Resistance to pentamidine is mediated by AdeAB, regulated by AdeRS, and influenced by growth conditions in *Acinetobacter baumannii*. *ATCC* 17978. *PLoS One* 13:e0197412. <https://doi.org/10.1371/journal.pone.0197412>.
40. Robinson JT, Thorvaldsdóttir H, Winkler W, Guttman M, Lander ES, Getz G, Mesirov JP. 2011. Integrative genomics viewer. *Nat Biotechnol* 29:24–26. <https://doi.org/10.1038/nbt.1754>.
41. Abernethy C, Blanc G, Monchois V, Renesto P, Sigollet C, Ogata H, Raoult D, Claverie JM. 2006. Impact of the excision of an ancient repeat insertion on *Rickettsia conorii* guanylate kinase activity. *Mol Biol Evol* 23:2112–2122. <https://doi.org/10.1093/molbev/mls082>.
42. Delhas N. 2007. Enterobacterial small mobile sequences carry open reading frames and are found intragenically—evolutionary implications for formation of new peptides. *Gene Regul Syst Bio* 1:191–205.
43. Yee L, Hinoiyama A, Ohji S, Tsuchikane K, Shimodaira J, Yamazoe A, Fujita N, Suzuki-Minakuchi C, Nohji H. 2014. Complete genome sequence of a dimethyl sulfide-utilizing bacterium, *Acinetobacter guillouiae* strain 208 (JBR110550). *Genome Announc* 2:e01048-14. <https://doi.org/10.1128/genomeA.01048-14>.
44. Delhas N. 2011. Impact of small repeat sequences on bacterial genome

- evolution. *Genome Biol Evol* 3:959–973. <https://doi.org/10.1093/gbe/evn077>.
45. Gillings MR, Labbate M, Sajad A, Giguere NJ, Holley MP, Stokes HW. 2009. Mobilization of a *Tn402*-like class 1 integron with a novel cassette array via flanking miniature inverted-repeat transposable element-like structures. *Appl Environ Microbiol* 75:6002–6004. <https://doi.org/10.1128/AEM.01033-09>.
 46. Hamidian M, Ambrose SJ, Hall RM. 2016. A large conjugative *Acinetobacter baumannii* plasmid carrying the *su2* sulphonamide and *stbA8* streptomycin resistance genes. *Plasmid* 87:88–93. <https://doi.org/10.1016/j.plasmid.2016.09.001>.
 47. Domingues S, Nielsen KM, da Silva GI. 2011. The *bla*IMP-5-carrying integron in a clinical *Acinetobacter baumannii* strain is flanked by miniature inverted-repeat transposable elements (MITEs). *J Antimicrob Chemother* 66:2667–2668. <https://doi.org/10.1093/jac/dkr327>.
 48. Domingues S, Toleman MA, Nielsen KM, da Silva GI. 2013. Identical miniature inverted repeat transposable elements flank class 1 integrons in clinical isolates of *Acinetobacter* spp. *J Clin Microbiol* 51:2362–2364. <https://doi.org/10.1128/JCM.00692-13>.
 49. Zong Z. 2014. The complex genetic context of *bla*_{IMP-5} flanked by miniature inverted-repeat transposable elements in *Acinetobacter johnsonii*. *PLoS One* 9:e009046. <https://doi.org/10.1371/journal.pone.0090466>.
 50. Gallagher LA, Ramage E, Weiss EJ, Radey M, Hayden HS, Held KG, Huse HK, Zurawski DV, Brittnacher MJ, Manoil C. 2015. Resources for genetic and genomic analysis of emerging pathogen *Acinetobacter baumannii*. *J Bacteriol* 197:2027–2035. <https://doi.org/10.1128/JB.00131-15>.
 51. Wibberg D, Salto IP, Elomvyr FG, Maus I, Winkler A, Nordmann P, Pühler A, Pöhlert A, Schlöter A. 2016. Complete genome sequencing of *Acinetobacter baumannii* strain K50 discloses the large conjugative plasmid pK50a encoding carbapenemase OXA-23 and extended-spectrum β -lactamase GES-11. *Antimicrob Agents Chemother* 62:e00212-16. <https://doi.org/10.1128/AAC.00212-16>.
 52. Nigro SJ, Hall RM. 2017. A large plasmid, pO46-4, carrying a complex resistance region in an extensively antibiotic-resistant ST25 *Acinetobacter baumannii*. *J Antimicrob Chemother* 72:3496–3498. <https://doi.org/10.1093/jac/dkx287>.
 53. Mindlin S, Petrenko A, Kuzakov A, Beletsky A, Mardanov A, Petrova M. 2016. Resistance of permafrost and modern *Acinetobacter* *lwoelfii* strains to heavy metals and arsenic revealed by genome analysis. *Biomed Res Int* 2016:3970831. <https://doi.org/10.1155/2016/3970831>.
 54. Wachter S, Raghavan R, Wachter J, Mirnick WF. 2018. Identification of novel MITEs (miniature inverted-repeat transposable elements) in *Caecilia* *buettii*: implications for protein and small RNA evolution. *BMC Genomics* 19:247. <https://doi.org/10.1186/s12864-018-4608-y>.
 55. Siddique A, Buisine N, Chalmers R. 2011. The transposon-like *Correlia* elements encode numerous strong promoters and provide a potential new mechanism for phase variation in the meningococcus. *PLoS Genet* 7:e1001277. <https://doi.org/10.1371/journal.pgen.1001277>.
 56. Klein BA, Chen Y, Scott JC, Koenigsberg AL, Duncan MJ, Hu LT. 2015. Identification and characterization of a minisatellite contained within a novel miniature inverted-repeat transposable element (MITE) of *Porphyromonas gingivalis*. *Mob DNA 6:18*. <https://doi.org/10.1186/s13100-015-0049-1>.
 57. Turton JF, Ward ME, Woodford N, Kaufmann ME, Pike R, Livermore DM, Pitt TL. 2006. The role of IS*Aba1* in expression of OXA carbapenemase genes in *Acinetobacter baumannii*. *FEMS Microbiol Lett* 258:72–77. <https://doi.org/10.1111/j.1574-6968.2006.00195.x>.
 58. Lopes BS, Amyes SG. 2012. Role of IS*Aba1* and IS*Aba125* in governing the expression of *bla*_{OXA} in clinically relevant *Acinetobacter baumannii* strains resistant to cephalosporins. *J Med Microbiol* 61:1103–1108. <https://doi.org/10.1099/jmm.0.044156-0>.
 59. Liu SV, Saunders NJ, Jeffries A, Rest RF. 2002. Genome analysis and strain comparison of *Correlia* repeats and *Correlia* repeat-enclosed elements in pathogenic *Neisseria*. *J Bacteriol* 184:6163–6173. <https://doi.org/10.1128/JB.184.22.6163-6173.2002>.
 60. Zhou F, Tran Y, Xu Y. 2008. *Nezha*, a novel active miniature inverted-repeat transposable element in cyanobacteria. *Biochem Biophys Res Commun* 365:790–794. <https://doi.org/10.1016/j.bbrc.2007.11.038>.
 61. Juárez-Rodríguez MD, Torres-Escobar A, Demuth DR. 2013. *ggiW* and *ggiC* are co-expressed in *Aggregatibacter actinomycetemcomitans* and regulate biofilm growth. *Microbiology* 159:989–1001. <https://doi.org/10.1099/mic.0.060183-0>.
 62. Steele KH, O'Connor LH, Burpo N, Kohler K, Johnston JW. 2012. Characterization of a ferrous iron-responsive two-component system in non-typeable *Haemophilus influenzae*. *J Bacteriol* 194:6162–6173. <https://doi.org/10.1128/JB.01465-12>.
 63. Lee J, Hibel SL, Reardon KF, Wood TK. 2010. Identification of stress-related proteins in *Escherichia coli* using the pollutant *cis*-dichloroethylene. *J Appl Microbiol* 108:2088–2102. <https://doi.org/10.1111/j.1365-2672.2009.04611.x>.
 64. Moreira CG, Herrera CM, Needham BD, Parker CT, Libby SJ, Fang FC, Trent MS, Sperandio V. 2013. Virulence and stress-related periplasmic protein (VspP) in bacterial/host associations. *Proc Natl Acad Sci U S A* 110:1470–1475. <https://doi.org/10.1073/pnas.1215416110>.
 65. Ginalski K, Kirsch L, Rychlewski L, Grishin NV. 2004. BOF: a novel family of bacterial CBP proteins. *FEBS Lett* 567:297–301. <https://doi.org/10.1016/j.febslet.2004.04.086>.
 66. Wu Y, Aandahl RZ, Tanaka MM. 2015. Dynamics of bacterial insertion sequences: can transposition bursts help the elements persist? *BMC Evol Biol* 15:288. <https://doi.org/10.1186/s12862-015-0560-5>.
 67. Dorman CJ. 2007. H-NS, the genome sentinel. *Nat Rev Microbiol* 5:157–161. <https://doi.org/10.1038/nrmicro1598>.
 68. Elgami A, Miyoshi S. 2015. Role of the histone-like nucleoid structuring protein (H-NS) in the regulation of virulence factor expression and stress response in *Vibrio vulnificus*. *Biocontrol Sci* 20:265–274. <https://doi.org/10.4265/bio.20.265>.
 69. Davison Lucas D, Crane R, Wright A, Han ML, Moffatt J, Bulach D, Gladman SL, Powell D, Aranda J, Seemann T, Machado D, Pacheco T, Marques T, Viveiros M, Nation R, Li J, Harper M, Boyce JD. 2018. Emergence of high-level colistin resistance in an *Acinetobacter baumannii* clinical isolate mediated by inactivation of the global regulator H-NS. *Antimicrob Agents Chemother* 62:e02442-17. <https://doi.org/10.1128/AAC.02442-17>.
 70. Smith MG, Gianouis TA, Pskatzki S, Mekalanos JJ, Ormston LM, Gerstein M, Stryder M. 2007. New insights into *Acinetobacter baumannii* pathogenesis revealed by high-density pyrosequencing and transposon mutagenesis. *Genes Dev* 21:601–614. <https://doi.org/10.1101/gad.1510307>.
 71. Tucker AT, Nowicki EM, Boll JM, Knauf GA, Burdick NC, Trent MS, Davies BW. 2014. Defining gene-phenotype relationships in *Acinetobacter baumannii* through one-step chromosomal gene inactivation. *mBio* 5:e01313. <https://doi.org/10.1128/mBio.01313-14>.
 72. Altschul SF, Gish W, Miller W, Myers EW, Lipman DJ. 1990. Basic local alignment search tool. *J Mol Biol* 215:403–410. [https://doi.org/10.1016/S0022-2836\(05\)80360-2](https://doi.org/10.1016/S0022-2836(05)80360-2).
 73. Lim JY, Hwang I, Garzong M, Huang SL, Cho GS, Franz C, Lee K. 2018. Complete genome sequences of three *Moraxella osloensis* strains isolated from human skin. *Genome Announc* 6:e01509-17. <https://doi.org/10.1128/genomeA.01509-17>.
 74. Sullivan MJ, Petty NK, Beaton SA. 2011. Easyfig: a genome comparison visualizer. *Bioinformatics* 27:1009–1010. <https://doi.org/10.1093/bioinformatics/btr039>.
 75. Vettath YK, Anzures ACM, Uchida A, Purboljati RW, Houghton JN, Chenard C, Drautz-Moses D, Wong A, Kolundzija S, Clare ME, Kishwaha KK, Panicker D, Putra A, Gaultier NE, Heinle CE, Premkrisnan BN, Schuster SC. 2018. Complete genome sequence of *Acinetobacter indicus* type strain SGAr0564 isolated from tropical air collected in Singapore. *Genome Announc* 6:e00230-18. <https://doi.org/10.1128/genomeA.00230-18>.
 76. Feng Y, Yang P, Wang X, Zong Z. 2016. Characterization of *Acinetobacter johnsonii* isolate XBB1 carrying nine plasmids and encoding NDM-1, OXA-58 and PER-1 by genome sequencing. *J Antimicrob Chemother* 71:71–75. <https://doi.org/10.1093/jac/dkv524>.
 77. Fomenkov A, Vincze T, Degtyarev SK, Roberts RJ. 2017. Complete genome sequence and methylome analysis of *Acinetobacter calcoaceticus* 65. *Genome Announc* 5:e00050-17. <https://doi.org/10.1128/genomeA.00050-17>.
 78. Vijaykumar S, Balaji V, Biswas I. 2015. Complete genome sequence of *Acinetobacter baumannii* strain BB300, which displays high twitching motility. *Genome Announc* 3:e00956-15. <https://doi.org/10.1128/genomeA.00956-15>.
 79. Weingarten RA, Johnson RC, Conlan S, Ramsburg AM, Dekker JP, Lau AF, Khil P, Odom RT, Deming C, Park M, Thomas PJ, Henderson DK, Palmone TN, Segre JA, Frank KM. 2018. Genomic analysis of hospital plumbing reveals diverse reservoir of bacterial plasmids conferring carbapenem resistance. *mBio* 9:e02011-17. <https://doi.org/10.1128/mBio.02011-17>.
 80. Vijaykumar S, Balaji V, Biswas I. 2015. Complete genome sequence of *Acinetobacter baumannii* strain BB342, a motility-positive clinical

- isolate. *Genome Announc* 3:e00925-15. <https://doi.org/10.1128/genomeA.00925-15>.
81. Blaschke U, Wilharm G. 2017. Complete genome sequence of *Acinetobacter* sp. strain NCu20-2 isolated from a mouse. *Genome Announc* 5:e01415-16. <https://doi.org/10.1128/genomeA.01415-16>.
 82. Poirot L, Nordmann P. 2006. Genetic structures at the origin of acquisition and expression of the carbapenem-hydrolyzing oxacillinase gene *bla_{OXA-58}* in *Acinetobacter baumannii*. *Antimicrob Agents Chemother* 50:1442-1448. <https://doi.org/10.1128/AAC.50.4.1442-1448.2006>.
 83. Kee C, Junqueira ACM, Uchida A, Purbojati RW, Houghton JNL, Chenard C, Wong A, Clare ME, Kuswaha KK, Panicker D, Putra A, Gaultier NE, Premkrishnan BN, Heirle CE, Vettath VK, Drautz-Moses DI, Schuster SC. 2018. Complete genome sequence of *Acinetobacter schindleri* SGAir0122 isolated from Singapore air. *Genome Announc* 6:e00567-18. <https://doi.org/10.1128/genomeA.00567-18>.
 84. Lutz S, Mäkitar N, Shabbir MZ, Rivera I, Ivanov YV, Tahir Z, Yaqub T, Harvill ET. 2018. Virulent epidemic pneumonia in sheep caused by the human pathogen *Acinetobacter baumannii*. *Front Microbiol* 9:2616. <https://doi.org/10.3389/fmicb.2018.02616>.
 85. Kholodii G, Mindlin S, Gorlenko Z, Petrova M, Hobman J, Nikiforov V. 2004. Translocation of transposition-deficient (*Int1* PK1A2-like) transposons in the natural environment: mechanistic insights from the study of adjacent DNA sequences. *Microbiology* 150:979-992. <https://doi.org/10.1099/mic.0.26844-0>.
 86. Zou D, Huang Y, Liu W, Yang Z, Dong D, Huang S, He X, Ao D, Liu N, Wang S, Wang Y, Tong Y, Yuan J, Huang L. 2017. Complete sequences of two novel *bla_{OXA-58}*-harbouring plasmids from two *Acinetobacter baumannii* isolates in China associated with the acquisition of Tn125. *Sci Rep* 7:9405. <https://doi.org/10.1038/s41598-017-09624-0>.
 87. Purins L, Van Den Bosch L, Richardson V, Morona R. 2008. Coiled-coil regions play a role in the function of the *Shigella flexneri* O-antigen chain length regulator WzqH52. *Microbiology* 154:1104-1116. <https://doi.org/10.1099/mic.0.2007/014225-0>.
 88. Macrina FL, Evans RP, Tobian JA, Hartley DL, Creswell DE, Jones KR. 1983. Novel shuttle plasmid vehicles for *Escherichia*-*Streptococcus* transgeneric cloning. *Gene* 25:145-150. [https://doi.org/10.1016/0378-1119\(83\)90176-2](https://doi.org/10.1016/0378-1119(83)90176-2).

Appendix F – Adams, 2017; *Microbiology Australia**In Focus*

A key regulatory mechanism of antimicrobial resistance in pathogenic *Acinetobacter baumannii*



Felise G Adams

Molecular Microbiology Lab
College of Science and Engineering
Flinders University
Adelaide, SA 5042, Australia
Tel. +61 8 8201 5579
Email: felise.adams@flinders.edu.au

Acinetobacter baumannii is a Gram-negative bacterial pathogen that has become a pressing global health issue in recent decades. Although virulence factors for this pathogen have been identified, details of how they are regulated are largely unknown. One widely employed regulatory mechanism that bacteria, such as *A. baumannii*, have adopted is through two component signal transduction systems (TCS). TCS consist of two proteins; a histidine kinase and response regulator. The histidine kinase allows the bacterium to sense alterations in the extracellular milieu, transmitting the information to the response regulator which prompts the cell to modify gene expression levels accordingly. Bacteria can encode multiple TCS, where each system can mediate specific responses to particular conditions or stressors. Identifying those conditions in which these TCS are expressed, and the genes they regulate known as their 'regulon', is vital for understanding how *A. baumannii* survives and persists within the hospital environment or the human host during infection. As we enter the post-antibiotic era, knowledge of TCS could prove to be invaluable, as they offer an alternative target for the treatment of multidrug resistant bacterial infections.

Acinetobacter baumannii is a Gram-negative opportunistic 'superbug' that causes a diverse range of nosocomial infections, primarily in patients whom are immunocompromised, such as those within intensive care units¹. The *Acinetobacter* species is one of the leading causes of bacterial pneumonia within the hospital environment^{2,3} and have been responsible for numerous

outbreaks of nosocomial infections, worldwide⁴. Within Australia, *A. baumannii* isolates are not only confined to hospitals but are also seen within community-based settings, primarily in tropical regions of Northern Australia^{5,6}. These community-acquired infections have been shown to be predominant in individuals whom have underlying medical conditions such as diabetes mellitus or other risk factors including excessive alcohol consumption⁶.

High levels of innate and acquired multidrug resistance mechanisms represent a leading factor in the pathogenic success of this organism. Intrinsic resistance mechanisms include low outer membrane permeability, production of chromosomally-encoded antibiotic inactivating enzymes and efflux pump systems^{7,8}. Acquired mechanisms contributing to resistance include the uptake of foreign resistance determinants via horizontal gene transfer^{9,10} and over-expression of resistance genes through introduction of insertional elements or mutations particularly within their regulators^{11,12}. This ability of the bacterium to acquire and modulate expression of an array of antimicrobial resistance determinants provides a strong ecological advantage to survive the selective pressures typically found within the hospital setting, resulting in the growing emergence of multidrug resistant *A. baumannii* lineages¹.

Infections caused by multidrug resistant *A. baumannii* isolates, particularly those resistant to carbapenems, have been linked to increased morbidity and mortality, as well as a significant rise in hospital associated costs¹³. Recently, the World Health Organization recognised the impending threat of carbapenem resistant *A. baumannii* isolates, listing them as one of the top three critical priorities for research and development towards new therapeutic treatments for antibiotic-resistant bacterial species (excluding *Mycobacteriota*)¹⁴. Despite the risk this bacterium poses to susceptible individuals and our healthcare facilities, virulence traits including antimicrobial resistance, are not completely understood. Furthermore, the regulatory mechanisms that modulate these characteristics are even more ill-defined.

One simple yet highly sophisticated mechanism that bacteria utilise to effectively regulate the expression of virulence factors employs TCS^{15,16}. TCS consist of two proteins; a histidine kinase which

senses variations in the extracellular milieu and a response regulator which alters gene expression upon activation by its cognate histidine kinase²⁷ (Figure 1). TCS not only modulate virulence-associated mechanisms but also fundamental biological processes such as pathways involved in metabolism^{18,19} and osmoregulation²⁰. The proportion of genes coding for TCS within a bacterial genome is thought to be dependent on a range of factors, including genome size and the diversity of different environments the bacterium may encounter²¹. Generally, histidine kinase and response regulator genes are co-transcribed in an operon, but they can also exist in the genome separated from their cognate partner, and are defined as orphans²². In *A. baumannii*, genomic analyses have identified 12 response regulator genes in an avirulent isolate that increases to 16 to 19 in pathogenic isolates²³. Of these, only a handful have been experimentally examined^{24–26}.

An aspect of my research has focused on the AdeRS TCS which was originally identified as a regulator of the AdeABC three component

efflux system in many *A. baumannii* clinical isolates (Figure 2a). When overexpressed, AdeABC exports a broad range of structurally-unrelated antimicrobials including antibiotics, biocides and dyes^{25,30–34}. Importantly, within this group of substrates are compounds from the carbapenem class of antibiotics as well as tigecycline, one of the last lines of defence against *A. baumannii*³⁵. Analysis of many multidrug resistant *A. baumannii* isolates has shown a high incidence of mutations or the presence of insertional elements in the AdeRS regulatory system, deeming this TCS to be a significant contributor to the observed multidrug resistance phenotype^{31,36,37}. At a genetic level, the *adeRS* genes lie adjacent to *adeABC*, but are divergently transcribed (Figure 2b). The AdeR response regulator protein binds to a 10 base-pair direct repeat DNA sequence and modulates *adeABC* expression³⁸; however, the external signal(s) that interact with the AdeS histidine kinase remain unknown. Aside from changes in antimicrobial resistance, deletion of *adeRS* seen in some clinical isolates, has identified significant alterations in persistence strategies, such as

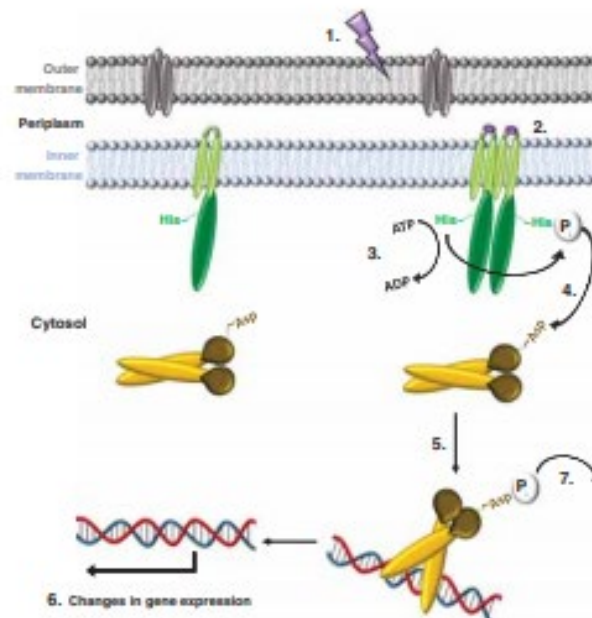


Figure 1. Schematic representation of a typical two component signal transduction system cascade in Gram-negative bacteria. Two component signal transduction systems consist of a histidine kinase (HK) and response regulator (RR) protein (green and yellow, respectively). HK proteins are generally localised in the inner membrane and possess a variable N-terminal sensing domain and a highly conserved C-terminal kinase region (light and dark green, respectively). In contrast, cytosolic RR proteins contain a highly conserved N-terminal domain and a variable C-terminal output domain (brown and yellow, respectively). The HK detects the presence of an external stimulus (1). Binding of the stimulating agent induces a conformational change in the HK (2) resulting in trans-autophosphorylation between HK homodimers whereby one monomer catalyzes phosphorylation using ATP of the conserved histidine (His) residue in the second monomer (3). This phosphate (P) is subsequently transferred to the highly conserved aspartate (Asp) residue on the RR protein (4). Phosphorylation of the RR induces conformational changes that alters its DNA binding properties (5) modulating target gene expression (6). Resetting the system to pre-stimulus state is attained by de-phosphorylation of the RR (7) through phosphatase activity of the HK or by other phosphatase enzymes.

In Focus

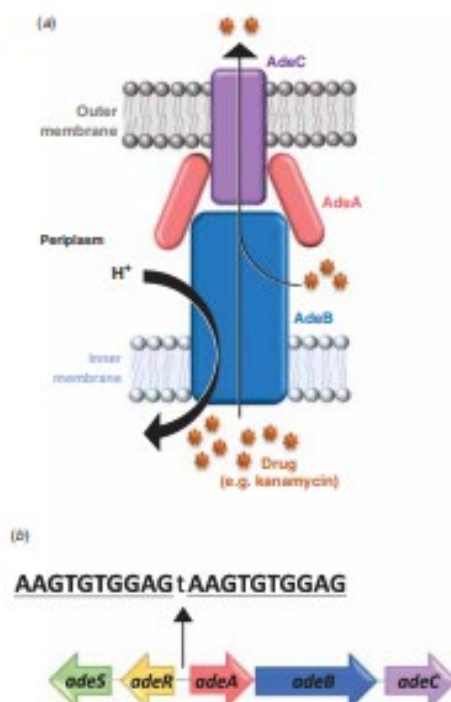


Figure 2. Composition of the AdeABC tripartite pump and genetic organisation of the *adeRS* and *adeABC* operons typically found in the *Acinetobacter baumannii* membrane and chromosome, respectively. (a) The pump is constituted of three proteins; AdeB the cytoplasmic membrane transporter (blue), AdeA the membrane fusion protein (pink) and AdeC the outer membrane protein (purple), that come together to form a functional complex. Activity of the AdeABC pump is coupled to the proton gradient (H^+), where substrates of the pump, e.g. kanamycin (orange stars), can be directly expelled into the external environment. (b) The *adeRS* genes is adjacent to the *adeABC* genes and are divergently transcribed (arrows indicate the coding sequence and the direction of transcription). Located within the intergenic region between *adeR* and *adeA* is a 10 base-pair direct repeat, separated by a thymine nucleotide. This repeat is predicted to be where the AdeR response regulator binds to modulate *adeABC* gene expression.

the production of an extracellular protective matrix known as a biofilm^{34,35}.

Many clinical *A. baumannii* isolates harbour different genetic arrangements of the *adeRS* and *adeABC* operons³⁹. Examination into one *A. baumannii* clinical isolate identified that insertional-inactivation of the outer membrane component of the pump (AdeC) did not affect resistance towards two previously identified AdeABC substrates²⁵. It was suggested that in the absence of AdeC, AdeAB can utilise an alternative outer membrane protein to form a functional tripartite complex²⁵. Given that AdeC may not be essential to confer antimicrobial resistance, and the diverse genetic arrangements of these operons across clinical *A. baumannii*

isolates, a key aim of my studies was to (1) ascertain whether clinical isolates which naturally lack *adeC* also confer antimicrobial resistance and to (2) determine if the previously observed regulatory properties governed by AdeRS are also maintained. The well characterised *A. baumannii* 'type' strain ATCC 17978⁴⁰ isolated from an infant with fatal meningitis, which does not carry *adeC*, was chosen for genetic manipulation. Through double homologous recombination techniques, mutant derivatives targeting either *adeRS* or *adeAB* genes were generated and compared to the ATCC 17978 parent. Antibigram analysis of the *adeAB* mutant identified changes in resistance to a subset of structurally related antimicrobials, including a commonly utilised clinical disinfectant. The role of the AdeRS TCS in modulating expression of *adeABC* is of current debate. As deletion of *adeRS* exhibited similar resistance levels to the *adeAB* deletion strain, my research supports the hypothesis that the AdeRS TCS activates expression of the *adeABC* operon²⁷. These research findings shed new light on the resistance capabilities of the AdeABC pump, questioning the views that AdeABC does not contribute towards the intrinsic resistance of *A. baumannii* and that antibacterial efflux can only occur when AdeABC is constitutively over-expressed³².

To identify the effects of the deletion of *adeRS* on the global transcriptional landscape, RNA-sequencing methodologies were employed. Numerous changes in gene transcription levels were identified including expression of *adeAB*. Additionally, other genes known to be important for virulence, such as iron sequestering and pilus assembly operons were differentially expressed. AdeR has previously been found to bind to a 10 base-pair direct repeat only found within the intergenic region between the *adeRS* and *adeABC* operons⁴¹. Genomic analyses within ATCC 17978 also support this finding. Therefore, in the *adeRS* deletion strain, aside from alterations in *adeAB* expression, the transcriptional changes in the aforementioned virulence associated genes are likely to be indirect. Interestingly, these direct/indirect transcriptional changes differed from an *adeRS* deletion mutant constructed in a different *A. baumannii* clinical isolate³⁷, emphasising that changes in the global transcriptional landscape are dependent on the isolate under investigation.

With a lack of currently effective antimicrobial treatments and a less than promising pipeline for the generation of new antibiotics, research into novel antimicrobial treatments is of significant interest. Histidine kinases of TCS are seen as attractive targets, primarily due to their presence in many pathogenic bacterial species⁴² and the absence of homologues in higher eukaryotes, including humans⁴³. A number of novel inhibitors towards some TCS regulatory cascades present across a number of clinically relevant

pathogenic bacterial species have been identified⁴²; however, no inhibitors have been recognised for TCS found within *A. baumannii*. Results from this research area have made promising leads but progress is slow and many challenges still remain⁴².

In recent decades, *A. baumannii* has fast become an extremely problematic hospital-acquired pathogen, propelled by its ability to flourish within hostile clinical environments and accrue resistance to the current armamentarium of therapeutic treatments. The AdeABC efflux system is a known contributor to the multidrug resistance phenotype displayed by this organism. My research into this system has identified that AdeAB in ATCC 17978 is functional despite the absence of AdeC and can provide intrinsic antimicrobial resistance, albeit to a limited substrate range. Antibacterial drug research efforts over recent decades have highlighted the eligibility of targeting TCS regulatory cascades for the development as an alternate therapy to treat bacterial infections. In light of this research, the AdeRS system holds particular interest due to its direct role in regulating a key aspect of multidrug resistance in many clinical *A. baumannii* isolates. Further examination into the AdeRS TCS is required, particularly identifying the activating stimuli of this system. This knowledge may be instrumental in the identification of novel inhibitors, which could aid in the future treatment of infections caused by this formidable pathogen.

References

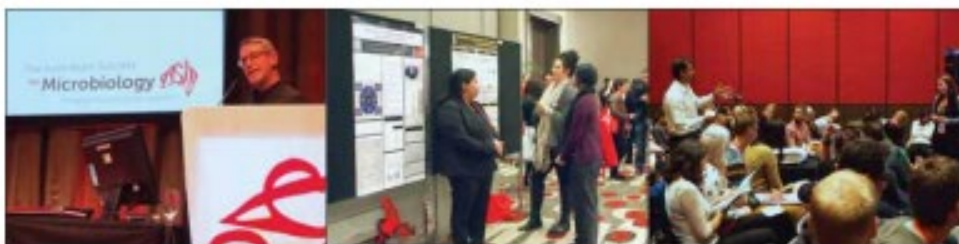
1. Bolog, A.Y. *et al.* (2008) *Acinetobacter baumannii*: emergence of a successful pathogen. *Clin. Microbiol. Rev.* **21**, 538–582. doi:10.1128/CMR.00158-07
2. Jones, R.N. (2010) Microbial etiologies of hospital-acquired bacterial pneumonia and ventilator-associated bacterial pneumonia. *Clin. Infect. Dis.* **51**, 581–587. doi:10.1093/cid/cir053
3. Severin, D.M. *et al.* (2013) Antimicrobial-resistant pathogens associated with healthcare-associated infections: summary of data reported to the National Healthcare Safety Network at the Centers for Disease Control and Prevention, 2009–2010. *Infect. Control Hosp. Epidemiol.* **34**, 1–14. doi:10.1017/S0950268812001770
4. Wong, D. *et al.* (2017) Clinical and pathophysiological overview of *Acinetobacter* infections: a century of challenges. *Clin. Microbiol. Rev.* **30**, 409–447.
5. Anstey, M.M. *et al.* (2002) Community-acquired bacteremic *Acinetobacter baumannii* pneumonia in tropical Australia is caused by diverse strains of *Acinetobacter baumannii*, with carriage in the throat in at-risk groups. *J. Clin. Microbiol.* **40**, 685–686. doi:10.1128/JCM.40.2.685-686.2002
6. Dohor, C. *et al.* (2015) Community-acquired *Acinetobacter baumannii*: clinical characteristics, epidemiology and pathogenesis. *Expert Rev. Anticancer Ther.* **15**, 567–573. doi:10.1586/14737210.2015.1025055
7. Vila, J. *et al.* (2007) Peris, efflux pumps and multidrug resistance in *Acinetobacter baumannii*. *J. Antimicrob. Chemother.* **59**, 1230–1235. doi:10.1093/jac/dk159
8. Sugimura, E. and Nikaido, H. (2012) OmpA is the principal nonspecific slow porin of *Acinetobacter baumannii*. *J. Bacteriol.* **194**, 4089–4094. doi:10.1128/JB.00435-12
9. Rautman, P.E. *et al.* (2006) Comparative genomics of multidrug resistance in *Acinetobacter baumannii*. *PLoS Genet.* **2**, e7. doi:10.1371/journal.pgen.0020007
10. Blackwell, G.A. *et al.* (2016) IncM Plasmid R1215 is the source of chromosomally located regions containing multiple antibiotic resistance genes in the globally disseminated *Acinetobacter baumannii* GC1 and GC2 clones. *ISphere* **1**, e00117–16. doi:10.1128/isphere.00117-16
11. Wright, M.S. *et al.* (2017) Transcriptome remodeling of *Acinetobacter baumannii* during infection and treatment. *Mbio* **8**, e02193-16. doi:10.1128/mbio.02193-16
12. Yoon, E.J. *et al.* (2013) RND-type efflux pumps in multidrug-resistant clinical isolates of *Acinetobacter baumannii*: major role for AdeABC overexpression and AdeRS mutations. *Antimicrob. Agents Chemother.* **57**, 2989–2995. doi:10.1128/AAC.02556-12
13. Lemos, E.V. *et al.* (2014) Carbapenem resistance and mortality in patients with *Acinetobacter baumannii* infection: systematic review and meta-analysis. *Clin. Microbiol. Infect.* **20**, 416–423. doi:10.1111/1469-0691.12353
14. World Health Organization (2017) Global priority list of antibiotic-resistant bacteria to guide research, discovery, and development of new antibiotics. <http://www.who.int/medicines/publications/global-priority-list-antibiotic-resistant-bacteria/en/>
15. Calva, E. and Ortopeda, R. (2006) Two-component signal transduction systems, environmental signals, and virulence. *Microb. Drug Resist.* **11**, 166–176. doi:10.1007/s10248-005-0087-1
16. Beier, D. and Gross, R. (2006) Regulation of bacterial virulence by two-component systems. *Curr. Opin. Microbiol.* **9**, 143–152. doi:10.1016/j.cob.2006.01.005
17. Casino, P. *et al.* (2010) The mechanism of signal transduction by two-component systems. *Curr. Opin. Struct. Biol.* **20**, 763–771. doi:10.1016/j.csb.2010.09.010
18. Kaspar, S. *et al.* (1999) The periplasmic domain of the histidine autokinase CiaA functions as a highly specific citrate receptor. *Mol. Microbiol.* **33**, 859–872. doi:10.1046/j.1365-2958.1999.01536.x
19. Zurek, E. *et al.* (1998) Furanoic regulation of gene expression in *Escherichia coli* by the DcuSR(ynfX) genes: a two-component regulatory system. *J. Bacteriol.* **180**, 5421–5425.
20. Fox, S.A. and Roberts, D.L. (1994) Signal transduction by the EnvZ-OmpK phosphotransfer system in bacteria. *Res. Microbiol.* **145**, 363–373. doi:10.1016/0923-2508(94)90001-3
21. Galpin, M.Y. (2005) A census of membrane-bound and intracellular signal transduction proteins in bacteria (bacterial IQ), eubacteria and eucobacteria. *BMC Microbiol.* **5**, 35. doi:10.1186/1471-2180-5-35
22. Lutz, M.T. *et al.* (2007) Phosphotransfer profiling: systematic mapping of two-component signal transduction pathways and phosphotransfers. *Methods Enzymol.* **423**, 533–548. doi:10.1016/S0076-6879(07)23026-5
23. Adams, M.D. *et al.* (2008) Comparative genome sequence analysis of multidrug-resistant *Acinetobacter baumannii*. *J. Bacteriol.* **190**, 8051–8064. doi:10.1128/JB.00834-08
24. Tomaras, A.P. *et al.* (2008) Characterisation of a two-component regulatory system from *Acinetobacter baumannii* that controls biofilm formation and cellular morphology. *Microbiology* **154**, 3388–3409. doi:10.1099/mic.0.2008/019471-0
25. Marchand, I. *et al.* (2004) Expression of the RND-type efflux pump AdeABC in *Acinetobacter baumannii* is regulated by the AdeRS two-component system. *Antimicrob. Agents Chemother.* **48**, 3298–3304. doi:10.1128/AAC.48.9.3298-3304.2004
26. Adams, M.D. *et al.* (2009) Resistance to colistin in *Acinetobacter baumannii* associated with mutations in the PhoAR two-component system. *Antimicrob. Agents Chemother.* **53**, 3628–3634. doi:10.1128/AAC.00284-09
27. Corqueira, G.M. *et al.* (2014) A global virulence regulator in *Acinetobacter baumannii* and its control of the phenylacetic acid catabolic pathway. *J. Infect. Dis.* **210**, 46–55. doi:10.1093/infdis/jiu224
28. Gebhardt, M.J. and Shuman, H.A. (2017) GtgA and GtgB are master regulators of antibiotic resistance, stress responses and virulence in *Acinetobacter baumannii*. *J. Bacteriol.* **199**, e00066-17. doi:10.1128/JB.00066-17
29. Tipton, K.A. and Rother, P.N. (2017) An *ompA* and *ompB* two-component system ortholog regulates phase variation, osmotic tolerance, motility, and virulence in *Acinetobacter baumannii* strain AB5075. *J. Bacteriol.* **199**, e00705-16. doi:10.1128/JB.00705-16

In Focus

30. Magnet, S. *et al.* (2011) Resistance-modulation-cell division-type efflux pump involved in aminoglycoside resistance in *Acinetobacter baumannii* strain BM4454. *Antimicrob. Agents Chemother.* **45**, 3375–3380. doi:10.1128/AAC-45.12.3375-3380.2011
31. Kazi, A. *et al.* (2007) AdeABC multidrug efflux pump is associated with decreased susceptibility to tigecycline in *Acinetobacter calcoaceticus*-*Acinetobacter baumannii* complex. *J. Antimicrob. Chemother.* **59**, 1001–1004. doi:10.1093/jac/dkq058
32. Yoon, K.J. *et al.* (2015) Contribution of resistance-modulation-cell division efflux systems to antibiotic resistance and biofilm formation in *Acinetobacter baumannii*. *MBio* **6**, e00909-15. doi:10.1128/mBio.00909-15
33. Richmond, G.E. *et al.* (2016) The *Acinetobacter baumannii* two-component system AdeRS regulates genes required for multidrug efflux, biofilm formation, and virulence in a strain-specific manner. *MBio* **7**, e00436-16.
34. Rajanathan, G. *et al.* (2010) Novel role of *Acinetobacter baumannii* RND efflux transporters in mediating decreased susceptibility to bicyclics. *J. Antimicrob. Chemother.* **65**, 228–232. doi:10.1093/jac/dkp427
35. Dai, Y. *et al.* (2015) *Acinetobacter baumannii*: evolution of antimicrobial resistance-treatment options. *Semin Respir. Crit. Care Med.* **36**, 95–98. doi:10.1053/s0894-3886(15)00388
36. Hanessey, M. *et al.* (2010) AdeABC-mediated efflux and tigecycline MICs for epidemic clones of *Acinetobacter baumannii*. *J. Antimicrob. Chemother.* **65**, 1589–1593. doi:10.1093/jac/dkq218
37. Sun, J.R. *et al.* (2012) A truncated AdeK kinase protein generated by IS_{AbdI} insertion correlates with tigecycline resistance in *Acinetobacter baumannii*. *PLoS One* **7**, e49534. doi:10.1371/journal.pone.0049534
38. Chang, T.Y. *et al.* (2016) AdeK protein regulates adeABC expression by binding to a direct-repeat motif in the intergenic space. *Microbiol. Res.* **183**, 60–67. doi:10.1016/j.micres.2015.11.010
39. Neme, A. *et al.* (2007) Relationship between the AdeABC efflux system gene content, meritacin susceptibility and multidrug resistance in a geographically diverse collection of *Acinetobacter baumannii* strains. *J. Antimicrob. Chemother.* **60**, 483–489. doi:10.1093/jac/dkm251
40. Smith, M.G. *et al.* (2007) New insights into *Acinetobacter baumannii* pathogenesis revealed by high-density pyrosequencing and transposon mutagenesis. *Genes Dev.* **21**, 601–614. doi:10.1301/jgd.1510307
41. Thomson, P. and Kay, R. (2000) Bacterial signal transduction via histidine-aspartate phosphorylation. *J. Cell Sci.* **113**, 3141–3150.
42. Ben, A.E. *et al.* (2015) Bacterial histidine kinases as novel antibacterial drug targets. *ACS Chem. Biol.* **10**, 213–224. doi:10.1021/acschembio.5b00735

Biography

Felise Adams is a PhD candidate from Flinders University, Adelaide, Australia, who is working under the supervision of Professor Melissa H Brown. Her research interests include molecular genetics, particularly gene regulation and antibiotic resistance strategies of pathogenic bacterial species.



ASM Membership

Some benefits of ASM membership:

- Access to hard copies of ASM'S official journal, *Microbiology Australia*, published 4 times per year
- Reduced registration fees for ASM annual scientific meeting and other affiliated conferences
- Professional development and networking opportunities
- Eligibility to apply for many ASM awards for researchers, teachers, students, early career scientists and clinical laboratory scientists

Contact:

Kara Taglieri
ASM National Office, 9/397 Smith Street, Fitzroy, Vic. 3065
Tel: 1300 656 423
Email: admin@theasm.com.au



Appendix G – List of Abbreviations

A	Adenine
ABC	(Adenosine triphosphate) binding cassette
Acb	<i>A. calcoaceticus</i> - <i>A. baumannii</i>
Ade	<i>Acinetobacter</i> drug efflux
AMP	Ampicillin
ATP	Adenosine triphosphate
BAP	Biofilm-associated protein
BAP _{Ab}	Biofilm-associated protein of <i>Acinetobacter baumannii</i>
Blastn	Basic local alignment search tool for nucleotide sequences
bp	Base pair
CA	Catalytic ATP-binding domain
°C	Degree Celsius
CDART	Conserved domain architecture retrieval tool
cDNA	Complimentary deoxyribonucleic acid
CDS	Coding sequence
CFU	Colony forming units
CHX	Chlorhexidine
CHL	Chloramphenicol
DAPI	4',6-diamidino-2-phenylindole
dH ₂ O	Distilled H ₂ O
DNA	Deoxyribonucleic acid
DR	Direct repeat
ERY	Erythromycin
Fur	Ferric uptake regulator
GAF	c-GMP-specific and c-GMP-stimulated phosphodiesterases, Anabaena adenylate cyclases and <i>Escherichia coli</i> FhlA
GEI	Genomic island
GEO	Gene expression omnibus
GEN	Gentamicin
HAMP	Histidine kinases, adenylyl cyclases, methyl-accepting chemotaxis proteins, and phosphatases domain
HATPase	Histidine kinase-, DNA gyrase-B-, and HSP90-like ATPase
HGT	Horizontal gene transfer
HHK	Hybrid histidine kinase
HisKA	Histidine phosphotransfer kinase A

HK	Histidine kinase
H-NS	Histone-like nucleoid-structuring
Hpt	Histidine phosphotransfer
HTH	Helix-turn-helix
ICU	Intensive care unit
IC	International clonal lineage
IHF	Integration host factor
IRL	Inverted repeat left
IRR	Inverted repeat right
IS	Insertion sequence
kb	Kilo base
KL	Capsular biosynthesis locus
LB	Lysogeny broth
LOS	Lipooligosaccharides
MATE	Multidrug and toxic compound extrusion
MDR	Multidrug resistant
MFP	Membrane fusion protein
MFS	Major facilitator superfamily
MGE	Mobile genetic element
mg/L	Miligram per litre
MH	Mueller-Hinton
MHA	Mueller-Hinton agar
MIC	Minimal inhibitory concentration
mL	Millilitre
MITE	Miniature inverted-repeat transposable element
MLST	Multi-locus sequence typing
mM	Millimolar
mm	Millimetre
mRNA	Messenger ribonucleic acid
NCBI	National center for biotechnology information
ND	Not determined
nm	nanometres
OD	Optical density
OMP	Outer membrane porin
Omp _A _{Ab}	Outer membrane protein A of <i>Acinetobacter baumannii</i>
ON	Overnight

ORF	Open reading frame
<i>P</i>	Probability value
PAS	Per-Arnt-Sim domain
PBS	Phosphate buffered saline
PCR	Polymerase chain reaction
PACE	Proteobacterial antimicrobial compound efflux
PFGE	Pulsed-field gel electrophoresis
PNAG	poly- β -(1-6)- <i>N</i> -acetylglucosamine
qRT-PCR	Quantative reverse transcription polymerase chain reaction
^R	Resistant
rDNA	Ribosomal deoxyribonucleic acid
REC	Receiver domain
RNA	Ribonucleic acid
RNA-seq	RNA sequencing
RND	Resistance-nodulation-cell division
ROS	Reactive oxygen species
rpm	Rotations per minute
RR	Response regulator
SD	Standard deviation
SEM	Standard error of the mean
SLC	Solute carrier domain
SMART	Simple modular architecture research tool
SNP	Single nucleotide polymorphism
sp.	Species
STAC	SLC and (two component signal transduction system)-associated component
T	Thymine
T6SS	Type VI secretion system
TCS	Two component signal transduction system
TET	Tetracycline
TIR	Terminal inverted repeat
TM	Transmembrane
Tn	Transposon
UT	Untreated
w/v	Weight/volume
WGS	Whole genome sequencing
WT	Wildtype

μg	Microgram
μL	Microlitre
μM	Micromolar

CHAPTER 7: References

- Abergel, C., Blanc, G., Monchois, V., Renesto, P., Sigoillot, C., Ogata, H., *et al.* (2006) Impact of the excision of an ancient repeat insertion on *Rickettsia conorii* guanylate kinase activity. *Mol Biol Evol* **23**, 2112-22.
- Abramson, J., and Wright, E. M. (2009) Structure and function of Na⁺-symporters with inverted repeats. *Curr Opin Struct Biol* **19**, 425-32.
- Adams-Haduch, J. M., Onuoha, E. O., Bogdanovich, T., Tian, G. B., Marschall, J., Urban, C. M., *et al.* (2011) Molecular epidemiology of carbapenem-nonsusceptible *Acinetobacter baumannii* in the United States. *J Clin Microbiol* **49**, 3849-54.
- Adams, M. D., Bishop, B., and Wright, M. S. (2016) Quantitative assessment of insertion sequence impact on bacterial genome architecture. *Microb Genom* **2**, e000062.
- Adams, M. D., Chan, E. R., Molyneaux, N. D., and Bonomo, R. A. (2010) Genomewide analysis of divergence of antibiotic resistance determinants in closely related isolates of *Acinetobacter baumannii*. *Antimicrob Agents Chemother* **54**, 3569-77.
- Adams, M. D., Goglin, K., Molyneaux, N., Hujer, K. M., Lavender, H., Jamison, J. J., *et al.* (2008) Comparative genome sequence analysis of multidrug-resistant *Acinetobacter baumannii*. *J Bacteriol* **190**, 8053-64.
- Adams, M. D., Nickel, G. C., Bajaksouzian, S., Lavender, H., Murthy, A. R., Jacobs, M. R., *et al.* (2009) Resistance to colistin in *Acinetobacter baumannii* associated with mutations in the PmrAB two-component system. *Antimicrob Agents Chemother* **53**, 3628-34.
- Adebali, O., Ortega, D. R., and Zhulin, I. B. (2015) CDvist: a webserver for identification and visualization of conserved domains in protein sequences. *Bioinformatics* **31**, 1475-7.
- Adegoke, A. A., Mvuyo, T., and Okoh, A. I. (2012) Ubiquitous *Acinetobacter* species as beneficial commensals but gradually being emboldened with antibiotic resistance genes. *J Basic Microbiol* **52**, 620-7.
- Agrawal, R., Pandey, A., Rajankar, M. P., Dixit, N. M., and Saini, D. K. (2015) The two-component signalling networks of *Mycobacterium tuberculosis* display extensive cross-talk *in vitro*. *Biochem J* **469**, 121-34.
- Ainsaar, K., Mumm, K., Ilves, H., and Horak, R. (2014) The ColRS signal transduction system responds to the excess of external zinc, iron, manganese, and cadmium. *BMC Microbiol* **14**, 162.
- Al Atrouni, A., Joly-Guillou, M. L., Hamze, M., and Kempf, M. (2016) Reservoirs of non-*baumannii* *Acinetobacter* species. *Front Microbiol* **7**, 49.
- Ali, S. S., Xia, B., Liu, J., and Navarre, W. W. (2012) Silencing of foreign DNA in bacteria. *Curr Opin Microbiol* **15**, 175-81.
- Altting-Mees, M. A., and Short, J. M. (1989) pBluescript II: gene mapping vectors. *Nucleic Acids Res* **17**, 9494.
- Altschul, S. F., Gish, W., Miller, W., Myers, E. W., and Lipman, D. J. (1990) Basic local alignment search tool. *J Mol Biol* **215**, 403-10.

- Álvarez-Fraga, L., Pérez, A., Rumbo-Feal, S., Merino, M., Vallejo, J. A., Ohneck, E. J., *et al.* (2016) Analysis of the role of the LH92_11085 gene of a biofilm hyper-producing *Acinetobacter baumannii* strain on biofilm formation and attachment to eukaryotic cells. *Virulence* **7**, 443-55.
- Álvarez-Fraga, L., Vázquez-Ucha, J. C., Martínez-Gutián, M., Vallejo, J. A., Bou, G., Beceiro, A., *et al.* (2018) Pneumonia infection in mice reveals the involvement of the *feoA* gene in the pathogenesis of *Acinetobacter baumannii*. *Virulence* **9**, 496-509.
- Amos, H., and Vollmayer, E. (1957) Effect of pentamidine on the growth of *Escherichia coli*. *J Bacteriol* **73**, 172-7.
- Ansaldi, F., Canepa, P., Bassetti, M., Zancolli, M., Molinari, M. P., Talamini, A., *et al.* (2011) Sequential outbreaks of multidrug-resistant *Acinetobacter baumannii* in intensive care units of a tertiary referral hospital in Italy: combined molecular approach for epidemiological investigation. *J Hosp Infect* **79**, 134-40.
- Antunes, L. C., Imperi, F., Carattoli, A., and Visca, P. (2011a) Deciphering the multifactorial nature of *Acinetobacter baumannii* pathogenicity. *PLoS One* **6**, e22674.
- Antunes, L. C., Imperi, F., Towner, K. J., and Visca, P. (2011b) Genome-assisted identification of putative iron-utilization genes in *Acinetobacter baumannii* and their distribution among a genotypically diverse collection of clinical isolates. *Res Microbiol* **162**, 279-84.
- Appleby, J. L., Parkinson, J. S., and Bourret, R. B. (1996) Signal transduction via the multi-step phosphorelay: not necessarily a road less traveled. *Cell* **86**, 845-8.
- Aranda, J., Bardina, C., Beceiro, A., Rumbo, S., Cabral, M. P., Barbe, J., *et al.* (2011) *Acinetobacter baumannii* RecA protein in repair of DNA damage, antimicrobial resistance, general stress response, and virulence. *J Bacteriol* **193**, 3740-7.
- Aravind, L., Iyer, L. M., Leipe, D. D., and Koonin, E. V. (2004) A novel family of P-loop NTPases with an unusual phyletic distribution and transmembrane segments inserted within the NTPase domain. *Genome Biol* **5**, R30.
- Aravind, L., and Ponting, C. P. (1999) The cytoplasmic helical linker domain of receptor histidine kinase and methyl-accepting proteins is common to many prokaryotic signalling proteins. *FEMS Microbiol Lett* **176**, 111-6.
- Arroyo, L. A., Herrera, C. M., Fernandez, L., Hankins, J. V., Trent, M. S., and Hancock, R. E. (2011) The *pmrCAB* operon mediates polymyxin resistance in *Acinetobacter baumannii* ATCC 17978 and clinical isolates through phosphoethanolamine modification of lipid A. *Antimicrob Agents Chemother* **55**, 3743-51.
- Baikalov, I., Schroder, I., Kaczor-Grzeskowiak, M., Grzeskowiak, K., Gunsalus, R. P., and Dickerson, R. E. (1996) Structure of the *Escherichia coli* response regulator NarL. *Biochemistry* **35**, 11053-61.
- Baker, M. D., Wolanin, P. M., and Stock, J. B. (2006) Signal transduction in bacterial chemotaxis. *Bioessays* **28**, 9-22.
- Barbe, V., Vallenet, D., Fonknechten, N., Kreimeyer, A., Oztas, S., Labarre, L., *et al.* (2004) Unique features revealed by the genome sequence of *Acinetobacter* sp.

- ADP1, a versatile and naturally transformation competent bacterium. *Nucleic Acids Res* **32**, 5766-79.
- Barlow, M.** (2009) What antimicrobial resistance has taught us about horizontal gene transfer. *Methods Mol Biol* **532**, 397-411.
- Batchelor, J. D., Lee, P. S., Wang, A. C., Doucleff, M., and Wemmer, D. E.** (2013) Structural mechanism of GAF-regulated σ^{54} activators from *Aquifex aeolicus*. *J Mol Biol* **425**, 156-70.
- Baumann, P.** (1968) Isolation of *Acinetobacter* from soil and water. *J Bacteriol* **96**, 39-42.
- Beceiro, A., Llobet, E., Aranda, J., Bengoechea, J. A., Doumith, M., Hornsey, M., et al.** (2011) Phosphoethanolamine modification of lipid A in colistin-resistant variants of *Acinetobacter baumannii* mediated by the *pmrAB* two-component regulatory system. *Antimicrob Agents Chemother* **55**, 3370-9.
- Beceiro, A., Moreno, A., Fernandez, N., Vallejo, J. A., Aranda, J., Adler, B., et al.** (2014) Biological cost of different mechanisms of colistin resistance and their impact on virulence in *Acinetobacter baumannii*. *Antimicrob Agents Chemother* **58**, 518-26.
- Bem, A. E., Velikova, N., Pellicer, M. T., Baarlen, P., Marina, A., and Wells, J. M.** (2015) Bacterial histidine kinases as novel antibacterial drug targets. *ACS Chem Biol* **10**, 213-24.
- Bentancor, L. V., O'Malley, J. M., Bozkurt-Guzel, C., Pier, G. B., and Maira-Litrán, T.** (2012) Poly-N-acetyl- β -(1-6)-glucosamine is a target for protective immunity against *Acinetobacter baumannii* infections. *Infect Immun* **80**, 651-6.
- Bergogne-Bérézin, E., and Towner, K. J.** (1996) *Acinetobacter* spp. as nosocomial pathogens: microbiological, clinical, and epidemiological features. *Clin Microbiol Rev* **9**, 148-65.
- Berlau, J., Aucken, H., Malnick, H., and Pitt, T.** (1999) Distribution of *Acinetobacter* species on skin of healthy humans. *Eur J Clin Microbiol Infect Dis* **18**, 179-83.
- Bertels, F., and Rainey, P. B.** (2011) Within-genome evolution of REPINs: a new family of miniature mobile DNA in bacteria. *PLoS Genet* **7**, e1002132.
- Bertini, A., Poirel, L., Mugnier, P. D., Villa, L., Nordmann, P., and Carattoli, A.** (2010) Characterization and PCR-based replicon typing of resistance plasmids in *Acinetobacter baumannii*. *Antimicrob Agents Chemother* **54**, 4168-77.
- Bhuiyan, M. S., Ellett, F., Murray, G. L., Kostoulias, X., Cerqueira, G. M., Schulze, K. E., et al.** (2016) *Acinetobacter baumannii* phenylacetic acid metabolism influences infection outcome through a direct effect on neutrophil chemotaxis. *Proc Natl Acad Sci U S A* **113**, 9599-604.
- Bingle, L. E., Bailey, C. M., and Pallen, M. J.** (2008) Type VI secretion: a beginner's guide. *Curr Opin Microbiol* **11**, 3-8.
- Biondi, E. G., Skerker, J. M., Arif, M., Prasol, M. S., Perchuk, B. S., and Laub, M. T.** (2006) A phosphorelay system controls stalk biogenesis during cell cycle progression in *Caulobacter crescentus*. *Mol Microbiol* **59**, 386-401.
- Blackwell, G. A., Hamidian, M., and Hall, R. M.** (2016a) IncM plasmid R1215 is the source of chromosomally located regions containing multiple antibiotic resistance

genes in the globally disseminated *Acinetobacter baumannii* GC1 and GC2 clones. *mSphere* **1**, e00117-16.

- Blackwell, G. A., Nigro, S. J., and Hall, R. M.** (2016b) Evolution of AbGRI2-0, the progenitor of the AbGRI2 resistance island in global clone 2 of *Acinetobacter baumannii*. *Antimicrob Agents Chemother* **60**, 1421-9.
- Blaschke, U., Suwono, B., Zafari, S., Ebersberger, I., Skiebe, E., Jeffries, C. M., et al.** (2018) Recombinant production of A1S_0222 from *Acinetobacter baumannii* ATCC 17978 and confirmation of its DNA-(adenine N6)-methyltransferase activity. *Protein Expr Purif* **151**, 78-85.
- Blaschke, U., and Wilharm, G.** (2017) Complete genome sequence of *Acinetobacter* sp. strain NCu2D-2 isolated from a mouse. *Genome Announc* **5**, e01415-16.
- Boinett, C. J., Cain, A. K., Hawkey, J., Do Hoang, N. T., Khanh, N. N. T., Thanh, D. P., et al.** (2019) Clinical and laboratory-induced colistin-resistance mechanisms in *Acinetobacter baumannii*. *Microb Genom* **5**, e000246.
- Boll, J. M., Tucker, A. T., Klein, D. R., Beltran, A. M., Brodbelt, J. S., Davies, B. W., et al.** (2015) Reinforcing lipid A acylation on the cell surface of *Acinetobacter baumannii* promotes cationic antimicrobial peptide resistance and desiccation survival. *MBio* **6**, e00478-15.
- Bonnin, R. A., Poirel, L., and Nordmann, P.** (2012) AbaR-type transposon structures in *Acinetobacter baumannii*. *J Antimicrob Chemother* **67**, 234-6.
- Boucher, Y., Labbate, M., Koenig, J. E., and Stokes, H. W.** (2007) Integrons: mobilizable platforms that promote genetic diversity in bacteria. *Trends Microbiol* **15**, 301-9.
- Bouillet, S., Genest, O., Méjean, V., and Iobbi-Nivol, C.** (2017) Protection of the general stress response σ^S factor by the CrsR regulator allows a rapid and efficient adaptation of *Shewanella oneidensis*. *J Biol Chem* **292**, 14921-8.
- Bourret, R. B.** (2010) Receiver domain structure and function in response regulator proteins. *Curr Opin Microbiol* **13**, 142-9.
- Bouvet, P. J., and Grimont, P. A.** (1987) Identification and biotyping of clinical isolates of *Acinetobacter*. *Ann Inst Pasteur Microbiol* **138**, 569-78.
- Bouvet, P. J. M., and Grimont, P. A. D.** (1986) Taxonomy of the Genus *Acinetobacter* with the recognition of *Acinetobacter baumannii* sp. nov., *Acinetobacter haemolyticus* sp. nov., *Acinetobacter johnsonii* sp. nov., and *Acinetobacter junii* sp. nov. and emended descriptions of *Acinetobacter calcoaceticus* and *Acinetobacter lwoffii*. *Int J Syst Bacteriol* **36**, 228-40.
- Branda, S. S., Vik, S., Friedman, L., and Kolter, R.** (2005) Biofilms: the matrix revisited. *Trends Microbiol* **13**, 20-6.
- Breisch, J., Waclawska, I., and Averhoff, B.** (2019) Identification and characterization of a carnitine transporter in *Acinetobacter baumannii*. *Microbiologyopen* **8**, e00752.
- Brown, M. H., and Skurray, R. A.** (2001) Staphylococcal multidrug efflux protein QacA. *J Mol Microbiol Biotechnol* **3**, 163-70.
- Brügger, K., Redder, P., She, Q., Confalonieri, F., Zivanovic, Y., and Garrett, R. A.** (2002) Mobile elements in archaeal genomes. *FEMS Microbiol Lett* **206**, 131-41.

- Brügger, K., Torarinsson, E., Redder, P., Chen, L., and Garrett, R. A.** (2004) Shuffling of *Sulfolobus* genomes by autonomous and non-autonomous mobile elements. *Biochem Soc Trans* **32**, 179-83.
- Buisine, N., Tang, C. M., and Chalmers, R.** (2002) Transposon-like Correia elements: structure, distribution and genetic exchange between pathogenic *Neisseria* sp. *FEBS Lett* **522**, 52-8.
- Cabral, M. P., Soares, N. C., Aranda, J., Parreira, J. R., Rumbo, C., Poza, M., et al.** (2011) Proteomic and functional analyses reveal a unique lifestyle for *Acinetobacter baumannii* biofilms and a key role for histidine metabolism. *J Proteome Res* **10**, 3399-417.
- Cai, S. J., and Inouye, M.** (2002) EnvZ-OmpR interaction and osmoregulation in *Escherichia coli*. *J Biol Chem* **277**, 24155-61.
- Cai, Y., Chai, D., Wang, R., Liang, B., and Bai, N.** (2012) Colistin resistance of *Acinetobacter baumannii*: clinical reports, mechanisms and antimicrobial strategies. *J Antimicrob Chemother* **67**, 1607-15.
- Camarena, L., Bruno, V., Euskirchen, G., Poggio, S., and Snyder, M.** (2010) Molecular mechanisms of ethanol-induced pathogenesis revealed by RNA-sequencing. *PLoS Pathog* **6**, e1000834.
- Cambray, G., Guerout, A. M., and Mazel, D.** (2010) Integrons. *Annu Rev Genet* **44**, 141-66.
- Capra, E. J., Perchuk, B. S., Ashenberg, O., Seid, C. A., Snow, H. R., Skerker, J. M., et al.** (2012) Spatial tethering of kinases to their substrates relaxes evolutionary constraints on specificity. *Mol Microbiol* **86**, 1393-403.
- Carrano, C. J., and Raymond, K. N.** (1979) Ferric ion sequestering agents. 2. Kinetics and mechanism of iron removal from transferrin by enterobactin and synthetic tricatechols. *J Am Chem Soc* **101**, 5401-4.
- Carruthers, M. D., Nicholson, P. A., Tracy, E. N., and Munson, R. S., Jr.** (2013) *Acinetobacter baumannii* utilizes a type VI secretion system for bacterial competition. *PLoS One* **8**, e59388.
- Cartron, M. L., Maddocks, S., Gillingham, P., Craven, C. J., and Andrews, S. C.** (2006) Feo--transport of ferrous iron into bacteria. *Biometals* **19**, 143-57.
- Casella, L. G., Weiss, A., Pérez-Rueda, E., Ibarra, J. A., and Shaw, L. N.** (2017) Towards the complete proteinaceous regulome of *Acinetobacter baumannii*. *Microb Genom* **3**, mgen000107.
- Casino, P., Rubio, V., and Marina, A.** (2009) Structural insight into partner specificity and phosphoryl transfer in two-component signal transduction. *Cell* **139**, 325-36.
- Casino, P., Rubio, V., and Marina, A.** (2010) The mechanism of signal transduction by two-component systems. *Curr Opin Struct Biol* **20**, 763-71.
- Cassat, J. E., and Skaar, E. P.** (2013) Iron in infection and immunity. *Cell Host Microbe* **13**, 509-19.
- Catalano, M., Quelle, L. S., JERIC, P. E., Di Martino, A., and Maimone, S. M.** (1999) Survival of *Acinetobacter baumannii* on bed rails during an outbreak and during sporadic cases. *J Hosp Infect* **42**, 27-35.

- Cerqueira, G. M., Kostoulias, X., Khoo, C., Aibinu, I., Qu, Y., Traven, A., *et al.* (2014) A global virulence regulator in *Acinetobacter baumannii* and its control of the phenylacetic acid catabolic pathway. *J Infect Dis* **210**, 46-55.
- Chambonnier, G., Roux, L., Redelberger, D., Fadel, F., Filloux, A., Sivaneson, M., *et al.* (2016) The hybrid histidine kinase LadS forms a multicomponent signal transduction system with the GacS/GacA two-component system in *Pseudomonas aeruginosa*. *PLoS Genet* **12**, e1006032.
- Chandler, M., and Fayet, O. (1993) Translational frameshifting in the control of transposition in bacteria. *Mol Microbiol* **7**, 497-503.
- Chang, T. Y., Huang, B. J., Sun, J. R., Perng, C. L., Chan, M. C., Yu, C. P., *et al.* (2016) AdeR protein regulates *adeABC* expression by binding to a direct-repeat motif in the intercistronic spacer. *Microbiol Res* **183**, 60-7.
- Chang, Y. W., Rettberg, L. A., Ortega, D. R., and Jensen, G. J. (2017) *In vivo* structures of an intact type VI secretion system revealed by electron cryotomography. *EMBO Rep* **18**, 1090-9.
- Chau, S. L., Chu, Y. W., and Houang, E. T. (2004) Novel resistance-nodulation-cell division efflux system AdeDE in *Acinetobacter* genomic DNA group 3. *Antimicrob Agents Chemother* **48**, 4054-5.
- Chen, R., Lv, R., Xiao, L., Wang, M., Du, Z., Tan, Y., *et al.* (2017) A1S_2811, a CheA/Y-like hybrid two-component regulator from *Acinetobacter baumannii* ATCC17978, is involved in surface motility and biofilm formation in this bacterium. *Microbiologyopen* **6**, e510.
- Chen, Y., Zhou, F., Li, G., and Xu, Y. (2009) MUST: a system for identification of miniature inverted-repeat transposable elements and applications to *Anabaena variabilis* and *Haloquadratum walsbyi*. *Gene* **436**, 1-7.
- Chin, C. Y., Tipton, K. A., Farokhyfar, M., Burd, E. M., Weiss, D. S., and Rather, P. N. (2018) A high-frequency phenotypic switch links bacterial virulence and environmental survival in *Acinetobacter baumannii*. *Nat Microbiol* **3**, 563-9.
- Chitsaz, M., and Brown, M. H. (2017) The role played by drug efflux pumps in bacterial multidrug resistance. *Essays Biochem* **61**, 127-39.
- Choi, A. H., Slamti, L., Avci, F. Y., Pier, G. B., and Maira-Litrán, T. (2009) The *pgaABCD* locus of *Acinetobacter baumannii* encodes the production of poly- β -1-6-*N*-acetylglucosamine, which is critical for biofilm formation. *J Bacteriol* **191**, 5953-63.
- Choi, C. H., Hyun, S. H., Lee, J. Y., Lee, J. S., Lee, Y. S., Kim, S. A., *et al.* (2008a) *Acinetobacter baumannii* outer membrane protein A targets the nucleus and induces cytotoxicity. *Cell Microbiol* **10**, 309-19.
- Choi, C. H., Lee, E. Y., Lee, Y. C., Park, T. I., Kim, H. J., Hyun, S. H., *et al.* (2005) Outer membrane protein 38 of *Acinetobacter baumannii* localizes to the mitochondria and induces apoptosis of epithelial cells. *Cell Microbiol* **7**, 1127-38.
- Choi, C. H., Lee, J. S., Lee, Y. C., Park, T. I., and Lee, J. C. (2008b) *Acinetobacter baumannii* invades epithelial cells and outer membrane protein A mediates interactions with epithelial cells. *BMC Microbiol* **8**, 216.

- Chopra, T., Marchaim, D., Johnson, P. C., Awali, R. A., Doshi, H., Chalana, I., et al.** (2014) Risk factors and outcomes for patients with bloodstream infection due to *Acinetobacter baumannii-calcoaceticus* complex. *Antimicrob Agents Chemother* **58**, 4630-5.
- Chuanchuen, R., Narasaki, C. T., and Schweizer, H. P.** (2002) The MexJK efflux pump of *Pseudomonas aeruginosa* requires OprM for antibiotic efflux but not for efflux of triclosan. *J Bacteriol* **184**, 5036-44.
- Chusri, S., Chongsuvivatwong, V., Rivera, J. I., Silpapojakul, K., Singkhamanan, K., McNeil, E., et al.** (2014) Clinical outcomes of hospital-acquired infection with *Acinetobacter nosocomialis* and *Acinetobacter pittii*. *Antimicrob Agents Chemother* **58**, 4172-9.
- Cianfanelli, F. R., Monlezun, L., and Coulthurst, S. J.** (2016) Aim, load, fire: the type VI secretion system, a bacterial nanoweapon. *Trends Microbiol* **24**, 51-62.
- Clemmer, K. M., Bonomo, R. A., and Rather, P. N.** (2011) Genetic analysis of surface motility in *Acinetobacter baumannii*. *Microbiology* **157**, 2534-44.
- Cock, P. J., and Whitworth, D. E.** (2007) Evolution of prokaryotic two-component system signaling pathways: gene fusions and fissions. *Mol Biol Evol* **24**, 2355-7.
- Collis, C. M., and Hall, R. M.** (1992) Gene cassettes from the insert region of integrons are excised as covalently closed circles. *Mol Microbiol* **6**, 2875-85.
- Conrad, R. S., Wulf, R. G., and Clay, D. L.** (1979) Effects of carbon sources on antibiotic resistance in *Pseudomonas aeruginosa*. *Antimicrob Agents Chemother* **15**, 59-66.
- Correia, F. F., Inouye, S., and Inouye, M.** (1986) A 26-base-pair repetitive sequence specific for *Neisseria gonorrhoeae* and *Neisseria meningitidis* genomic DNA. *J Bacteriol* **167**, 1009-15.
- Correia, F. F., Inouye, S., and Inouye, M.** (1988) A family of small repeated elements with some transposon-like properties in the genome of *Neisseria gonorrhoeae*. *J Biol Chem* **263**, 12194-8.
- Corvec, S., Caroff, N., Espaze, E., Giraudeau, C., Drugeon, H., and Reynaud, A.** (2003) AmpC cephalosporinase hyperproduction in *Acinetobacter baumannii* clinical strains. *J Antimicrob Chemother* **52**, 629-35.
- Corvec, S., Poirel, L., Naas, T., Drugeon, H., and Nordmann, P.** (2007) Genetics and expression of the carbapenem-hydrolyzing oxacillinase gene *bla_{OXA-23}* in *Acinetobacter baumannii*. *Antimicrob Agents Chemother* **51**, 1530-3.
- Cosgaya, C., Mari-Almirall, M., Van Assche, A., Fernandez-Orth, D., Mosqueda, N., Telli, M., et al.** (2016) *Acinetobacter dijkschoorniae* sp. nov., a member of the *Acinetobacter calcoaceticus-Acinetobacter baumannii* complex mainly recovered from clinical samples in different countries. *Int J Syst Evol Microbiol* **66**, 4105-11.
- Coyne, S., Courvalin, P., and Perichon, B.** (2011) Efflux-mediated antibiotic resistance in *Acinetobacter* spp. *Antimicrob Agents Chemother* **55**, 947-53.
- Coyne, S., Rosenfeld, N., Lambert, T., Courvalin, P., and Perichon, B.** (2010) Overexpression of resistance-nodulation-cell division pump AdeFGH confers

multidrug resistance in *Acinetobacter baumannii*. *Antimicrob Agents Chemother* **54**, 4389-93.

- Crooks, G. E., Hon, G., Chandonia, J. M., and Brenner, S. E.** (2004) WebLogo: a sequence logo generator. *Genome Res* **14**, 1188-11890.
- Cucarella, C., Solano, C., Valle, J., Amorena, B., Lasa, I., and Penadés, J. R.** (2001) Bap, a *Staphylococcus aureus* surface protein involved in biofilm formation. *J Bacteriol* **183**, 2888-96.
- Cuthbertson, L., and Nodwell, J. R.** (2013) The TetR family of regulators. *Microbiol Mol Biol Rev* **77**, 440-75.
- Damier-Piolle, L., Magnet, S., Bremont, S., Lambert, T., and Courvalin, P.** (2008) AdeIJK, a resistance-nodulation-cell division pump effluxing multiple antibiotics in *Acinetobacter baumannii*. *Antimicrob Agents Chemother* **52**, 557-62.
- Damo, S. M., Kehl-Fie, T. E., Sugitani, N., Holt, M. E., Rathi, S., Murphy, W. J., et al.** (2013) Molecular basis for manganese sequestration by calprotectin and roles in the innate immune response to invading bacterial pathogens. *Proc Natl Acad Sci U S A* **110**, 3841-6.
- Daniel, C., Haentjens, S., Bissinger, M. C., and Courcol, R. J.** (1999) Characterization of the *Acinetobacter baumannii* Fur regulator: cloning and sequencing of the *fur* homolog gene. *FEMS Microbiol Lett* **170**, 199-209.
- David, S. A., Bechtel, B., Annaiah, C., Mathan, V. I., and Balaram, P.** (1994) Interaction of cationic amphiphilic drugs with lipid A: implications for development of endotoxin antagonists. *Biochim Biophys Acta* **1212**, 167-75.
- Davis, K. A., Moran, K. A., McAllister, C. K., and Gray, P. J.** (2005) Multidrug-resistant *Acinetobacter* extremity infections in soldiers. *Emerg Infect Dis* **11**, 1218-24.
- de Been, M., Bart, M. J., Abee, T., Siezen, R. J., and Francke, C.** (2008) The identification of response regulator-specific binding sites reveals new roles of two-component systems in *Bacillus cereus* and closely related low-GC Gram-positives. *Environ Microbiol* **10**, 2796-809.
- de Breij, A., Gaddy, J., van der Meer, J., Koning, R., Koster, A., van den Broek, P., et al.** (2009) CsuA/BABCDE-dependent pili are not involved in the adherence of *Acinetobacter baumannii* ATCC19606(T) to human airway epithelial cells and their inflammatory response. *Res Microbiol* **160**, 213-8.
- De Gregorio, E., Abrescia, C., Carlomagno, M. S., and Di Nocera, P. P.** (2002) The abundant class of nemis repeats provides RNA substrates for ribonuclease III in *Neisseriae*. *Biochim Biophys Acta* **1576**, 39-44.
- De Gregorio, E., Abrescia, C., Carlomagno, M. S., and Di Nocera, P. P.** (2003) Asymmetrical distribution of *Neisseria* miniature insertion sequence DNA repeats among pathogenic and nonpathogenic *Neisseria* strains. *Infect Immun* **71**, 4217-21.
- De Gregorio, E., Del Franco, M., Martinucci, M., Roscetto, E., Zarrilli, R., and Di Nocera, P. P.** (2015) Biofilm-associated proteins: news from *Acinetobacter*. *BMC Genomics* **16**, 933.

- De Silva, P. M., and Kumar, A.** (2017) Effect of sodium chloride on surface-associated motility of *Acinetobacter baumannii* and the role of AdeRS two-component system. *J Membr Biol* **251**, 5-13.
- De Silva, P. M., and Kumar, A.** (2019) Signal transduction proteins in *Acinetobacter baumannii*: role in antibiotic resistance, virulence, and potential as drug targets. *Front Microbiol* **10**, 49.
- Delihhas, N.** (2007) Enterobacterial small mobile sequences carry open reading frames and are found intragenically- evolutionary implications for formation of new peptides. *Gene Regul Syst Bio* **1**, 191-205.
- Delihhas, N.** (2008) Small mobile sequences in bacteria display diverse structure/function motifs. *Mol Microbiol* **67**, 475-81.
- Delihhas, N.** (2011) Impact of small repeat sequences on bacterial genome evolution. *Genome Biol Evol* **3**, 959-73.
- Deutscher, J., and Saier, M. H., Jr.** (2005) Ser/Thr/Tyr protein phosphorylation in bacteria - for long time neglected, now well established. *J Mol Microbiol Biotechnol* **9**, 125-31.
- Deveson Lucas, D., Crane, B., Wright, A., Han, M. L., Moffatt, J., Bulach, D., et al.** (2018) Emergence of high-level colistin resistance in an *Acinetobacter baumannii* clinical isolate mediated by inactivation of the global regulator H-NS. *Antimicrob Agents Chemother* **62**, e02442-17.
- Dexter, C., Murray, G. L., Paulsen, I. T., and Peleg, A. Y.** (2015) Community-acquired *Acinetobacter baumannii*: clinical characteristics, epidemiology and pathogenesis. *Expert Rev Anti Infect Ther* **13**, 567-73.
- Diancourt, L., Passet, V., Nemec, A., Dijkshoorn, L., and Brisse, S.** (2010) The population structure of *Acinetobacter baumannii*: expanding multiresistant clones from an ancestral susceptible genetic pool. *PLoS One* **5**, e10034.
- Dijkshoorn, L., Aucken, H., Gerner-Smidt, P., Janssen, P., Kaufmann, M. E., Garaizar, J., et al.** (1996) Comparison of outbreak and nonoutbreak *Acinetobacter baumannii* strains by genotypic and phenotypic methods. *J Clin Microbiol* **34**, 1519-25.
- Dijkshoorn, L., Nemec, A., and Seifert, H.** (2007) An increasing threat in hospitals: multidrug-resistant *Acinetobacter baumannii*. *Nat Rev Microbiol* **5**, 939-51.
- Dintner, S., Heermann, R., Fang, C., Jung, K., and Gebhard, S.** (2014) A sensory complex consisting of an ATP-binding cassette transporter and a two-component regulatory system controls bacitracin resistance in *Bacillus subtilis*. *J Biol Chem* **289**, 27899-910.
- Dobrindt, U., Hochhut, B., Hentschel, U., and Hacker, J.** (2004) Genomic islands in pathogenic and environmental microorganisms. *Nat Rev Microbiol* **2**, 414-24.
- Domingues, S., da Silva, G. J., and Nielsen, K. M.** (2012) Integrons: Vehicles and pathways for horizontal dissemination in bacteria. *Mob Genet Elements* **2**, 211-23.
- Domingues, S., Nielsen, K. M., and da Silva, G. J.** (2011) The *bla*IMP-5-carrying integron in a clinical *Acinetobacter baumannii* strain is flanked by miniature

- inverted-repeat transposable elements (MITEs). *J Antimicrob Chemother* **66**, 2667-8.
- Domingues, S., Toleman, M. A., Nielsen, K. M., and da Silva, G. J.** (2013) Identical miniature inverted repeat transposable elements flank class 1 integrons in clinical isolates of *Acinetobacter* spp. *J Clin Microbiol* **51**, 2382-4.
- Doolittle, W. F., Kirkwood, T. B., and Dempster, M. A.** (1984) Selfish DNAs with self-restraint. *Nature* **307**, 501-2.
- Dorman, C. J.** (2007) H-NS, the genome sentinel. *Nat Rev Microbiol* **5**, 157-61.
- Dorsey, C. W., Tomaras, A. P., and Actis, L. A.** (2002) Genetic and phenotypic analysis of *Acinetobacter baumannii* insertion derivatives generated with a transposome system. *Appl Environ Microbiol* **68**, 6353-60.
- Dortay, H., Gruhn, N., Pfeifer, A., Schwerdtner, M., Schmulling, T., and Heyl, A.** (2008) Toward an interaction map of the two-component signaling pathway of *Arabidopsis thaliana*. *J Proteome Res* **7**, 3649-60.
- Dragoš, A., and Kovács, A. T.** (2017) The peculiar functions of the bacterial extracellular matrix. *Trends Microbiol* **25**, 257-66.
- Ducus-Mowchun, K., De Silva, P., Crisostomo, L., Fernando, D., Chao, T., et al.** (2019) Next generation of Tn7-based single-copy insertion elements for use in multi- and pan-drug-resistant strains of *Acinetobacter baumannii*. *Appl Environ Microbiol* **85**, e00066-19.
- Durand, E., Cambillau, C., Cascales, E., and Journet, L.** (2014) VgrG, Tae, Tle, and beyond: the versatile arsenal of Type VI secretion effectors. *Trends Microbiol* **22**, 498-507.
- Durante-Mangoni, E., and Zarrilli, R.** (2011) Global spread of drug-resistant *Acinetobacter baumannii*: molecular epidemiology and management of antimicrobial resistance. *Future Microbiol* **6**, 407-22.
- Dutta, R., and Inouye, M.** (1996) Reverse phosphotransfer from OmpR to EnvZ in a kinase-/phosphatase+ mutant of EnvZ (EnvZ.N347D), a bifunctional signal transducer of *Escherichia coli*. *J Biol Chem* **271**, 1424-9.
- Eijkelkamp, B. A.** (2011). *Factors contributing to the success of Acinetobacter baumannii as a human pathogen*. PhD thesis, Flinders University of South Australia.
- Eijkelkamp, B. A., Hassan, K. A., Paulsen, I. T., and Brown, M. H.** (2011a) Investigation of the human pathogen *Acinetobacter baumannii* under iron limiting conditions. *BMC Genomics* **12**, 126.
- Eijkelkamp, B. A., Stroehrer, U. H., Hassan, K. A., Elbourne, L. D., Paulsen, I. T., and Brown, M. H.** (2013) H-NS plays a role in expression of *Acinetobacter baumannii* virulence features. *Infect Immun* **81**, 2574-83.
- Eijkelkamp, B. A., Stroehrer, U. H., Hassan, K. A., Papadimitriou, M. S., Paulsen, I. T., and Brown, M. H.** (2011b) Adherence and motility characteristics of clinical *Acinetobacter baumannii* isolates. *FEMS Microbiol Lett* **323**, 44-51.
- Eijkelkamp, B. A., Stroehrer, U. H., Hassan, K. A., Paulsen, I. T., and Brown, M. H.** (2014) Comparative analysis of surface-exposed virulence factors of *Acinetobacter baumannii*. *BMC Genomics* **15**, 1020.

- Elgaml, A., and Miyoshi, S.** (2015) Role of the histone-like nucleoid structuring protein (H-NS) in the regulation of virulence factor expression and stress response in *Vibrio vulnificus*. *Biocontrol Sci* **20**, 263-74.
- Enriquez, R., Abad, R., Chanto, G., Corso, A., Cruces, R., Gabastou, J. M., et al.** (2010) Deletion of the Correia element in the *mtr* gene complex of *Neisseria meningitidis*. *J Med Microbiol* **59**, 1055-60.
- Erickson, M. G., Ulijasz, A. T., and Weisblum, B.** (2005) Bacterial 2-component signal transduction systems: a fluorescence polarization screen for response regulator-protein binding. *J Biomol Screen* **10**, 270-4.
- Espinal, P., Marti, S., and Vila, J.** (2012) Effect of biofilm formation on the survival of *Acinetobacter baumannii* on dry surfaces. *J Hosp Infect* **80**, 56-60.
- Eveillard, M., Kempf, M., Belmonte, O., Pailhories, H., and Joly-Guillou, M. L.** (2013) Reservoirs of *Acinetobacter baumannii* outside the hospital and potential involvement in emerging human community-acquired infections. *Int J Infect Dis* **17**, e802-5.
- Eyre, D. W., Golubchik, T., Gordon, N. C., Bowden, R., Piazza, P., Batty, E. M., et al.** (2012) A pilot study of rapid benchtop sequencing of *Staphylococcus aureus* and *Clostridium difficile* for outbreak detection and surveillance. *BMJ Open* **2**.
- Eze, E. C., Chenia, H. Y., and El Zowalaty, M. E.** (2018) *Acinetobacter baumannii* biofilms: effects of physicochemical factors, virulence, antibiotic resistance determinants, gene regulation, and future antimicrobial treatments. *Infect Drug Resist* **11**, 2277-99.
- Ezraty, B., and Barras, F.** (2016) The 'liaisons dangereuses' between iron and antibiotics. *FEMS Microbiol Rev* **40**, 418-35.
- Farrow, J. M., 3rd, Wells, G., and Pesci, E. C.** (2018) Desiccation tolerance in *Acinetobacter baumannii* is mediated by the two-component response regulator BfmR. *PLoS One* **13**, e0205638.
- Farrugia, D. N., Elbourne, L. D., Hassan, K. A., Eijkelkamp, B. A., Tetu, S. G., Brown, M. H., et al.** (2013) The complete genome and phenome of a community-acquired *Acinetobacter baumannii*. *PLoS One* **8**, e58628.
- Fattash, I., Rooke, R., Wong, A., Hui, C., Luu, T., Bhardwaj, P., et al.** (2013) Miniature inverted-repeat transposable elements: discovery, distribution, and activity. *Genome* **56**, 475-86.
- Feng, Y.** (2003) Plant MITEs: useful tools for plant genetics and genomics. *Geno Prot Bioinfo* **1**, 90-9.
- Feng, Y., Yang, P., Wang, X., and Zong, Z.** (2016) Characterization of *Acinetobacter johnsonii* isolate XBB1 carrying nine plasmids and encoding NDM-1, OXA-58 and PER-1 by genome sequencing. *J Antimicrob Chemother* **71**, 71-5.
- Fernando, D. M., Xu, W., Loewen, P. C., Zhanel, G. G., and Kumar, A.** (2014) Triclosan can select for an AdeIJK overexpressing mutant of *Acinetobacter baumannii* ATCC17978 that displays reduced susceptibility to multiple antibiotics. *Antimicrob Agents Chemother* **58**, 6424-31.

- Ferris, H. U., Dunin-Horkawicz, S., Mondejar, L. G., Hulko, M., Hantke, K., Martin, J., et al.** (2011) The mechanisms of HAMP-mediated signaling in transmembrane receptors. *Structure* **19**, 378-85.
- Fisher, S. L., Kim, S. K., Wanner, B. L., and Walsh, C. T.** (1996) Kinetic comparison of the specificity of the vancomycin resistance VanS for two response regulators, VanR and PhoB. *Biochemistry* **35**, 4732-40.
- Fitzsimons, T. C., Lewis, J. M., Wright, A., Kleifeld, O., Schittenhelm, R. B., Powell, D., et al.** (2018) Identification of novel *Acinetobacter baumannii* type VI secretion system antibacterial effector and immunity pairs. *Infect Immun* **86**, e00297.
- Fluman, N., Adler, J., Rotenberg, S. A., Brown, M. H., and Bibi, E.** (2014) Export of a single drug molecule in two transport cycles by a multidrug efflux pump. *Nat Commun* **5**, 4615.
- Fomenkov, A., Vincze, T., Degtyarev, S. K., and Roberts, R. J.** (2017) Complete genome sequence and methylome analysis of *Acinetobacter calcoaceticus* 65. *Genome Announc* **5**, e00060-17.
- Fournier, P. E., Vallenet, D., Barbe, V., Audic, S., Ogata, H., Poirel, L., et al.** (2006) Comparative genomics of multidrug resistance in *Acinetobacter baumannii*. *PLoS Genet* **2**, e7.
- Fralick, J. A.** (1996) Evidence that TolC is required for functioning of the Mar/AcrAB efflux pump of *Escherichia coli*. *J Bacteriol* **178**, 5803-5.
- Francis, V. I., Waters, E. M., Finton-James, S. E., Gori, A., Kadioglu, A., Brown, A. R., et al.** (2018) Multiple communication mechanisms between sensor kinases are crucial for virulence in *Pseudomonas aeruginosa*. *Nat Commun* **9**, 2219.
- Fricke, W. F., and Rasko, D. A.** (2014) Bacterial genome sequencing in the clinic: bioinformatic challenges and solutions. *Nat Rev Genet* **15**, 49-55.
- Gaddy, J. A., Arivett, B. A., McConnell, M. J., Lopez-Rojas, R., Pachon, J., and Actis, L. A.** (2012) Role of acinetobactin-mediated iron acquisition functions in the interaction of *Acinetobacter baumannii* strain ATCC 19606T with human lung epithelial cells, *Galleria mellonella* caterpillars, and mice. *Infect Immun* **80**, 1015-24.
- Gaddy, J. A., Tomaras, A. P., and Actis, L. A.** (2009) The *Acinetobacter baumannii* 19606 OmpA protein plays a role in biofilm formation on abiotic surfaces and in the interaction of this pathogen with eukaryotic cells. *Infect Immun* **77**, 3150-60.
- Gallagher, L. A., Lee, S. A., and Manoel, C.** (2017) Importance of core genome functions for an extreme antibiotic resistance trait. *MBio* **8**, e01655-17.
- Gallagher, L. A., Ramage, E., Weiss, E. J., Radey, M., Hayden, H. S., Held, K. G., et al.** (2015) Resources for genetic and genomic analysis of emerging pathogen *Acinetobacter baumannii*. *J Bacteriol* **197**, 2027-35.
- Galperin, M. Y.** (2005) A census of membrane-bound and intracellular signal transduction proteins in bacteria: bacterial IQ, extroverts and introverts. *BMC Microbiol* **5**, 35.
- Galperin, M. Y.** (2006) Structural classification of bacterial response regulators: diversity of output domains and domain combinations. *J Bacteriol* **188**, 4169-82.

- Galperin, M. Y.** (2010) Diversity of structure and function of response regulator output domains. *Curr Opin Microbiol* **13**, 150-9.
- Gao, R., Mack, T. R., and Stock, A. M.** (2007) Bacterial response regulators: versatile regulatory strategies from common domains. *Trends Biochem Sci* **32**, 225-34.
- Gao, R., and Stock, A. M.** (2009) Biological insights from structures of two-component proteins. *Annu Rev Microbiol* **63**, 133-54.
- García Véscovi, E., Soncini, F. C., and Groisman, E. A.** (1996) Mg²⁺ as an extracellular signal: environmental regulation of *Salmonella* virulence. *Cell* **84**, 165-74.
- Gauthier, J. D., Jones, M. K., Thiaville, P., Joseph, J. L., Swain, R. A., Krediet, C. J., et al.** (2010) Role of GacA in virulence of *Vibrio vulnificus*. *Microbiology* **156**, 3722-33.
- Gayoso, C. M., Mateos, J., Méndez, J. A., Fernández-Puente, P., Rumbo, C., Tomás, M., et al.** (2014) Molecular mechanisms involved in the response to desiccation stress and persistence in *Acinetobacter baumannii*. *J Proteome Res* **13**, 460-76.
- Gebhardt, M. J., Gallagher, L. A., Jacobson, R. K., Usacheva, E. A., Peterson, L. R., Zurawski, D. V., et al.** (2015) Joint transcriptional control of virulence and resistance to antibiotic and environmental stress in *Acinetobacter baumannii*. *MBio* **6**, e01660-15.
- Geer, L. Y., Domrachev, M., Lipman, D. J., and Bryant, S. H.** (2002) CDART: protein homology by domain architecture. *Genome Res* **12**, 1619-23.
- Geisinger, E., and Isberg, R. R.** (2015) Antibiotic modulation of capsular exopolysaccharide and virulence in *Acinetobacter baumannii*. *PLoS Pathog* **11**, e1004691.
- Geisinger, E., Mortman, N. J., Vargas-Cuebas, G., Tai, A. K., and Isberg, R. R.** (2018) A global regulatory system links virulence and antibiotic resistance to envelope homeostasis in *Acinetobacter baumannii*. *PLoS Pathog* **14**, e1007030.
- Gerson, S., Nowak, J., Zander, E., Ertel, J., Wen, Y., Krut, O., et al.** (2018) Diversity of mutations in regulatory genes of resistance-nodulation-cell division efflux pumps in association with tigecycline resistance in *Acinetobacter baumannii*. *J Antimicrob Chemother* **73**, 1501-8.
- Ghosh, S., and O'Connor, T. J.** (2017) Beyond paralogs: the multiple layers of redundancy in bacterial pathogenesis. *Front Cell Infect Microbiol* **7**, 467.
- Giammanco, A., Calà, C., Fasciana, T., and Dowzicky, M. J.** (2017) Global assessment of the activity of tigecycline against multidrug-resistant Gram-negative pathogens between 2004 and 2014 as part of the tigecycline evaluation and surveillance trial. *mSphere* **2**, e00310-16.
- Gil-Marqués, M. L., Moreno-Martinez, P., Costas, C., Pachón, J., Blázquez, J., and McConnell, M. J.** (2018) Peptidoglycan recycling contributes to intrinsic resistance to fosfomicin in *Acinetobacter baumannii*. *J Antimicrob Chemother* **73**, 2960-8.
- Giles, S. K., Stroehrer, U. H., Eijkelkamp, B. A., and Brown, M. H.** (2015) Identification of genes essential for pellicle formation in *Acinetobacter baumannii*. *BMC Microbiol* **15**, 116.

- Gillings, M. R., Labbate, M., Sajjad, A., Giguere, N. J., Holley, M. P., and Stokes, H. W.** (2009) Mobilization of a Tn402-like class 1 integron with a novel cassette array via flanking miniature inverted-repeat transposable element-like structures. *Appl Environ Microbiol* **75**, 6002-4.
- Ginalski, K., Kinch, L., Rychlewski, L., and Grishin, N. V.** (2004) BOF: a novel family of bacterial OB-fold proteins. *FEBS Lett* **567**, 297-301.
- Goh, H. M., Beatson, S. A., Totsika, M., Moriel, D. G., Phan, M. D., Szubert, J., et al.** (2013) Molecular analysis of the *Acinetobacter baumannii* biofilm-associated protein. *Appl Environ Microbiol* **79**, 6535-43.
- Gohl, O., Friedrich, A., Hoppert, M., and Averhoff, B.** (2006) The thin pili of *Acinetobacter* sp. strain BD413 mediate adhesion to biotic and abiotic surfaces. *Appl Environ Microbiol* **72**, 1394-401.
- Gotoh, Y., Doi, A., Furuta, E., Dubrac, S., Ishizaki, Y., Okada, M., et al.** (2010) Novel antibacterial compounds specifically targeting the essential WalR response regulator. *J Antibiot* **63**, 127-34.
- Greene, C., Wu, J., Rickard, A. H., and Xi, C.** (2016) Evaluation of the ability of *Acinetobacter baumannii* to form biofilms on six different biomedical relevant surfaces. *Lett Appl Microbiol* **63**, 233-9.
- Hamidian, M., Ambrose, S. J., and Hall, R. M.** (2016a) A large conjugative *Acinetobacter baumannii* plasmid carrying the *sul2* sulphonamide and *strAB* streptomycin resistance genes. *Plasmid* **87-88**, 43-50.
- Hamidian, M., and Hall, R. M.** (2011) AbaR4 replaces AbaR3 in a carbapenem-resistant *Acinetobacter baumannii* isolate belonging to global clone 1 from an Australian hospital. *J Antimicrob Chemother* **66**, 2484-91.
- Hamidian, M., and Hall, R. M.** (2014) pACICU2 is a conjugative plasmid of *Acinetobacter* carrying the aminoglycoside resistance transposon Tn ϕ A6. *J Antimicrob Chemother* **69**, 1146-8.
- Hamidian, M., Holt, K. E., and Hall, R. M.** (2015) Genomic resistance island AGI1 carrying a complex class 1 integron in a multiply antibiotic-resistant ST25 *Acinetobacter baumannii* isolate. *J Antimicrob Chemother* **70**, 2519-23.
- Hamidian, M., Holt, K. E., Pickard, D., and Hall, R. M.** (2016b) A small *Acinetobacter* plasmid carrying the *tet39* tetracycline resistance determinant. *J Antimicrob Chemother* **71**, 269-71.
- Hamidian, M., Kenyon, J. J., Holt, K. E., Pickard, D., and Hall, R. M.** (2014) A conjugative plasmid carrying the carbapenem resistance gene *blaOXA-23* in AbaR4 in an extensively resistant GC1 *Acinetobacter baumannii* isolate. *J Antimicrob Chemother* **69**, 2625-8.
- Hamm, R. E., Shull Jr., C. M., and Grant, D. M.** (1953) Citrate complexes with iron(II) and iron(III). *J Am Chem Soc* **76**, 2111-4.
- Hanahan, D.** (1983) Studies on transformation of *Escherichia coli* with plasmids. *J Mol Biol* **166**, 557-80.
- Hancock, C. N., Zhang, F., and Wessler, S. R.** (2010) Transposition of the *Tourist*-MITE *mPing* in yeast: an assay that retains key features of catalysis by the class 2 PIF/Harbinger superfamily. *Mob DNA* **1**, 5.

- Harding, C. M., Hennon, S. W., and Feldman, M. F.** (2018) Uncovering the mechanisms of *Acinetobacter baumannii* virulence. *Nat Rev Microbiol* **16**, 91-102.
- Harding, C. M., Nasr, M. A., Kinsella, R. L., Scott, N. E., Foster, L. J., Weber, B. S., et al.** (2015) *Acinetobacter* strains carry two functional oligosaccharyl-transferases, one devoted exclusively to type IV pilin, and the other one dedicated to *O*-glycosylation of multiple proteins. *Mol Microbiol* **96**, 1023-41.
- Harding, C. M., Pulido, M. R., Di Venanzio, G., Kinsella, R. L., Webb, A. I., Scott, N. E., et al.** (2017) Pathogenic *Acinetobacter* species have a functional type I secretion system and contact-dependent inhibition systems. *J Biol Chem* **292**, 9075-87.
- Harding, C. M., Tracy, E. N., Carruthers, M. D., Rather, P. N., Actis, L. A., and Munson, R. S., Jr.** (2013) *Acinetobacter baumannii* strain M2 produces type IV pili which play a role in natural transformation and twitching motility but not surface-associated motility. *MBio* **4**, e00360-13.
- Haren, L., Ton-Hoang, B., and Chandler, M.** (1999) Integrating DNA: transposases and retroviral integrases. *Annu Rev Microbiol* **53**, 245-81.
- Hartman, J. L. t., Garvik, B., and Hartwell, L.** (2001) Principles for the buffering of genetic variation. *Science* **291**, 1001-4.
- Hassan, K. A., Brzoska, A. J., Wilson, N. L., Eijkelkamp, B. A., Brown, M. H., and Paulsen, I. T.** (2011) Roles of DHA2 family transporters in drug resistance and iron homeostasis in *Acinetobacter* spp. *J Mol Microbiol Biotechnol* **20**, 116-24.
- Hassan, K. A., Cain, A. K., Huang, T., Liu, Q., Elbourne, L. D., Boinett, C. J., et al.** (2016) Fluorescence-based flow sorting in parallel with transposon insertion site sequencing identifies multidrug efflux systems in *Acinetobacter baumannii*. *MBio* **7**, e01200-16.
- Hassan, K. A., Jackson, S. M., Penesyan, A., Patching, S. G., Tetu, S. G., Eijkelkamp, B. A., et al.** (2013) Transcriptomic and biochemical analyses identify a family of chlorhexidine efflux proteins. *Proc Natl Acad Sci USA* **110**, 20254-9.
- Hassan, K. A., Liu, Q., Henderson, P. J., and Paulsen, I. T.** (2015) Homologs of the *Acinetobacter baumannii* AceI transporter represent a new family of bacterial multidrug efflux systems. *MBio* **6**, e01982-14.
- Hassan, K. A., Pederick, V. G., Elbourne, L. D., Paulsen, I. T., Paton, J. C., McDevitt, C. A., et al.** (2017) Zinc stress induces copper depletion in *Acinetobacter baumannii*. *BMC Microbiol* **17**, 59.
- Hawkey, J.** (2017). *Dynamics of insertion sequences in bacterial genomes*. PhD thesis, The University of Melbourne.
- Heath, C. H., Orrell, T. C., Lee, R. C., Pearman, J. W., McCullough, C., and Christiansen, K. J.** (2003) A review of the Royal Perth Hospital Bali experience: an infection control perspective. *Australian Infection Control* **8**, 43-6.
- Henig, O., Weber, G., Hoshen, M. B., Paul, M., German, L., Neuberger, A., et al.** (2015) Risk factors for and impact of carbapenem-resistant *Acinetobacter baumannii* colonization and infection: matched case-control study. *Eur J Clin Microbiol Infect Dis* **34**, 2063-8.

- Henrichsen, J.** (1984) Not gliding but twitching motility of *Acinetobacter calcoaceticus*. *J Clin Pathol* **37**, 102-3.
- Henry, J. T., and Crosson, S.** (2011) Ligand-binding PAS domains in a genomic, cellular, and structural context. *Annu Rev Microbiol* **65**, 261-86.
- Henry, R., Crane, B., Powell, D., Deveson Lucas, D., Li, Z., Aranda, J., et al.** (2015) The transcriptomic response of *Acinetobacter baumannii* to colistin and doripenem alone and in combination in an *in vitro* pharmacokinetics/pharmacodynamics model. *J Antimicrob Chemother* **70**, 1303-13.
- Héritier, C., Poirel, L., and Nordmann, P.** (2006) Cephalosporinase over-expression resulting from insertion of IS*Abal* in *Acinetobacter baumannii*. *Clin Microbiol Infect* **12**, 123-30.
- Higgins, P. G., Dammhayn, C., Hackel, M., and Seifert, H.** (2010) Global spread of carbapenem-resistant *Acinetobacter baumannii*. *J Antimicrob Chemother* **65**, 233-8.
- Higgins, P. G., Hujer, A. M., Hujer, K. M., Bonomo, R. A., and Seifert, H.** (2012) Interlaboratory reproducibility of DiversiLab rep-PCR typing and clustering of *Acinetobacter baumannii* isolates. *J Med Microbiol* **61**, 137-41.
- Higgins, P. G., Prior, K., Harmsen, D., and Seifert, H.** (2017) Development and evaluation of a core genome multilocus typing scheme for whole-genome sequence-based typing of *Acinetobacter baumannii*. *PLoS One* **12**, e0179228.
- Hoang, T. T., Karkhoff-Schweizer, R. R., Kutchma, A. J., and Schweizer, H. P.** (1998) A broad-host-range FLP-FRT recombination system for site-specific excision of chromosomally-located DNA sequences: application for isolation of unmarked *Pseudomonas aeruginosa* mutants. *Gene* **212**, 77-86.
- Hoch, J. A.** (2000) Two-component and phosphorelay signal transduction. *Curr Opin Microbiol* **3**, 165-70.
- Hood, M. I., Mortensen, B. L., Moore, J. L., Zhang, Y., Kehl-Fie, T. E., Sugitani, N., et al.** (2012) Identification of an *Acinetobacter baumannii* zinc acquisition system that facilitates resistance to calprotectin-mediated zinc sequestration. *PLoS Pathog* **8**, e1003068.
- Hood, M. I., and Skaar, E. P.** (2012) Nutritional immunity: transition metals at the pathogen-host interface. *Nat Rev Microbiol* **10**, 525-37.
- Hu, D., Liu, B., Dijkshoorn, L., Wang, L., and Reeves, P. R.** (2013) Diversity in the major polysaccharide antigen of *Acinetobacter baumannii* assessed by DNA sequencing, and development of a molecular serotyping scheme. *PLoS One* **8**, e70329.
- Hug, I., and Feldman, M. F.** (2011) Analogies and homologies in lipopolysaccharide and glycoprotein biosynthesis in bacteria. *Glycobiology* **21**, 138-51.
- Hülter, N., Ilhan, J., Wein, T., Kadibalban, A. S., Hammerschmidt, K., and Dagan, T.** (2017) An evolutionary perspective on plasmid lifestyle modes. *Curr Opin Microbiol* **38**, 74-80.

- Hunger, M., Schmucker, R., Kishan, V., and Hillen, W.** (1990) Analysis and nucleotide sequence of an origin of DNA replication in *Acinetobacter calcoaceticus* and its use for *Escherichia coli* shuttle plasmids. *Gene* **87**, 45-51.
- Iacono, M., Villa, L., Fortini, D., Bordoni, R., Imperi, F., Bonnal, R. J., et al.** (2008) Whole-genome pyrosequencing of an epidemic multidrug-resistant *Acinetobacter baumannii* strain belonging to the European clone II group. *Antimicrob Agents Chemother* **52**, 2616-25.
- Illegheems, K., De Vuyst, L., and Weckx, S.** (2013) Complete genome sequence and comparative analysis of *Acetobacter pasteurianus* 386B, a strain well-adapted to the cocoa bean fermentation ecosystem. *BMC Genomics* **14**, 526.
- Imperi, F., Antunes, L. C., Blom, J., Villa, L., Iacono, M., Visca, P., et al.** (2011) The genomics of *Acinetobacter baumannii*: insights into genome plasticity, antimicrobial resistance and pathogenicity. *IUBMB Life* **63**, 1068-74.
- Itou, H., and Tanaka, I.** (2001) The OmpR-family of proteins: insight into the tertiary structure and functions of two-component regulator proteins. *J Biochem* **129**, 343-50.
- Iwashkiw, J. A., Seper, A., Weber, B. S., Scott, N. E., Vinogradov, E., Stratilo, C., et al.** (2012) Identification of a general O-linked protein glycosylation system in *Acinetobacter baumannii* and its role in virulence and biofilm formation. *PLoS Pathog* **8**, e1002758.
- Izaguirre-Mayoral, M. L., Lazarovits, G., and Baral, B.** (2018) Ureide metabolism in plant-associated bacteria: purine plant-bacteria interactive scenarios under nitrogen deficiency. *Plant and Soil* **428**, 1-34.
- Jacobs, A. C., Thompson, M. G., Black, C. C., Kessler, J. L., Clark, L. P., McQueary, C. N., et al.** (2014) AB5075, a highly virulent isolate of *Acinetobacter baumannii*, as a model strain for the evaluation of pathogenesis and antimicrobial treatments. *MBio* **5**, e01076-14.
- Jamet, A., and Nassif, X.** (2015) New players in the toxin field: polymorphic toxin systems in bacteria. *MBio* **6**, e00285-15.
- Jawad, A., Seifert, H., Snelling, A. M., Heritage, J., and Hawkey, P. M.** (1998) Survival of *Acinetobacter baumannii* on dry surfaces: comparison of outbreak and sporadic isolates. *J Clin Microbiol* **36**, 1938-41.
- Jenal, U., and Galperin, M. Y.** (2009) Single domain response regulators: molecular switches with emerging roles in cell organization and dynamics. *Curr Opin Microbiol* **12**, 152-60.
- Jiang, J. H., Hassan, K. A., Begg, S. L., Rupasinghe, T. W. T., Naidu, V., Pederick, V. G., et al.** (2019) Identification of novel *Acinetobacter baumannii* host fatty acid stress adaptation strategies. *MBio* **10**, e02056-18.
- Juárez-Rodríguez, M. D., Torres-Escobar, A., and Demuth, D. R.** (2013) *ygiW* and *qseBC* are co-expressed in *Aggregatibacter actinomycetemcomitans* and regulate biofilm growth. *Microbiology* **159**, 989-1001.
- Juhas, M., van der Meer, J. R., Gaillard, M., Harding, R. M., Hood, D. W., and Crook, D. W.** (2009) Genomic islands: tools of bacterial horizontal gene transfer and evolution. *FEMS Microbiol Rev* **33**, 376-93.

- Kalivoda, E. J., Horzempa, J., Stella, N. A., Sadaf, A., Kowalski, R. P., Nau, G. J., et al.** (2011) New vector tools with a hygromycin resistance marker for use with opportunistic pathogens. *Mol Biotechnol* **48**, 7-14.
- Kanehisa, M., Sato, Y., Kawashima, M., Furumichi, M., and Tanabe, M.** (2016) KEGG as a reference resource for gene and protein annotation. *Nucleic Acids Res* **44**, D457-62.
- Kaniga, K., Delor, I., and Cornelis, G. R.** (1991) A wide-host-range suicide vector for improving reverse genetics in Gram-negative bacteria: inactivation of the *blaA* gene of *Yersinia enterocolitica*. *Gene* **109**, 137-41.
- Karaiskos, I., Galani, L., Baziaka, F., and Giamarellou, H.** (2013) Intraventricular and intrathecal colistin as the last therapeutic resort for the treatment of multidrug-resistant and extensively drug-resistant *Acinetobacter baumannii* ventriculitis and meningitis: a literature review. *Int J Antimicrob Agents* **41**, 499-508.
- Kee, C., Junqueira, A. C. M., Uchida, A., Purbojati, R. W., Houghton, J. N. I., Chenard, C., et al.** (2018) Complete genome sequence of *Acinetobacter schindleri* SGAir0122 isolated from Singapore air. *Genome Announc* **6**.
- Kentache, T., Ben Abdelkrim, A., Jouenne, T., De, E., and Hardouin, J.** (2017) Global dynamic proteome study of a pellicle-forming *Acinetobacter baumannii* strain. *Mol Cell Proteomics* **16**, 100-12.
- Kenyon, J. J., and Hall, R. M.** (2013) Variation in the complex carbohydrate biosynthesis loci of *Acinetobacter baumannii* genomes. *PLoS One* **8**, e62160.
- Kenyon, J. J., Shneider, M. M., Senchenkova, S. N., Shashkov, A. S., Siniagina, M. N., Malanin, S. Y., et al.** (2016) K19 capsular polysaccharide of *Acinetobacter baumannii* is produced via a Wzy polymerase encoded in a small genomic island rather than the KL19 capsule gene cluster. *Microbiology* **162**, 1479-89.
- Kholodii, G., Mindlin, S., Gorlenko, Z., Petrova, M., Hobman, J., and Nikiforov, V.** (2004) Translocation of transposition-deficient (Tn^d PKLH2-like) transposons in the natural environment: mechanistic insights from the study of adjacent DNA sequences. *Microbiology* **150**, 979-92.
- Khorchid, A., and Ikura, M.** (2006) Bacterial histidine kinase as signal sensor and transducer. *Int J Biochem Cell Biol* **38**, 307-12.
- Kim, D. H., and Ko, K. S.** (2015) IS*Aba15* inserted into outer membrane protein gene *carO* in *Acinetobacter baumannii*. *J Bacteriol Virol* **45**, 51-3.
- Kim, S. W., Choi, C. H., Moon, D. C., Jin, J. S., Lee, J. H., Shin, J. H., et al.** (2009) Serum resistance of *Acinetobacter baumannii* through the binding of factor H to outer membrane proteins. *FEMS Microbiol Lett* **301**, 224-31.
- Kleckner, N.** (1990) Regulation of transposition in bacteria. *Annu Rev Cell Biol* **6**, 297-327.
- Klein, B. A., Chen, T., Scott, J. C., Koenigsberg, A. L., Duncan, M. J., and Hu, L. T.** (2015) Identification and characterization of a minisatellite contained within a novel miniature inverted-repeat transposable element (MITE) of *Porphyromonas gingivalis*. *Mob DNA* **6**, 18.

- Knauf, G. A., Cunningham, A. L., Kazi, M. I., Riddington, I. M., Crofts, A. A., Cattoir, V., et al.** (2018) Exploring the antimicrobial action of quaternary amines against *Acinetobacter baumannii*. *MBio* **9**, e02394-17.
- Kohler, T., van Delden, C., Curty, L. K., Hamzehpour, M. M., and Pechere, J. C.** (2001) Overexpression of the MexEF-OprN multidrug efflux system affects cell-to-cell signaling in *Pseudomonas aeruginosa*. *J Bacteriol* **183**, 5213-22.
- Koretke, K. K., Lupas, A. N., Warren, P. V., Rosenberg, M., and Brown, J. R.** (2000) Evolution of two-component signal transduction. *Mol Biol Evol* **17**, 1956-70.
- Korycinski, M., Albrecht, R., Ursinus, A., Hartmann, M. D., Coles, M., Martin, J., et al.** (2015) STAC- A new domain associated with transmembrane solute transport and two-component signal transduction systems. *J Mol Biol* **427**, 3327-39.
- Koteva, K., Hong, H. J., Wang, X. D., Nazi, I., Hughes, D., Naldrett, M. J., et al.** (2010) A vancomycin photoprobe identifies the histidine kinase VanSsc as a vancomycin receptor. *Nat Chem Biol* **6**, 327-9.
- Krahn, T., Wibberg, D., Maus, I., Winkler, A., Bontron, S., Sczyrba, A., et al.** (2016) Intraspecies transfer of the chromosomal *Acinetobacter baumannii* bla_{NDM-1} carbapenemase gene. *Antimicrob Agents Chemother* **60**, 3032-40.
- Krawczyk, B., and Kur, J.** (1998) *In vitro* interaction of the IHF-like proteins *Acinetobacter junii* and *Proteus vulgaris* with *ihf* sites. *FEMS Microbiol Lett* **161**, 187-92.
- Kreamer, N. N., Costa, F., and Newman, D. K.** (2015) The ferrous iron-responsive BqsRS two-component system activates genes that promote cationic stress tolerance. *MBio* **6**, e02549.
- Krizova, L., Dijkshoorn, L., and Nemec, A.** (2011) Diversity and evolution of AbaR genomic resistance islands in *Acinetobacter baumannii* strains of European clone I. *Antimicrob Agents Chemother* **55**, 3201-6.
- Kröger, C., Kary, S. C., Schauer, K., and Cameron, A. D.** (2016) Genetic regulation of virulence and antibiotic resistance in *Acinetobacter baumannii*. *Genes* **8**, 12.
- Kröger, C., MacKenzie, K. D., Alshabib, E. Y., Kirzinger, M. W. B., Suchan, D. M., Chao, T. C., et al.** (2018) The primary transcriptome, small RNAs and regulation of antimicrobial resistance in *Acinetobacter baumannii* ATCC 17978. *Nucleic Acids Res* **46**, 9684-98.
- Kumar, A., and Schweizer, H. P.** (2005) Bacterial resistance to antibiotics: active efflux and reduced uptake. *Adv Drug Deliv Rev* **57**, 1486-513.
- Kuo, S. C., Chang, S. C., Wang, H. Y., Lai, J. F., Chen, P. C., Shiau, Y. R., et al.** (2012) Emergence of extensively drug-resistant *Acinetobacter baumannii* complex over 10 years: nationwide data from the Taiwan Surveillance of Antimicrobial Resistance (TSAR) program. *BMC Infect Dis* **12**, 200.
- La, M. V., Jureen, R., Lin, R. T., and Teo, J. W.** (2014) Unusual detection of an *Acinetobacter* class D carbapenemase gene, bla_{OXA-23}, in a clinical *Escherichia coli* isolate. *J Clin Microbiol* **52**, 3822-3.

- Lassak, J., Henche, A. L., Binnenkade, L., and Thormann, K. M.** (2010) ArcS, the cognate sensor kinase in an atypical Arc system of *Shewanella oneidensis* MR-1. *Appl Environ Microbiol* **76**, 3263-74.
- Laub, M. T., Biondi, E. G., and Skerker, J. M.** (2007) Phosphotransfer profiling: systematic mapping of two-component signal transduction pathways and phosphorelays. *Methods Enzymol* **423**, 531-48.
- Lean, S. S., and Yeo, C. C.** (2017) Small, enigmatic plasmids of the nosocomial pathogen, *Acinetobacter baumannii*: good, bad, who knows? *Front Microbiol* **8**, 1547.
- Lean, S. S., Yeo, C. C., Suhaili, Z., and Thong, K. L.** (2015) Comparative genomics of two ST 195 carbapenem-resistant *Acinetobacter baumannii* with different susceptibility to polymyxin revealed underlying resistance mechanism. *Front Microbiol* **6**, 1445.
- Lee, C. R., Lee, J. H., Park, M., Park, K. S., Bae, I. K., Kim, Y. B., et al.** (2017) Biology of *Acinetobacter baumannii*: pathogenesis, antibiotic resistance mechanisms, and prospective treatment options. *Front Cell Infect Microbiol* **7**, 55.
- Lee, H. Y., Chang, R. C., Su, L. H., Liu, S. Y., Wu, S. R., Chuang, C. H., et al.** (2012a) Wide spread of Tn2006 in an AbaR4-type resistance island among carbapenem-resistant *Acinetobacter baumannii* clinical isolates in Taiwan. *Int J Antimicrob Agents* **40**, 163-7.
- Lee, J., Hiibel, S. R., Reardon, K. F., and Wood, T. K.** (2010a) Identification of stress-related proteins in *Escherichia coli* using the pollutant cis-dichloroethylene. *J Appl Microbiol* **108**, 2088-102.
- Lee, J. H., Choi, C. H., Kang, H. Y., Lee, J. Y., Kim, J., Lee, Y. C., et al.** (2007) Differences in phenotypic and genotypic traits against antimicrobial agents between *Acinetobacter baumannii* and *Acinetobacter* genomic species 13TU. *J Antimicrob Chemother* **59**, 633-9.
- Lee, J. S., Choi, C. H., Kim, J. W., and Lee, J. C.** (2010b) *Acinetobacter baumannii* outer membrane protein A induces dendritic cell death through mitochondrial targeting. *J Microbiol* **48**, 387-92.
- Lee, Y., Kim, C. K., Lee, H., Jeong, S. H., Yong, D., and Lee, K.** (2011) A novel insertion sequence, IS*Aba10*, inserted into IS*Aba1* adjacent to the *bla*_{OXA-23} gene and disrupting the outer membrane protein gene *carO* in *Acinetobacter baumannii*. *Antimicrob Agents Chemother* **55**, 361-3.
- Lee, Y. T., Fung, C. P., Wang, F. D., Chen, C. P., Chen, T. L., and Cho, W. L.** (2012b) Outbreak of imipenem-resistant *Acinetobacter calcoaceticus*-*Acinetobacter baumannii* complex harboring different carbapenemase gene-associated genetic structures in an intensive care unit. *J Microbiol Immunol Infect* **45**, 43-51.
- Lees-Miller, R. G., Iwashkiw, J. A., Scott, N. E., Seper, A., Vinogradov, E., Schild, S., et al.** (2013) A common pathway for O-linked protein-glycosylation and synthesis of capsule in *Acinetobacter baumannii*. *Mol Microbiol* **89**, 816-30.
- Lemos, E. V., de la Hoz, F. P., Einarson, T. R., McGhan, W. F., Quevedo, E., Castaneda, C., et al.** (2014) Carbapenem resistance and mortality in patients with *Acinetobacter baumannii* infection: systematic review and meta-analysis. *Clin Microbiol Infect* **20**, 416-23.

- Leonardo, M. R., and Forst, S.** (1996) Re-examination of the role of the periplasmic domain of EnvZ in sensing of osmolarity signals in *Escherichia coli*. *Mol Microbiol* **22**, 405-13.
- Leong, C. G., Bloomfield, R. A., Boyd, C. A., Dornbusch, A. J., Lieber, L., Liu, F., et al.** (2017) The role of core and accessory type IV pilus genes in natural transformation and twitching motility in the bacterium *Acinetobacter baylyi*. *PLoS One* **12**, e0182139.
- Lessel, E. F.** (1971) Minutes of the meeting. International committee on nomenclature of bacteria subcommittee on the taxonomy of *Moraxella* and allied bacteria. *Int J Syst Bacteriol* **21**, 213-4.
- Letunic, I., and Bork, P.** (2018) 20 years of the SMART protein domain annotation resource. *Nucleic Acids Res* **46**, D493-D6.
- Leung, W. S., Chu, C. M., Tsang, K. Y., Lo, F. H., Lo, K. F., and Ho, P. L.** (2006) Fulminant community-acquired *Acinetobacter baumannii* pneumonia as a distinct clinical syndrome. *Chest* **129**, 102-9.
- Leus, I. V., Weeks, J. W., Bonifay, V., Smith, L., Richardson, S., and Zgurskaya, H. I.** (2018) Substrate specificities and efflux efficiencies of RND efflux pumps of *Acinetobacter baumannii*. *J Bacteriol* **200**, e00049-18.
- Levy-Blitchtein, S., Roca, I., Plasencia-Rebata, S., Vicente-Taboada, W., Velasquez-Pomar, J., Munoz, L., et al.** (2018) Emergence and spread of carbapenem-resistant *Acinetobacter baumannii* international clones II and III in Lima, Peru. *Emerg Microbes Infect* **7**, 119.
- Li, G. W., Burkhardt, D., Gross, C., and Weissman, J. S.** (2014a) Quantifying absolute protein synthesis rates reveals principles underlying allocation of cellular resources. *Cell* **157**, 624-35.
- Li, L., Hassan, K. A., Brown, M. H., and Paulsen, I. T.** (2016a) Rapid multiplexed phenotypic screening identifies drug resistance functions for three novel efflux pumps in *Acinetobacter baumannii*. *J Antimicrob Chemother* **71**, 1223-32.
- Li, L., Wang, Q., Zhang, H., Yang, M., Khan, M. I., and Zhou, X.** (2016b) Sensor histidine kinase is a β -lactam receptor and induces resistance to β -lactam antibiotics. *Proc Natl Acad Sci USA* **113**, 1648-53.
- Li, X., Quan, J., Yang, Y., Ji, J., Liu, L., Fu, Y., et al.** (2016c) *abrp*, a new gene, confers reduced susceptibility to tetracycline, glycolcine, chloramphenicol and fosfomycin classes in *Acinetobacter baumannii*. *Eur J Clin Microbiol Infect Dis* **35**, 1371-5.
- Li, X. Z., and Nikaido, H.** (2004) Efflux-mediated drug resistance in bacteria. *Drugs* **64**, 159-204.
- Li, Y. C., Chang, C. K., Chang, C. F., Cheng, Y. H., Fang, P. J., Yu, T., et al.** (2014b) Structural dynamics of the two-component response regulator RstA in recognition of promoter DNA element. *Nucleic Acids Res* **42**, 8777-88.
- Lim, J. Y., Hwang, I., Ganzorig, M., Huang, S. L., Cho, G. S., Franz, C., et al.** (2018) Complete genome sequences of three *Moraxella osloensis* strains isolated from human skin. *Genome Announc* **6**, e01509-17.

- Lin, M. F., and Lan, C. Y.** (2014) Antimicrobial resistance in *Acinetobacter baumannii*: From bench to bedside. *World J Clin Cases* **2**, 787-814.
- Lin, M. F., Lin, Y. Y., and Lan, C. Y.** (2015) The role of the two-component system BaeSR in disposing chemicals through regulating transporter systems in *Acinetobacter baumannii*. *PLoS One* **10**, e0132843.
- Lin, M. F., Lin, Y. Y., Yeh, H. W., and Lan, C. Y.** (2014) Role of the BaeSR two-component system in the regulation of *Acinetobacter baumannii* *adeAB* genes and its correlation with tigecycline susceptibility. *BMC Microbiol* **14**, 119.
- Lin, M. F., Liou, M. L., Tu, C. C., Yeh, H. W., and Lan, C. Y.** (2013) Molecular epidemiology of integron-associated antimicrobial gene cassettes in the clinical isolates of *Acinetobacter baumannii* from northern Taiwan. *Ann Lab Med* **33**, 242-7.
- Linz, B., Mukhtar, N., Shabbir, M. Z., Rivera, I., Ivanov, Y. V., Tahir, Z., et al.** (2018) Virulent epidemic pneumonia in sheep caused by the human pathogen *Acinetobacter baumannii*. *Front Microbiol* **9**, 2616.
- Liou, M. L., Soo, P. C., Ling, S. R., Kuo, H. Y., Tang, C. Y., and Chang, K. C.** (2014) The sensor kinase BfmS mediates virulence in *Acinetobacter baumannii*. *J Microbiol Immunol Infect* **47**, 275-81.
- Liu, F., Zhu, Y., Yi, Y., Lu, N., Zhu, B., and Hu, Y.** (2014) Comparative genomic analysis of *Acinetobacter baumannii* clinical isolates reveals extensive genomic variation and diverse antibiotic resistance determinants. *BMC Genomics* **15**, 1163.
- Liu, Q., Hassan, K. A., Ashwood, H. E., Gamage, H., Li, L., Mabbutt, B. C., et al.** (2018) Regulation of the *aceI* multidrug efflux pump gene in *Acinetobacter baumannii*. *J Antimicrob Chemother* **73**, 1492-500.
- Liu, S. V., Saunders, N. J., Jeffries, A., and Rest, R. F.** (2002) Genome analysis and strain comparison of *Correia* repeats and *Correia* repeat-enclosed elements in pathogenic *Neisseria*. *J Bacteriol* **184**, 6163-73.
- Livak, K. J., and Schmittgen, T. D.** (2001) Analysis of relative gene expression data using real-time quantitative PCR and the $2^{(-\Delta\Delta C(T))}$ method. *Methods* **25**, 402-8.
- Lob, S. H., Hoban, D. J., Sahm, D. F., and Badal, R. E.** (2016) Regional differences and trends in antimicrobial susceptibility of *Acinetobacter baumannii*. *Int J Antimicrob Agents* **47**, 317-23.
- Loehfelm, T. W., Luke, N. R., and Campagnari, A. A.** (2008) Identification and characterization of an *Acinetobacter baumannii* biofilm-associated protein. *J Bacteriol* **190**, 1036-44.
- Logan Draughn, G., Milton, M. E., Feldmann, E. A., Bobay, B. G., Roth, B. M., Olson, A. L., et al.** (2018) The structure of the biofilm-controlling response regulator BfmR from *Acinetobacter baumannii* reveals details of its DNA-binding mechanism. *J Mol Biol* **430**, 806-21.
- Lonergan, Z. R., Nairn, B. L., Wang, J., Hsu, Y. P., Hesse, L. E., Beavers, W. N., et al.** (2019) An *Acinetobacter baumannii*, zinc-regulated peptidase maintains cell wall integrity during immune-mediated nutrient sequestration. *Cell Rep* **26**, 2009-18.e6.

- Lopes, B. S., and Amyes, S. G.** (2012) Role of IS*Aba1* and IS*Aba125* in governing the expression of *bla*_{ADC} in clinically relevant *Acinetobacter baumannii* strains resistant to cephalosporins. *J Med Microbiol* **61**, 1103-8.
- Lopes, B. S., and Amyes, S. G.** (2013) Insertion sequence disruption of *adeR* and ciprofloxacin resistance caused by efflux pumps and *gyrA* and *parC* mutations in *Acinetobacter baumannii*. *Int J Antimicrob Agents* **41**, 117-21.
- Lopes, B. S., Evans, B. A., and Amyes, S. G.** (2012) Disruption of the *bla*_{OXA-51-like} gene by IS*Aba16* and activation of the *bla*_{OXA-58} gene leading to carbapenem resistance in *Acinetobacter baumannii* Ab244. *J Antimicrob Chemother* **67**, 59-63.
- López-Pérez, M., Gonzaga, A., and Rodríguez-Valera, F.** (2013) Genomic diversity of "deep ecotype" *Alteromonas macleodii* isolates: evidence for pan-Mediterranean clonal frames. *Genome Biol Evol* **5**, 1220-32.
- López-Rojas, R., Dominguez-Herrera, J., McConnell, M. J., Docobo-Perez, F., Smani, Y., Fernández-Reyes, M., et al.** (2011) Impaired virulence and *in vivo* fitness of colistin-resistant *Acinetobacter baumannii*. *J Infect Dis* **203**, 545-8.
- López, D., Vlamakis, H., and Kolter, R.** (2010) Biofilms. *Cold Spring Harb Perspect Biol* **2**, a000398.
- Lucidi, M., Runci, F., Rampioni, G., Frangipani, E., Leoni, L., and Visca, P.** (2018) New shuttle vectors for gene cloning and expression in multidrug-resistant *Acinetobacter* species. *Antimicrob Agents Chemother* **62**, e02480-17.
- Luna, C. M., Rodríguez-Noriega, E., Bavestrello, L., and Guzmán-Blanco, M.** (2014) Gram-negative infections in adult intensive care units of latin america and the Caribbean. *Crit Care Res Pract* **2014**, 480463.
- Lupski, J. R.** (1987) Molecular mechanisms for transposition of drug-resistance genes and other movable genetic elements. *Rev Infect Dis* **9**, 357-68.
- Ma, P., Patching, S. G., Ivanova, E., Baldwin, J. M., Sharples, D., Baldwin, S. A., et al.** (2016) Allantoin transport protein, PucI, from *Bacillus subtilis*: evolutionary relationships, amplified expression, activity and specificity. *Microbiology* **162**, 823-36.
- Mackie, A. M., Hassan, K. A., Paulsen, I. T., and Tetu, S. G.** (2014) Biolog Phenotype Microarrays for phenotypic characterization of microbial cells. *Methods Mol Biol* **1096**, 123-30.
- Macrina, F. L., Evans, R. P., Tobian, J. A., Hartley, D. L., Clewell, D. B., and Jones, K. R.** (1983) Novel shuttle plasmid vehicles for *Escherichia-Streptococcus* transgeneric cloning. *Gene* **25**, 145-50.
- Madrid, C., Nieto, J. M., Paytubi, S., Falconi, M., Gualerzi, C. O., and Juarez, A.** (2002) Temperature- and H-NS-dependent regulation of a plasmid-encoded virulence operon expressing *Escherichia coli* hemolysin. *J Bacteriol* **184**, 5058-66.
- Magnet, S., Courvalin, P., and Lambert, T.** (2001) Resistance-nodulation-cell division-type efflux pump involved in aminoglycoside resistance in *Acinetobacter baumannii* strain BM4454. *Antimicrob Agents Chemother* **45**, 3375-80.
- Mahillon, J., and Chandler, M.** (1998) Insertion sequences. *Microbiol Mol Biol Rev* **62**, 725-74.

- Maiden, M. C., Bygraves, J. A., Feil, E., Morelli, G., Russell, J. E., Urwin, R., et al.** (1998) Multilocus sequence typing: a portable approach to the identification of clones within populations of pathogenic microorganisms. *Proc Natl Acad Sci USA* **95**, 3140-5.
- Mann, T. H., Seth Childers, W., Blair, J. A., Eckart, M. R., and Shapiro, L.** (2016) A cell cycle kinase with tandem sensory PAS domains integrates cell fate cues. *Nat Commun* **7**, 11454.
- Marchand, I., Damier-Piolle, L., Courvalin, P., and Lambert, T.** (2004) Expression of the RND-type efflux pump AdeABC in *Acinetobacter baumannii* is regulated by the AdeRS two-component system. *Antimicrob Agents Chemother* **48**, 3298-304.
- Marchler-Bauer, A., Bo, Y., Han, L., He, J., Lanczycki, C. J., Lu, S., et al.** (2017) CDD/SPARCLE: functional classification of proteins via subfamily domain architectures. *Nucleic Acids Res* **45**, D200-D3.
- Marí-Almirall, M., Cosgaya, C., Higgins, P. G., Van Assche, A., Telli, M., Huys, G., et al.** (2017) MALDI-TOF/MS identification of species from the *Acinetobacter baumannii* (Ab) group revisited: inclusion of the novel *A. seifertii* and *A. dijkshoorniae* species. *Clin Microbiol Infect* **23**, 210.e1-.e9.
- Martí, S., Nait Chabane, Y., Alexandre, S., Coquet, L., Vila, J., Jouenne, T., et al.** (2011a) Growth of *Acinetobacter baumannii* in pellicle enhanced the expression of potential virulence factors. *PLoS One* **6**, e26030.
- Martí, S., Rodríguez-Baño, J., Catel-Ferreira, M., Jouenne, T., Vila, J., Seifert, H., et al.** (2011b) Biofilm formation at the solid-liquid and air-liquid interfaces by *Acinetobacter* species. *BMC Res Notes* **4**, 5.
- Martinez-Garcia, P. M., Ruano-Rosa, D., Schiliro, E., Prieto, P., Ramos, C., Rodriguez-Palenzuela, P., et al.** (2015) Complete genome sequence of *Pseudomonas fluorescens* strain PICF7, an indigenous root endophyte from olive (*Olea europaea* L.) and effective biocontrol agent against *Verticillium dahliae*. *Stand Genomic Sci* **10**, 10.
- Martins, N., Picao, R. C., Adams-Sapper, S., Riley, L. W., and Moreira, B. M.** (2015) Association of class 1 and 2 integrons with multidrug-resistant *Acinetobacter baumannii* international clones and *Acinetobacter nosocomialis* isolates. *Antimicrob Agents Chemother* **59**, 698-701.
- Mascher, T., Helmann, J. D., and Uden, G.** (2006) Stimulus perception in bacterial signal-transducing histidine kinases. *Microbiol Mol Biol Rev* **70**, 910-38.
- McCleary, W. R., Stock, J. B., and Ninfa, A. J.** (1993) Is acetyl phosphate a global signal in *Escherichia coli*? *J Bacteriol* **175**, 2793-8.
- McQueary, C. N., Kirkup, B. C., Si, Y., Barlow, M., Actis, L. A., Craft, D. W., et al.** (2012) Extracellular stress and lipopolysaccharide modulate *Acinetobacter baumannii* surface-associated motility. *J Microbiol* **50**, 434-43.
- Miethke, M., and Marahiel, M. A.** (2007) Siderophore-based iron acquisition and pathogen control. *Microbiol Mol Biol Rev* **71**, 413-51.
- Mike, L. A., Dutter, B. F., Stauff, D. L., Moore, J. L., Vitko, N. P., Aranmolate, O., et al.** (2013) Activation of heme biosynthesis by a small molecule that is toxic to fermenting *Staphylococcus aureus*. *Proc Natl Acad Sci USA* **110**, 8206-11.

- Milton, M. E., Minrovic, B. M., Harris, D. L., Kang, B., Jung, D., Lewis, C. P., et al.** (2018) Re-sensitizing multidrug resistant bacteria to antibiotics by targeting bacterial response regulators: characterization and comparison of interactions between 2-aminoimidazoles and the response regulators BfmR from *Acinetobacter baumannii* and QseB from *Francisella* spp. *Front Mol Biosci* **5**, 15.
- Mindlin, S., Petrenko, A., Kurakov, A., Beletsky, A., Mardanov, A., and Petrova, M.** (2016) Resistance of permafrost and modern *Acinetobacter lwoffii* strains to heavy metals and arsenic revealed by genome analysis. *Biomed Res Int* **2016**, 3970831.
- Mine, T., Morita, Y., Kataoka, A., Mizushima, T., and Tsuchiya, T.** (1999) Expression in *Escherichia coli* of a new multidrug efflux pump, MexXY, from *Pseudomonas aeruginosa*. *Antimicrob Agents Chemother* **43**, 415-7.
- Mirshekar, M., Shahcheraghi, F., Azizi, O., Solgi, H., and Badmasti, F.** (2018) Diversity of class 1 integrons, and disruption of *carO* and *dacD* by insertion sequences among *Acinetobacter baumannii* isolates in Tehran, Iran. *Microb Drug Resist* **24**, 359-66.
- Mizuno, T., and Tanaka, I.** (1997) Structure of the DNA-binding domain of the OmpR family of response regulators. *Mol Microbiol* **24**, 665-7.
- Moffatt, J. H., Harper, M., Adler, B., Nation, R. L., Li, J., and Boyce, J. D.** (2011) Insertion sequence *ISAbal1* is involved in colistin resistance and loss of lipopolysaccharide in *Acinetobacter baumannii*. *Antimicrob Agents Chemother* **55**, 3022-4.
- Monk, I. R., Howden, B. P., Seemann, T., and Stinear, T. P.** (2017) Correspondence: Spontaneous secondary mutations confound analysis of the essential two-component system WalkR in *Staphylococcus aureus*. *Nat Commun* **8**, 14403.
- Monteagudo-Cascales, E., Garcia-Mauriño, S. M., Santero, E., and Canosa, I.** (2019) Unraveling the role of the CbrA histidine kinase in the signal transduction of the CbrAB two-component system in *Pseudomonas putida*. *Sci Rep* **9**, 9110.
- Moon, K. H., Weber, B. S., and Feldman, M. F.** (2017) Subinhibitory concentrations of trimethoprim and sulfamethoxazole prevent biofilm formation by *Acinetobacter baumannii* through inhibition of Csu pilus expression. *Antimicrob Agents Chemother* **61**, e00778-17.
- Moore, J. L., Becker, K. W., Nicklay, J. J., Boyd, K. L., Skaar, E. P., and Caprioli, R. M.** (2014) Imaging mass spectrometry for assessing temporal proteomics: analysis of calprotectin in *Acinetobacter baumannii* pulmonary infection. *Proteomics* **14**, 820-8.
- Moreira, C. G., Herrera, C. M., Needham, B. D., Parker, C. T., Libby, S. J., Fang, F. C., et al.** (2013) Virulence and stress-related periplasmic protein (VisP) in bacterial/host associations. *Proc Natl Acad Sci USA* **110**, 1470-5.
- Moreno-Paz, M., Gómez, M. J., Arcas, A., and Parro, V.** (2010) Environmental transcriptome analysis reveals physiological differences between biofilm and planktonic modes of life of the iron oxidizing bacteria *Leptospirillum* spp. in their natural microbial community. *BMC Genomics* **11**, 404.
- Moriel, D. G., Beatson, S. A., Wurpel, D. J., Lipman, J., Nimmo, G. R., Paterson, D. L., et al.** (2013) Identification of novel vaccine candidates against multidrug-resistant *Acinetobacter baumannii*. *PLoS One* **8**, e77631.

- Morris, A. R., and Visick, K. L.** (2013) The response regulator SypE controls biofilm formation and colonization through phosphorylation of the syp-encoded regulator SypA in *Vibrio fischeri*. *Mol Microbiol* **87**, 509-25.
- Mortensen, B. L., Rathi, S., Chazin, W. J., and Skaar, E. P.** (2014) *Acinetobacter baumannii* response to host-mediated zinc limitation requires the transcriptional regulator Zur. *J Bacteriol* **196**, 2616-26.
- Mu, X., Wang, N., Li, X., Shi, K., Zhou, Z., Yu, Y., et al.** (2016) The effect of colistin resistance-associated mutations on the fitness of *Acinetobacter baumannii*. *Front Microbiol* **7**, 1715.
- Mugnier, P. D., Poirel, L., and Nordmann, P.** (2009) Functional analysis of insertion sequence IS*Aba1*, responsible for genomic plasticity of *Acinetobacter baumannii*. *J Bacteriol* **191**, 2414-8.
- Muller, S., Pflock, M., Schar, J., Kennard, S., and Beier, D.** (2007) Regulation of expression of atypical orphan response regulators of *Helicobacter pylori*. *Microbiol Res* **162**, 1-14.
- Murray, G. L., Tsyganov, K., Kostoulias, X. P., Bulach, D. M., Powell, D., Creek, D. J., et al.** (2017) Global gene expression profile of *Acinetobacter baumannii* during bacteremia. *J Infect Dis* **215**, S52-7.
- Mussi, M. A., Gaddy, J. A., Cabruja, M., Arivett, B. A., Viale, A. M., Rasia, R., et al.** (2010) The opportunistic human pathogen *Acinetobacter baumannii* senses and responds to light. *J Bacteriol* **192**, 6336-45.
- Mussi, M. A., Limansky, A. S., and Viale, A. M.** (2005) Acquisition of resistance to carbapenems in multidrug-resistant clinical strains of *Acinetobacter baumannii*: natural insertional inactivation of a gene encoding a member of a novel family of β -barrel outer membrane proteins. *Antimicrob Agents Chemother* **49**, 1432-40.
- Nagy, Z., and Chandler, M.** (2004) Regulation of transposition in bacteria. *Res Microbiol* **155**, 387-98.
- Nait Chabane, Y., Marti, S., Rihouey, C., Alexandre, S., Hardouin, J., Lesouhaitier, O., et al.** (2014) Characterisation of pellicles formed by *Acinetobacter baumannii* at the air-liquid interface. *PLoS One* **9**, e111660.
- Naville, M., Ghuillot-Gaudeffroy, A., Marchais, A., and Gautheret, D.** (2011) ARNold: a web tool for the prediction of Rho-independent transcription terminators. *RNA Biol* **8**, 11-3.
- Nemec, A., Dijkshoorn, L., and van der Reijden, T. J.** (2004) Long-term predominance of two pan-European clones among multi-resistant *Acinetobacter baumannii* strains in the Czech Republic. *J Med Microbiol* **53**, 147-53.
- Nemec, A., Krizova, L., Maixnerova, M., Sedo, O., Brisse, S., and Higgins, P. G.** (2015) *Acinetobacter seifertii* sp. nov., a member of the *Acinetobacter calcoaceticus*-*Acinetobacter baumannii* complex isolated from human clinical specimens. *Int J Syst Evol Microbiol* **65**, 934-42.
- Nemec, A., Krizova, L., Maixnerova, M., van der Reijden, T. J., Deschaght, P., Passet, V., et al.** (2011) Genotypic and phenotypic characterization of the *Acinetobacter calcoaceticus*-*Acinetobacter baumannii* complex with the proposal of *Acinetobacter pittii* sp. nov. (formerly *Acinetobacter* genomic species 3) and

Acinetobacter nosocomialis sp. nov. (formerly *Acinetobacter* genomic species 13TU). *Res Microbiol* **162**, 393-404.

- Nemec, A., Maixnerova, M., van der Reijden, T. J., van den Broek, P. J., and Dijkshoorn, L.** (2007) Relationship between the AdeABC efflux system gene content, netilmicin susceptibility and multidrug resistance in a genotypically diverse collection of *Acinetobacter baumannii* strains. *J Antimicrob Chemother* **60**, 483-9.
- Nigro, S. J., Farrugia, D. N., Paulsen, I. T., and Hall, R. M.** (2013) A novel family of genomic resistance islands, AbGRI2, contributing to aminoglycoside resistance in *Acinetobacter baumannii* isolates belonging to global clone 2. *J Antimicrob Chemother* **68**, 554-7.
- Nigro, S. J., and Hall, R. M.** (2012) Antibiotic resistance islands in A320 (RUH134), the reference strain for *Acinetobacter baumannii* global clone 2. *J Antimicrob Chemother* **67**, 335-8.
- Nigro, S. J., and Hall, R. M.** (2016a) Loss and gain of aminoglycoside resistance in global clone 2 *Acinetobacter baumannii* in Australia via modification of genomic resistance islands and acquisition of plasmids. *J Antimicrob Chemother* **71**, 2432-40.
- Nigro, S. J., and Hall, R. M.** (2016b) Structure and context of *Acinetobacter* transposons carrying the *oxa23* carbapenemase gene. *J Antimicrob Chemother* **71**, 1135-47.
- Nigro, S. J., and Hall, R. M.** (2017) A large plasmid, pD46-4, carrying a complex resistance region in an extensively antibiotic-resistant ST25 *Acinetobacter baumannii*. *J Antimicrob Chemother* **72**, 3496-8.
- Nigro, S. J., Holt, K. E., Pickard, D., and Hall, R. M.** (2015) Carbapenem and amikacin resistance on a large conjugative *Acinetobacter baumannii* plasmid. *J Antimicrob Chemother* **70**, 1259-61.
- Nikaido, H.** (2011) Structure and mechanism of RND-type multidrug efflux pumps. *Adv Enzymol Relat Areas Mol Biol* **77**, 1-60.
- Nikaido, H., and Takatsuka, Y.** (2009) Mechanisms of RND multidrug efflux pumps. *Biochim Biophys Acta* **1794**, 769-81.
- Niu, C., Clemmer, K. M., Bonomo, R. A., and Rather, P. N.** (2008) Isolation and characterization of an autoinducer synthase from *Acinetobacter baumannii*. *J Bacteriol* **190**, 3386-92.
- Norton, M. D., Spilka, A. J., and Godoy, V. G.** (2013) Antibiotic resistance acquired through a DNA damage-inducible response in *Acinetobacter baumannii*. *J Bacteriol* **195**, 1335-45.
- Nowak-Zaleska, A., Wieczor, M., Czub, J., Nierzwicki, L., Kotlowski, R., Mikucka, A., et al.** (2016) Correlation between the number of Pro-Ala repeats in the EmrA homologue of *Acinetobacter baumannii* and resistance to netilmicin, tobramycin, imipenem and ceftazidime. *J Glob Antimicrob Resist* **7**, 145-9.
- Nowak, J., Schneiders, T., Seifert, H., and Higgins, P. G.** (2016) The Asp20-to-Asn substitution in the response regulator AdeR leads to enhanced efflux activity of AdeB in *Acinetobacter baumannii*. *Antimicrob Agents Chemother* **60**, 1085-90.

- Nowak, J., Zander, E., Stefanik, D., Higgins, P. G., Roca, I., Vila, J., et al.** (2017) High incidence of pandrug-resistant *Acinetobacter baumannii* isolates collected from patients with ventilator-associated pneumonia in Greece, Italy and Spain as part of the MagicBullet clinical trial. *J Antimicrob Chemother* **72**, 3277-82.
- Ogata, H., Audic, S., Barbe, V., Artiguenave, F., Fournier, P. E., Raoult, D., et al.** (2000) Selfish DNA in protein-coding genes of *Rickettsia*. *Science* **290**, 347-50.
- Ohtsubo, Y., Genka, H., Komatsu, H., Nagata, Y., and Tsuda, M.** (2005) High-temperature-induced transposition of insertion elements in *Burkholderia multivorans* ATCC 17616. *Appl Environ Microbiol* **71**, 1822-8.
- Omasits, U., Ahrens, C. H., Muller, S., and Wollscheid, B.** (2014) Protter: interactive protein feature visualization and integration with experimental proteomic data. *Bioinformatics* **30**, 884-6.
- Oncul, O., Keskin, O., Acar, H. V., Kucukardali, Y., Evrenkaya, R., Atasoyu, E. M., et al.** (2002) Hospital-acquired infections following the 1999 Marmara earthquake. *J Hosp Infect* **51**, 47-51.
- Ophir, T., and Gutnick, D. L.** (1994) A role for exopolysaccharides in the protection of microorganisms from desiccation. *Appl Environ Microbiol* **60**, 740-5.
- Ortet, P., Whitworth, D. E., Santaella, C., Achouak, W., and Barakat, M.** (2015) P2CS: updates of the prokaryotic two-component systems database. *Nucleic Acids Res* **43**, D536-41.
- Owen-Hughes, T. A., Pavitt, G. D., Santos, D. S., Sidebotham, J. M., Hulton, C. S., Hinton, J. C., et al.** (1992) The chromatin-associated protein H-NS interacts with curved DNA to influence DNA topology and gene expression. *Cell* **71**, 255-65.
- Pagano, M., Martins, A. F., and Barth, A. L.** (2016) Mobile genetic elements related to carbapenem resistance in *Acinetobacter baumannii*. *Braz J Microbiol* **47**, 785-92.
- Pakharukova, N., Garnett, J. A., Tuittila, M., Paavilainen, S., Diallo, M., Xu, Y., et al.** (2015) Structural insight into archaic and alternative chaperone-usher pathways reveals a novel mechanism of pilus biogenesis. *PLoS Pathog* **11**, e1005269.
- Pakharukova, N., Tuittila, M., Paavilainen, S., Malmi, H., Parilova, O., Teneberg, S., et al.** (2018) Structural basis for *Acinetobacter baumannii* biofilm formation. *Proc Natl Acad Sci USA* **115**, 5558-63.
- Palmer, L. D., and Skaar, E. P.** (2016) Transition metals and virulence in bacteria. *Annu Rev Genet* **50**, 67-91.
- Parkins, M. D., Ceri, H., and Storey, D. G.** (2001) *Pseudomonas aeruginosa* GacA, a factor in multihost virulence, is also essential for biofilm formation. *Mol Microbiol* **40**, 1215-26.
- Partridge, S. R., Kwong, S. M., Firth, N., and Jensen, S. O.** (2018) Mobile genetic elements associated with antimicrobial resistance. *Clin Microbiol Rev* **31**, e00088-17.
- Partridge, S. R., Tsafnat, G., Coiera, E., and Iredell, J. R.** (2009) Gene cassettes and cassette arrays in mobile resistance integrons. *FEMS Microbiol Rev* **33**, 757-84.

- Patching, S. G.** (2018) Recent developments in nucleobase cation symporter-1 (NCS1) family transport proteins from bacteria, archaea, fungi and plants. *J Biosci* **43**, 797-815.
- Patel, S.** (2016) Drivers of bacterial genomes plasticity and roles they play in pathogen virulence, persistence and drug resistance. *Infect Genet Evol* **45**, 151-64.
- Pazos, F., and Valencia, A.** (2008) Protein co-evolution, co-adaptation and interactions. *EMBO J* **27**, 2648-55.
- Pecsok, R. L., and Sandera, J.** (1955) The gluconate complexes. II. The ferric-gluconate system. *J Am Chem Soc* **77**, 1489-94.
- Pedrosa, F. O., Monteiro, R. A., Wassem, R., Cruz, L. M., Ayub, R. A., Colauto, N. B., et al.** (2011) Genome of *Herbaspirillum seropedicae* strain SmR1, a specialized diazotrophic endophyte of tropical grasses. *PLoS Genet* **7**, e1002064.
- Peleg, A. Y., Adams, J., and Paterson, D. L.** (2007) Tigecycline efflux as a mechanism for nonsusceptibility in *Acinetobacter baumannii*. *Antimicrob Agents Chemother* **51**, 2065-9.
- Peleg, A. Y., Seifert, H., and Paterson, D. L.** (2008a) *Acinetobacter baumannii*: emergence of a successful pathogen. *Clin Microbiol Rev* **21**, 538-82.
- Peleg, A. Y., Tampakakis, E., Fuchs, B. B., Eliopoulos, G. M., Moellering, R. C., Jr., and Mylonakis, E.** (2008b) Prokaryote-eukaryote interactions identified by using *Caenorhabditis elegans*. *Proc Natl Acad Sci USA* **105**, 14585-90.
- Penwell, W. F., Arivett, B. A., and Actis, L. A.** (2012) The *Acinetobacter baumannii* *entA* gene located outside the acinetobactin cluster is critical for siderophore production, iron acquisition and virulence. *PLoS One* **7**, e36493.
- Penwell, W. F., DeGrace, N., Tentarelli, S., Gauthier, L., Gilbert, C. M., Arivett, B. A., et al.** (2015) Discovery and characterization of new hydroxamate siderophores, baumannoferrin A and B, produced by *Acinetobacter baumannii*. *Chembiochem* **16**, 1896-904.
- Pérez-Losada, M., Cabezas, P., Castro-Nallar, E., and Crandall, K. A.** (2013) Pathogen typing in the genomics era: MLST and the future of molecular epidemiology. *Infect Genet Evol* **16**, 38-53.
- Pérez-Varela, M., Corral, J., Aranda, J., and Barbé, J.** (2019) Roles of efflux pumps from different superfamilies in the surface-associated motility and virulence of *Acinetobacter baumannii* ATCC 17978. *Antimicrob Agents Chemother* **63**, e02190-18.
- Pérez-Varela, M., Corral, J., Vallejo, J. A., Rumbo-Feal, S., Bou, G., Aranda, J., et al.** (2017) Mutations in the β -subunit of the RNA polymerase impair the surface-associated motility and virulence of *Acinetobacter baumannii*. *Infect Immun* **85**, e00327-17.
- Peters, M., Tomikas, A., and Nurk, A.** (2004) Organization of the horizontally transferred *pheBA* operon and its adjacent genes in the genomes of eight indigenous *Pseudomonas* strains. *Plasmid* **52**, 230-6.
- Pflüger, T., Hernández, C. F., Lewe, P., Frank, F., Mertens, H., Svergun, D., et al.** (2018) Signaling ammonium across membranes through an ammonium sensor histidine kinase. *Nat Commun* **9**, 164.

- Piddock, L. J.** (2006) Clinically relevant chromosomally encoded multidrug resistance efflux pumps in bacteria. *Clin Microbiol Rev* **19**, 382-402.
- Pirrung, M. C.** (1999) Histidine kinases and two-component signal transduction systems. *Chem Biol* **6**, 167-75.
- Podgornaia, A. I., and Laub, M. T.** (2013) Determinants of specificity in two-component signal transduction. *Curr Opin Microbiol* **16**, 156-62.
- Poirel, L., Carrer, A., Pitout, J. D., and Nordmann, P.** (2009) Integron mobilization unit as a source of mobility of antibiotic resistance genes. *Antimicrob Agents Chemother* **53**, 2492-8.
- Poirel, L., Menuteau, O., Agoli, N., Cattoen, C., and Nordmann, P.** (2003) Outbreak of extended-spectrum β -lactamase VEB-1-producing isolates of *Acinetobacter baumannii* in a French hospital. *J Clin Microbiol* **41**, 3542-7.
- Poirel, L., and Nordmann, P.** (2006) Genetic structures at the origin of acquisition and expression of the carbapenem-hydrolyzing oxacillinase gene *bla_{OXA-58}* in *Acinetobacter baumannii*. *Antimicrob Agents Chemother* **50**, 1442-8.
- Porter, S. L., Roberts, M. A., Manning, C. S., and Armitage, J. P.** (2008) A bifunctional kinase-phosphatase in bacterial chemotaxis. *Proc Natl Acad Sci USA* **105**, 18531-6.
- Post, V., and Hall, R. M.** (2009) AbaR5, a large multiple-antibiotic resistance region found in *Acinetobacter baumannii*. *Antimicrob Agents Chemother* **53**, 2667-71.
- Post, V., White, P. A., and Hall, R. M.** (2010) Evolution of AbaR-type genomic resistance islands in multiply antibiotic-resistant *Acinetobacter baumannii*. *J Antimicrob Chemother* **65**, 1162-70.
- Potron, A., Munoz-Price, L. S., Nordmann, P., Cleary, T., and Poirel, L.** (2011) Genetic features of CTX-M-15-producing *Acinetobacter baumannii* from Haiti. *Antimicrob Agents Chemother* **55**, 5946-8.
- Potts, M.** (1994) Desiccation tolerance of prokaryotes. *Microbiol Rev* **58**, 755-805.
- Pratt, L. A., and Kolter, R.** (1998) Genetic analysis of *Escherichia coli* biofilm formation: roles of flagella, motility, chemotaxis and type I pili. *Mol Microbiol* **30**, 285-93.
- Procaccini, A., Lunt, B., Szurmant, H., Hwa, T., and Weigt, M.** (2011) Dissecting the specificity of protein-protein interaction in bacterial two-component signaling: orphans and crosstalks. *PLoS One* **6**, e19729.
- Proschak, A., Lubuta, P., Grun, P., Lohr, F., Wilharm, G., De Berardinis, V., et al.** (2013) Structure and biosynthesis of fimsbactins A-F, siderophores from *Acinetobacter baumannii* and *Acinetobacter baylyi*. *Chembiochem* **14**, 633-8.
- Purins, L., Van Den Bosch, L., Richardson, V., and Morona, R.** (2008) Coiled-coil regions play a role in the function of the *Shigella flexneri* O-antigen chain length regulator WzzpHS2. *Microbiology* **154**, 1104-16.
- Rajamohan, G., Srinivasan, V. B., and Gebreyes, W. A.** (2010a) Molecular and functional characterization of a novel efflux pump, AmvA, mediating antimicrobial and disinfectant resistance in *Acinetobacter baumannii*. *J Antimicrob Chemother* **65**, 1919-25.

- Rajamohan, G., Srinivasan, V. B., and Gebreyes, W. A.** (2010b) Novel role of *Acinetobacter baumannii* RND efflux transporters in mediating decreased susceptibility to biocides. *J Antimicrob Chemother* **65**, 228-32.
- Ramirez, M. S., Don, M., Merkier, A. K., Bistue, A. J., Zorreguieta, A., Centron, D., et al.** (2010) Naturally competent *Acinetobacter baumannii* clinical isolate as a convenient model for genetic studies. *J Clin Microbiol* **48**, 1488-90.
- Rasko, D., Moreira, C., Li, D., Reading, N., Ritchie, J., Waldor, M. et al.** (2008) Targeting QseC signalling and virulence for antibiotic development. *Science* **321**, 1078-1080.
- Repizo, G. D., Gagne, S., Foucault-Grunenwald, M. L., Borges, V., Charpentier, X., Limansky, A. S., et al.** (2015) Differential role of the T6SS in *Acinetobacter baumannii* virulence. *PLoS One* **10**, e0138265.
- Ribera, A., Roca, I., Ruiz, J., Gibert, I., and Vila, J.** (2003) Partial characterization of a transposon containing the *tet(A)* determinant in a clinical isolate of *Acinetobacter baumannii*. *J Antimicrob Chemother* **52**, 477-80.
- Richmond, G. E., Evans, L. P., Anderson, M. J., Wand, M. E., Bonney, L. C., Ivens, A., et al.** (2016) The *Acinetobacter baumannii* two-component system AdeRS regulates genes required for multidrug efflux, biofilm formation, and virulence in a strain-specific manner. *MBio* **7**, e00430-16.
- Ringel, P. D., Hu, D., and Basler, M.** (2017) The role of type VI secretion system effectors in target cell lysis and subsequent horizontal gene transfer. *Cell Rep* **21**, 3927-40.
- Rivera, G., Bulnes, J., Castillo, C., Ajenjo, M. C., Garcia, P., and Labarca, J.** (2016) Extensively drug-resistant *Acinetobacter baumannii* isolated in a university hospital: Role of inter-hospital transmission. *J Infect Dev Ctries* **10**, 96-9.
- Roberson, E. B., and Firestone, M. K.** (1992) Relationship between desiccation and exopolysaccharide production in a soil *Pseudomonas* sp. *Appl Environ Microbiol* **58**, 1284-91.
- Robertson, A. E., Wechter, W. P., Denny, T. P., Fortnum, B. A., and Kluepfel, D. A.** (2004) Relationship between avirulence gene (*avrA*) diversity in *Ralstonia solanacearum* and bacterial wilt incidence. *Mol Plant Microbe Interact* **17**, 1376-84.
- Robinson, J. T., Thorvaldsdottir, H., Winckler, W., Guttman, M., Lander, E. S., Getz, G., et al.** (2011) Integrative genomics viewer. *Nat Biotechnol* **29**, 24-6.
- Robinson, V. L., Buckler, D. R., and Stock, A. M.** (2000) A tale of two components: a novel kinase and a regulatory switch. *Nat Struct Biol* **7**, 626-33.
- Roca, I., Espinal, P., Vila-Farres, X., and Vila, J.** (2012) The *Acinetobacter baumannii* oxymoron: commensal hospital dweller turned pan-drug-resistant menace. *Front Microbiol* **3**, 148.
- Roca, I., Marti, S., Espinal, P., Martínez, P., Gibert, I., and Vila, J.** (2009) CraA, a major facilitator superfamily efflux pump associated with chloramphenicol resistance in *Acinetobacter baumannii*. *Antimicrob Agents Chemother* **53**, 4013-4.

- Rolain, J. M., Diene, S. M., Kempf, M., Gimenez, G., Robert, C., and Raoult, D.** (2013) Real-time sequencing to decipher the molecular mechanism of resistance of a clinical pan-drug-resistant *Acinetobacter baumannii* isolate from Marseille, France. *Antimicrob Agents Chemother* **57**, 592-6.
- Rosenfeld, N., Bouchier, C., Courvalin, P., and Périchon, B.** (2012) Expression of the resistance-nodulation-cell division pump AdeIJK in *Acinetobacter baumannii* is regulated by AdeN, a TetR-type regulator. *Antimicrob Agents Chemother* **56**, 2504-10.
- Royer, S., de Campos, P. A., Araújo, B. F., Ferreira, M. L., Gonçalves, I. R., Batistão, D., et al.** (2018) Molecular characterization and clonal dynamics of nosocomial *bla_{OXA-23}* producing XDR *Acinetobacter baumannii*. *PLoS One* **13**, e0198643.
- Ruppitsch, W., Pietzka, A., Prior, K., Bletz, S., Fernandez, H. L., Allerberger, F., et al.** (2015) Defining and evaluating a core genome multilocus sequence typing scheme for whole-genome sequence-based typing of *Listeria monocytogenes*. *J Clin Microbiol* **53**, 2869-76.
- Russo, T. A., Luke, N. R., Beanan, J. M., Olson, R., Sauberan, S. L., MacDonald, U., et al.** (2010) The K1 capsular polysaccharide of *Acinetobacter baumannii* strain 307-0294 is a major virulence factor. *Infect Immun* **78**, 3993-4000.
- Russo, T. A., Manohar, A., Beanan, J. M., Olson, R., MacDonald, U., Graham, J., et al.** (2016) The response regulator BfmR is a potential drug target for *Acinetobacter baumannii*. *mSphere* **1**, e00082-16.
- Ryan, K. R.** (2006) Partners in crime: phosphotransfer profiling identifies a multicomponent phosphorelay. *Mol Microbiol* **59**, 361-3.
- Salto, I. P., Torres Tejerizo, G., Wibberg, D., Puhler, A., Schluter, A., and Pistorio, M.** (2018) Comparative genomic analysis of *Acinetobacter* spp. plasmids originating from clinical settings and environmental habitats. *Sci Rep* **8**, 7783.
- Sanchez-Larrayoz, A. F., Elhosseiny, N. M., Chevrette, M. G., Fu, Y., Giunta, P., Spallanzani, R. G., et al.** (2017) Complexity of complement resistance factors expressed by *Acinetobacter baumannii* needed for survival in human serum. *J Immunol* **199**, 2803-14.
- Sapula, S., and Brown, M. H.** (2016). "The role of efflux pumps in *Staphylococcus aureus*," in *Efflux-mediated drug resistance mechanisms in bacteria: mechanisms, regulation and clinical implications* eds. X.-Z. Li, C.A. Elkins & H.I. Zgurskaya. (Switzerland: Springer), 165-96.
- Saranathan, R., Pagal, S., Sawant, A. R., Tomar, A., Madhangi, M., Sah, S., et al.** (2017) Disruption of TetR type regulator *adeN* by mobile genetic element confers elevated virulence in *Acinetobacter baumannii*. *Virulence* **8**, 1316-34.
- Saroj, S. D., Clemmer, K. M., Bonomo, R. A., and Rather, P. N.** (2012) Novel mechanism for fluoroquinolone resistance in *Acinetobacter baumannii*. *Antimicrob Agents Chemother* **56**, 4955-7.
- Schmidt, H., and Hensel, M.** (2004) Pathogenicity islands in bacterial pathogenesis. *Clin Microbiol Rev* **17**, 14-56.
- Schurch, A. C., Arredondo-Alonso, S., Willems, R. J. L., and Goering, R. V.** (2018) Whole genome sequencing options for bacterial strain typing and epidemiologic

analysis based on single nucleotide polymorphism versus gene-by-gene-based approaches. *Clin Microbiol Infect* **24**, 350-4.

- Schweizer, H. D.** (1993) Small broad-host-range gentamycin resistance gene cassettes for site-specific insertion and deletion mutagenesis. *Biotechniques* **15**, 831-4.
- Scott, P., Deye, G., Srinivasan, A., Murray, C., Moran, K., Hulten, E., et al.** (2007) An outbreak of multidrug-resistant *Acinetobacter baumannii-calcoaceticus* complex infection in the US military health care system associated with military operations in Iraq. *Clin Infect Dis* **44**, 1577-84.
- Seifert, H., Dijkshoorn, L., Gerner-Smidt, P., Pelzer, N., Tjernberg, I., and Vanechoutte, M.** (1997) Distribution of *Acinetobacter* species on human skin: comparison of phenotypic and genotypic identification methods. *J Clin Microbiol* **35**, 2819-25.
- Semmler, A. B., Whitchurch, C. B., and Mattick, J. S.** (1999) A re-examination of twitching motility in *Pseudomonas aeruginosa*. *Microbiology* **145** (Pt 10), 2863-73.
- Seo, Y. S., Lim, J., Choi, B. S., Kim, H., Goo, E., Lee, B., et al.** (2011) Complete genome sequence of *Burkholderia gladioli* BSR3. *J Bacteriol* **193**, 3149.
- Sepulveda, E., and Lupas, A. N.** (2017) Characterization of the CrbS/R two-component system in *Pseudomonas fluorescens* reveals a new set of genes under Its control and a DNA motif required for CrbR-mediated transcriptional activation. *Front Microbiol* **8**, 2287.
- Sevvana, M., Vijayan, V., Zweckstetter, M., Reinelt, S., Madden, D. R., Herbst-Irmer, R., et al.** (2008) A ligand-induced switch in the periplasmic domain of sensor histidine kinase CitA. *J Mol Biol* **377**, 512-23.
- Sewitz, S., Crellin, P., and Chalmers, R.** (2003) The positive and negative regulation of Tn10 transposition by IHF is mediated by structurally asymmetric transposon arms. *Nucleic Acids Res* **31**, 5868-76.
- Shapiro, J. A., and Wencewicz, T. A.** (2016) Acinetobactin isomerization enables adaptive iron acquisition in *Acinetobacter baumannii* through pH-triggered siderophore swapping. *ACS Infect Dis* **2**, 157-68.
- Sharan, A., Soni, P., Nongpiur, R. C., Singla-Pareek, S. L., and Pareek, A.** (2017) Mapping the 'two-component system' network in rice. *Sci Rep* **7**, 9287.
- Sharma, A., Sharma, R., Bhattacharyya, T., Bhandu, T., and Pathania, R.** (2016) Fosfomycin resistance in *Acinetobacter baumannii* is mediated by efflux through a major facilitator superfamily (MFS) transporter-AbaF. *J Antimicrob Chemother* **72**, 68-74.
- Shashkov, A. S., Liu, B., Kenyon, J. J., Popova, A. V., Shneider, M. M., Senchenkova, S. N., et al.** (2017) Structures of the K35 and K15 capsular polysaccharides of *Acinetobacter baumannii* LUH5535 and LUH5554 containing amino and diamino uronic acids. *Carbohydr Res* **448**, 28-34.
- Shiga, Y., Sekine, Y., Kano, Y., and Ohtsubo, E.** (2001) Involvement of H-NS in transpositional recombination mediated by IS1. *J Bacteriol* **183**, 2476-84.

- Siddique, A., Buisine, N., and Chalmers, R.** (2011) The transposon-like *Correia* elements encode numerous strong promoters and provide a potential new mechanism for phase variation in the meningococcus. *PLoS Genet* **7**, e1001277.
- Sievers, F., and Higgins, D. G.** (2018) Clustal Omega for making accurate alignments of many protein sequences. *Protein Sci* **27**, 135-45.
- Siguier, P., Gourbeyre, E., and Chandler, M.** (2014) Bacterial insertion sequences: their genomic impact and diversity. *FEMS Microbiol Rev* **38**, 865-91.
- Siguier, P., Gourbeyre, E., Varani, A., Ton-Hoang, B., and Chandler, M.** (2015) Everyman's guide to bacterial insertion sequences. *Microbiol Spectr* **3**, MDNA3-0030-2014.
- Siguier, P., Perochon, J., Lestrade, L., Mahillon, J., and Chandler, M.** (2006) ISfinder: the reference centre for bacterial insertion sequences. *Nucleic Acids Res* **34**, D32-D6.
- Simon, R., Priefer, U., and Pühler, A.** (1983) A broad host range mobilization system for *in vivo* genetic engineering: transposon mutagenesis in Gram negative bacteria. *Bio/Technology* **1**, 784-91.
- Singkhom-In, U., and Chatsuwana, T.** (2018) *In vitro* activities of carbapenems in combination with amikacin, colistin, or fosfomycin against carbapenem-resistant *Acinetobacter baumannii* clinical isolates. *Diagn Microbiol Infect Dis* **67**, 1667-72.
- Siryaporn, A., and Goulian, M.** (2008) Cross-talk suppression between the CpxA-CpxR and EnvZ-OmpR two-component systems in *E. coli*. *Mol Microbiol* **70**, 494-506.
- Skerker, J. M., Prasol, M. S., Perchuk, B. S., Biondi, E. G., and Laub, M. T.** (2005) Two-component signal transduction pathways regulating growth and cell cycle progression in a bacterium: a system-level analysis. *PLoS Biol* **3**, e334.
- Skiebe, E., de Berardinis, V., Morczinek, P., Kerrinnes, T., Faber, F., Lepka, D., et al.** (2012) Surface-associated motility, a common trait of clinical isolates of *Acinetobacter baumannii*, depends on 1,3-diaminopropane. *Int J Med Microbiol* **302**, 117-28.
- Smillie, C., Garcillán-Barcia, M. P., Francia, M. V., Rocha, E. P., and de la Cruz, F.** (2010) Mobility of plasmids. *Microbiol Mol Biol Rev* **74**, 434-52.
- Smith, M. G., Gianoulis, T. A., Pukatzki, S., Mekalanos, J. J., Ornston, L. N., Gerstein, M., et al.** (2007) New insights into *Acinetobacter baumannii* pathogenesis revealed by high-density pyrosequencing and transposon mutagenesis. *Genes Dev* **21**, 601-14.
- Snitkin, E. S., Zelazny, A. M., Gupta, J., Palmore, T. N., Murray, P. R., and Segre, J. A.** (2013) Genomic insights into the fate of colistin resistance and *Acinetobacter baumannii* during patient treatment. *Genome Res* **23**, 1155-62.
- Snitkin, E. S., Zelazny, A. M., Montero, C. I., Stock, F., Mijares, L., Murray, P. R., et al.** (2011) Genome-wide recombination drives diversification of epidemic strains of *Acinetobacter baumannii*. *Proc Natl Acad Sci USA* **108**, 13758-63.
- Spaulding, C. N., Schreiber, H. L. t., Zheng, W., Dodson, K. W., Hazen, J. E., Conover, M. S., et al.** (2018) Functional role of the type 1 pilus rod structure in mediating host-pathogen interactions. *Elife* **7**, e31662.

- Spellberg, B., and Rex, J. H.** (2013) The value of single-pathogen antibacterial agents. *Nat Rev Drug Discov* **12**, 963.
- Srinivasan, V. B., Rajamohan, G., and Gebreyes, W. A.** (2009) Role of AbeS, a novel efflux pump of the SMR family of transporters, in resistance to antimicrobial agents in *Acinetobacter baumannii*. *Antimicrob Agents Chemother* **53**, 5312-6.
- Srinivasan, V. B., Vaidyanathan, V., and Rajamohan, G.** (2015) AbuO, a TolC-like outer membrane protein of *Acinetobacter baumannii*, is involved in antimicrobial and oxidative stress resistance. *Antimicrob Agents Chemother* **59**, 1236-45.
- Stavrinides, J., Kirzinger, M. W., Beasley, F. C., and Guttman, D. S.** (2012) E622, a miniature, virulence-associated mobile element. *J Bacteriol* **194**, 509-17.
- Steele, K. H., O'Connor, L. H., Burpo, N., Kohler, K., and Johnston, J. W.** (2012) Characterization of a ferrous iron-responsive two-component system in nontypeable *Haemophilus influenzae*. *J Bacteriol* **194**, 6162-73.
- Stock, A. M., Robinson, V. L., and Goudreau, P. N.** (2000) Two-component signal transduction. *Annu Rev Biochem* **69**, 183-215.
- Stock, J. B., Ninfa, A. J., and Stock, A. M.** (1989) Protein phosphorylation and regulation of adaptive responses in bacteria. *Microbiol Rev* **53**, 450-90.
- Stokes, J. M., MacNair, C. R., Ilyas, B., French, S., Cote, J. P., Bouwman, C., et al.** (2017) Pentamidine sensitizes Gram-negative pathogens to antibiotics and overcomes acquired colistin resistance. *Nat Microbiol* **2**, 17028.
- Su, C. C., Morgan, C. E., Kambakam, S., Rajavel, M., Scott, H., Huang, W., et al.** (2019) Cryo-electron microscopy structure of an *Acinetobacter baumannii* multidrug efflux pump. *MBio* **10**, e01295-19.
- Su, X. Z., Chen, J., Mizushima, T., Kuroda, T., and Tsuchiya, T.** (2005) AbeM, an H⁺-coupled *Acinetobacter baumannii* multidrug efflux pump belonging to the MATE family of transporters. *Antimicrob Agents Chemother* **49**, 4362-4.
- Subashchandrabose, S., Smith, S., DeOrnellas, V., Crepin, S., Kole, M., Zahdeh, C., et al.** (2016) *Acinetobacter baumannii* genes required for bacterial survival during bloodstream infection. *mSphere* **1**, e00013-15.
- Sugawara, E., and Nikaido, H.** (2012) OmpA is the principal nonspecific slow porin of *Acinetobacter baumannii*. *J Bacteriol* **194**, 4089-96.
- Sugawara, E., and Nikaido, H.** (2014) Properties of AdeABC and AdeIJK efflux systems of *Acinetobacter baumannii* compared with those of AcrAB-TolC system of *Escherichia coli*. *Antimicrob Agents Chemother* **58**, 7250-7.
- Sullivan, M. J., Petty, N. K., and Beatson, S. A.** (2011) Easyfig: a genome comparison visualizer. *Bioinformatics* **27**, 1009-10.
- Sun, J. R., Perng, C. L., Chan, M. C., Morita, Y., Lin, J. C., Su, C. M., et al.** (2012) A truncated AdeS kinase protein generated by IS*AbaI* insertion correlates with tigecycline resistance in *Acinetobacter baumannii*. *PLoS One* **7**, e49534.
- Szuplewska, M., Ludwiczak, M., Lyzwa, K., Czarnecki, J., and Bartosik, D.** (2014) Mobility and generation of mosaic non-autonomous transposons by Tn3-derived inverted-repeat miniature elements (TIMEs). *PLoS One* **9**, e105010.

- Takahashi, K., Sekine, Y., Chibazakura, T., and Yoshikawa, H.** (2007) Development of an intermolecular transposition assay system in *Bacillus subtilis* 168 using IS4*BsuI* from *Bacillus subtilis* (natto). *Microbiology* **153**, 2553-9.
- Tang, Y. T., Gao, R., Havranek, J. J., Groisman, E. A., Stock, A. M., and Marshall, G. R.** (2012) Inhibition of bacterial virulence: drug-like molecules targeting the *Salmonella enterica* PhoP response regulator. *Chem Biol Drug Des* **79**, 1007-17.
- Tipton, K. A., Chin, C. Y., Farokhyfar, M., Weiss, D. S., and Rather, P. N.** (2018) Role of capsule in resistance to disinfectants, host antimicrobials and desiccation in *Acinetobacter baumannii*. *Antimicrob Agents Chemother* **62**, e01188-18.
- Tipton, K. A., Dimitrova, D., and Rather, P. N.** (2015) Phase-variable control of multiple phenotypes in *Acinetobacter baumannii* strain AB5075. *J Bacteriol* **197**, 2593-9.
- Tipton, K. A., Farokhyfar, M., and Rather, P. N.** (2017) Multiple roles for a novel RND-type efflux system in *Acinetobacter baumannii* AB5075. *Microbiologyopen* **6**, e10.1002.
- Tipton, K. A., and Rather, P. N.** (2017) An *ompR/envZ* two-component system ortholog regulates phase variation, osmotic tolerance, motility, and virulence in *Acinetobacter baumannii* strain AB5075. *J Bacteriol* **199**, e00705-16.
- Tiwari, S., Jamal, S. B., Hassan, S. S., Carvalho, P., Almeida, S., Barh, D., et al.** (2017) Two-component signal transduction systems of pathogenic bacteria as targets for antimicrobial therapy: an overview. *Front Microbiol* **8**, 1878.
- Tomaras, A. P., Dorsey, C. W., Edelmann, R. E., and Actis, L. A.** (2003) Attachment to and biofilm formation on abiotic surfaces by *Acinetobacter baumannii*: involvement of a novel chaperone-usher pili assembly system. *Microbiology* **149**, 3473-84.
- Tomaras, A. P., Flagler, M. J., Dorsey, C. W., Gaddy, J. A., and Actis, L. A.** (2008) Characterisation of a two-component regulatory system from *Acinetobacter baumannii* that controls biofilm formation and cellular morphology. *Microbiology* **154**, 3398-409.
- Tomich, M., and Mohr, C. D.** (2004) Genetic characterization of a multicomponent signal transduction system controlling the expression of cable pili in *Burkholderia cenocepacia*. *J Bacteriol* **186**, 3826-36.
- Toussaint, A., and Chandler, M.** (2012) Prokaryote genome fluidity: toward a system approach of the mobilome. *Methods Mol Biol* **804**, 57-80.
- Trebosc, V., Gartenmann, S., Royet, K., Manfredi, P., Totzl, M., Schellhorn, B., et al.** (2016) A novel genome editing platform for drug resistant *Acinetobacter baumannii* revealed an AdeR-unrelated tigecycline resistance mechanism. *Antimicrob Agents Chemother* **60**, 7263-71.
- Tucker, A. T., Nowicki, E. M., Boll, J. M., Knauf, G. A., Burdis, N. C., Trent, M. S., et al.** (2014) Defining gene-phenotype relationships in *Acinetobacter baumannii* through one-step chromosomal gene inactivation. *MBio* **5**, e01313-14.
- Turabelidze, G., Lawrence, S. J., Gao, H., Sodergren, E., Weinstock, G. M., Abubucker, S., et al.** (2013) Precise dissection of an *Escherichia coli* O157:H7 outbreak by single nucleotide polymorphism analysis. *J Clin Microbiol* **51**, 3950-4.

- Turton, J. F., Ward, M. E., Woodford, N., Kaufmann, M. E., Pike, R., Livermore, D. M., et al.** (2006) The role of IS*AbaI* in expression of OXA carbapenemase genes in *Acinetobacter baumannii*. *FEMS Microbiol Lett* **258**, 72-7.
- Uckay, I., Sax, H., Harbarth, S., Bernard, L., and Pittet, D.** (2008) Multi-resistant infections in repatriated patients after natural disasters: lessons learned from the 2004 tsunami for hospital infection control. *J Hosp Infect* **68**, 1-8.
- Ulrich, L. E., and Zhulin, I. B.** (2007) MiST: a microbial signal transduction database. *Nucleic Acids Res* **35**, 386-90.
- Umland, T. C., Schultz, L. W., MacDonald, U., Beanan, J. M., Olson, R., and Russo, T. A.** (2012) *In vivo*-validated essential genes identified in *Acinetobacter baumannii* by using human ascites overlap poorly with essential genes detected on laboratory media. *MBio* **3**, e00113-12.
- Urwin, R., and Maiden, M. C.** (2003) Multi-locus sequence typing: a tool for global epidemiology. *Trends Microbiol* **11**, 479-87.
- Valencia, R., Arroyo, L. A., Conde, M., Aldana, J. M., Torres, M. J., Fernández-Cuenca, F., et al.** (2009) Nosocomial outbreak of infection with pan-drug-resistant *Acinetobacter baumannii* in a tertiary care university hospital. *Infect Control Hosp Epidemiol* **30**, 257-63.
- Valladares, A., Montesinos, M. L., Herrero, A., and Flores, E.** (2002) An ABC-type, high-affinity urea permease identified in cyanobacteria. *Mol Microbiol* **43**, 703-15.
- van Dessel, H., Dijkshoorn, L., van der Reijden, T., Bakker, N., Paauw, A., van den Broek, P., et al.** (2004) Identification of a new geographically widespread multiresistant *Acinetobacter baumannii* clone from European hospitals. *Res Microbiol* **155**, 105-12.
- Vandecraen, J., Chandler, M., Aertsen, A., and Van Houdt, R.** (2017) The impact of insertion sequences on bacterial genome plasticity and adaptability. *Crit Rev Microbiol* **43**, 709-30.
- Vanechoutte, M., Young, D. M., Ornston, L. N., De Baere, T., Nemeč, A., Van Der Reijden, T., et al.** (2006) Naturally transformable *Acinetobacter* sp. strain ADP1 belongs to the newly described species *Acinetobacter baylyi*. *Appl Environ Microbiol* **72**, 932-6.
- Vettath, V. K., Junqueira, A. C. M., Uchida, A., Purbojati, R. W., Houghton, J. N. I., Chenard, C., et al.** (2018) Complete genome sequence of *Acinetobacter indicus* type strain SGAir0564 isolated from tropical air collected in Singapore. *Genome Announc* **6**.
- Viehman, J. A., Nguyen, M. H., and Doi, Y.** (2014) Treatment options for carbapenem-resistant and extensively drug-resistant *Acinetobacter baumannii* infections. *Drugs* **74**, 1315-33.
- Vijaykumar, S., Balaji, V., and Biswas, I.** (2015a) Complete genome sequence of *Acinetobacter baumannii* strain B8300, which displays high twitching motility. *Genome Announc* **3**, e00956-15.
- Vijaykumar, S., Balaji, V., and Biswas, I.** (2015b) Complete genome sequence of *Acinetobacter baumannii* strain B8342, a motility-positive clinical isolate. *Genome Announc* **3**, e00925-15.

- Vila, J., Marti, S., and Sánchez-Céspedes, J. (2007) Porins, efflux pumps and multidrug resistance in *Acinetobacter baumannii*. *J Antimicrob Chemother* **59**, 1210-5.
- Wachter, S., Raghavan, R., Wachter, J., and Minnick, M. F. (2018) Identification of novel MITEs (miniature inverted-repeat transposable elements) in *Coxiella burnetii*: implications for protein and small RNA evolution. *BMC Genomics* **19**, 247.
- Walthers, D., Tran, V. K., and Kenney, L. J. (2003) Interdomain linkers of homologous response regulators determine their mechanism of action. *J Bacteriol* **185**, 317-24.
- Wang, J., Zhou, Z., He, F., Ruan, Z., Jiang, Y., Hua, X., *et al.* (2018) The role of the type VI secretion system *vgrG* gene in the virulence and antimicrobial resistance of *Acinetobacter baumannii* ATCC 19606. *PLoS One* **13**, e0192288.
- Wang, N., Ozer, E. A., Mandel, M. J., and Hauser, A. R. (2014) Genome-wide identification of *Acinetobacter baumannii* genes necessary for persistence in the lung. *MBio* **5**, e01163-14.
- Wang, X., Preston, J. F., 3rd, and Romeo, T. (2004) The *pgaABCD* locus of *Escherichia coli* promotes the synthesis of a polysaccharide adhesin required for biofilm formation. *J Bacteriol* **186**, 2724-34.
- Wang, X., Wang, Q., Yang, M., Xiao, J., Liu, Q., Wu, H., *et al.* (2011a) QseBC controls flagellar motility, fimbrial hemagglutination and intracellular virulence in fish pathogen *Edwardsiella tarda*. *Fish Shellfish Immunol* **30**, 944-53.
- Wang, X., Zong, Z., and Lu, X. (2011b) Tn2008 is a major vehicle carrying *bla*_{OXA-23} in *Acinetobacter baumannii* from China. *Diagn Microbiol Infect Dis* **69**, 218-22.
- Wang, Y., Hao, P., Lu, B., Yu, H., Huang, W., Hou, H., *et al.* (2010) Causes of infection after earthquake, China, 2008. *Emerg Infect Dis* **16**, 974-5.
- Wardle, S. J., O'Carroll, M., Derbyshire, K. M., and Haniford, D. B. (2005) The global regulator H-NS acts directly on the transpososome to promote Tn10 transposition. *Genes Dev* **19**, 2224-35.
- Weber, B. S., Harding, C. M., and Feldman, M. F. (2015a) Pathogenic *Acinetobacter* from the cell surface to infinity and beyond. *J Bacteriol* **198**, 880-7.
- Weber, B. S., Hennon, S. W., Wright, M. S., Scott, N. E., de Berardinis, V., Foster, L. J., *et al.* (2016) Genetic dissection of the type VI secretion system in *Acinetobacter* and identification of a novel peptidoglycan hydrolase, TagX, required for its biogenesis. *MBio* **7**, e01253-16.
- Weber, B. S., Ly, P. M., Irwin, J. N., Pukatzki, S., and Feldman, M. F. (2015b) A multidrug resistance plasmid contains the molecular switch for type VI secretion in *Acinetobacter baumannii*. *Proc Natl Acad Sci USA* **112**, 9442-7.
- Weber, B. S., Miyata, S. T., Iwashkiw, J. A., Mortensen, B. L., Skaar, E. P., Pukatzki, S., *et al.* (2013) Genomic and functional analysis of the type VI secretion system in *Acinetobacter*. *PLoS One* **8**, e55142.
- Weigel, W. A., and Demuth, D. R. (2016) QseBC, a two-component bacterial adrenergic receptor and global regulator of virulence in *Enterobacteriaceae* and *Pasteurellaceae*. *Mol Oral Microbiol* **31**, 379-97.

- Weigel, W. A., Demuth, D. R., Torres-Escobar, A., and Juárez-Rodríguez, M. D. (2015) *Aggregatibacter actinomycetemcomitans* QseBC is activated by catecholamines and iron and regulates genes encoding proteins associated with anaerobic respiration and metabolism. *Mol Oral Microbiol* **30**, 384-98.
- Weingarten, R. A., Johnson, R. C., Conlan, S., Ramsburg, A. M., Dekker, J. P., Lau, A. F., *et al.* (2018) Genomic analysis of hospital plumbing reveals diverse reservoir of bacterial plasmids conferring carbapenem resistance. *MBio* **9**, e02011-17.
- Wen, H., Wang, K., Liu, Y., Tay, M., Lauro, F. M., Huang, H., *et al.* (2014) Population dynamics of an *Acinetobacter baumannii* clonal complex during colonization of patients. *J Clin Microbiol* **52**, 3200-8.
- Wen, Y. O., Z., Yu, Y., Zhou, X., Pei, Y. D., B., Higgins, P., and Zheng, F. (2017) Mechanistic insight into how multidrug resistant *Acinetobacter baumannii* response regulator AdeR recognizes an intercistronic region *Nucleic Acids Res* **45**, 9773-87.
- West, A. H., and Stock, A. M. (2001) Histidine kinases and response regulator proteins in two-component signaling systems. *Trends Biochem Sci* **26**, 369-76.
- Wheeler, D. L., Church, D. M., Federhen, S., Lash, A. E., Madden, T. L., Pontius, J. U., *et al.* (2003) Database resources of the National Center for Biotechnology. *Nucleic Acids Res* **31**, 28-33.
- Whitchurch, C. B., Leech, A. J., Young, M. D., Kennedy, D., Sargent, J. L., Bertrand, J. J., *et al.* (2004) Characterization of a complex chemosensory signal transduction system which controls twitching motility in *Pseudomonas aeruginosa*. *Mol Microbiol* **52**, 873-93.
- Whitman, T. J., Qasba, S. S., Timpone, J. G., Babel, B. S., Kasper, M. R., English, J. F., *et al.* (2008) Occupational transmission of *Acinetobacter baumannii* from a United States serviceman wounded in Iraq to a health care worker. *Clin Infect Dis* **47**, 439-43.
- Wibberg, D., Salto, I. P., Eikmeyer, F. G., Maus, I., Winkler, A., Nordmann, P., *et al.* (2018) Complete genome sequencing of *Acinetobacter baumannii* strain K50 discloses the large conjugative plasmid pK50a encoding carbapenemase OXA-23 and extended-spectrum β -lactamase GES-11. *Antimicrob Agents Chemother* **62**, e00212-18.
- Wiegand, I., Hilpert, K., and Hancock, R. E. (2008) Agar and broth dilution methods to determine the minimal inhibitory concentration (MIC) of antimicrobial substances. *Nat Protoc* **3**, 163-75.
- Wilharm, G., Piesker, J., Laue, M., and Skiebe, E. (2013) DNA uptake by the nosocomial pathogen *Acinetobacter baumannii* occurs during movement along wet surfaces. *J Bacteriol* **195**, 4146-53.
- Willett, J. W., and Kirby, J. R. (2012) Genetic and biochemical dissection of a HisKA domain identifies residues required exclusively for kinase and phosphatase activities. *PLoS Genet* **8**, e1003084.
- Willett, J. W., Tiwari, N., Muller, S., Hummels, K. R., Houtman, J. C., Fuentes, E. J., *et al.* (2013) Specificity residues determine binding affinity for two-component signal transduction systems. *MBio* **4**, e00420-13.

- Williams, R. H., and Whitworth, D. E.** (2010) The genetic organisation of prokaryotic two-component system signalling pathways. *BMC Genomics* **11**, 720-32.
- Withers, R., Doherty, G. P., Jordan, M., Yang, X., Dixon, N. E., and Lewis, P. J.** (2014) AtfA, a new factor in global regulation of transcription in *Acinetobacter* spp. *Mol Microbiol* **93**, 1130-43.
- Wong, D., Nielsen, T. B., Bonomo, R. A., Pantapalangkoor, P., Luna, B., and Spellberg, B.** (2017) Clinical and pathophysiological overview of *Acinetobacter* infections: a century of challenges. *Clin Microbiol Rev* **30**, 409-47.
- Wong, I. L., and Chow, L. M.** (2006) The role of *Leishmania enriettii* multidrug resistance protein 1 (LeMDR1) in mediating drug resistance is iron-dependent. *Mol Biochem Parasitol* **150**, 278-87.
- Wood, C. R., Ohneck, E. J., Edelmann, R. E., and Actis, L. A.** (2018) A light-regulated type I pilus contributes to *Acinetobacter baumannii* biofilm, motility and virulence functions. *Infect Immun* **86**, e00442-18.
- World Health Organisation** (2017) *Global priority list of antibiotic-resistant bacteria to guide research, discovery, and development of new antibiotics*. World Health Organisation <http://www.who.int/medicines/publications/global-priority-list-antibiotic-resistant-bacteria/en/>
- Worthington, R. J., Blackledge, M. S., and Melander, C.** (2013) Small-molecule inhibition of bacterial two-component systems to combat antibiotic resistance and virulence. *Future Med Chem* **5**, 1265-84.
- Wosten, M. M., Kox, L. F., Chamnongpol, S., Soncini, F. C., and Groisman, E. A.** (2000) A signal transduction system that responds to extracellular iron. *Cell* **103**, 113-25.
- Wright, M. S., Haft, D. H., Harkins, D. M., Perez, F., Hujer, K. M., Bajaksouzian, S., et al.** (2014) New insights into dissemination and variation of the health care-associated pathogen *Acinetobacter baumannii* from genomic analysis. *MBio* **5**, e00963-13.
- Wright, M. S., Iovleva, A., Jacobs, M. R., Bonomo, R. A., and Adams, M. D.** (2016) Genome dynamics of multidrug-resistant *Acinetobacter baumannii* during infection and treatment. *Genome Med* **8**, 26.
- Wright, M. S., Jacobs, M. R., Bonomo, R. A., and Adams, M. D.** (2017a) Transcriptome remodeling of *Acinetobacter baumannii* during infection and treatment. *MBio* **8**, e02193-16.
- Wright, M. S., Mountain, S., Beerli, K., and Adams, M. D.** (2017b) Assessment of insertion sequence mobilization as an adaptive response to oxidative stress in *Acinetobacter baumannii* using IS-seq. *J Bacteriol* **199**, e00833-16.
- Wu, R., Gu, M., Wilton, R., Babnigg, G., Kim, Y., Pokkuluri, P. R., et al.** (2013) Insight into the sporulation phosphorelay: crystal structure of the sensor domain of *Bacillus subtilis* histidine kinase, KinD. *Protein Sci* **22**, 564-76.
- Wu, Y., Aandahl, R. Z., and Tanaka, M. M.** (2015) Dynamics of bacterial insertion sequences: can transposition bursts help the elements persist? *BMC Evol Biol* **15**, 288.

- Wuichet, K., Cantwell, B. J., and Zhulin, I. B.** (2010) Evolution and phyletic distribution of two-component signal transduction systems. *Curr Opin Microbiol* **13**, 219-25.
- Xing, D., Zuo, Y., Cheng, S., Regan, J. M., and Logan, B. E.** (2008) Electricity generation by *Rhodopseudomonas palustris* DX-1. *Environ Sci Technol* **42**, 4146-51.
- Yakkala, H., Samantarrai, D., Gribskov, M., and Siddavattam, D.** (2019) Comparative genome analysis reveals niche-specific genome expansion in *Acinetobacter baumannii* strains. *PLoS One* **14**, e0218204.
- Yamamoto, S., Okujo, N., and Sakakibara, Y.** (1994) Isolation and structure elucidation of acinetobactin, a novel siderophore from *Acinetobacter baumannii*. *Arch Microbiol* **162**, 249-54.
- Yang, G.** (2013) MITE Digger, an efficient and accurate algorithm for genome wide discovery of miniature inverted repeat transposable elements. *BMC Bioinformatics* **14**, 186.
- Yang, G., Nagel, D. H., Feschotte, C., Hancock, C. N., and Wessler, S. R.** (2009) Tuned for transposition: molecular determinants underlying the hyperactivity of a Stowaway MITE. *Science* **325**, 1391-4.
- Ye, C., Ji, G., and Liang, C.** (2016) detectMITE: A novel approach to detect miniature inverted repeat transposable elements in genomes. *Sci Rep* **6**, 19688.
- Yee, L., Hosoyama, A., Ohji, S., Tsuchikane, K., Shimodaira, J., Yamazoe, A., et al.** (2014) Complete genome sequence of a dimethyl sulfide-utilizing bacterium, *Acinetobacter guillouiae* strain 20B (NBRC 110550). *Genome Announc* **2**, e01048-14.
- Yoon, E. J., Balloy, V., Fiette, L., Chignard, M., Courvalin, P., and Grillot-Courvalin, C.** (2016) Contribution of the Ade resistance-nodulation-cell division-type efflux pumps to fitness and pathogenesis of *Acinetobacter baumannii*. *MBio* **7**, e00697-16.
- Yoon, E. J., Chabane, Y. N., Goussard, S., Snesrud, E., Courvalin, P., Dé, E., et al.** (2015) Contribution of resistance-nodulation-cell division efflux systems to antibiotic resistance and biofilm formation in *Acinetobacter baumannii*. *MBio* **6**, e00309-15.
- Yoon, E. J., Courvalin, P., and Grillot-Courvalin, C.** (2013) RND-type efflux pumps in multidrug-resistant clinical isolates of *Acinetobacter baumannii*: major role for AdeABC overexpression and AdeRS mutations. *Antimicrob Agents Chemother* **57**, 2989-95.
- Yu, H., Yuan, M., Lu, W., Yang, J., Dai, S., Li, Q., et al.** (2011) Complete genome sequence of the nitrogen-fixing and rhizosphere-associated bacterium *Pseudomonas stutzeri* strain DSM4166. *J Bacteriol* **193**, 3422-3.
- Zackular, J. P., Chazin, W. J., and Skaar, E. P.** (2015) Nutritional immunity: S100 proteins at the host-pathogen interface. *J Biol Chem* **290**, 18991-8.
- Zarrilli, R., Pournaras, S., Giannouli, M., and Tsakris, A.** (2013) Global evolution of multidrug-resistant *Acinetobacter baumannii* clonal lineages. *Int J Antimicrob Agents* **41**, 11-9.

- Zha, D., Xu, L., Zhang, H., and Yan, Y.** (2014) Two-component system GacS/A activates lipA translation by RsmE but not RsmA in *Pseudomonas protegens* Pf-5. *Appl Environ Microbiol* **80**, 6627-37.
- Zhang, R., Hu, Y. Y., Yang, X. F., Gu, D. X., Zhou, H. W., Hu, Q. F., et al.** (2014) Emergence of NDM-producing non-baumannii *Acinetobacter* spp. isolated from China. *Eur J Clin Microbiol Infect Dis* **33**, 853-60.
- Zhang, W., and Shi, L.** (2005) Distribution and evolution of multiple-step phosphorelay in prokaryotes: lateral domain recruitment involved in the formation of hybrid-type histidine kinases. *Microbiology* **151**, 2159-73.
- Zhang, X. X., Gauntlett, J. C., Oldenburg, D. G., Cook, G. M., and Rainey, P. B.** (2015) Role of the transporter-like sensor kinase CbrA in histidine uptake and signal transduction. *J Bacteriol* **197**, 2867-78.
- Zhang, Z., and Saier, M. H., Jr.** (2011) Transposon-mediated adaptive and directed mutations and their potential evolutionary benefits. *J Mol Microbiol Biotechnol* **21**, 59-70.
- Zheng, Y. L., Wan, Y. F., Zhou, L. Y., Ye, M. L., Liu, S., Xu, C. Q., et al.** (2013) Risk factors and mortality of patients with nosocomial carbapenem-resistant *Acinetobacter baumannii* pneumonia. *Am J Infect Control* **41**, e59-63.
- Zhou, F., Tran, T., and Xu, Y.** (2008) *Nezha*, a novel active miniature inverted-repeat transposable element in cyanobacteria. *Biochem Biophys Res Commun* **365**, 790-4.
- Zhou, H., Zhang, T., Yu, D., Pi, B., Yang, Q., Zhou, J., et al.** (2011) Genomic analysis of the multidrug-resistant *Acinetobacter baumannii* strain MDR-ZJ06 widely spread in China. *Antimicrob Agents Chemother* **55**, 4506-12.
- Zhu, Y., Yi, Y., Liu, F., Lv, N., Yang, X., Li, J., et al.** (2014) Distribution and molecular profiling of class 1 integrons in MDR *Acinetobacter baumannii* isolates and whole genome-based analysis of antibiotic resistance mechanisms in a representative strain. *Microbiol Res* **169**, 811-16.
- Zimblér, D. L., Penwell, W. F., Gaddy, J. A., Menke, S. M., Tomaras, A. P., Connerly, P. L., et al.** (2009) Iron acquisition functions expressed by the human pathogen *Acinetobacter baumannii*. *Biomaterials* **22**, 23-32.
- Zong, Z.** (2014) The complex genetic context of *bla*_{PER-1} flanked by miniature inverted-repeat transposable elements in *Acinetobacter johnsonii*. *PLoS One* **9**, e90046.
- Zou, D., Huang, Y., Liu, W., Yang, Z., Dong, D., Huang, S., et al.** (2017) Complete sequences of two novel *bla*_{NDM-1}-harbouring plasmids from two *Acinetobacter towneri* isolates in China associated with the acquisition of Tn125. *Sci Rep* **7**, 9405.
- Zoued, A., Brunet, Y. R., Durand, E., Aschtgen, M. S., Logger, L., Douzi, B., et al.** (2014) Architecture and assembly of the Type VI secretion system. *Biochim Biophys Acta* **1843**, 1664-73.
- Zschiedrich, C. P., Keidel, V., and Szurmant, H.** (2016) Molecular mechanisms of two-component signal transduction. *J Mol Biol* **428**, 3752-75.
- Zuker, M.** (2003) Mfold web server for nucleic acid folding and hybridization prediction. *Nucleic Acids Res* **31**, 3406-15.